

P2 PURINOCEPTOR-DEPENDENT CARDIOPROTECTION IN ISCHAEMIC- REPERFUSED MYOCARDIUM

Shirley Sheau Yan Wee
BBioMedSc (Hons1), GradCertResMgt

School of Medical Science
Griffith Health
Griffith University

Submitted in fulfilment of the requirements of the degree of
Doctor of Philosophy

November 2011

ABSTRACT

The P2 purinoceptor family are perhaps the earliest (or most 'primitive') group of regulatory cell surface receptors, and have been studied intensely for several decades. The P2 receptors are subdivided into two major families, P2X subtypes (P2X₁, P2X₂, P2X₃, P2X₄, P2X₅, P2X₆ and P2X₇,) and P2Y subtypes (P2Y₁, P2Y₂, P2Y₄, P2Y₆, P2Y₁₁, P2Y₁₂, P2Y₁₃, and P2Y₁₄). In the cardiovascular system P2 purinoceptors have been implicated both in vasoconstriction and vasodilatation, cardiac inotropy, cardioprotection (including pre- and postconditioning responses), and disease-dependent cardiac dysfunction. Furthermore, increasing evidence indicates that P2 purinoceptors form functional heteromeric assemblies under certain conditions, adding to the complexity of purinoceptor functionality. Thus, full characterisation of the regulatory function of these receptors is yet to be accomplished. This thesis comprises a series of studies aimed at elucidating the roles of P2 purinoceptors (primarily the P2Y₂ subtype) in protecting the heart during ischaemia-reperfusion (relevant to the injurious effects of acute myocardial infarction).

The Langendorff perfused mouse heart model is the predominant model employed throughout this thesis. Despite common use in studies of myocardial ischaemia-reperfusion, few laboratories have rigorously characterised and refined this technically challenging model, and thus variability persists in its preparation and functional properties across laboratories. Thus, prior to analysis of P2 purinoceptor responses in normoxic and ischaemic-reperfused hearts, the Langendorff perfused heart model is characterised in **Chapter 3**, in which functional stability, responses to ischaemia-reperfusion, and effects of substrate (± 2 mM pyruvate) and of a known cardioprotectant (50 μ M adenosine; Ado) were assessed. Results from this work

showed an unavoidable though moderate degree of functional decay over time in this *in vitro* model, identified end-diastolic pressure (EDP) and left ventricular developed pressure (LVDP) as being sensitive markers of ischaemic injury (with systolic force not reliably impacted ischaemia-reperfusion), and confirmed predicted protective effects of both pyruvate and Ado, thus supporting application of the model in subsequent studies of ischaemia-reperfusion injury.

Chapter 4 outlines a real-time PCR based investigation of mRNA expression profiles for P2 purinoceptor subtypes in murine heart (left vs. right ventricular myocardium) and vascular tissue (ascending aorta). Expression of mRNA for all nine P2 purinoceptors studied (P2X₁, P2X₄, P2X₅, P2X₇, P2Y₁, P2Y₂, P2Y₄, P2Y₆ and P2Y₁₂) was detected in aorta and ventricular tissue of the mouse. Abundance of mRNAs varied considerably between subtypes and tissues. The P2X₁, P2X₇ and P2Y₄ transcripts were most abundant in vascular tissue; P2X₇ and P2Y₂ most abundant in left ventricle; and P2X₄, P2X₅, P2Y₁, P2Y₆ and P2Y₁₂ most abundant in the right ventricle. The LinRegPCR application was used to determine mean RT-PCR reaction efficiencies, which ranged between 1.93 - 2.30. These data established presence of mRNA transcript for all nine P2 subtypes in the mouse heart, with predominant expression of P2Y₁ and P2Y₂ in myocardial vs. vascular tissue suggestive of specific cardiac roles for these latter subtypes (whereas P2X₁ is very highly expressed in vascular tissue).

Having established expression of transcript for a range of P2Y and P2X subtypes in ventricular myocardium, investigations outlined in **Chapter 5** address the potential role of intrinsic P2 purinoceptor activity in dictating myocardial stress resistance -

specifically tolerance to the damaging effects of global ischaemia and reperfusion. Perfused C57/B16 mouse hearts were subjected to 20 min ischaemia and 45 min reperfusion, with effects of P2Y antagonists (reactive blue 2 and suramin), P2Y₁ selective antagonist (MRS2179), and P2X antagonists (MRS2159 and PPNDS) on post-ischaemic recoveries and oncosis (LDH efflux) assessed. Post-ischaemic recovery was reduced by blocking endogenous activation of P2Y receptors (reactive blue 2, suramin, MRS2179) and of P2X purinoceptors (MRS2159 and PPNDS). These data support a protective function for intrinsic P2Y and also P2X purinoceptor activity during ischaemia-reperfusion.

Having acquired evidence of ventricular expression of P2Y₁ and P2Y₂, and of potential protective functions of intrinsic P2Y_{1/2} activity, work in **Chapter 6** specifically addresses concentration and temporal dependence of P2Y agonist mediated cardioprotection. Concentration and time-dependent effects of the P2Y agonist uridine 5'-triphosphate (UTP) were investigated in murine hearts subjected to 20 min global ischaemia and 45 min aerobic reperfusion. Six experimental groups were studied, with hearts subjected to either 250 nM or 1 μ M UTP treatment as follows: i) 5 min pre-ischaemic treatment; ii) 5 min post-ischaemic treatment (early reperfusion); or iii) 5 min pre- and 5 min post-ischaemic treatment. Pre-ischaemic application of 250 nM UTP did not modify recovery of LVDP, while diastolic dysfunction was significantly reduced. In contrast, pre-ischaemic application of 1 μ M UTP did improve recovery of LVDP while also reducing diastolic dysfunction. Pre-ischaemic UTP treatment also improved recovery of coronary flow compared with untreated hearts. Contrasting pre-ischaemic treatment, post-ischaemic UTP (at 250 nM or 1 μ M) failed to modify contractile outcomes. Interestingly, a combination of

pre- and post-ischaemic UTP at 250 nM significantly reduced diastolic contracture and resulted in higher recovery of LVDP whereas the higher 1 μ M concentration was paradoxically ineffective. Data suggest that UTP (a P2Y_{2/4} agonist) enhances tolerance to ischaemia when applied before but not after the ischaemic event, and in a concentration dependent manner. Paradoxically, a high level of UTP throughout ischaemia-reperfusion fails to modify outcome. These data thus implicate P2Y_{2/4} subtypes, and possibly P2Y₆ receptors, in functional protection from myocardial ischaemia-reperfusion.

P2 purinoceptor modulation of injury during ischaemia-reperfusion was further investigated under **Chapter 7**. Effects of P2 agonism or antagonism on functional and cell death outcomes were assessed in isolated hearts subjected to 20 min ischaemia and 45 min reperfusion, together with interstitial accumulation of endogenous P2 agonists (UTP, ATP, ADP). A 250 nM concentration of UTP (a P2Y_{2/4} agonist) improved contractile function and reduced diastolic contracture and LDH loss. In contrast, P2Y₁ agonism with 2-MeSATP was ineffective. Co-treatment with the antagonist suramin negated UTP-mediated protection. Ischaemia substantially elevated interstitial [UTP], [ATP] and [ADP], providing potentially active levels of endogenous P2 agonists. This was consistent with effects of applied antagonists: 200 μ M suramin worsened LDH efflux and contractile dysfunction as did P2Y antagonism with reactive blue 2 (RB2). On the other hand, P2X antagonism with PPADS and P2X₁ selective antagonism with MRS2159 did not modify outcomes. These data collectively support cardioprotection with low concentrations of UTP, are consistent with P2Y₂ involvement, and indicate that endogenous interstitial nucleotides may contribute to intrinsic ischaemic tolerance via P2Y but not P2X receptors.

While UTP is thought to primarily target P2Y₂ and P2Y₄ receptors, it is not highly selective. Thus, in **Chapter 8** more selective P2Y agonists were employed to identify subtype involvement. The stable pyrimidines *UDPβS* and *UTPγS* were employed, and were not readily available at the time of earlier studies. These agents selectively activate P2Y₆ and P2Y_{2/4} purinoceptors, respectively. Interestingly, significant changes in normoxic function were apparent with *UTPγS* and *UDPβS*. A reduction in rate of relaxation and coronary flow occurred with *UTPγS* and *UDPβS*, although *UDPβS* treatment also unexpectedly depressed LVDP. In terms of post-ischaemic outcomes, diastolic contracture was significantly and concentration-dependently reduced by 50 and 150 nM *UTPγS*. However, only 50 nM *UTPγS* improved relative (%) recovery of LVDP, while hearts treated 150 nM *UTPγS* exhibited comparable relative recoveries to untreated hearts. Recovery of contractile function was also improved with *UDPβS*, with significantly enhanced recovery of LVDP and $-dP/dt$ (but not diastolic pressure) In addition, *UDPβS* enhanced recovery of coronary flow. Paradoxically, *UTPγS* failed to alter LDH efflux, while *UDPβS* actually enhanced LDH loss, suggesting exaggeration of tissue damage. Results in this study thus provide mixed support for a cardioprotective role of selective P2Y_{2/4} purinoceptor activation, which appears restricted to functional protection. Data also provides the first evidence of P2Y₆ mediated functional protection in ischaemic-reperfused mouse hearts, though evidence suggests cell damage may be paradoxically exaggerated.

The mechanistic basis of P2Y_{2/4} purinoceptor mediated cardioprotection is unclear. Work described in **Chapter 9** presents a basic interrogation of downstream signalling pathways associated with P2Y-mediated protection. While P2Y activation has been linked to multiple signalling pathways, stimulation of PIP₂–PLC signals predominates

(ultimately leading to activation of other signalling, including PKC, PLA₂, Ca²⁺-dependent K⁺ channels, NOS, voltage-operated Ca²⁺ channels, and MAPK paths). To identify potential signalling mechanisms ischaemic-reperfused mouse hearts were either untreated or subjected to: i) P2Y agonist (UTP); ii) UTP+P2 antagonist suramin; iii) K_{ATP} inhibitor 5-HD; iv) 5-HD+UTP; v) PI3K inhibitor wortmannin; vi) wortmannin+UTP; vii) Raf-1 inhibitor GW5074; or viii) GW5074+UTP. Treatment with UTP induced cardioprotection, reducing EDP and enhancing recovery of LVDP. Suramin abolished UTP cardioprotection, confirming P2 purinoceptor involvement. UTP mediated protection was also significantly attenuated by co-treatment with wortmannin, GW5074 and 5-HD (impairing diastolic and LVDP recoveries). Shifts in LDH efflux (a marker of oncosis) show that UTP reduces cell death, indicate that wortmannin and 5-HD exaggerate cell death, and show that UTP is unable to modify outcomes in the presence of these inhibitors (supporting PI3K and K_{ATP} dependent reductions in cell death, and involvement in UTP protection). UTP was also unable to reduce LDH efflux in GW5074 treated hearts. These results suggest that UTP mediated cardioprotection involves Raf-1 (immediately downstream of Ras in MAPK signalling), PI3K activation, and the opening of mitochondrial K_{ATP} channels.

In summary, the data presented throughout this thesis support a role for exogenous and endogenous P2 purinoceptor activity in modifying myocardial resistance to ischaemia and reperfusion. Data support involvement of P2Y *vs.* P2X subtypes, with evidence of P2Y₂, P2Y₄ and P2Y₆ subtype involvement. Thus, the P2Y system may be a potential target for therapeutic manipulation, and an intrinsic determinant of ischaemic tolerance. Signalling harnessed by these receptors is consistent with that engaged in other conventional protective responses such as pre- and postconditioning.

ACKNOWLEDGEMENTS

This work was undertaken in the Heart Foundation Research Centre (HFRC), School of Medical Science, Griffith University. This work was funded by the Australian Postgraduate Awards (APA) scholarship, and supported by the Heart Foundation Research Centre.

Without a doubt, if not for my supervisor, Professor John Headrick's inspiring guidance, support and friendship the completion of this work will not be possible. I am grateful for his patience and understanding in times of personal difficulties, and in times of triumphs such as a pregnancy amid my PhD candidature.

I would also like to thank my associate supervisors, Professor Roger Willis (whom is now retired) and Dr Jason Peart for his guidance and support. He had always made himself available to assist even without prior arrangements. In addition, a special thanks to Dr Roselyn Rose-Meyer for her words of encouragement and unwavering support.

To my colleagues in HFRC: Grant Williams-Pritchard, Dr Kevin Ashton, Dr Amanda Zatta, Dr Laura Shoo, Dr Melissa Reichelt, Kirsty Holmgren, Dr Ben Hack, Dr Tamsin Jenner, Dr Glen Harrison, Sussi Owen, Boris Budiono, Melinda John, Dr Helen Massa and Assoc. Professor Jay Browning, and in the School of Medical Science: Professor Lyn Griffiths, Sassy Braisby, Emma Cowie, Dr Larisa Haupt, Saras Menon, Javed Fowdar, Emily Camilleri; I would like to thank you all for your help, encouragement and timely kind words.

Last but not least, I would like to thank my husband, Brad Moran who has been a tower of strength in supporting me through every step of the way. To him I dedicate this work. Without his persistent encouragement, love and support, this work would have been insurmountable. To my beautiful daughters, Emma and Ella, thank you for keeping my spirit up. In addition, I would also like to thank my mother-in-law, Beverley Moran for her undying faith in me.

To all that are listed above and those that I have been in contact with during my PhD candidature at Griffith, you have enriched my research experience in ways more than you can imagine, you have made this experience an unforgettable chapter in my life. Thank you.

STATEMENT OF ORIGINALITY

The work presented within this thesis was performed in the Heart Foundation Research Centre, School of Medical Science, Griffith University. The research was carried out under the supervision of Prof. John P. Headrick, Prof. Roger Willis (now retired) and Dr Jason N. Peart.

I declare that this work has not previously been submitted for a degree or diploma in any university. To the best of my knowledge and belief, this thesis contains no material previously published or written by another person except where due reference is made in the thesis itself.

Shirley Wee
November 2011

TABLE OF CONTENTS

ABSTRACT	2
ACKNOWLEDGEMENTS	8
STATEMENT OF ORIGINALITY	10
TABLE OF CONTENTS	11
LIST OF FIGURES	15
LIST OF TABLES	19
LIST OF ABBREVIATIONS	20
CHAPTER 1 GENERAL INTRODUCTION	24
1.1 MYOCARDIAL METABOLISM.....	26
1.1.1 Fatty acid β -oxidation	26
1.1.2 Glucose and lactate oxidation	27
1.1.3 Oxidative phosphorylation	28
1.2 MYOCARDIAL ISCHAEMIA.....	29
1.2.1 Reperfusion injury	30
1.3 METABOLIC ALTERATIONS IN ISCHAEMIA-REPERFUSION	31
1.3.1 Oxidative stress	31
1.3.2 The Ca^{2+} hypothesis of injury.....	33
1.3.3 Excitation-contraction uncoupling and SR dysfunction	34
1.3.4 Desensitisation of contractile proteins to Ca^{2+}	34
1.3.5 Ca^{2+} overload.....	35
1.4 MYOCARDIAL CELL DEATH	37
1.4.1 Apoptosis or programmed cell death	38
1.4.2 Bcl-2 proteins and cardiac BNIP3-mediated apoptosis	40
1.4.3 mPTP.....	42
1.4.4 mPTP structure and mechanisms of activation and inhibition	44
1.4.5 mPTP and cardiac ischaemia-reperfusion	45
1.5 ENDOGENOUS PROTECTIVE MECHANISMS.....	46
1.5.1 Ischaemic preconditioning	47
1.5.2 Antioxidants	49
1.5.3 K_{ATP} channels.....	51
1.6 CYTOPROTECTIVE MEMBRANE RECEPTORS	53
1.6.1 Stress sensing and protection via nucleosides and nucleotides	54
1.6.2 Adenosine 5'-triphosphate (ATP).....	55
1.6.3 Cardiac effects of ATP/Uridine 5'-triphosphate (UTP)	57
1.6.4 Purinoceptors - P1 purinoceptors	58

1.7	P2X PURINOCEPTORS	60
1.7.1	<i>P2X purinoceptor signal transduction mechanisms</i>	62
1.7.2	<i>P2X purinoceptors in the heart</i>	63
1.8	P2Y PURINOCEPTORS	64
1.8.1	<i>P2Y purinoceptor signal transduction mechanisms</i>	64
1.8.2	<i>P2Y purinoceptor oligomers and interactions</i>	68
1.8.3	<i>P2Y purinoceptors in the heart</i>	69
1.9	CARDIOPROTECTION AND P2 PURINOCEPTORS	70
1.9.1	<i>UTP and P2Y purinoceptors</i>	71
1.9.2	<i>P2 purinoceptors and cell death</i>	71
CHAPTER 2 GENERAL METHODS		74
2.1	ANIMALS AND THE ISOLATED LANGENDORFF HEART MODEL	75
2.1.1	<i>Experimental exclusion criteria</i>	77
2.2	ONCOTIC DAMAGE VIA LACTATE DEHYDROGENASE (LDH) EFFLUX	77
2.3	REAL-TIME POLYMERASE CHAIN REACTION (PCR) ANALYSES	78
2.3.1	<i>Necessary equipment</i>	79
2.3.2	<i>Tissue preparation</i>	80
2.3.3	<i>Isolation of RNA from aorta, left and right ventricles</i>	80
2.3.4	<i>cDNA synthesis</i>	80
2.3.5	<i>Quantitative real-time PCR</i>	81
2.4	DATA ANALYSIS	82
CHAPTER 3 CHARACTERISATION OF THE <i>EX VIVO</i> MOUSE HEART MODEL		83
3.1	ABSTRACT	84
3.2	INTRODUCTION	86
3.3	MATERIALS AND METHODS	87
3.4	RESULTS	91
3.5	DISCUSSION	98
CHAPTER 4 P2 PURINOCEPTOR GENE EXPRESSION PROFILES IN MOUSE MYOCARDIUM AND AORTA		102
4.1	ABSTRACT	103
4.2	INTRODUCTION	104
4.3	MATERIALS AND METHODS	105
4.4	RESULTS	109
4.5	DISCUSSION	115
4.6	CONCLUSION	120

CHAPTER 5 P2 PURINOCEPTOR ANTAGONIST EFFECTS IN ISCHAEMIC-REPERFUSED MOUSE HEART - ROLES FOR INTRINSIC P2 ACTIVITY..... 121

5.1	ABSTRACT	122
5.2	INTRODUCTION.....	123
5.3	MATERIALS AND METHODS.....	124
5.4	RESULTS.....	126
5.5	DISCUSSION	134
5.6	CONCLUSION	137

CHAPTER 6 PRE- VS. POST-ISCHAEMIC CARDIOPROTECTION VIA THE P2 AGONIST UTP 138

6.1	ABSTRACT	139
6.2	INTRODUCTION.....	140
6.3	MATERIALS AND METHODS.....	141
6.4	RESULTS.....	143
6.5	DISCUSSION	151
6.6	CONCLUSION	156

CHAPTER 7 P2 PURINOCEPTOR-MEDIATED CARDIOPROTECTION IN ISCHAEMIC-REPERFUSED MOUSE HEART 157

7.1	ABSTRACT	158
7.2	INTRODUCTION.....	159
7.3	MATERIALS AND METHODS.....	160
7.4	RESULTS.....	163
7.5	DISCUSSION	170
7.6	CONCLUSION	176

CHAPTER 8 EFFECTS OF SELECTIVE P2Y₆ AND P2Y_{2/4} AGONISTS IN ISCHAEMIC-REPERFUSED MYOCARDIUM..... 178

8.1	ABSTRACT	179
8.2	INTRODUCTION.....	181
8.3	MATERIALS AND METHODS.....	182
8.4	RESULTS.....	183
8.5	DISCUSSION	193
8.6	CONCLUSION	197

CHAPTER 9 PHARMACOLOGICAL INTERROGATION OF P2 PURINOCEPTOR COUPLED SIGNALING IN ISCHAEMIC-REPERFUSED MOUSE HEART 198

9.1	ABSTRACT	199
9.2	INTRODUCTION.....	201
9.3	MATERIALS AND METHODS.....	203
9.4	RESULTS.....	204
9.5	DISCUSSION	210
9.6	CONCLUSION	214

CHAPTER 10 GENERAL CONCLUSIONS	215
REFERENCES.....	219

LIST OF FIGURES

Figure 1.1. Basic scheme of myocardial metabolism. Fatty acid and glucose oxidative pathways..	27
Figure 1.2. Overview of oxidative stress in ischaemia-reperfused cardiomyocytes. Ros may be initially generated at onset of reperfusion, from oxidation of hypoxanthine by xanthine oxidase (XO) in endothelial cells (ECs), and from the mitochondrial electron transport chain (METC) in myocytes. This promotes interactions among neutrophils (PMNs), macrophages (Ms) and ECs. Further ROS generation can arise from activated PMNs and Ms in the vascular space. Effects of migrated PMNs or Ms can generate ROS via the NADPH reaction catalyzed by NADPH oxidase (NADPHO) later in reperfusion.	32
Figure 1.3. Ca^{2+} overload in cardiomyocytes following ischaemia. Ischaemia causes intracellular Ca^{2+} overload. During the early phase of reoxygenation, the Ca^{2+} overload may be exaggerated by a reverse-mode action of the $\text{Na}^+/\text{Ca}^{2+}$ exchanger. Reoxygenation leads to the re-energizing of the sarcoplasmic reticulum where Ca^{2+} begins to accumulate. Once full, Ca^{2+} movement into the cytosol causes further elevation of Ca^{2+} concentration and the resultant Ca^{2+} oscillations provoke hypercontracture of the myofibrils, fuelled by the ATP resupply from the mitochondrion.	36
Figure 1.4. Diagrammatic representation of oncosis vs. apoptosis. Apoptosis is characterised by cell shrinkage, plasma membrane blebbing, chromatin condensation, and genomic DNA fragmentation. Oncosis involves cell swelling, random genetic damage and ultimately cell membrane rupture.	38
Figure 1.5. Molecular pathways of apoptotic and non-apoptotic cell death.	41
Figure 1.6. Model for BNIP3-mediated mitochondrial damage and cell death in myocytes. Ischaemia or hypoxia-induced activation of BNIP3 expression and the resulting acidotic condition are shown to mediate stable homo-dimerisation and mitochondrial membrane insertion of BNIP3 resulting in loss of $\Delta\Psi_m$ and generation of ROS. As a consequence of the mitochondrial damage, cells are shown to undergo three different fates, BAX/BAK dependent apoptosis, autophagy (by the release of Beclin-1 from the BCL-2/BCL-xL complex) and possibly necrosis.	43
Figure 1.7. Metabolic inducers and inhibitors of mPTP opening in cardiac ischaemia-reperfusion. ANT, adenine nucleotide translocase; CK, creatine kinase; CyPD, cyclophilin D; HK, hexokinase; Pi, inorganic phosphate; PBR, peripheral benzodiazepine receptor; VDAC, voltage dependent anion channel.	47
Figure 1.8. Reperfusion injury survival kinase (RISK) signalling in cardioprotection.	49
Akt, protein kinase B; cyto C, cytochrome C; eNOS, enzyme nitric oxide synthase; ERK, extracellular signal-regulated kinase 1/2; GC, guanylate cyclase; GPCR, G-protein coupled receptor; GSK-3 β , glycogen synthase kinase 3 beta; MEK, extracellular protein kinase; mK_{ATP} , mitochondrial ATP-dependent potassium channel; mPTP, mitochondrial permeability transition pore; NO, nitric oxide; PI3K, phosphoinositide 3 kinase - PKC- ϵ , protein kinase C-epsilon; PKG, protein kinase G; ROS, reactive oxygen species; TK, tyrosine kinase	
Figure 1.9. The purinergic cascade. ATP is released into the extracellular space where it forms the basis of a purinergic cascade. ATP acts directly on P2X and P2Y receptors and is degraded to ADP and AMP by ectonucleotidase activity. AMP gives rise to adenosine (ADO) that activated the P1 receptors. LGIC = Ligand gated ion channel, GPC = G-protein coupled	56
Figure 1.10. Schematic representation of a P2X receptor.	60
Figure 1.11. Schematic representation of a P2Y receptor.	64
Figure 2.1. Simplified schematic of the Langendorff isolated heart perfusion apparatus employed throughout this thesis.	76

Figure 2.2. Example of a real-time PCR amplification output. The threshold and CT are described in the text.....	79
Figure 3.1 - Schematic overview of all experimental groups undertaken in the characterisation of the <i>ex vivo</i> mouse heart model.....	91
Figure 3.2. Functional outcomes from 20 min ischaemia after 30 vs. 45 min of aerobic reperfusion in pyruvate perfused hearts. Recoveries are shown for: systolic pressure (A); coronary flow rate (%Pre-ischaemia) (B); left ventricular developed pressure (C); and end-diastolic pressure (D). Values are means±SEM. *, $P<0.05$ vs. 30 min reperfusion..	94
Figure 3.3. Effects of pyruvate ($n=23$) vs. glucose ($n=6$) on post-ischaemic recoveries for: (A) left ventricular developed pressure; and (B) left ventricular diastolic pressure. Values are means±SEM. *, $P<0.05$ vs. pyruvate.....	95
Figure 3.4 Effects of 50 μ M Ado on post-ischaemic recoveries of: (A) left ventricular developed pressure; and (B) left ventricular diastolic pressure. Data are shown for recoveries in control ($n=23$) vs. Ado ($n=6$) hearts. Values are means±SEM. *, $P<0.05$ vs. control.....	97
Figure 4.1. Relative vascular vs. ventricular mRNA expression of P2X ₁ purinoceptor. Data expressed as a % of the maximum level achieved in the tissue (% Max Gene expression).....	109
Figure 4.2. Relative vascular vs. ventricular mRNA expression of P2X ₄ purinoceptor. Data expressed as a % of the maximum level achieved in the tissue (% Max Gene expression).....	109
Figure 4.3. Relative vascular vs. ventricular mRNA expression of P2X ₅ purinoceptor. Data expressed as a % of the maximum level achieved in the tissue (% Max Gene expression).....	110
Figure 4.4. Relative vascular vs. ventricular mRNA expression of P2X ₇ purinoceptor. Data expressed as a % of the maximum level achieved in the tissue (% Max Gene expression).....	110
Figure 4.5. Relative vascular vs. ventricular mRNA expression of P2Y ₁ purinoceptor. Data expressed as a % of the maximum level achieved in the tissue (% Max Gene expression).....	111
Figure 4.6. Relative vascular vs. ventricular mRNA expression of P2Y ₂ purinoceptor. Data expressed as a % of the maximum level achieved in the tissue (% Max Gene expression).....	111
Figure 4.7. Relative vascular vs. ventricular mRNA expression of P2Y ₄ purinoceptor. Data expressed as a % of the maximum level achieved in the tissue (% Max Gene expression).....	112
Figure 4.8. Relative vascular vs. ventricular mRNA expression of P2Y ₆ purinoceptor. Data expressed as a % of the maximum level achieved in the tissue (% Max Gene expression).....	112
Figure 4.9. Relative vascular vs. ventricular mRNA expression of P2Y ₁₂ purinoceptor. Data expressed as a % of the maximum level achieved in the tissue (% Max Gene expression).....	113
Figure 5.1. Experimental time course in investigations of P2 antagonism in ischaemia-reperfusion.	125
Figure 5.2. Effects of P2 purinoceptor antagonists on left ventricular developed pressure at the end of 45 min reperfusion. Data are shown for treatment with RB2 (100 μ M, 1 μ M), suramin (SU; 200 μ M), MRS2179 (3 μ M), MRS2159 (3 μ M), and PPNDS (200 nM). Values shown are means±SEM. *, $P<0.05$ vs. untreated control hearts.....	128
Figure 5.3. Effects of P2 purinoceptor antagonists on left ventricular diastolic pressure at the end of 45 min reperfusion. Data are shown for treatment with RB2 (100 μ M, 1 μ M), suramin (SU; 200 μ M), MRS2179 (3 μ M), MRS2159 (3 μ M), and PPNDS (200 nM). Values shown are means±SEM. *, $P<0.05$ vs. untreated control hearts.....	129

Figure 5.4. Effects of P2 purinoceptor antagonists on coronary flow (% Pre-ischæmia) at the end of 45 min reperfusion. Data are shown for treatment with RB2 (100 μ M, 1 μ M), suramin (200 μ M), MRS2179 (3 μ M), MRS2159 (3 μ M), and PPNDS (200 nM). Values shown are means \pm SEM. *, $P<0.05$ vs. untreated control hearts.....	129
Figure 5.5. Effects of P2Y purinoceptor antagonists on post-ischæmic recoveries for (A) left ventricular developed pressure and (B) left ventricular diastolic pressure. Data are shown for recoveries in CTRL ($n=10$), 100 μ M RB2-100 ($n=7$), 1 μ M RB2-1 ($n=8$), 200 μ M suramin ($n=9$) and 3 μ M MRS2179 ($n=4$) treated hearts. Values are means \pm SEM. *, $P<0.05$ vs. CTRL. †, $P<0.05$ vs. RB2-100. ‡, $P<0.05$ vs. SU. §, $P<0.05$ vs. RB2-1.....	131
Figure 5.6. Effects of P2X purinoceptor antagonism on post-ischæmic recoveries for (A) left ventricular developed pressure and (B) left ventricular diastolic pressure. Data are shown for recoveries in CTRL ($n=10$), 3 μ M MRS2159 ($n=8$) and 200 nM PPNDS ($n=9$) hearts. Values are means \pm SEM. *, $P<0.05$ vs. CTRL. †, $P<0.05$ vs. MRS2159.....	132
Figure 5.7. Post-ischæmic efflux of lactate dehydrogenase (LDH) following 20 min ischæmia for control hearts and hearts treated with RB2 (100 μ M, 1 μ M), suramin (200 μ M) and MRS2179 (3 μ M). Values shown are means \pm SEM.	133
Figure 6.1. Overview of experimental groups in the investigations of P2 agonism with UTP pre-ischæmia, post-ischæmia, and pre-and post-ischæmia.....	142
Figure 6.2. Effects of UTP treatment (250 nM or 1 μ M) on final post-ischæmic recoveries of left ventricular (LV) developed pressure. Values are means \pm SEM. *, $P<0.05$ vs. control.	145
Figure 6.3. Effects of UTP treatment (250 nM or 1 μ M) on final post-ischæmic recoveries of left ventricular diastolic pressure. Values are means \pm SEM. *, $P<0.05$ vs. control.	145
Figure 6.4. Effects of UTP treatment (250 nM or 1 μ M) on final post-ischæmic recoveries of coronary flow (% pre-ischæmia). Values are means \pm SEM. *, $P<0.05$ vs. control.....	146
Figure 6.5. Effects of 250 nM UTP treatment (5 min pre-ischæmia, 5 min post-ischæmia, 5 min pre-and post-ischæmia) on post-ischæmic recoveries for: (A) left ventricular developed pressure; and (B) left ventricular diastolic pressure. Data are shown for recoveries for Control ($n=19$) versus UTP Pre ($n=10$), UTP Post ($n=8$) and UTP Pre & Post ($n=12$) treated hearts. Values are means \pm SEM. *, $P<0.05$ vs. CTRL.	149
Figure 6.6. Effects of 1 μ M UTP treatment (5 min pre-ischæmia, 5 min post-ischæmia, 5 min pre-and post-ischæmia) on post-ischæmic recoveries for: (A) left ventricular developed pressure; and (B) left ventricular diastolic pressure. Data are shown for recoveries in Control ($n=19$) versus UTP Pre ($n=8$), UTP Post ($n=8$) and UTP Pre & Post ($n=12$) treated hearts. Values are means \pm SEM. *, $P<0.05$ vs. CTRL.	150
Figure 7.1. Effects of UTP on post-ischæmic recoveries of left ventricular contractile function and coronary flow. Measures were made at the end of 45 min reperfusion (following 20 min global ischæmia) in untreated hearts ($n=19$), and in hearts treated with 250 nM UTP ($n=12$), 200 μ M suramin ($n=8$), 250 nM UTP + 200 μ M suramin ($n=8$), 10 μ M suramin ($n=7$), or 250 nM UTP + 10 μ M suramin ($n=9$). Shown are recoveries for left ventricular (LV) diastolic pressure (A), left ventricular (LV) developed pressure (B), and coronary flow rate (C). Values are means \pm SEM. * $P<0.05$ vs. corresponding values from control (Untreated) hearts.	166
Figure 7.2. Myocardial LDH efflux (indicating extent of oncosis) throughout post-ischæmic reperfusion. Efflux was measured in untreated hearts ($n=19$), and in hearts treated with 250 nM UTP ($n=12$), 200 μ M suramin ($n=8$), or UTP + suramin ($n=8$). Values are means \pm SEM. *, $P<0.05$ vs. corresponding values from control (Untreated) hearts.	167

Figure 7.3. Microdialysate levels of ATP, ADP and UTP during ischaemia-reperfusion in control (untreated; $n=7$) hearts. Microdialysate levels are also shown for normally perfused, non-ischaemic hearts (closed symbols; $n=7$). Values are means \pm SEM. *, $P<0.05$ vs. pre-ischaemic levels..... 168

Figure 7.4. Effects of P2 antagonists on post-ischaemic recoveries of contractile function and coronary flow. Measures were made after 45 min reperfusion in untreated hearts ($n=19$), and in hearts treated with 10 μ M ($n=7$) or 200 μ M ($n=8$) suramin, 10 μ M ($n=7$) or 100 μ M ($n=8$) RB2, 50 μ M PPADS ($n=8$), or 30 μ M MRS2159 ($n=8$). Shown are recoveries for left ventricular (LV) diastolic pressure (A), left ventricular (LV) developed pressure (B), and coronary flow rate (C). Values are means \pm SEM. *, $P<0.05$ vs. corresponding values from control (Untreated) hearts. 169

Figure 8.1. Effects of $UTP\gamma S$ (50 nM or 150 nM) or $UDP\beta S$ (50 nM) on post-ischaemic recoveries of: A) LVDP (absolute units); and B) LVDP (% of pre-ischaemic levels). Values are means \pm SEM. *, $P<0.05$ vs. control; †, $P<0.05$ vs. $UTP\gamma S$ (50 nM); ‡, $P<0.05$ vs. $UTP\gamma S$ (150 nM). 186

Figure 8.2. Effects of $UTP\gamma S$ (50 nM or 150 nM) or $UDP\beta S$ (50 nM) on post-ischaemic recoveries of: A) $+dP/dt$ (absolute units); and B) $+dP/dt$ (% of pre-ischaemia). Values are means \pm SEM. *, $P<0.05$ vs. control; †, $P<0.05$ vs. $UTP\gamma S$ (50 nM); ‡, $P<0.05$ vs. $UTP\gamma S$ (150 nM). 187

Figure 8.3. Effects of $UTP\gamma S$ (50 nM or 150 nM) or $UDP\beta S$ (50 nM) on post-ischaemic recoveries of: A) $-dP/dt$ (absolute units); and B) $-dP/dt$ (% of pre-ischaemia). Values are means \pm SEM. *, $P<0.05$ vs. control; †, $P<0.05$ vs. $UTP\gamma S$ (50 nM); ‡, $P<0.05$ vs. $UTP\gamma S$ (150 nM). 188

Figure 8.4. Effects of $UTP\gamma S$ (50 nM or 150 nM) or $UDP\beta S$ (50 nM) treatment on post-ischaemic recovery of end-diastolic pressure. Values are means \pm SEM. *, $P<0.05$ vs. control; †, $P<0.05$ vs. $UTP\gamma S$ (50 nM); ‡, $P<0.05$ vs. $UTP\gamma S$ (150 nM). 189

Figure 8.5. Effects of $UTP\gamma S$ (50 nM or 150 nM) or $UDP\beta S$ (50 nM) treatment on post-ischaemic recovery of: A) coronary flow (absolute units); and (B) coronary flow (% of pre-ischaemia). Values are means \pm SEM. *, $P<0.05$ vs. control; †, $P<0.05$ vs. $UTP\gamma S$ (50 nM); ‡, $P<0.05$ vs. $UTP\gamma S$ (150 nM). 190

Figure 8.6. Effects of $UTP\gamma S$ (50 nM or 150 nM) or $UDP\beta S$ (50 nM) on post-ischaemic recoveries for: A) LVDP; and B) left ventricular diastolic pressure. Data are shown for recoveries in untreated control hearts ($n=10$) vs. 50 nM $UTP\gamma S$ ($n=10$), 150 nM $UTP\gamma S$ ($n=10$), and 50 nM $UDP\beta S$ ($n=8$) treated hearts. Values are means \pm SEM. *, $P<0.05$ vs. Control; †, $P<0.05$ vs. 50 nM $UTP\gamma S$; ‡, $P<0.05$ vs. 150 nM $UTP\gamma S$ 191

Figure 8.7. Effects of $UTP\gamma S$ (50 nM or 150 nM) and $UDP\beta S$ (50 nM) on post-ischaemic LDH efflux (indicating extent of oncosis). Values are means \pm SEM. *, $P<0.05$ vs. control; †, $P<0.05$ vs. 50 nM $UTP\gamma S$; ‡, $P<0.05$ vs. 150 nM $UTP\gamma S$ 192

Figure 9.1. Effects of UTP and signalling inhibitors on post-ischaemic recoveries for: (A) left ventricular developed pressure (mmHg); and (B) left ventricular end diastolic pressure (mmHg). Data are shown for untreated hearts ($n=30$) and UTP ($n=15$), suramin+UTP ($n=8$), 5-HD ($n=11$), 5-HD+UTP ($n=9$), wortmannin ($n=9$), wortmannin+UTP ($n=9$), GW5074 ($n=13$), and GW5074+UTP ($n=13$) treated hearts. Values are means \pm SEM. *, $P<0.05$ vs. Control; †, $P<0.05$ vs. UTP. 207

Figure 9.2. Effects of UTP and signalling inhibitors on post-ischaemic recoveries for: (A) left ventricular developed pressure (% pre-ischaemia); and (B) coronary flow (% pre-ischaemia). Data are shown for untreated hearts ($n=30$), and UTP ($n=15$), suramin+UTP ($n=8$), 5-HD ($n=11$), 5HD+UTP ($n=9$), wortmannin ($n=9$), wortmannin+UTP ($n=9$), GW5074 ($n=13$), and GW5074+UTP ($n=13$) treated hearts. Values are means \pm SEM. *, $P<0.05$ vs. Control; †, $P<0.05$ vs. UTP; ‡, $P<0.05$ vs. wortmannin. 208

Figure 9.3. Effects of UTP and signalling inhibitors on post-ischaemic efflux of lactate dehydrogenase (LDH) over 45 min reperfusion. Values are means \pm SEM. *, $P<0.05$ vs. Control; †, $P<0.05$ vs. UTP. 209

LIST OF TABLES

Table 1.1 - Cardiac and vascular effects of P2 purinoceptors	58
Table 1.2 - Transduction mechanisms of the various P2X purinoceptor subtypes [169].....	63
Table 1.3 - Transduction mechanisms of the eight known P2Y purinoceptor.....	65
Table 3.1 - Recipe for formulation of modified Krebs–Henseleit solution.....	89
Table 3.2 - Functional parameters after stabilisation and 80 min of normoxic perfusion.....	92
Table 3.3 - Functional parameters in post-ischaemic hearts after 30 And 45 min of aerobic reperfusion.....	93
Table 3.4 - Final post-ischaemic functional recoveries in pyruvate vs. glucose perfused mouse hearts.....	94
Table 3.5 - Final post-ischaemic functional recovery in control vs. Ado treated hearts.....	96
Table 4.1 - Purinoceptors and respective Taqman products employed.....	106
Table 4.2 - Overview of mRNA expression for P2 purinoceptor subtypes in mouse heart and aorta.....	113
Table 4.3 - Comparison of RT-PCR efficiency, Ct(E) values and mean reaction efficiency.....	114
Table 5.1 - Summary of experimental groups, antagonists used selectivity and concentrations used in targeting P2 purinoceptors in ischaemic-reperfused hearts.....	125
Table 5.2 - Pre-ischaemic contractile function and coronary flow in all experimental groups...	127
Table 6.1 - Pre-ischaemic contractile function and coronary flow.....	143
Table 6.2 - Final post-ischaemic functional recoveries in mouse hearts untreated (Control) or treated with UTP (250 nM or 1 μ M) at different times.....	147
Table 7.1 - Pre-ischaemic contractile function and coronary flow in all experimental groups...	164
Table 8.1 - Effects of <i>UTPγS</i> and <i>UDPβS</i> on normoxic cardiovascular function.....	184
Table 9.1 - Pre-ischaemic contractile function and coronary flow.....	205

LIST OF ABBREVIATIONS

<i>Name or term</i>	<i>Abbreviations</i>
AC	Adenylyl cyclase
ADO	Adenosine
ADP	Adenosine 5'-diphosphate
Akt	Also known as Protein Kinase B
AMP	Adenosine monophosphate
ANOVA	Analysis of variance
ANT	Adenine nucleotide translocase
Apaf-1	Apoptotic protease-activating factor
ATP	Adenosine 5'-triphosphate
ATPase	Adenosine Tri-phosphatease
BKA	Bongkreikic acid
CAT	Carboxyatractyloside
CD39	Nucleoside triphosphate diphosphohydrolase-1
CD73	Ecto-5'-nucleotidase
CK	Creatine kinase
CyPD	Cyclophilin D
2-Cl-ATP	2-Chloroadenosine
DAG	Diacylglycerol
DMSO	Dimethylsulfoxide
EDP	End diastolic pressure
EDTA	Ethylene diamine tetra-acetic acid
ERK	Extracellular signal-regulated kinase

+dP/dt	First derivative of positive pressure development over time
-dP/dt	First derivative of negative pressure development over time
GAPDH	Glyceraldehyde-3-phosphate dehydrogenase
GDP	Guanosine diphosphate
GLUT	Glucose transporter
GPCR	G-protein-coupled receptor
GPRK2	G-protein-coupled receptor kinase 2
Gs	Guanine nucleotide binding stimulatory protein
GSSG	Glutathione disulphide
GTP	Guanosine-5'-triphosphate
Gi/o	Guanine nucleotide binding inhibitory protein
GW5074	(3-(3,5-Dibromo-4-hydroxybenzyliden)-5-iodo-1,3-dihydroindol-2-one)
HK	Hexokinase
H ₂ O ₂	Hydrogen peroxide
5-HD	5'-hydroxydecanoate
ICa	L-type calcium channel current
I _{Ca(N)}	Current mediated by N-type voltage-dependent calcium channels
IHD	Ischaemic heart disease
I _{Kir}	Current mediated by inwardly-rectifying potassium channels
I _{K(M)}	M-type potassium current
IP ₃	Inositol triphosphate
JNK	c-Jun N-terminal kinase
KATP	ATP-sensitive potassium channel
LDH	Lactate dehydrogenase

LGIC	Ligand gated ion channel
LVDP	Left ventricular developed pressure
LVEDP	Left ventricular end diastolic pressure
MAPK	Mitogen activated protein kinase
2-MethioATP	2-Methylthio-adenosine 5'triphosphate
2MeSADP	2-methylthioadenosine 5'-diphosphate
mitoKATP	Mitochondrial potassium activated channels
MPT	Mitochondrial permeability transition
mPTP	Mitochondrial permeability transition pore
mRNA	Messenger ribonucleic acid
MRS2159	Pyridoxal-5-phosphate-6-phenylazo-4 -carboxylic acid
MRS2179	2'-Deoxy-N6-methyladenosine 3',5-diphosphate
NO	Nitric oxide
NOS	Nitric oxide synthase
PKD1	3- phosphoinositide-dependent protein kinase-1
PI3K	Phosphatidylinositol 3-kinase
PIP ₂	Phosphatidylinositol 4,5-biphosphate
PKA	Protein kinase A
PKB	Protein kinase B (also known as Akt)
PKC	Protein kinase C
PLA ₂	Phospholipase A2
PLC	Phospholipase C
PLD	Phospholipase D
PPADS	Pyridoxal phosphate-6-azo(benzene-2,4-disulfonic acid)
PPNDS	Pyridoxal-5'-phosphate-6-(2'-naphthylazo-6'-nitro-4',8'-disulfonate

PTX	Pertussis toxin
RAFTK	Related Adhesion Focal Tyrosine Kinase
Reactive Blue 2	(1-amino-4-[[4-[[4-chloro-6[[3 (or4)-sulfophenyl]amino]-1,3,5-triazin-2-yl]amino]-3-sulfophenyl]amino]-9,10-dihydro-9,10-dioxo-2-anthracenesulfonic acid
RISK	Reperfusion injury salvage kinase
RNS	Reactive nitrogen species
ROS	Reactive oxygen species
ROCK	Rho-dependent kinase
RT-PCR	Reverse transcriptase polymerase chain reaction
SAPK	Stress activated protein kinase
SEM	Standard error of the mean
SD	Standard deviation
SOD	Superoxide dismutase
Suramin	(8,8'-[Carbonylbis[imino-3,1-phenylenecarbonylimino(4-methyl-3, 1-phenylene)carbonylimino]]bis-1,3,5-naphthlene trisulfonic acid hexa sodium salt
TnI	Troponin I
TnT	Troponin T
UDP	Uridine 5'-diphosphate
UDP β S	Uridine-5'-O-(2-thiodiphosphate)
UTP γ (S	Uridine-5'-O-(3-thiotriphosphate)
UTP	Uridine 5'-triphosphate
VDAC	Voltage-dependent anion channel

CHAPTER 1

GENERAL INTRODUCTION

*...What of the wonder of my Heart,
That plays so faithfully its part?
I hear it running sound and sweet;
It does not seem to miss a beat;
Between the cradle and the grave
It never falters, stanch and brave.
Alas! I wish I had the art
To tell the wonder of my Heart...*

Excerpts from *'The Wonderer'* by Robert Service

The Australian health authorities have invested a significant amount of funding and effort in preventing cardiovascular disease and reducing associated death in Australia. Cardiovascular disease was the underlying cause for 46,106 deaths (~33% of all deaths) in Australia during 2009 and contributed to a total of 80,375 deaths as either an underlying or associated cause of death. While ischaemic heart diseases (IHD) have been the leading cause of death in Australia since 2000 and despite a steady decline in the number of deaths due to IHD in Australia from almost 24% in 1995 [4], it remained the underlying cause of 16% of all death in 2009 [5]. At \$5.9 billion - about 11% of the Australian health system expenditure in 2004-05, cardiovascular disease is the most expensive disease burden for this country [6]. On a global scale, the incidence and prevalence of cardiovascular disease is expected to increase and become a leading public health problem in coming decades, due in part to ageing of populations and in westernising of less developed countries. Economic affluence brings about sedentary lifestyles and ready access to calorie dense foods, with a

higher incidence of chronic diseases such as obesity and Type II diabetes, conditions compounding the incidence and management of cardiovascular disease.

1.1 MYOCARDIAL METABOLISM

The heart relies on a continuous supply of energy to function normally, as a tireless pump responsible for transporting vital signalling molecules such as hormones and neurotransmitters, delivering essential nutrients and O₂, and removing waste throughout the body. Energy in the form of adenosine triphosphate (ATP) is a product of aerobic metabolism, critical for homeostasis and contraction and relaxation of the myocardium. It is the metabolism of carbohydrates into glucose and lactate, and fatty acids into oxidised lipids, driving oxidative ATP generation that sustains the viability and continuous contractile activity of the heart. Under aerobic conditions in a healthy human heart, the oxidation of free fatty acids accounts for up to 90% of ATP produced via mitochondrial respiration, whilst only 10 – 40% of ATP is derived from pyruvate, a product of carbohydrate metabolism [7, 8].

1.1.1 Fatty acid β -oxidation

The heart readily extracts free fatty acids from the plasma, oxidising up to 80% of fatty acids to CO₂ in studies of human mitochondria [7]. Free fatty acids in the heart are bound to albumin and fatty esters in chylomicrons and low-density lipoproteins. Within the cytoplasm, fatty acids bind to binding proteins and are activated by acyl-CoA synthetase to long chain acylcoenzyme A (acyl-CoA). A complex of enzymes including carnitine palmitoyltransferase 1 (CPT-I), carnitine-acylcarnitine translocase and carnitine palmitoyltransferase 2 (CPT-II) aid the transfer of the acyl-CoA into the mitochondria to enter the β -oxidation enzyme system, producing acetylcoenzyme A

(acetyl-CoA). This results in the formation of one reduced nicotinamide-adenine dinucleotide (NADH) and one reduced flavin adenine dinucleotide with hydrogen (FADH₂). Acetyl-CoA gained from β -oxidation then enters the Krebs cycle releasing two CO₂, three NADH and one FADH₂ [9]. An overview of the energy metabolism is shown in Figure 1.1.

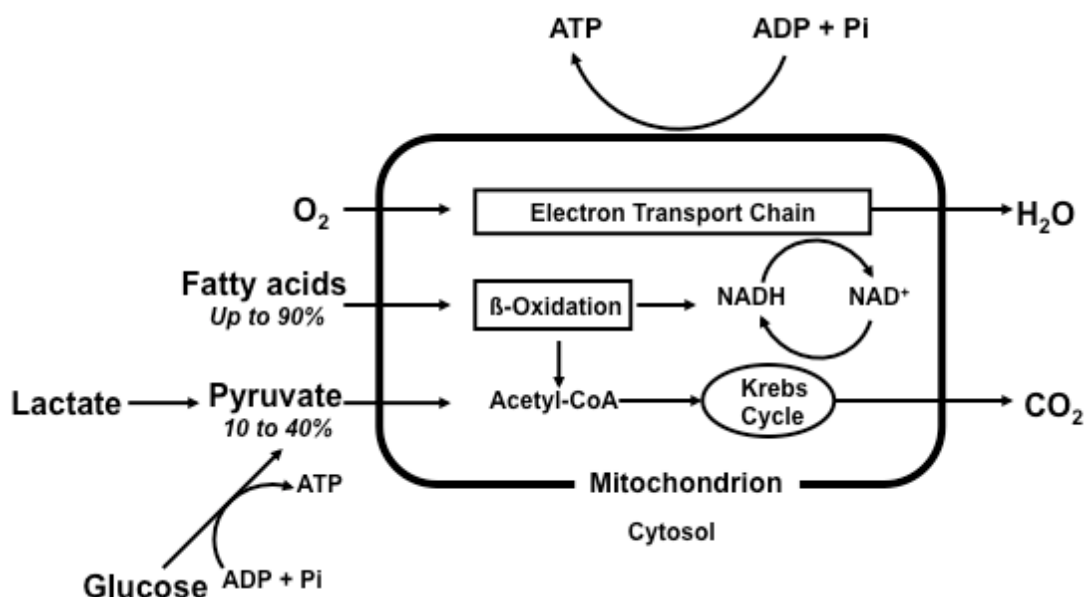


Figure 1.1. Basic scheme of myocardial metabolism. Fatty acid and glucose oxidative pathways [7].

1.1.2 Glucose and lactate oxidation

The transmembrane glucose gradient and plasma membrane transporters such as glucose transporter (GLUT) 1 and GLUT 4 regulate glucose entry into the myocyte. Within the cell, glucose is phosphorylated by hexokinase to form glucose 6-phosphate, destined for either glycolysis or glycogenesis. Glycolysis derived pyruvate that is transported into the mitochondria is converted into acetyl-CoA, then entering the Krebs cycle to liberate two CO₂, three NADH and one FADH₂ [9]. The presence

of insulin leads to translocation of GLUT-1 and GLUT-4 to the plasma membrane, increasing the capacity of cells to take up glucose. Russell *et al.* have shown a similar translocation of these membrane transporters in myocardial ischaemia, and the effects of insulin and ischaemia are thought to be additive [10]. Pyruvate is also converted by cytoplasmic lactate dehydrogenase (LDH) to lactate. Extracellular lactate can be converted to pyruvate, and transported into the mitochondria for oxidation [9].

1.1.3 Oxidative phosphorylation

A constant resynthesis of ATP through mitochondrial oxidative phosphorylation is essential for normal cardiac function. The reducing equivalents NADH and FADH₂ from glycolysis, the Krebs cycle, pyruvate dehydrogenase, and β -oxidation are utilised within the mitochondrial electron transport chain. In the presence of O₂, the transfer of H₂ from these products to water is coupled to the conversion of adenosine diphosphate (ADP) to ATP [9]. The rate of ATP breakdown and oxidative phosphorylation, and the rate of carbon electron transfer to the electron transport chain via NADH and FADH₂, are determined by the work rate of the myocardium. In a healthy heart, the rate of ATP hydrolysis corresponds with the rate of ATP resynthesis and the content of ATP is maintained constant within cardiac tissue. The mechanistic basis of this ‘coupling’ remains incompletely defined, but may involve effects of Ca²⁺, levels of reducing equivalents, and kinetic control by ADP and P_i. Pathological defects in energy delivery, as in ischaemia or hypoxia, lead to cellular dysfunction and ultimately death.

Ischaemia differs from hypoxia (where there is a diminished level of oxygen within blood and tissues), and describes a deficiency in blood supply to a part of the body. Within this thesis the focus is on the myocardial effects of ischaemia and subsequent reperfusion.

1.2 MYOCARDIAL ISCHAEMIA

Myocardial ischaemia occurs as a result of the partial or total occlusion of coronary vessels that gradually narrow due to damaging effects of conditions such as atherosclerosis or thrombosis. Ischaemia in the myocardium is characterised by a significant loss in contractile and systolic function, arrhythmogenesis, and ultimately true infarction or cell death.

Some resultant metabolic changes include loss of ATP, and ability to replenish ATP stores, loss of creatine phosphate, extracellular movement of K^+ ions, accumulation of lactate, myocyte swelling, acidosis, loss of ion homeostasis, contracture and mitochondrial abnormalities [3, 8]. The disruption in the supply and breakdown of ATP leads to an increase in ADP and AMP, and a subsequent conversion of AMP to adenosine (Ado), which is further broken down to hypoxanthine and xanthine, leading to the activation of xanthine oxidase causing superoxide-induced tissue injury [3].

Several injurious outcomes are associated to myocardial ischaemia; these are further classed into reversible and irreversible injuries [11]. Myocardial stunning refers to a reversible, transient dysfunction of myocardial tissue that persists after reperfusion, in the absence of irreversible damage and major alterations in coronary flow. Clinical observations suggest that stunning of the myocardium occurs in open heart surgery,

rest and exercise-induced angina, myocardial infarction with early reperfusion, and might heighten morbidity among patients with coronary artery disease [1]. Irreversible injury is characterised by lack of recovery in contractile function due to cell death, leading to fibrosis and remodelling.

1.2.1 Reperfusion injury

Reperfusion is essential to cell survival. Infarct size is reduced when coronary reperfusion occurs soon after an acute myocardial infarction, however there is evidence that reperfusion of ischaemic myocardium also paradoxically results in injury. This may arise from production of oxygen-derived free radicals during reperfusion, together with effects on ion handling and osmotic gradients. Reperfusion injury can lead to the development of cellular necrosis within minutes to the first few hours of reperfusion [12]. Myocardial damage sustained in the early minutes of reperfusion can be in the form of contracture development caused by cellular Ca^{2+} overload and rigor from a low level of re-energisation during reperfusion. Severe contracture contributes to tissue necrosis [13].

1.3 METABOLIC ALTERATIONS IN ISCHAEMIA-REPERFUSION

Alterations in metabolism depend highly on the duration and the level of severity in ischaemia. The complete lack of flow to the myocardium, leads to a rapid depletion of ATP, creatine phosphate, glycogen and the accumulation of lactate, ionic disturbances and Ca^{2+} overload, the loss of normal contractility, and eventual tissue necrosis/apoptosis and infarction. These changes contribute to and are associated with enhanced oxidative stress.

1.3.1 Oxidative stress

The role of oxidative stress in ischaemic heart disease has been investigated extensively, with reactive oxygen species (ROS) generation and resultant oxidative damage observed in post-ischaemic reperfusion. Oxidative stress can be detected through the accumulation of peroxides such as lipid peroxides, or by-products such as malondialdehyde (MDA) and GSSG. During ischaemia, ATP is catabolised to yield hypoxanthine, triggering the conversion of NAD-reducing xanthine dehydrogenase to xanthine oxidase [2]. During reperfusion, the introduction of O_2 that reacts with hypoxanthine and xanthine oxidase generates a surge in superoxide dismutase (SOD) and hydrogen peroxide (H_2O_2). Mechanisms associated with the production of ROS also include the accumulation of reducing agents during deprivation of O_2 , the increased univalent reduction in O_2 due to derangements within the mitochondrial electron transport system, the activation of the arachidonate cascade and the auto-oxidation of catecholamines and other associated compounds.

Electron paramagnetic resonance spectroscopy has been used to demonstrate a burst of free radical production in reperfusion following a reversible episode of ischaemia

[1]. In the presence of catalytic Fe, SOD and H_2O_2 react via the Haber-Weiss reaction to form superoxide and hydroxyl radicals [2]. Whilst the transient ischaemia delivers damage insufficient to cause cell death, dysfunction to key organelles is sustained. Postulated sites of free radical or ROS damage include the sarcoplasmic reticulum (SR) – causing impairment of Ca^{2+} homeostasis and excitation-contraction coupling, the sarcolemma – with loss of selective permeability, the mitochondria – with impairment of oxidative phosphorylation, and other targets such as myofibrillar creatine kinase (impairing energy use), and the extracellular collagen matrix (contributing to loss of mechanical coupling) [1]. Consequently, there is dysfunction in contractile activity and high energy phosphate metabolism. An overview of oxidative stress in ischaemia-reperfused in cardiomyocytes is provided in Figure 1.2.

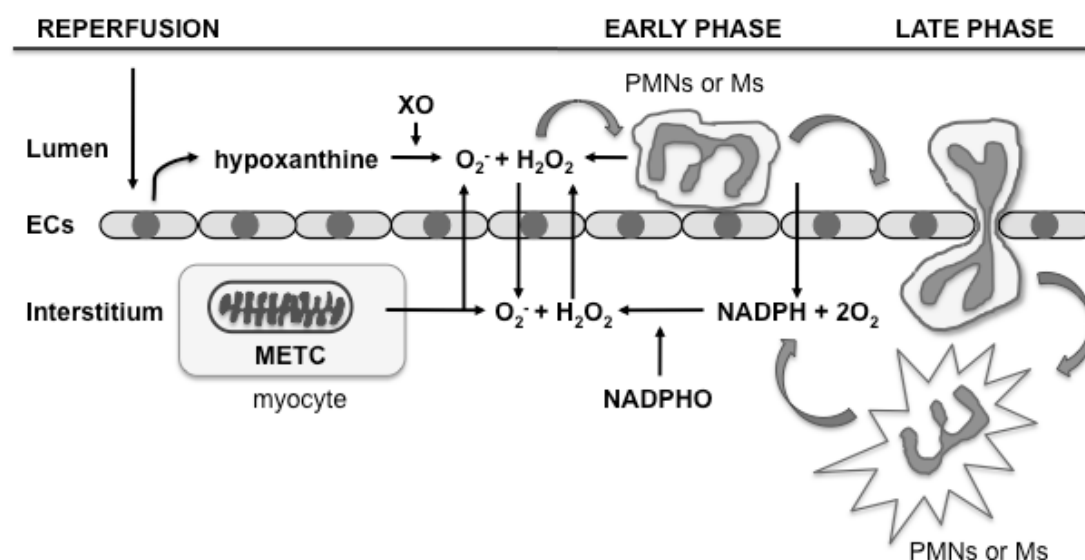


Figure 1.2. Overview of oxidative stress in ischaemia-reperfused cardiomyocytes [1-3]. ROS may be initially generated at onset of reperfusion, from oxidation of hypoxanthine by xanthine oxidase (XO) in endothelial cells (ECs), and from the mitochondrial electron transport chain (METC) in myocytes. This promotes interactions among neutrophils (PMNs), macrophages (Ms) and ECs. Further ROS generation can arise from activated PMNs and Ms in the vascular space. Effects of migrated PMNs or Ms can generate ROS via the NADPH reaction catalyzed by NADPH oxidase (NADPHO) later in reperfusion.

The generation of cytotoxic radicals have been proposed to mediate myocardial stunning in ischaemia-reperfusion. It has been determined from infarcted human heart that there is also an increased release of oxidative products of nitric oxide (NO) including NO_2^- and NO_3^- during the inflammatory phase of myocardial ischaemia [14]. Enhanced nitric oxide production during ischaemia was found to be critical to the coordination of ATP supply and demand, and Kawahara *et al.* found that NO has a role in cytoprotection from ischaemia-reperfusion injury in rat cardiac myocytes [15]. Interestingly, a study in isolated rabbit hearts by Ambrosio *et al.* demonstrated that ischaemia and reperfusion have no significant effects on cardiac tolerance towards oxidants [16]. The full effects of varied ROS and reactive nitrogen species (RNS) following ischaemic-reperfusion are yet to be completely understood.

1.3.2 The Ca^{2+} hypothesis of injury

Disturbance of cellular Ca^{2+} homeostasis can result in both myocardial stunning (reversible cellular injury) and contribute to irreversible cell death during ischaemia-reperfusion. Muscle contraction involves the hydrolysis of ATP during repeated cycles of actin and myosin interactions during cross bridge cycling. The free intracellular Ca^{2+} concentration is critical to muscle function, with elevations in $[\text{Ca}^{2+}]_i$ perpetuating cross bridge cycling vs. relaxation of the muscle with reductions in $[\text{Ca}^{2+}]_i$ (given sufficient energy). Three Ca^{2+} -dependent mechanisms are forwarded as explanations for myocardial dysfunction with ischaemia-reperfusion: i) excitation and contraction uncoupling due to SR dysfunction; ii) desensitisation of contractile proteins to Ca^{2+} ; and iii) Ca^{2+} overload.

1.3.3 Excitation-contraction uncoupling and SR dysfunction

Two mechanisms of contractile dysfunction have been forwarded based on electrical activity remaining normal [17] in stunned myocardium. One involves reduced availability of activator Ca^{2+} due to irregular entry or exit from the cytosol as a result of lesions in Ca^{2+} handling pathways. The other involves a decrease in Ca^{2+} -dependent myocardial force production due to reduced Ca^{2+} sensitivity of the contractile machinery [18-20]. Changes in intracellular free Ca^{2+} or responsiveness of contractile machinery can lead to excitation-contraction uncoupling and a resultant fall in contractility [18, 20]. Sarcoplasmic reticular dysfunction following ischaemia injury can also affect Ca^{2+} availability from a lower Ca^{2+} uptake. It was demonstrated by Krause *et al.* that ischaemic-reperfusion injury in a stunned myocardium can lead to a reduction in the SR's ability to transport Ca^{2+} affecting contractile protein activation, attenuating Ca^{2+} release during systole [21]. Similarly, ischaemic-reperfusion studies in isolated rat hearts [22], have also reported diminished uptake of Ca^{2+} in sarcoplasmic reticular, lowering transient Ca^{2+} and inhibiting contractility.

1.3.4 Desensitisation of contractile proteins to Ca^{2+}

The mechanisms and role of contractile protein desensitisation to Ca^{2+} remain incompletely defined. Results of some *in vitro* studies suggest that myocardial stunning may be caused by reduced Ca^{2+} sensitivity rather than lack of Ca^{2+} availability [23-25]. Gao *et al.* found that trabeculae from stunned myocardium exhibited comparable $[\text{Ca}^{2+}]_i$ to normoxic tissue, suggesting blunted responsiveness to Ca^{2+} by myofilaments [24]. Carrozza *et al.* report that cardiac $[\text{Ca}^{2+}]_i$ returns to baseline levels during reperfusion, also implicating a reduction in cardiac Ca^{2+} responsiveness in stunning [23]. Other studies suggest structural changes to

myofibrillar proteins, implicating damage such as thiol group oxidation by ROS, and resulting in impaired protein Ca^{2+} responsiveness [26, 27]. Ferrari *et al.* documented decreased Ca^{2+} sensitivity in cardiac muscles when glutathione is oxidised, while reduced glutathione produces an opposing response [26]. Thus, desensitisation of stunned myofilaments may arise from shifts in the 'oxidative balance', for example with alterations in cytosolic glutathione [26, 28].

1.3.5 Ca^{2+} overload

In the early minutes of reperfusion, the myocardium is further damaged by development of severe contracture, contributing to stiffening of the myocardium and tissue oncosis. Myocardial contracture usually occurs by means of a rigor-bond mechanism, and with cytoskeletal defects render cardiomyocytes susceptible to mechanical damage sustained in reperfusion (if the preceding ischaemia is sufficiently protracted). Functionally, this translates to a profound increase in end diastolic ventricular pressure and a major fall in ventricular compliance [13].

Cardiomyocyte Ca^{2+} -induced contracture is activated with ischaemia-dependent Ca^{2+} overload and subsequent rapid re-energisation of the tissue. Ischaemia leads to severe acidosis and accumulation of intracellular Na^+ via Na^+/H^+ exchange and de-energisation (impairing Na^+-K^+ ATPase activity). Cellular Na^+ overload can drive excess Ca^{2+} loading via $\text{Na}^+-\text{Ca}^{2+}$ exchange, though this may be limited during ischaemia itself due to de-energisation [18, 29]. Reperfusion leads to re-energisation, reversal of acidosis, activation of $\text{Na}^+-\text{Ca}^{2+}$ exchange and cellular Ca^{2+} overload [3, 18]. At the same time rapid recovery of oxidative phosphorylation and reactivation of the contractile machinery results in uncontrolled Ca^{2+} -dependent contraction [29].

Post-ischaemic Ca^{2+} overload produces a number of injurious effects, including activation of proteases, excess mitochondrial activation, and opening of the inner membrane mitochondrial permeability transition pore (mPTP) with resultant loss of ATP generation [30]. Additionally, propagation of contracture may arise from movement of Na^+ through gap junctions from hypercontracting cells to neighbouring cells, facilitating further Na^+ - Ca^{2+} exchange and exacerbating cytosolic Ca^{2+} overload [31]. Figure 1.3 illustrates in a basic fashion energy-dependent exchange of these ions.

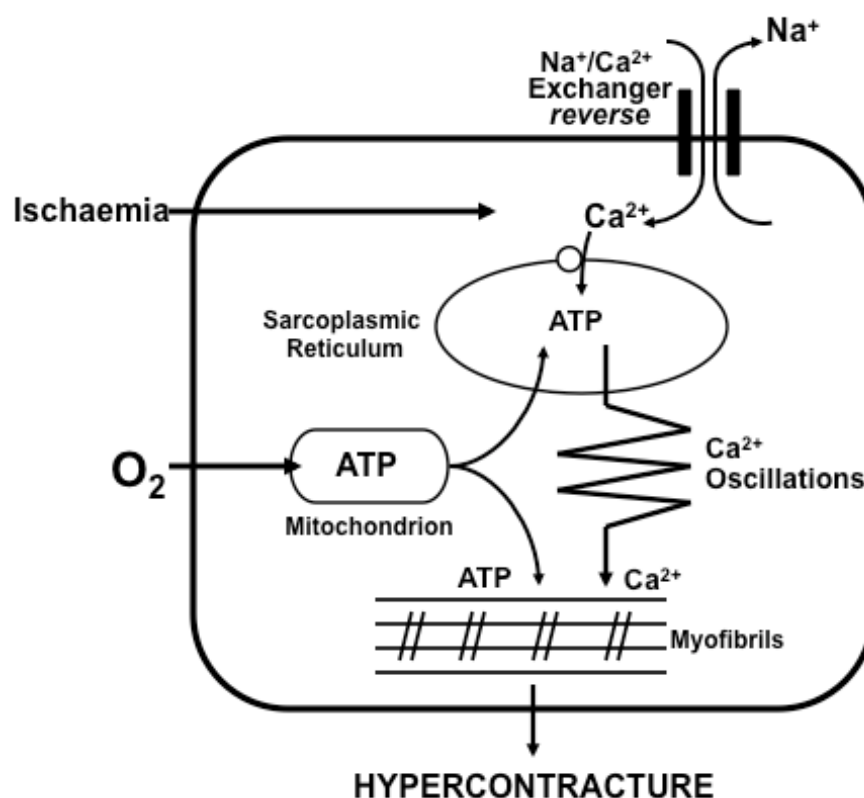


Figure 1.3. Ca^{2+} overload in cardiomyocytes following ischaemia [29]. Ischaemia causes intracellular Ca^{2+} overload. During the early phase of reoxygenation, the Ca^{2+} overload may be exaggerated by a reverse-mode action of the Na^+ / Ca^{2+} exchanger. Reoxygenation leads to the re-energizing of the sarcoplasmic reticulum where Ca^{2+} begins to accumulate. Once full, Ca^{2+} movement into the cytosol causes further elevation of Ca^{2+} concentration and the resultant Ca^{2+} oscillations provoke hypercontracture of the myofibrils, fuelled by the ATP resupply from the mitochondrion.

Severe impairment of coronary blood flow results in myocardial ischaemic injury that can ultimately lead to cell death. Both myocyte oncosis (or necrosis) and apoptosis, the two fundamental forms of cell death, are associated with ischaemia and reperfusion.

1.4 MYOCARDIAL CELL DEATH

Cell death that takes place during acute ischaemia was commonly thought to be "accidental" cell death - necrosis or oncosis. However, in 1995, Majno and Joris specified that necrosis is not a type of cell death but the end stage of cell death itself [32]. Necrosis refers to the morphological changes that take place following cell death: a post-mortem condition rather than the death processes of oncosis and apoptosis [33]. Compared to programmed apoptosis, oncosis progresses rapidly with cell swelling, membrane failure and release of cellular debris, and subsequent activation of the inflammation cascade [34]. Ischaemia, toxic agents disrupting ATP generation, and failure of ion pumps all contribute to the loss of membrane integrity in oncosis [32, 35]. Unlike apoptosis, oncosis is not energy dependent nor involves a programmed process of self-destruction. Although condensation of the chromatin within the nucleus (pyknosis) and disintegration of the nucleus (karyolysis) are both common events in apoptosis and oncosis, karyolysis - the disappearance of the nucleus - appears oncosis-specific, and apoptotic cells eventually undergo lysis when phagocytosed [33].

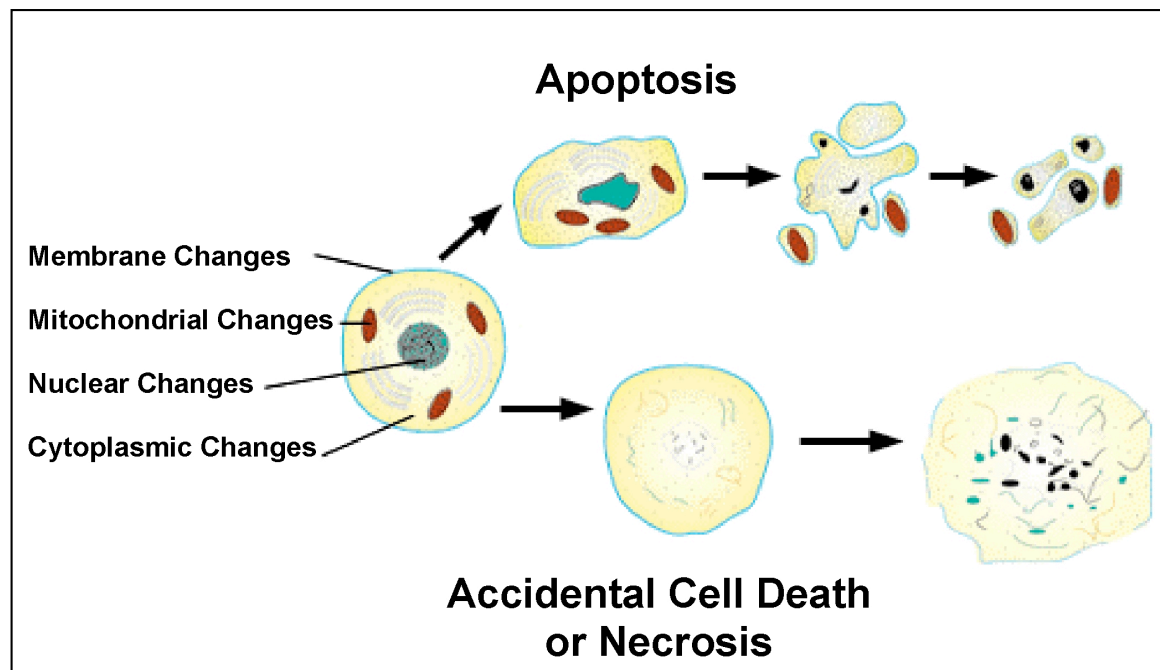


Figure 1.4. Diagrammatic representation of oncosis vs. apoptosis. Apoptosis is characterised by cell shrinkage, plasma membrane blebbing, chromatin condensation, and genomic DNA fragmentation. Oncosis involves cell swelling, random genetic damage and ultimately cell membrane rupture.

1.4.1 Apoptosis or programmed cell death

Apoptosis is characterised by cell death with cell shrinkage, chromatin condensation and fragmentation, without the loss of membrane integrity or an inflammatory response [36]. Apoptosis occurs predominantly during reperfusion of previously ischaemic myocardium since it requires energy for execution [36-40]. The ATP level within an injured cell may dictate whether there is adequate energy to die via apoptosis or with more severe lack of energy via oncosis [41, 42]. This, in turn, may involve varying degrees of mitochondrial permeability transition (discussed later).

Induction of apoptosis in ischaemic-reperfused hearts may arise via a variety of paths (which are often interrelated). Pathways involved during reperfusion may include: i) activation by FAS (apoll)/TNFR-1 (tumour necrosis factor receptor-1) death receptors [43]; ii) activation of p53 and c-Jun kinase pathways; iii) down-regulation of anti-apoptotic Bcl-2 protein and up-regulation of pro-apoptotic Bax protein [36]; and iv) infiltration/activation of neutrophils and/or macrophages, with subsequent cell death activation [44-46]. Mitochondria play a key role in multiple paths of apoptosis, in the provision of ATP necessary for execution of apoptotic programs, release of cytochrome *c* and apoptosis-inducing factor proteins involved in caspase activation and nuclear fragmentation, and the release of proteins (second mitochondria-derived activator of caspases SMAC/DIABLO) that neutralize endogenous inhibitors of apoptosis [44].

Caspase activation is central to apoptosis, and caspase inhibition has been demonstrated to limit reperfusion injury [47]. Three primary pathways of caspase activation via the abovementioned paths have been described: i) the binding of extracellular FAS/TNF α to surface receptor leading to the activation of caspase-8 and to proteolytic activation of caspase-3; ii) mitochondria release of cytochrome *c* binding to cytosolic protein Apaf-1 and complex in the presence of dATP of ATP to form the apoptosome that facilitates activation of caspase-9, which in turn activates downstream caspase-3; iii) by endoplasmic reticulum (ER) stress due to depletion of Ca²⁺ or accumulation of unfolded proteins, leading to the activation of caspase-9. Mitochondria are involved in both the death receptor and the so-called mitochondrial paths of caspase activation.

Mitochondrial cytochrome *c* release involves two mechanisms: formation of a large channel in the outer mitochondrial membrane as a result of oligomerisation of Bcl-2 proteins such as Bax or Bak; and the opening of the mPTP. Mitochondrial permeability transition (MPT) describes a significant increase in the permeability of the inner mitochondrial membrane to small molecules of up to 1.5kDa, and can be induced by high concentration of Ca^{2+} or oxidative stress, which accompany conditions such as ischaemia and reperfusion. Other proposed triggers of the MPT during ischaemia and reperfusion include phosphates, free fatty acids, decreased adenine nucleotides, and mitochondrial potential membrane changes. The mitochondrial apoptosis path is initiated by such changes to mitochondrial structure and function, leading to apoptosome formation and caspase-3 activation. The death receptor path, initiated by receptor ligation also results in truncation of Bid and promotion of mitochondrial permeability. Figure 1.5 illustrates the major pathways of apoptosis and the relationships between apoptotic and non-apoptotic cell death.

1.4.2 Bcl-2 proteins and cardiac BNIP3-mediated apoptosis

Bcl-2 family members are important regulators of cell death in myocardial and other cells. This family is divided into anti-apoptotic members (Bcl-2 and Bcl-x_L) and pro-apoptotic members (Bax, Bak and Bcl-2 homology domain 3 (BH3)-only proteins - Bad, Noxa, and Puma). BH3-only proteins function as sensors of cellular stress and relay signals downstream to the effectors, Bax and/or Bak. As many as 10 different BH3-only proteins have been identified, each differing in mode of activation. Their pro-apoptotic activity is regulated by transcription and/or post-translational modification [48]. It should be noted, however, that in the context of acute ischaemia-

reperfusion, transcriptional control is not relevant owing to temporal delays in translating such control to actual shifts in protein expression.

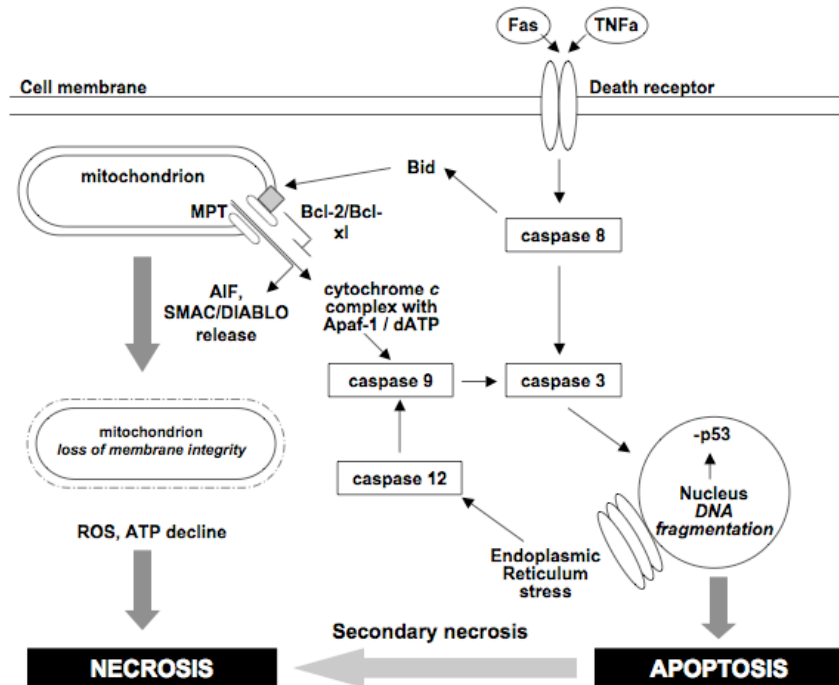


Figure 1.5. Molecular pathways of apoptotic and non-apoptotic cell death [40, 44, 49, 50].

The Bcl-2/adenovirus E1B 19-kDa protein-interacting protein 3 (*Bnip3*) is a BH3-only protein that is localized primarily to the mitochondria [51-53]. Overexpression of *Bnip3* leads to the activation of Bax/Bak, opening of the mPTP, and cell death [54-57]. *Bnip3* is transcriptionally up-regulated via hypoxia inducible factor-1(HIFα) in the heart and other tissues [53, 55, 57]. *Bnip3* has been identified as a significant mediator of post-ischaemic myocardial apoptosis. The targeted ablation of *Bnip3* in ischaemic cardiomyocytes preserves LV systolic performance, diminishes LV dilation, and decreases ventricular sphericalization, suggesting myocardial salvage by inhibition of apoptosis [58].

In 2008, Kubli *et al.* demonstrated that *Bnip3* acts as a mitochondrial sensor of oxidative stress, with an increase in ROS during ischaemia-reperfusion inducing homo-dimerisation and activation of *Bnip3*, leading to subsequent opening of the mitochondrial permeability transition pore, and cell death [59]. Several recent studies have further substantiated that *Bnip3*-induced cell death may involve autophagy [53, 60, 61]. Autophagy is essential for cellular homeostasis and can be a selective process where specific protein aggregates or organelles, (such as mitochondria) are targeted for removal by autophagosomes. The removal of damaged mitochondria is an important process for cellular survival, and defects in this process result in the accumulation of dysfunctional mitochondria, cell aging and death. Thomas *et al.* recently demonstrated that *Bnip3* mediated impairment of mitochondrial oxidative phosphorylation promotes mitochondrial turnover via autophagy in the absence of permeabilisation of the mitochondrial membrane and apoptosis [62]. Some studies have established a link between endonuclease-G (EndoG) and *Bnip3* induced mitochondrial damage and caspase-independent DNA fragmentation in ischaemic cardiomyocytes [63]. EndoG is a mitochondrial protein with DNase/RNase activity which is involved in apoptotic DNA degradation [64, 65] in cardiomyocytes [66] independently of caspase activation. Thus, caspase independent processes may mediate cardiac apoptosis.

1.4.3 mPTP

As highlighted in prior discussion, mitochondria play a critical role in regulating both cell survival and death signalling pathways. Whilst mitochondria provide over 90% of ATP through oxidative phosphorylation for the survival of the cell, they are regulators

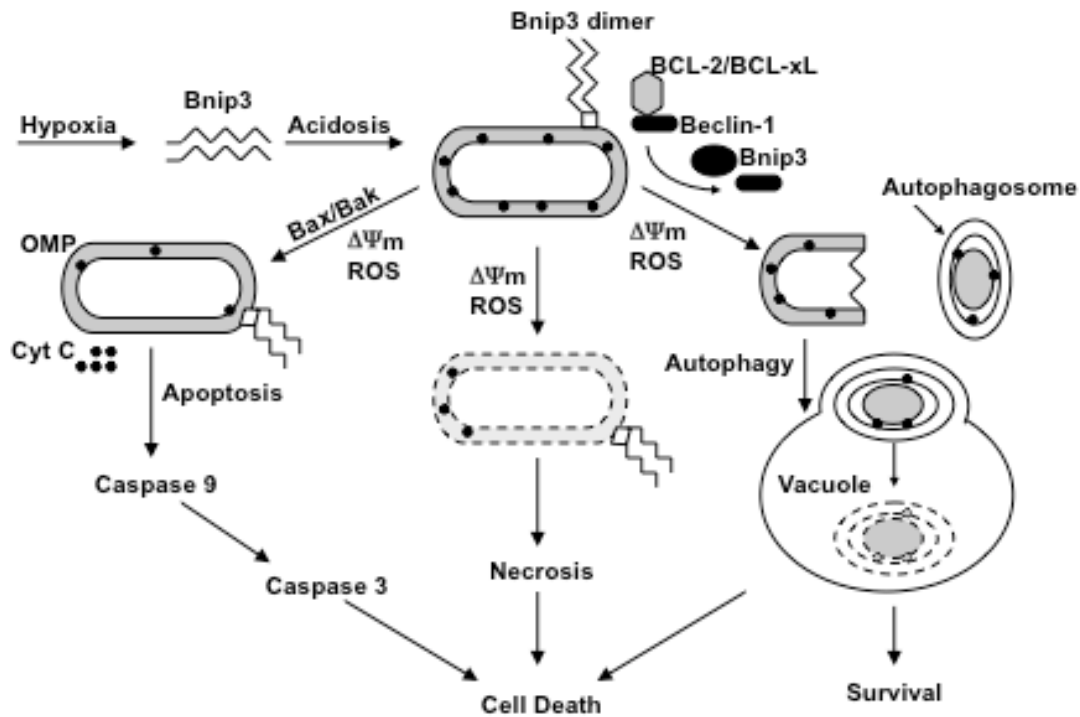


Figure 1.6. Model for BNIP3-mediated mitochondrial damage and cell death in myocytes. Ischaemia or hypoxia-induced activation of BNIP3 expression and the resulting acidotic condition are shown to mediate stable homo-dimerisation and mitochondrial membrane insertion of BNIP3 resulting in loss of $\Delta\Psi_m$ and generation of ROS. As a consequence of the mitochondrial damage, cells are shown to undergo three different fates, BAX/BAK dependent apoptosis, autophagy (by the release of Beclin-1 from the BCL-2/BCL-xL complex) and possibly necrosis [67].

of cell death through apoptosis, oncosis and autophagy [68]. The mPTP appears to play a key regulatory role in these processes.

Severe oxidative stress with Ca^{2+} overload in the mitochondrial matrix leads to increased permeability of the mitochondrial membranes, with formation of pathological and non-specific mPTPs [69-71]. The high conductance via opening of the mPTP depolarises of the mitochondrial inner membrane causing ATP depletion and ROS production. Increased permeability of the inner membrane enhances colloidal osmotic pressure, resulting in matrix swelling and rupture of the

mitochondrial outer membrane. This is followed by the release of pro-apoptotic proteins from the mitochondrial inter-membrane space to the cytoplasm which initiate both caspase-dependent and caspase-independent apoptosis. The translocation of pro-apoptotic Bcl-2 family proteins to the mitochondria induced by the formation of non-selective channels may also lead to the permeabilisation of the outer membrane. Over the last two decades, numerous studies have demonstrated that acute ischaemia-reperfusion injury is associated with opening of mPTP [69-71]. Additionally, pharmacological and conditional inhibition of mPTP formation significantly improves cardiac function, reducing ischaemic injury and myocardial infarct size in animal models [72-74] and patients [75, 76]. Given its key role in lethal functions, the mPTP has become a primary target for both cell survival and death interventions.

1.4.4 mPTP structure and mechanisms of activation and inhibition

Despite many studies of mPTP, its actual molecular composition and regulation remain unclear. Whilst adenine nucleotide translocase (ANT) in the inner membrane, mitochondrial cyclophilin D (CyPD) in the matrix and the voltage-dependent anion channel (VDAC) in the outer membrane were three proteins considered as key structural components of the mPTP, a number of genetic studies exclude VDAC and ANT as essential components of the mPTP complex [77, 78]. Recently, a different model of the mPTP, consisting of a phosphate carrier (PiC) and ANT, has been forwarded [79-81]. Strong evidence has been provided by several studies that CyP-D has a significant and essential regulatory role [79-81]. CyP-D binding to a phosphate carrier may regulate Ca^{2+} sensitivity of the mPTP [69, 82]. Studies of isolated mitochondria from CyP-D knockout mice revealed desensitisation of MPT with a

requirement for higher concentrations of Ca^{2+} to induce pore opening compared to wild types [79-81].

A high phosphate level within the matrix favours mPTP opening, as phosphates compete for the nucleotide binding site of ANT. The ANT conformational state is affected by specific ligands of the exchanger, such as carboxyatractyloside (CAT) which decrease ADP binding affinity, and bongkreikic acid (BKA) that increase matrix ADP binding affinity, leading to opening and closing of the mPTP. The opening of the mPTP is inhibited by H^+ , and divalent cations such as Mg^{2+} , Mn^{2+} , Sr^{2+} that antagonize Ca^{2+} binding to the ANT [83]. The conformational state and pore forming activity of mPTP components are also regulated by hexokinase (HK), the peripheral benzodiazepine receptor (PBR), and Bcl2 proteins on the mitochondria outer membrane (where they bind to VDAC), and creatine kinase (CK) in the inter-membrane space interacting with ANT. Whilst the role of ANT and VDAC as essential components of the mPTP is under investigation, most studies of the formation and regulation of the mPTP complex suggest that VDAC, ANT and CyPD are key players in pore formation [68].

1.4.5 mPTP and cardiac ischaemia-reperfusion

The opening of mPTP has been investigated specifically in ischaemic and reperfused myocytes [69-71]. Whilst expression of mPTP compounds is not affected in acute ischaemia-reperfusion, due to its short duration, conformational changes arise in essential mPTP proteins, modifying their interactions with pore effectors in the cytoplasm and mitochondrial matrix. Griffiths *et al.* demonstrated that mPTP opening takes place during reperfusion rather than ischaemia [84]. Griffiths *et al.* found that

H⁺ in ischaemia inhibit mPTP, with restoration of pH in reperfusion promoting opening at that time.

H⁺, which competes with Ca²⁺ at the trigger site of ANT, is a strong inhibitor of mPTP opening. Post-ischaemic recovery is highly dependent on the ATP supply by previously ischaemic mitochondria. A severe reduction in ATP levels after significant and prolonged ischaemia induces Ca²⁺-overload due to activation of reverse mode Na⁺/Ca²⁺ exchanger (NCE), and reduction of sarcoplasmic reticular Ca²⁺-ATPase activity. The increased concentration of Ca²⁺ along with a burst of ROS generation provokes mPTP opening. Kerr *et al.* reported that pore formation increases rapidly immediately following the return of pH to normal in the first minutes of reperfusion [85]. A delay in pH recovery has been showed to benefit post-ischaemia recovery with improved mitochondrial function and reduced mPTP opening [86, 87]. The mPTP has become a likely target of exogenous and endogenous protective responses, with mPTP formation directly or indirectly inhibited by targeting the main pore components, and mPTP function modulated through control of mPTP inducers such as ROS and Ca²⁺ (Figure 1.7).

1.5 ENDOGENOUS PROTECTIVE MECHANISMS

Cells possess mechanisms that provide resistance to differing stressors, allowing some resilience and resistance to environmental perturbations. Several intrinsic protective mechanisms exist to limit the severity and extent of ischaemic injury in myocardial cells. Known mechanisms include hormesis responses typified by preconditioning, antioxidant defences, ATP-sensitive potassium (K_{ATP}) channel activity and endogenous protectants such as Ado. These mechanisms are known to interact to

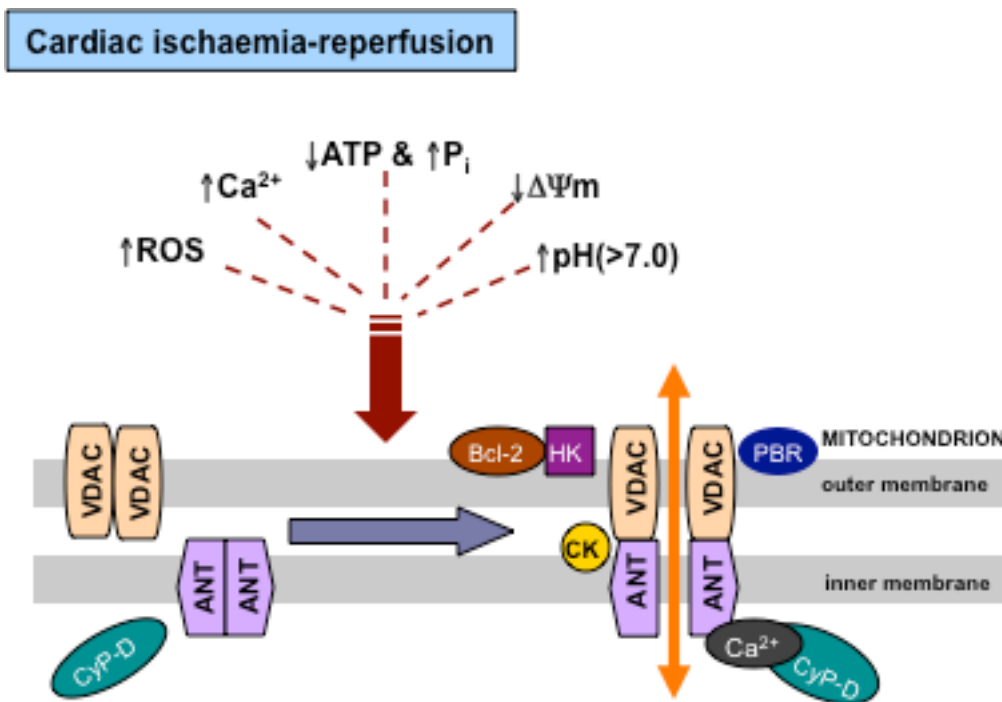


Figure 1.7. Metabolic inducers and inhibitors of mPTP opening in cardiac ischaemia-reperfusion [68]. ANT, adenine nucleotide translocase; CK, creatine kinase; CyPD, cyclophilin D; HK, hexokinase; P_i , inorganic phosphate; PBR, peripheral benzodiazepine receptor; VDAC, voltage dependent anion channel.

provide cardioprotection from ischaemia-reperfusion injury: Ado for example can be involved in ischaemic-preconditioning, activate antioxidant defence or K_{ATP} channels, and inhibit mPTP opening to improve post-ischaemic recovery. A variety of endogenous protection (or pro-survival) agents may contribute to cardiac stress resistance.

1.5.1 Ischaemic preconditioning

Ischaemic preconditioning refers to the ability of short periods of ischaemia and reperfusion to protect the heart from injury during subsequent prolonged ischaemia

[88-90]. First described in 1986 by Murray *et al.*, preconditioning in dog hearts achieved a remarkable 70% improvement in outcome [88]. Preconditioning produces several cardioprotective effects, including a reduction in infarct size, a reduced contractile dysfunction [91], decreased arrhythmias [92, 93], and decreased apoptosis [94, 95]. The reduction in contractile dysfunction is likely due to reduced infarct size, since it is not known to specifically reduce myocardial stunning [96-98].

Preconditioning becomes ineffective when ischaemia is permanent or prolonged (> 60-90 min), and the window of protective conditioning is bimodal. Preconditioning induces two distinct phases of cardioprotection, the first involving post-translation events (e.g. phosphorylation), the second shifts in protein expression (e.g. for NOS). The first window of protection, also known as 'classic' preconditioning, lasts up to 3 hours from the conditioning stimulus before the protection wanes [99]; the second window of protection, or 'delayed or late' preconditioning, emerges 24 hours after the initial stimulus and lasts 48-96 hours [100]. Preconditioning can be triggered by a variety of neuroendocrine and paracrine molecules, including Ado [101], catecholamines, angiotensin (Ang) II, bradykinin, endothelin, opioids [102], and NO [103]. These triggers activate downstream signalling pathways involving G-proteins, $[Ca^{2+}]_i$, phospholipase C (PLC) and protein kinase C (PKC) [104]. Reperfusion injury salvage kinase (RISK) signals are involved, transducing protective signals via a cascade of interrelated kinases, which may ultimately converge on mitochondrial targets such as K_{ATP} channels and the mPTP.

Cardiac K_{ATP} channels have a role in ischaemic preconditioning, with specific blockade abolishing the effects of ischaemic preconditioning [105]. In 2004

Hausenloy *et al.* demonstrated that preconditioning protects myocardium by inhibiting the mPTP [106]. Furthermore, Hausenloy *et al.* reported that the Ado-induced second window of protection in preconditioning is mediated by inhibition of mPTP opening at the time of reperfusion [107]. These protective paths are highlighted in Figure 1.8.

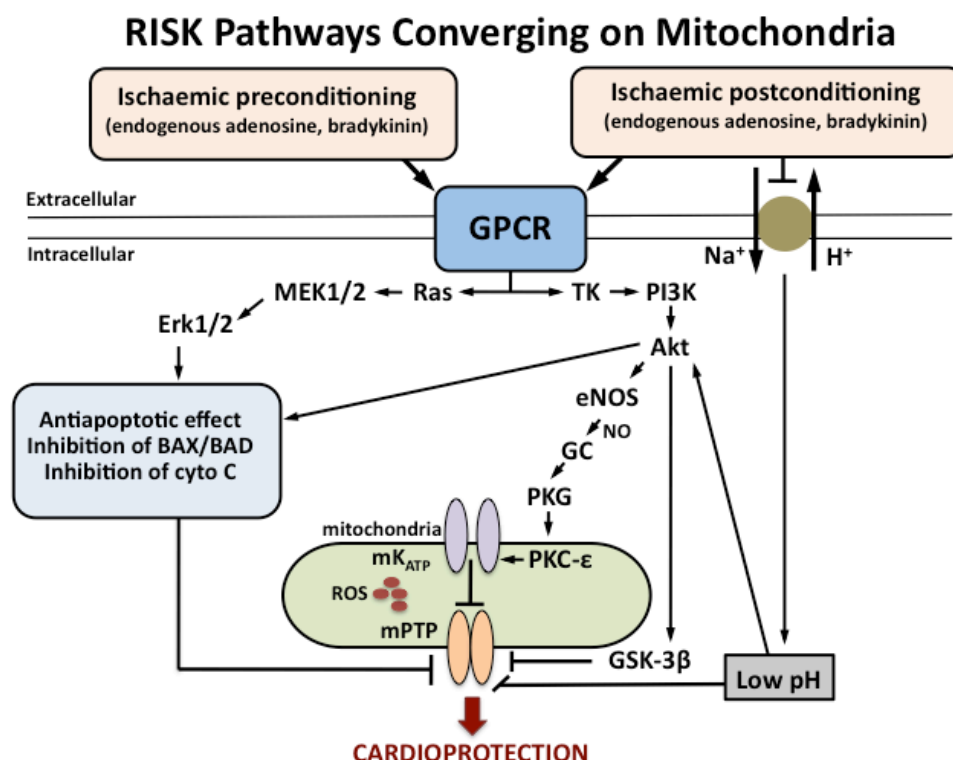


Figure 1.8. Reperfusion injury survival kinase (RISK) signalling in cardioprotection. Akt, protein kinase B; cyto C, cytochrome C; eNOS, enzyme nitric oxide synthase; ERK, extracellular signal-regulated kinase 1/2; GC, guanylate cyclase; GPCR, G-protein coupled receptor; GSK-3 β , glycogen synthase kinase 3 beta; MEK, extracellular protein kinase; mK_{ATP}, mitochondrial ATP-dependent potassium channel; mPTP, mitochondrial permeability transition pore; NO, nitric oxide; PI3K, phosphoinositide 3 kinase - PKC- ϵ , protein kinase C-epsilon; PKG, protein kinase G; ROS, reactive oxygen species; TK, tyrosine kinase

1.5.2 Antioxidants

Myocardial antioxidants act as endogenous protective agents within the myocardium, inhibiting or delaying oxidative damage to sub-cellular proteins, carbohydrates, lipids

and DNA [108]. It has been proposed that one antioxidant may equilibrate with another to establish a cellular redox potential and thus all endogenous antioxidants may act in concert to protect against oxidative insult. [108, 109]. Protective mechanisms include scavenging of ROS or their precursors, inhibiting ROS formation, inhibiting catalysis of ROS generation through metal ion binding, and promoting endogenous antioxidant generation [27, 108]. There is substantial evidence of the generation of free radicals/ROS during ischaemia-reperfusion, and their contribution to cellular injury [27, 110-114]. Oxidative stress by ROS produces cellular defects such as depression of sarcolemmal Ca^{2+} ATPase and Na^{+} - K^{+} ATPase activities, leading to decreased Ca^{2+} efflux, increased Ca^{2+} influx and subsequent Ca^{2+} overload [115, 116]. Radicals and ROS also promote pro-death mPTP activity. Recently, Kubli *et al.* demonstrated that *Bnip3* acts as a mitochondrial sensor of oxidative stress, with increased ROS inducing homodimerisation and activation of *Bnip3*, leading to opening of the mPTP, and cell death [59].

A variety of antioxidants enzyme systems limit oxidative stress. Two forms of SOD are found in mammalian hearts, a cytosolic form containing zinc and copper, and a mitochondrial form containing manganese. Both form of SOD catalyse the dismutation of $\text{O}_2^{\cdot -}$ to H_2O_2 [108]. Catalase is found in peroxisomal membranes and the mitochondrial matrix space. Hydrogen peroxide (H_2O_2) produced by SOD is reduced to water by catalase, or by oxidation of reduced glutathione (GSH) by glutathione peroxidase [27, 117, 118]. Glutathione act as a cellular reductant and is synthesised by γ -glutamylcysteine synthase and glutathione synthase from glutamate, cystine and glycine. Glutathione peroxidase catalyses the peroxidation of the reduced GSH to GSSG through H_2O_2 and phospholipid hydroperoxides. GSH is then cycled

back from GSSG by glutathione reductase, a process requiring NADPH produced by the hexose monophosphate shunt [27]. Other antioxidant may promote cardiac survival. For example, Petrosillo *et al.* demonstrated that melatonin, a known antioxidant, protects rat myocardium from reperfusion injury by inhibiting mPTP opening. It was proposed that melatonin inhibits cardiolipin oxidation, thereby preventing cytochrome *c* detachment from the mitochondrial membrane and thus mPTP opening [119]. Other antioxidants may limit the MPTP in a similar manner.

1.5.3 K_{ATP} channels

The activation of K_{ATP} channels can exert a protective effect, and has been implicated by multiple investigations in a variety of cardioprotective responses. Some demonstrate that activation of K_{ATP} channels plays an important role in ischaemic preconditioning [120-123], and may also contribute to more recently identified postconditioning [124-127]. Furthermore, K_{ATP} channel blockers have been found to have deleterious effect following ischaemia-reperfusion [128]. Thus, the activity of K_{ATP} channels appears important to myocardial ischaemic tolerance.

The K_{ATP} channels are linked to the metabolic state of the cell, and are modulated by pH, fatty acids, NO, nucleotides, G-proteins, Ado, acetylcholine and cyanoguanidines [128]. Two distinct types of K_{ATP} channels have been identified; the sarcolemmal K_{ATP} channels and the mitochondrial K_{ATP} channels [129]. The opening of cardiac K_{ATP} channels enhances a repolarising K^+ current and leads to action potential duration shortening and limiting Ca^{2+} influx; [130, 131]. However, some studies have demonstrated that cardioprotection is still elicited via K_{ATP} channel activation without action potential shortening, supporting a role for mitochondrial *vs.* sarcolemmal K_{ATP}

channels [131, 132] The protective role of mitochondrial K_{ATP} channels is verified by several studies: PKC activation primes the mitochondrial K_{ATP} channels to open sooner, linking between ischaemic preconditioning, PKC activity and mitochondrial K_{ATP} channels [120, 131-133]. Use of 5-HD to block mitochondrial K_{ATP} channels can prevent the protective effects ischaemic-preconditioning, supporting protective role for mitochondrial K_{ATP} channels [130-132]. As reviewed by Peart and Gross, both sarcolemmal and mitochondrial K_{ATP} channels may function as mediators of myocardial protection and preconditioning [129].

K_{ATP} channels are of intermediate conductance, and are inhibited by physiological concentrations of ATP. The lower the concentration of ATP the more likely the K_{ATP} channels operate in an open state. This regulation does not involve phosphorylation, as both intracellular ATP and its non-hydrolysable analogues inhibit K_{ATP} channels. Adenosine 5'-diphosphate (ADP) is also known to lower the sensitivity of K_{ATP} channels to ATP, and it has been proposed that a specific ratio of these nucleotides modulates the K_{ATP} channels [128, 134]. ADP may also compete for ATP binding sites, and in the absence of ATP also inhibits channel activity. An ADP site is also thought to exert weak agonist effects, while a regulatory nucleotide phosphate site can be stimulated by guanosine diphosphate (GDP) [128].

The stimulation of cell surface receptors linked to G-proteins releases GDP and enhances guanosine-5'-triphosphate (GTP) binding. Ado and acetylcholine are known ligands that interact with G_i , increasing K_{ATP} channel opening potential. Ado receptors are thought to activate PKC which in turn activates K_{ATP} channel opening by reducing channel sensitivity at the inhibitory site [123, 128]. Similarly, protein

kinase A (PKA) modulates K_{ATP} channel activity, and is involved in K_{ATP} channel opening induced by calcitonin gene-related peptide, Ado, prostacylin and β -adrenoceptor agonists. It has also been demonstrated that extracellular ATP enhance K_{ATP} channel currents through a P2 purinoceptor, involving activation of adenylate cyclase (AC) independently of PKA [128, 135].

Some studies demonstrate that K_{ATP} channel openers lengthen the time to onset of ischaemic contracture, suggesting an ATP conservation effect during ischaemia [128, 136]. K_{ATP} channel openers were found to be negatively inotropic, with ATP conservation considered comparable to that of Ca^{2+} channel blockers. Electron microscopy methods confirm that K_{ATP} channel openers enhance efficient use of O_2 and post-ischaemic recovery of ATP [128, 136, 137].

1.6 CYTOPROTECTIVE MEMBRANE RECEPTORS

Multiple surface receptors appear important in triggering cardioprotection during ischaemia-reperfusion, activating protection RISK paths, K_{ATP} channels and preventing mPTP opening and cell death. These include Ado, opioid, bradykinin, acetylcholine and other G-protein-coupled receptors (GPCR) (including P2 receptors). Agonised by locally generated ligands, these receptors activate kinase signals thought to converge on mitochondrial targets including K_{ATP} and mPTP. Two general models are forwarded regarding signal transduction to the mitochondria: Garlid *et al.* support a signalosome complex that communicates directly with mitochondria [138]; Clarke *et al.* suggest the receptor-coupled kinase paths (e.g. RISK) do not communicate with mitochondria directly, but rather reduce cellular oxidative stress, thus limiting the mPTP indirectly [139].

Ado and its receptors are 'prototypical' examples of protective GPCRs. Ado receptors couple to PKC through phospholipases to trigger preconditioning and protective effects. In 1991, Liu *et al.* discovered that stimulation of the G_i coupled Ado A_1 receptor was necessary to trigger ischaemic-preconditioning [140]. Unlike acetylcholine, Ado's cardioprotective effect is not dependent on Src tyrosine kinase or phosphatidylinositol 3-kinase (PI3K), but may directly stimulate PLC and phospholipase D (PLD) to activate PKC [141]. According to Cohen *et al.*, Ado completely bypasses K_{ATP} and ROS production [142] and directly activates downstream PKC. Others have demonstrated that the Ado A_{2B} receptor, a G_s -coupled receptor, is downstream from PKC and upstream from PI3K in survival kinase signalling during reperfusion [143, 144]. It may be that PKC activation sensitizes normally unresponsive A_{2B} receptors during ischaemia (via GPCR or other effects), leading to A_{2B} -dependent pro-survival signalling during the reperfusion phase. Such a scheme may link Ado protection with upstream effects of varied GPCRs targeting PKC.

1.6.1 Stress sensing and protection via nucleosides and nucleotides

Ado, a purine nucleoside is a major local (autocrine and paracrine) factor that accumulates in the tissue during disruptions to ATP supply. Ado acts on extracellular receptors to improve the balance between O_2 consumption and energy generation. There are four known Ado receptor subtypes, A_1 , A_{2A} , A_{2B} and A_3 receptors - coupled to the PLC-diacylglycerol (PLC-DAG) second messenger system through G-proteins, and ultimately impacting on K_{ATP} channel function [120, 131] and the mPTP (Hausenloy, 2004). Ado triggers and mediates ischaemic preconditioning by

stimulating the Ado A₁ receptor, found mainly on myocytes [140]. However, A₃ and also A_{2A}/A_{2B} receptors have also been implicated in cardioprotection, and pre- and post-conditioning [127, 145-147]. Ado is derived from ATP, which itself exerts receptor-triggered actions in the heart and vessels, affecting contractile responses as well as possessing vascular and arrhythmogenic properties. Previous studies from the host laboratory have shown Ado provides cardioprotection in isolated ischaemic-reperfused hearts [148-159]. The Ado receptor family are classified as P1 purinoceptors. The precursor ATP and other nucleotides can act at P2 purinoceptors.

1.6.2 Adenosine 5'-triphosphate (ATP)

ATP, apart from being the primary energy currency within the cell; exerts regulatory effects that were described as early as 1929 [160]. As a result of cell lysis, exocytosis of nucleotide-concentrating granules, or efflux from membrane transport proteins, ATP enters the extracellular compartment and can thus function as a paracrine or autocrine regulator [161].

Extracellular ATP acts at P2 purinoceptors to elicit diverse physiological and pathophysiological responses in many organs and tissues, including contractile responses of cardiac, vascular and visceral smooth muscle, stimulatory and inhibitory effects on neurons, stimulatory and inhibitory effects on ion; hormone; exocrine glands; mast cells; platelets, and many other effects [161, 162]. Roles and effects of ATP are still being defined, and are diverse. For example, exogenous and endogenous ATP increases the macromolecular permeability of blood capillaries via the P2Y purinoceptor [163]. In human HaCaT keratinocytes, ATP was found to act as an autocrine molecule, stimulating interleukin-6 production via P2Y receptors through

increased free Ca^{2+} concentrations [164]. In 2007, Deli *et al.* demonstrated that the activation of ionotropic P2X_4 , P2X_5 and P2X_7 and the metabotropic P2Y_1 and P2Y_4 purinoceptors contributed to ATP-evoked changes in intracellular concentration of Ca^{2+} in murine myotubes [165]. Locovei *et al.* showed that pannexin 1 channels can be activated by ATP binding to P2Y purinoceptors [166]. ATP's effect on increasing intracellular Ca^{2+} concentration also has a role in the proliferation of renal proximal tubule cells through activation of p38, p44/42 mitogen activated protein kinases (MAPK) and cyclin dependent kinases (CDKs) [167]. Another trophic effect of ATP involves P2 purinoceptor stimulation of neurite outgrowth, independent of neurotrophic factors and intracellular Ca^{2+} [168]. The P1/P2 system thus represents a regulatory network responsive to tissue energy state. As depicted in Figure 1.9, ATP, ADP and Ado are released from cells and nerves into the extracellular milieu where

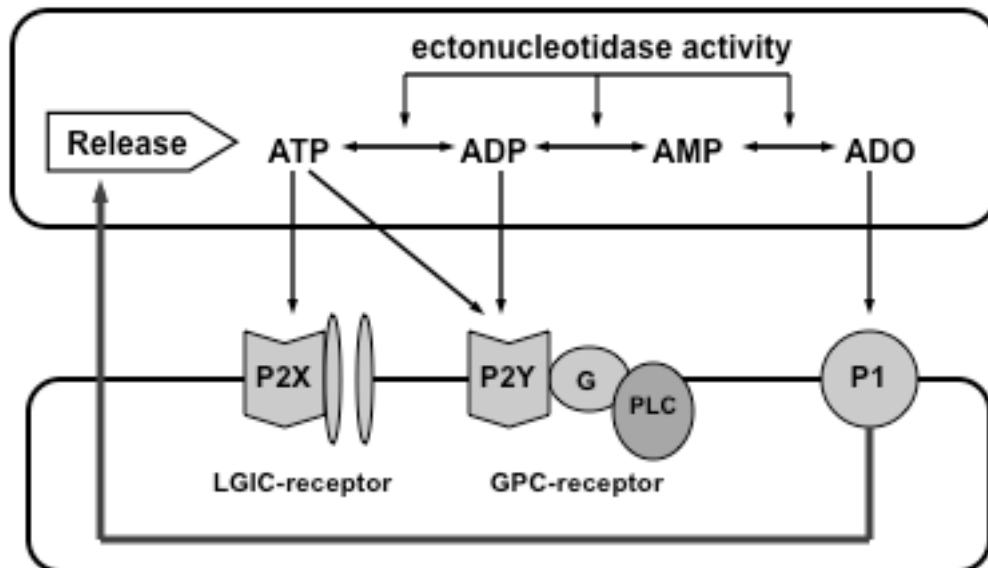


Figure 1.9. The purinergic cascade [169]. ATP is released into the extracellular space where it forms the basis of a purinergic cascade. ATP acts directly on P2X and P2Y receptors and is degraded to ADP and AMP by ectonucleotidase activity. AMP gives rise to adenosine (ADO) that activated the P1 receptors [170]. LGIC = Ligand gated ion channel, GPC = G-protein coupled.

they interact with purinoceptors and form the purinergic cascade. Whilst ATP interacts with P2 receptors and undergoes rapid degradation to ADP and AMP by ectonucleotidases, AMP gives rise to Ado that in turn activates P1 purinoceptors [170]. There is thus a complex interplay between P2 and P1 activities.

1.6.3 Cardiac effects of ATP/Uridine 5'-triphosphate (UTP)

In the cardiovascular system, ATP modulates ion exchange [171] and contractile functions [172-174]. ATP exerts a pronounced positive inotropic effect in the heart that appears mediated by an ATP receptor or P2 receptor found on the cell surface. ATP is also released from endothelial and smooth muscle cells by ischaemia, hypoxia and stress [161]. In 1987, Hopwood and Burnstock proposed that ATP causes coronary vasoconstriction via P2X receptors and coronary vasodilatation via P2Y receptors [175]. Released from and stored in vascular endothelial cells, ATP can act on P2Y receptors on endothelial cells to release NO and trigger vasodilatation [176]. Subsequently, endothelium-dependent dilation of human coronary arteries was reported for ATP, MeSATP, ADP β S and UTP [177]. Studies in rabbit atrial myocytes by Yamamoto *et al.*, indicate that both P1 and P2 purinoceptor activities inhibit L-type Ca²⁺ current in response to ATP lowering intracellular cyclic AMP (cAMP) via pertussis toxin (PTX)-sensitive G proteins [178]. In addition, ATP appears to have a role in inhibiting glucose transport in rat cardiomyocytes by promoting redistribution of glucose transporters from the cell surface to an intracellular compartment via a P2Y purinoceptor subtype [179]. ATP was also found to have an intermediate role in vasopressin induction of vascular, inotropic and arrhythmogenic effects in the heart [180]. Ninomiya *et al.* indicated a reciprocal

correlation between the interstitial fluid levels of ATP and Ado, which perform complementary roles in ischaemic preconditioning through activation of P2Y purinoceptors and Ado receptors [181]. More recently, it was found that endogenous ATP release during myocardial ischaemia activates ischaemia-sensitive cardiac spinal afferents through the stimulation of P2 purinoceptors, leading to chest pain and reflex cardiovascular responses [182]. Table 1.1 summarises some of the cardiac and vascular effects of P2 purinoceptors.

Table 1.1 - Cardiac and vascular effects of P2 purinoceptors.

<i>P2 subtype</i>	<i>Cardiac and vascular effects</i>
P2X subtypes	<p>Vasoconstriction [175]</p> <p>Foetal heart development (P2X₁, P2X₃ and P2X₄) [183]</p> <p>Congestive heart failure development (P2X₁) [184]</p> <p>Stimulating contractility (P2X₄) [185]</p> <p>Ventricular tachycardia [186]</p> <p>Pre- and postconditioning (P2X₇) [187]</p>
P2Y subtypes	<p>Vasodilatation (P2Y₁ and P2Y₂) [175, 188]</p> <p>Congestive heart failure development (P2Y₂) [184]</p> <p>Positive inotropy (P2Y₂, P2Y₆, P2Y₁₁) [173, 189]</p> <p>Triggers cardiac fibrosis (P2Y₆) [190]</p> <p>Inhibits DNA synthesis in fibroblasts (P2Y₁ and P2Y₂) [191]</p> <p>Preconditioning (P2Y₆ and P2Y₁₁) [192]</p> <p>Profibrotic in fibroblasts (P2Y₂) [193]</p>

1.6.4 Purinoceptors - P1 purinoceptors

As already noted, P1 purinoceptors are sensitive to activation by Ado and AMP, whilst P2 purinoceptors are activated by ATP and ADP. Thus, P2 purinoceptors are

otherwise known as ATP receptors. Unlike P1 receptors, P2 receptors are unaffected by methylxanthines such as caffeine and theophylline but are inhibited by quinidine, imidazolines, 2,2'-pyridylisatogen and apamin [194]. Lack of homogeneity in these purinoceptors led to classification into both P1 purinoceptors (A_1 , A_2 and A_3) and P2 purinoceptors (P2X and P2Y).

The initial pharmacological classification of P2 purinoceptors was based on the rank order agonist potency of a series of ATP analogues in a variety of mammalian tissues. P2X receptors were found to be most potently activated by stable analogues of ATP, α,β -methylene ATP (α,β -meATP), and β,γ -meATP. Whilst 2-methylthio ATP (2-MeSATP) was found to be the most potent agonist at the P2Y receptors, α,β -meATP and β,γ -meATP were weak or inactive [195]. The first defined receptor subtypes according to pharmacological profiles were P2X for excitatory and P2Y for inhibitory. P2U has been applied to those receptors that responded to both ATP and UTP, and P2T for ADP sensitive receptors inducing platelet aggregation. Finally, a large molecular pore activated by ATP^{4-} was labelled P2Z, while receptors activated by dinucleotides were referred to as P2D [174, 195]. In 1994, early successes in the cloning of P2 receptors enabled Abbracchio and Burnstock to propose a clear division of the P2 receptors into two main classes. They proposed that the characterisation of P2 receptors should include their molecular structure and signalling transduction properties, and not simply be based on receptor agonist potency. Thus, P2X receptors are a family of ionotropic ligand gated ion channels (LGICs) that mediate faster receptor responses, while P2Y receptors are a metabotropic, heptahelical GPCR family [196].

1.7 P2X PURINOCEPTORS

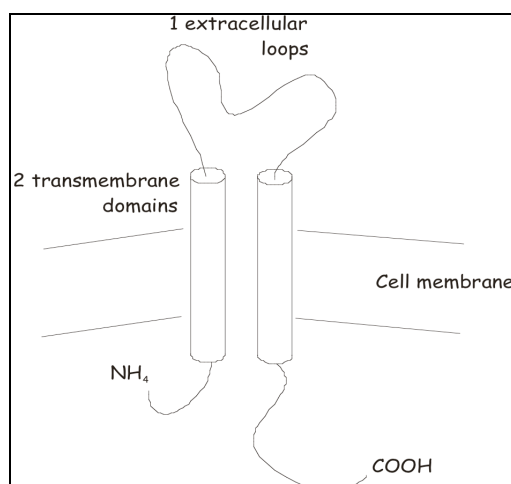


Figure 1.10. Schematic representation of a P2X receptor. [197].

The P2X class of purinoceptors are ATP-gated ion channels that function in fast excitatory neurotransmission in excitable tissues such as neurons, glia and smooth muscle cells. Activation by ATP results in selective permeability to Na^+ , K^+ and Ca^{2+} cations. The P2X subunit has a two-transmembrane motif that is structurally related to the amiloride-sensitive epithelial Na^+ channel [197]. The P2X receptor is made up of between 379-472 amino acids that are inserted in the membrane forming a pore comprised of two hydrophobic transmembrane domains and a large extracellular hydrophilic loop. To date, seven P2X receptor subunits have been cloned, and designated P2X₁ through to P2X₇.

P2X subunits have been found to function as both homo- and heteropolymers [198]. Radford and his team of researchers provided evidence for the heteromeric assembly of P2X₂ and P2X₃ subunits in baculovirus expression [199]. In 1998, Torres *et al.* provided both biochemical and functional evidence that the co-expression of P2X₁ and P2X₅ receptor subunits in mammalian cells formed a novel ATP-gated ion channel

[200]. In addition, Brown *et al.* found that co-expression of P2X₁ and P2X₂ receptors yielded a heteromeric formation of P2X_{1/2} ion channels that are sensitive to extracellular pH [201].

P2X purinoceptors are widely distributed in mammalian tissue and most tissues express more than one subtype of P2X purinoceptor. Although the principal distribution of P2X purinoceptors is on excitable tissue such as smooth muscle and nerves, P2X purinoceptors are also expressed by endocrine tissue and platelets [195], in addition to expression in urinary bladder, brain, spinal cord, liver, spleen, pancreas, testis, colon, heart, cochlea, adrenal medulla and macrophages [195, 197]. Zemkova *et al.* indicated P2X purinoceptors in rat gonadotrophs operate as pacemaking channels and modulators of GnRH-controlled Ca²⁺ mobilisation [202]. P2X₇ activation was demonstrated in mice deficient of P2X₇ expression to result in a signal that leads to the maturation and the release of interleukin (IL)-1 β and the initiation of a cytokine cascade [203].

In addition, Schwiebert *et al.* identified abundant P2X₄ and P2X₅ expression in human vascular endothelial cells from multiple vessels, proposing that a new extracellular autocrine and paracrine signalling cascade may have significant implications in vascular pathophysiology [204]. The vasoconstrictor role of P2X purinoceptors on vascular smooth muscle has been well established, however Harrington *et al.* demonstrated a novel bi-functional role for P2X purinoceptor causing constriction when activated on smooth muscle and dilation when activated on the endothelium [205]. This is comparable to the variable functions of P2Y purinoceptors, which

mediate dilation when activated on the endothelium and constriction when on smooth muscle cells [195, 206].

1.7.1 P2X purinoceptor signal transduction mechanisms

Table 1.2 summarises different transduction mechanisms for P2X subtypes. P2X purinoceptors mediate the rapid passage of cations (Na^+ , K^+ and Ca^{2+}) across the cell membrane, resulting increased intracellular Ca^{2+} and depolarization [207, 208]. Although this influx of Ca^{2+} contributes to the rise in Ca^{2+} level within the cell, the primary source arises from the secondary activation of voltage-dependent Ca^{2+} channels with membrane depolarization. This transduction mechanism is independent of the production and diffusion of second messengers within the cytosol and cell membrane, and thus plays an important role in fast neuronal signalling and muscle contraction. Cations such as Mg^{2+} , Ca^{2+} , Zn, Cu and H^+ can modulate ATP-activated P2X-dependent currents in regions of the extracellular loop adjacent to transmembrane regions. Mg^{2+} and Ca^{2+} generally inhibit P2X purinoceptor currents via allosteric changes in the receptor, whilst Zn potentiates cation conductance induced by ATP at most P2X purinoceptors. Extracellular protons modulate the affinity of the ATP-binding site: acid pH causes an increase while alkaline pH causes a decrease in receptor-dependent currents [195].

Table 1.2 - Transduction mechanisms of the various P2X purinoceptor subtypes [170].

<i>Subtype</i>	<i>Signal Transduction</i>
P2X ₁	$I_{\text{Na/K/Ca}}^{2+}$
P2X ₂	$I_{\text{Na/K}}$
P2X ₃	$I_{\text{Na/K/Ca}}^{2+}$
P2X ₄	$I_{\text{Na/K}}$
P2X ₅	$I_{\text{Na/K/Ca}}^{2+}$
P2X ₆	$I_{\text{Na/K/Ca}}^{2+}$
P2X ₇	$I_{\text{Na/K}}$, Pore Formation

Abbreviations: I_{Ca}^{2+} , Ca^{2+} current; I_{Na} , Na^{+} current; I_{K} , K^{+} current.

1.7.2 P2X purinoceptors in the heart

In 1997, studies by Froldi *et al.* (in isolated rat and guinea pig cardiac tissue) indicated that ATP and UTP may produce positive inotropic effects by interacting with P2X receptors, involving a Ca^{2+} -dependent mechanism [209]. Normal P2X purinoceptor function in the central nervous system are also proposed to be necessary for baroreflex regulation of heart rate [210]. Overexpression of P2X₄ purinoceptors in transgenic mice manifested in extended lifespan and enhanced LV contractility, supporting a beneficial role of this purinoceptor in heart failure [185, 211]. P2X purinoceptors were demonstrated to play a role in modulating heart rate in rats during development/maturation [212]. P2X₇ purinoceptors have been reported to combine with pannexin-1 to form channels that allow release of ATP and cardioprotectants in pre- and post-conditioned tissue, and ischaemic-reperfused rat hearts [187, 213].

1.8 P2Y PURINOCEPTORS

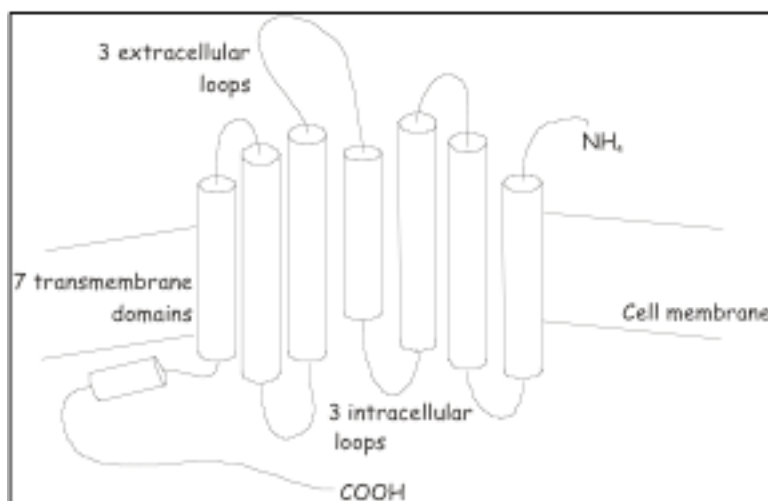


Figure 1.11. Schematic representation of a P2Y receptor [197].

P2Y purinoceptors are GPCRs with a typical seven transmembrane motif, sensitive to activation by both purines (ATP, UDP) and pyrimidines (UTP, UDP). P2Y purinoceptors consist of 308 to 377 amino acid, with a mass of 41 to 53kDa after glycosylation. The precise number of P2Y purinoceptor subtypes remains unclear with eight P2Y mammalian purinoceptor subtypes identified to date: P2Y₁, P2Y₂, P2Y₄, P2Y₆, P2Y₁₁, P2Y₁₂, P2Y₁₃ and P2Y₁₄ [214]. P2Y purinoceptors are also widely distributed, located in cardiac, vascular, connective, immune and neural tissues. In the rat, P2Y purinoceptor mRNA is expressed in varying levels in tissues including heart, brain, spleen, lung, liver, skeletal muscle and kidney [215].

1.8.1 P2Y purinoceptor signal transduction mechanisms

Table 1.3 summarises different transduction mechanisms for P2Y subtypes. Ca²⁺ plays an important role in P2 purinoceptor signalling pathways, with intracellular Ca²⁺ elevated via diverse mechanisms. Functional effects of most of P2Y purinoceptors (P2Y₁, P2Y₂, P2Y₄, P2Y₆, P2Y₁₁) arise from G-protein-coupled activation of PLC to

Table 1.3 - Transduction mechanisms of the eight known P2Y purinoceptor.

<i>Subtype</i>	<i>G protein</i>	<i>Signal</i>	<i>Response</i>
P2Y ₁	G _{q/11}	↑ PLC / Ca ²⁺	
	G _i	↓ AC / ↓ cAMP	
		↑ Rho - p160ROCK	
P2Y ₂	G _{q/11}	↑ PLC / Ca ²⁺	
	G _i	↓ AC / ↓ cAMP	
	G _o	↑ PLC / Ca ²⁺	
		↑ Rac	
	G _{α 12}	↑ Rho - p160ROCK	
P2Y ₄	G _{α and G_{βγ}}	PI3K/PDK1/PKCζ - ERK/MAPK	
	G _{q/11}	↑ PLC / Ca ²⁺	
	G _o	↑ PLC / Ca ²⁺	
	G _{α 12}	↑ Rho - p160ROCK	
P2Y ₆	G _{q/11}	↑ PLC / Ca ²⁺	
	G _i	↓ AC / ↓ cAMP	
	G _{α 12/13}	↑ Rho - p160ROCK	
P2Y ₁₁	G _{q/11}	↑ PLC / Ca ²⁺	
	G _s	↑ AC / ↑ cAMP	
	G _o	PLC-independent Ca ²⁺ release	
P2Y ₁₂	G _i	↓ AC / ↓ cAMP, ion channels	
P2Y ₁₃	G _{i/o}	↓ AC / ↓ cAMP, ↑ PLC / Ca ²⁺ , ion channels	
P2Y ₁₄	G _{i/o}	↓ AC / ↓ cAMP, ↑ PLC / Ca ²⁺ , ion channels	

PLC = phospholipase C; AC = adenylyl cyclase; ROCK = Rho-dependent kinase; PI3K = phosphatidylinositol 3-kinase; PDK1 = 3-phosphoinositide-dependent protein; PKCζ = protein kinase C-zeta ERK = extracellular signal-regulated kinase kinase-1; MAPK = mitogen activated protein kinase. [197, 216-221].

form inositol triphosphate (IP₃), in turn mobilising intracellular Ca²⁺. This leads to activation of other signalling intermediates and paths, including PKC, phospholipase A₂ (PLA₂), Ca²⁺-dependent K⁺ channels, NOS, voltage-operated Ca²⁺ channels, and MAPK pathways. Some P₂Y purinoceptors are linked to the inhibition of adenylate cyclase [222], including P₂Y₁₂, P₂Y₁₃ and P₂Y₁₄ receptors [218]. Sauzeau *et al.* proposed that in vascular myocytes, P₂Y₁, P₂Y₂, P₂Y₄ and P₂Y₆ purinoceptors are coupled to Rho and Rho kinase activation [223]. Studies by Montiel *et al.* in human umbilical vein endothelial cells suggest that P₂Y purinoceptors activate MAPK/extracellular signal-regulated kinase-1 (ERK) through PI3K-dependent mechanisms with 3-phosphoinositide-dependent protein (PDK1) and protein kinase C-zeta (PKC-ζ) identified as key molecules involved in this activation pathway [221]. As for P₂X receptors, P₂Y purinoceptors may form homo-and hetero-multimeric assemblies under certain conditions, and most tissues express multiple P₂Y subtypes.

The P₂Y₁ purinoceptor was the first P₂ purinoceptor to be cloned. Activation of this purinoceptor results in either activation of PLC via the G_q/G₁₁ coupling, or inhibition of adenylate cyclase via independent G_i subunits. Activation of P₂Y₁ purinoceptors can also directly modulate ion channel function, a G-protein-mediated effect independent of other secondary messengers [197]. Selective antagonism of platelet P₂Y₁ purinoceptor provides strong antithrombotic activity in mice [224]. White *et al.* demonstrated that activation of P₂Y₁ purinoceptor caused a dose-dependent decrease in human melanoma cell numbers whilst activation of P₂Y₂ purinoceptor led to a dose-dependent increase in cell numbers [225].

The P2Y₂ purinoceptor has been cloned from mouse, rat and human tissue. They are coupled to G_q and G_i proteins, mediating phospholipid breakdown, IP₃ formation and in turn mobilising Ca²⁺. P2Y₂ receptors on the pineal gland, was found to selectively inhibit β-adrenergic receptor-mediated signalling pathways via the inhibitory G-proteins [226]. P2Y₂ receptors have also been reported to negatively couple to adenylate cyclase, activating the inward-rectifier K⁺ channels of the Kir3.0 subfamily [227] and adenylate cyclase via a cyclooxygenase (COX) dependent mechanism [228]. Soltoff *et al.* demonstrated that activation of P2Y₂ purinoceptors by UTP and ATP stimulated Ca²⁺ dependent MAPK activity, involving related adhesion focal tyrosine kinase (RAFTK) and PKC [229, 230]. From studies in P2Y₂ deficient mice, it was demonstrated that this subtype is the only purinoceptor mediating nucleotide-induced inositol lipid hydrolysis and Ca²⁺ mobilisation in mouse lung fibroblasts [231]. In addition, Alvarez *et al.* demonstrated P2Y₂ receptors via G-protein and stimulation of PLCβ, induce opening of heteromeric transient receptor potential channel 3/7 (TRPC3/7), leading to a sustained depolarizing current that triggers arrhythmia during early infarct when ATP/UTP are released [232].

The P2Y₄ purinoceptor has been cloned from human placenta [233] and rat heart [234]. This receptor is a uridine-nucleotide specific receptor and similar to other P2Y purinoceptors (P2Y₁, P2Y₂, and P2Y₆), the P2Y₄ evokes Ca²⁺ signalling involving activation of PLC [235, 236]. The expression of P2Y₄ receptors was first thought to be restricted primary to placenta and pancreas, with low levels expressed in the lungs and vascular smooth muscle [195]. Hou *et al.* also identified P2Y₄ receptors (as well as P2X₁, P2Y₁, P2Y₂ and P2Y₆) in both rat and human myocardium [184], additionally, the expression of P2Y₄ subtype (amongst other P2 purinoceptors) was also identified

in the human foetal heart suggesting a contributing role for P2 purinoceptors in foetal heart development [183]. P2Y₄ receptors were also found to couple mitogenesis via p42/p44 MAPK to regulate aortic smooth muscle cells [236].

The P2Y₆ purinoceptor has been cloned from rat aortic smooth muscle, human placenta and spleen. Expression of P2Y₆ receptors is found abundantly in various tissues including thymus, lung, stomach, intestine, heart and aorta [195]. This P2Y₆ subtype is linked to G_q, activating PLC and forming IP₃. P2Y₆ mediates monocyte interleukin-8 production [237] and is also linked to a dual coupling to N-type Ca²⁺ and M-type K⁺ channels in rat sympathetic neurones [238]. Activation of luminal P2Y₆ receptors in the airways shifts electrolyte transport towards secretion by increasing intracellular Ca²⁺ and activation of PKA [239]. Activation of P2Y₆ purinoceptor by UDP stimulates mitogenesis in vascular smooth muscle [240]. P2Y₆ purinoceptors are also cited to play an important role in contraction of human cerebral arteries whilst it was also determined that this subtype is absent in human coronary arteries [241]. In cardiomyocytes, the P2Y₆ receptor has a role in mediating positive inotropy [189]. The human P2Y₁₁ receptor is coupled to both adenylate cyclase and phosphoinositide signalling [173], whilst P2Y₁₂, P2Y₁₃ and P2Y₁₄ receptors coupled to G_i protein to inhibit adenylate cyclase [197, 218]. Balogh *et al.* also showed that P2Y₁₁ receptor coupled both to IP₃ and cAMP in ATP induced inotropy [173].

1.8.2 P2Y purinoceptor oligomers and interactions

In 2003, Nakata and colleagues used bioluminescence resonance energy transfer technology (BRET) in transfected cultured cells to demonstrate heteromeric oligomerisation occur between A₁ Ado receptors and P2Y₁ purinoceptors providing

added diversity in purinergic signalling [216]. This interaction was later found to contribute to adenine nucleotide-mediated inhibition of neurotransmitter release [242]. Similarly, Suzuki *et al.* found that simultaneous activation of A₁ Ado receptor and P2Y₂ purinoceptor generates a hetero-oligomerisation complex that interferes with A₁ Ado receptor signalling via G_{i/o} whilst enhancing P2Y₂ purinoceptor signalling via G_{q/11} [243]. A complex signalling interplay was demonstrated between P2Y₁ and P2Y₁₂, whereby P2Y₁₂ receptors positively regulate the actions of P2Y₁ receptors, and the P2Y₁ receptors negatively regulates the actions of the P2Y₁₂ at the level of Ca²⁺ signalling in human platelets [244].

1.8.3 P2Y purinoceptors in the heart

Studies by Burnstock *et al.* indicated the involvement of P2 purinoceptors in the relaxation of coronary vasculature [176, 245]. In 1992, Chinellato *et al.* concluded that endothelial P2Y purinoceptors mediated ATP induced vasodilatation on isolated rabbit aorta [246]. Simonsen *et al.* indicated ATP acting through P2Y purinoceptors relaxes coronary small arteries in the non-adrenergic non-cholinergic inhibitory neurotransmission in the lamb isolated studies [247]. As already noted, the P2Y purinoceptor is predominantly linked to stimulation of phosphatidylinositol 4,5-biphosphate (PIP₂) - PLC, leading to increased IP₃ and DAG, with mobilization of intracellular Ca²⁺ to stimulate myocyte contractility, with DAG activation of PKC increasing myofilament Ca²⁺ sensitivity [162]. P2Y purinoceptors are also implicated a novel PLC- and cAMP-independent positive inotropic mechanism [248]. Subsequent studies in 2005 by Balogh *et al.* indicate that P2Y₁₁ purinoceptors couple both to activation of IP₃ and cAMP to enhance inotropy in cardiomyocytes and that down-regulation of this function is observed in heart failure [173]. In 1998, P2Y₁ and

P2Y₂ purinoceptor mRNA were detected in cultured cardiac fibroblasts, and stimulation of these purinoceptors activated *c-fos* expression, inhibiting fibroblast DNA synthesis [191]. Vascular P2Y₁, P2Y₂ and P2Y₆ receptors were pharmacologically characterised by Guns *et al.* with aortic tissue completely or partially relaxing in response to ATP, ADP and UTP [249]. PCR studies by Banfi *et al.* in heart transplant patients identified the presence of all known P2Y purinoceptors (P2Y₁, P2Y₂, P2Y₄, P2Y₆, P2Y₁₁, P2Y₁₂, P2Y₁₃ and P2Y₁₄) together with two P2Y-like receptors: GPR91 and GPR17 [250].

Despite cardiac and vascular expression of multiple P2Y subtypes, the specific roles and coupling mechanisms of these P2Y receptors, and possible interactions with P1 receptors, remain to be fully elucidated.

1.9 CARDIOPROTECTION AND P2 PURINOCEPTORS

Several studies over the past two decades indicate that P2 purinoceptors may exert cardioprotective effects. Opening of K_{ATP} channels is known to reduce myocardial damage caused by metabolic inhibition/dysfunction. Oketani *et al.* found that extracellular ATP modulates K_{ATP} channel activity through P2Y purinoceptors coupled to GTP-binding proteins, associated with reduced sarcolemmal PIP₂ and stimulation of PLC in ventricular myocytes [251]. During myocardial ischaemia, endogenously released ATP acts on P2 purinoceptors to activate sympathetic cardiac afferents to produce chest pain and reflex cardiovascular responses [182]. While not a protective function per se, this demonstrates that P2 agonists are released in stressed myocardium and may mediate different responses.

1.9.1 UTP and P2Y purinoceptors

In addition to ATP, there is evidence for endogenous release of UTP in stressed myocardium. Erlinge *et al.* demonstrated UTP release during cardiac ischaemia which stimulated blood flow, increased arrhythmia and t-PA release in the pig model. In this study, plasma UTP levels increased early during ischaemia and early after reperfusion; with a significant increase in cardiac blood flow, ventricular arrhythmias and t-PA release at the same time points [252]. Wihlborg *et al.* in 2007 provided evidence for UTP release in human hearts, and that UTP levels are increased during myocardial infarction. It was also found that UTP and UDP are positively inotropic in cardiomyocytes, possibly via the activation of P2Y₂ and P2Y₆ receptors, respectively [189]. Activation of P2Y₂ and P2Y₄ purinoceptors by UTP produces IP₃, resulting in increased intracellular Ca²⁺, an oscillatory Cl⁻ current, and membrane potential changes in rat aortic myocytes [253]. Further studies in UTP by Yitzhaki *et al.* found that UTP activation of P2Y₂ purinoceptors significantly reduced cardiomyocyte death induced by hypoxic stress [254]. Subsequent work by Yitzhaki *et al.* demonstrated that early or late preconditioning with applied UTP reduces infarct size and improves functional recovery through a reduction in mitochondrial Ca²⁺ overload [255].

1.9.2 P2 purinoceptors and cell death

Cell death either by necrosis or apoptosis is a common consequence of ischaemia-reperfusion. Caspase inhibition during early reperfusion has been shown to limit infarct size and provide cardioprotection against lethal reperfusion injury [47]. In terms of apoptotic signalling, Sellers *et al.* determined that the human P2Y₁ purinoceptor could activate the Ras-ERK cascade via collaborative effects of PI3K,

Src and PKC, leading to phosphorylation of the Elk-1 transcription factor. However, transient stress activated protein kinase (SAPK) activity did not sufficiently evoke transcription factor phosphorylation but seemed to regulate apoptotic processes through the caspase-3-dependent mechanism [256]. Mamedova *et al.* demonstrated opposing effects of P2Y₁ and P2Y₁₂ purinoceptors in terms of apoptosis - activation of P2Y₁ receptors induced apoptosis in 1321N1 human astrocytoma cells [256], while activation of P2Y₁₂ purinoceptors attenuates tumour necrosis factor alpha (TNF α)-induced apoptosis through phosphorylation of Erk1/2 (but not protein kinase B (Akt) or c-Jun N-terminal kinase (JNK)) [257]. Of the P2X subclass, P2X₇ is of particular interest in apoptosis, with several studies implicating a role in inducing apoptosis in mesangial, microglial and dendritic cell lines [258-261].

The specific roles of P2Y and P2X receptors in regulating apoptosis in myocytes remain to be clarified. Interestingly, Mazzola *et al.* recently reported opposing effects of uracil and adenine nucleotides on cardiomyocyte survival: ATP, ADP or BzATP induced apoptosis and necrosis, with cell death exacerbated by TNF- α , whereas uracil-preferring P2 receptors appear to counter this effect. A possible 'therapeutic' window was proposed, with uracil nucleotides-mediated protection apparent in cardiomyocytes exposed to adenine nucleotides and TNF α [262]. In hypoxic cardiomyocytes, Shainberg *et al.* proposed that UTP reduces cardiomyocyte death via a transient increase in [Ca²⁺]_i and phosphorylation of Erk1/2 and Akt, reducing mitochondrial Ca²⁺ overload [263]. In addition, Cosentino *et al.* very recently demonstrated that P2Y₂ and P2X₇ subtypes may induce cardiomyocyte death during ischaemic/hypoxic stress, whereas the P2Y₄ receptor has a protective effect [264]. Thus, a complex interplay may exist between P2 agonists and P2 subtypes in dictating

progression of cellular injury vs. survival during myocardial ischaemia-reperfusion, an interplay that awaits further interrogation. Importantly, given evidence for release of multiple P2 ligands from stressed tissue, the roles of intrinsic P2 activities in dictating cell death vs. stress resistance are yet to be clarified.

CHAPTER 2

GENERAL METHODS

2.1 ANIMALS AND THE ISOLATED LANGENDORFF HEART MODEL

This Chapter outlines the major methods and models employed in the thesis. Other techniques specific to individual chapters (e.g. cardiac microdialysis) are described in detail within relevant chapters, and the Langendorff model is described in more complete detail in **Chapter 3**.

For most studies male C57 mice weighing 25-35g were anaesthetized with a bolus injection sodium pentobarbital (50 mg/kg) given intraperitoneally. Successful anaesthesia was indicated by a lack of pedal withdrawal and other reflexes. A thoracotomy was performed with the mouse hearts excised *en bloc* with the lungs and arrested by immersion in ice-cold perfusion buffer. Each heart was cannulated via the aorta and retrogradely perfused at a constant pressure of 80 mmHg with Krebs-Henseleit buffer containing (in mM): NaCl, 119; NaHCO₃, 22; KCl, 4.7; CaCl₂, 2.5; MgCl₂ 1.2; KH₂PO₄ 1.2, glucose, 11; EDTA, 0.5 and pyruvate, 2.0. The perfusate was equilibrated with 95% O₂, 5% CO₂ and maintained at 37.0°C. Impurities were removed by an inline Sterivex-HV filter (Millipore, Bedford, MA, U.S.A.) A polyethylene apical drain was inserted into the left ventricle to prevent intra-ventricular pressure build up. A fluid-filled balloon was then inserted into the left ventricle via the left atrium for measurement of ventricular pressure via a P23XL pressure transducer. Coronary flow was monitored by Doppler flow probe in the aortic line (Transonic Systems Inc, Ithaca, NY, U.S.A.). Ventricular pressure was monitored using the application Chart 3.6.3 (ADInstruments, Castle Hill Australia) continuously, recording systolic, diastolic, developed pressure, heart rate and pressure derivatives ($-dP/dt$ and $+dP/dt$). Mouse hearts were electrically paced at 420 beats/min following 15 minutes of equilibration. The temperature of the perfusate

LANGENDORFF ISOLATED HEART PERFUSION APPARATUS

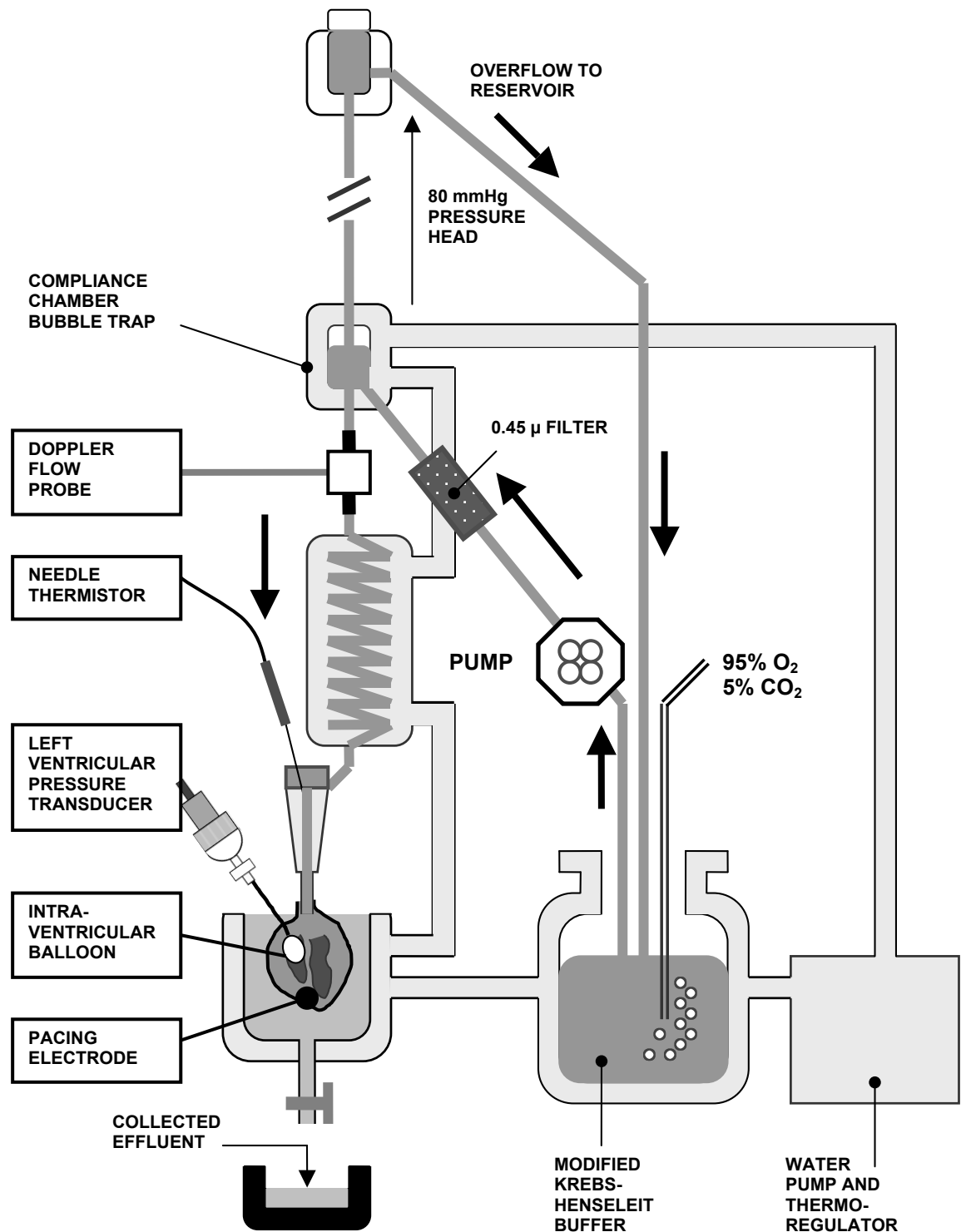


Figure 2.1. Simplified schematic of the Langendorff isolated heart perfusion apparatus employed throughout this thesis.

was maintained at 37.4°C and the temperature of the organ bath at 37.0°C. Temperature were monitored with the aid of a Physitemp TH-8 digital thermometer (Physitemp Instrument Inc, Clifton, NJ, U.S.A.)

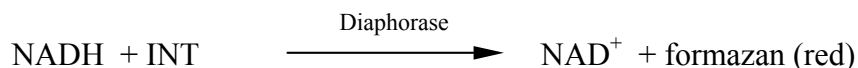
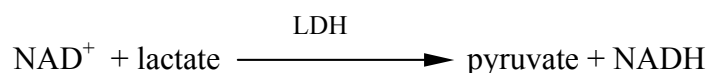
2.1.1 Experimental exclusion criteria

After the initial 15 min stabilization, hearts were excluded from further study if any exhibited one or more of the following exclusion criteria: coronary flow greater than 5 ml/min (normally indicative of an aortic tear); LV pressure development less than 100 mmHg; intrinsic heart rate less than 320 beats/min or irregular.

2.2 ONCOTIC DAMAGE VIA LACTATE DEHYDROGENASE (LDH) EFFLUX

Cellular oncosis or necrosis may be assessed by the release of LDH into the extracellular space. In humans, extracellular LDH activity is significantly elevated during myocardial infarction and LDH efflux has been shown to correlate linearly with infarct size in this rodent model [155]. Coronary effluent was collected on ice and stored at -80°C (≤ 7 days) until analysis for LDH via a CytoTox96® assay kit (Promega Corporation, Annandale, NSW, Australia), a colorimetric assay coupling LDH content to conversion of a tetrazolium salt to a coloured formazan product. Total LDH washed from hearts during reperfusion was calculated as the product of LDH content (per milliliter) and total coronary effluent over the reperfusion period (Headrick et al., 2001; Peart and Headrick, 2003).

The process is summarised in the following reactions:



Formazan formed in the reaction absorbs at 490 nm, permitting assessment of activity.

2.3 REAL-TIME POLYMERASE CHAIN REACTION (PCR) ANALYSES

The real time polymerase chain reaction (RT-PCR) was harnessed to measure the gene expression profile of P2 receptors in cardiovascular tissues. This method amplifies small amounts of mRNA and allows the simultaneous quantification of the PCR product in an attempt to measure the level of expression of mRNA for a specific protein. In this case, the genetic expression of the P2 receptors is quantified by performing RT-PCR on cDNA derived from the mRNA of the descending aorta and left and right ventricles of mouse hearts.

PCR product is quantitated in 'real time' by measuring the increase in fluorescence emission during the course of the amplification process. SYBR green I emits fluorescence when bound to double-stranded DNA. At the beginning of the PCR amplification process, a baseline fluorescent emission is detected from the sample. After every cycle of amplification, the degree of fluorescence emission (RFU) is detected and measured. As the amount of PCR product increases due to amplification, the amount of fluorescence detected increases as dye binds to double-stranded cDNA. The change in fluorescent emission is calculated between the baseline at time zero and the amplification cycle at time 'x'. An amplification plot is

derived from the data, as shown in Figure 2.2, characterized by a measurement threshold, an exponential or log phase, and a plateau. The individual curves represent different input quantities of mRNA. The C_T is the threshold cycle, which represents the cycle at which the exponential phase begins, while ΔR_n represents the fluorescent signal intensity.

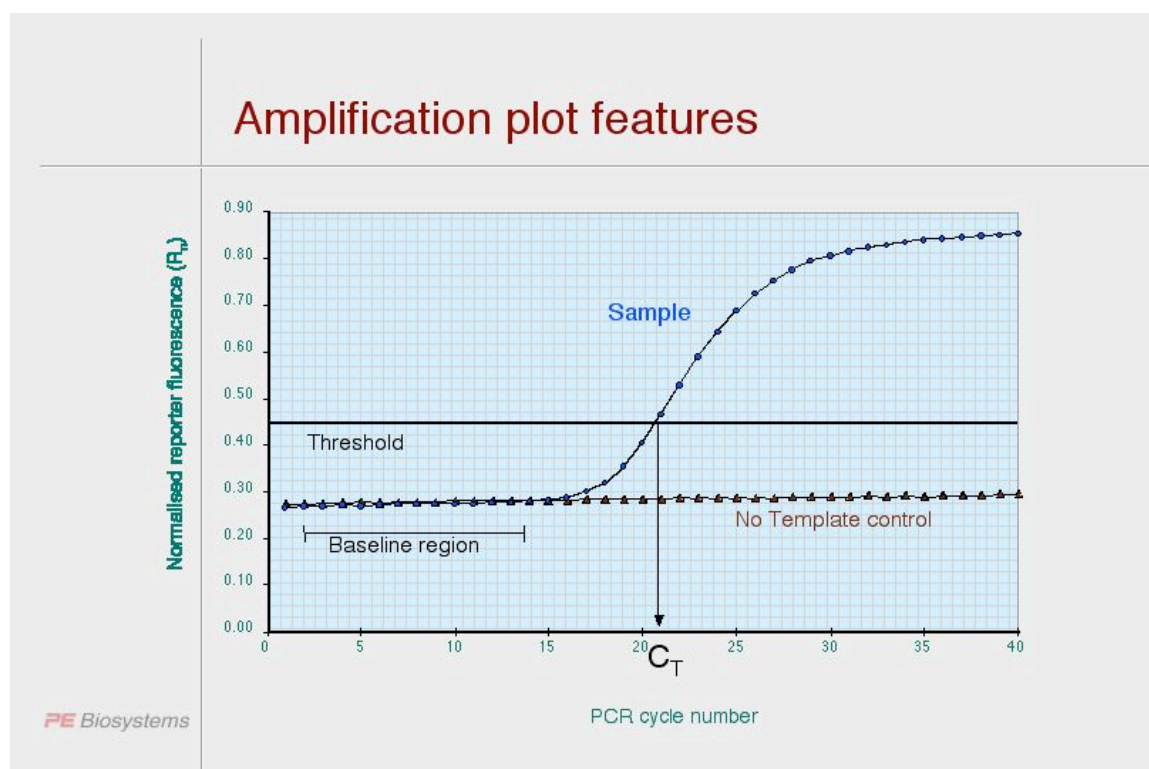


Figure 2.2. Example of a real-time PCR amplification output. The threshold and C_T are described in the text.

2.3.1 Necessary equipment

1. Real-time PCR instrument (e.g., Bio-Rad iCycler/MyiQ, or Applied Biosystems 7700).
2. Mechanical rotor homogeniser.
3. Pipettes: 20, 200, and 1000 μL .
4. UV spectrophotometer or fluorescent plate reader.
5. Water bath or heating block.

2.3.2 Tissue preparation

Investigations conformed to the Guide for the Care and Use of Laboratory Animals published by the US National Institutes of Health (NIH Publication No. 85-23, revised 1996). Hearts were acquired from male C57/B16 mice weighing 25-35g. Mouse heart tissue (descending aorta and heart complete) from 10 mice were excised and soaked in RNAlater solution. Heart tissues were dissected into aorta and left and right ventricle (with remaining septum discarded), and snap-frozen in liquid N₂ and stored at -80°C until subsequent RNA extraction.

2.3.3 Isolation of RNA from aorta, left and right ventricles

Snap-frozen aorta or ventricular tissue was homogenized in TRIzol reagent (Invitrogen, Carlsbad, CA), and total RNA isolated according to the manufacturer's protocol. Extracted total RNA was further treated with 50 U of DNase I (Promega, WI) for 15 min at 37°C and RNeasy spin-column purified (Qiagen, Hilden, Germany). Yield was determined spectrophotometrically and RNA integrity was assessed via formaldehyde agarose gel electrophoresis. Total RNA was stored at -80°C prior to cDNA synthesis.

2.3.4 cDNA synthesis

First-strand cDNA was synthesized from 5 µg of total RNA using 200 U of Superscript III (Invitrogen, Carlsbad, CA) with 200 ng of random hexamers according to manufacturer's instructions. Random hexamers were used to enable the use of β -actin as the invariant endogenous control. After heat inactivation, RNA was alkali hydrolysed and neutralised. Synthesized cDNA was diluted with nuclease free water 1:20 and stored at -20°C before use.

2.3.5 *Quantitative real-time PCR*

Real-time quantitative PCR was performed in triplicate on an ABI PRISM 7700 Detection System using TaqMan PCR Master Mix (Biorad icycler). The final reaction volume (20 μ l) included 0.5 μ l TaqMan Universal PCR master mix, and 5 μ L of diluted cDNA. The reaction cycle consisted of a 50°C step for 2 min, a second stage step to 95°C for 10 min, followed by 45 cycles consisting of 15 s at 95°C and 1 min at 60°C. Gene expression assays (Table 4.1) were purchased from Applied Biosystems, Foster City, CA. Sequences for actin primers and fluorogenic probe (Ribosomal RNA Control Reagents kit) are propriety from Applied Biosystems. Using a primer matrix, optimal reaction concentrations for β -actin were as follows: 20 nM forward, 20 nM reverse primer, and 100 nM probe. All reaction plates contained a serial dilution series (1:20, 1:40, 1:80, and 1:160) of cDNA pooled from all groups, these controls enabling inter-assay normalisation between reaction plates for the same transcript. All fluorescent signals were compared to non-template controls in which identical reaction constituents were added without cDNA (to determine baseline noise). Gene expression changes were confirmed on ≥ 2 separate reaction plates per tissue sample.

Relative expression and statistical analysis: Following baseline correction the threshold level was set during the geometric phase of PCR amplification for quantitative measurement. This was performed separately for each P2 gene and β -actin rRNA, according to Applied Biosystems guidelines. Gene expression levels per tissue type are normalised relative to maximum gene expression level in each tissue.

2.4 DATA ANALYSIS

All results are expressed as means \pm SEM. Data were compared and analysed using a multi-way ANOVA, with Student-Newman-Keuls post-hoc test when significant effects were detected (unless otherwise stated). In all statistical tests significance was accepted for $P<0.05$.

CHAPTER 3

CHARACTERISATION OF THE *EX VIVO* MOUSE HEART MODEL

3.1 ABSTRACT

The Langendorff mouse heart model has been widely used in physiological research and in studying cardiac responses to ischaemic insult. Unfortunately, few groups have fully characterised this technically challenging model and hence variability persists in its preparation and reported functional properties. In this chapter, the basic properties of the Langendorff isolated heart model and its applicability in investigation of ischaemia-reperfusion injury and cardioprotection, were examined. Functional stability of normoxic murine hearts, the time course of post-ischaemic functional recovery, and effects of substrate supplementation (glucose \pm 2 mM pyruvate) and of 50 μ M of the known cardioprotectant Ado were assessed.

Normoxic hearts ($n=13$) paced at 420 ± 5 beats/min exhibited >130 mmHg systolic pressure development, and 23 ml/min/g coronary flow under normoxic conditions. Following 80 min of further normoxic perfusion, systolic pressure declined by $\sim 30\%$, left ventricular developed pressure (LVDP) was reduced by $\sim 15\%$ and coronary flow rate fell by $\sim 40\%$ (in keeping with reduced metabolic demand at lower work levels). Post-ischaemic functional recoveries following 20 min ischaemia-reperfusion did not differ significantly at 30 or 45 min reperfusion (*i.e.* had plateaued by ~ 30 min). Despite a lack of effect of pyruvate on final post-ischaemic recovery of LVDP, significant functional differences were observed during ischaemia, with diastolic contracture profoundly reduced by pyruvate supplementation. Hearts ($n=6$) treated with Ado 5 min prior to ischaemia exhibited significantly reduced diastolic dysfunction across all time points (including final diastolic contracture: 23 ± 1 mmHg in untreated hearts *vs.* 17 ± 1 mmHg in Ado treated hearts), though other functional parameters were not modified. These data highlight the modest functional decay that

is unavoidable in an *in vitro* cardiac model, reveal that a 30-45 min reperfusion period is sufficient for stabilisation of early post-ischaemic outcomes, and confirm predicted beneficial effects of substrate and a protectant.

3.2 INTRODUCTION

Oscar Langendorff first devised the isolated perfused heart method to investigate the mechanical activity of the completely isolated mammalian heart in 1895. The Langendorff preparation was originally used to monitor cardiac contractile function. Over a century, the method of Langendorff was improved and modified by numerous physiologists and pharmacologists, and only those preparations in which the coronary arteries are perfused by retrograde flow from the aorta (without pulmonary or systemic circulation) are termed a 'Langendorff heart'. The Langendorff-perfused mouse heart is widely employed model for the analysis of functional contractility and responses to ischaemic insult. Several adaptations of perfusion methodologies for mouse hearts have facilitated detailed analysis of cardiac and coronary phenotypic outcomes of gene manipulation in the intact organ [265-268].

Whilst recent appraisal of the Langendorff heart model by Skrzypiec-Spring and colleagues indicates the preparation is a robust and useful tool in modern cardiovascular/pharmacological research [269], only a small number of research groups [265-268] have characterised this challenging model. Variability persists in baseline functional measures and outcomes from ischaemia-reperfusion. Baseline contractile function, expressed in terms of left ventricular (LV) pressure development, may vary from as low as 40–70 mmHg [270-277] to ≥ 120 mmHg [267, 278-283]. In terms of ischaemia-reperfusion, functional recoveries from comparable ischaemic insults also vary considerably, from arguably excessive (80–100% restoration of pre-ischaemic function; [103, 284, 285] to very poor (<25% recovery of function; [286, 287]. Such variance may stem from basic model differences (Ca^{2+} , perfusion mode and pressure, substrate) together with potentially poor technical preparation. Here the

basic properties of the Langendorff isolated heart model were characterised before application to studies of P2 biology.

3.3 MATERIALS AND METHODS

Investigations conformed to the *Guide for the Care and Use of Laboratory Animals* published by the US National Institutes of Health (NIH Publication no. 85-23, revised 1996). Mice were anaesthetised with an intraperitoneal injection of sodium pentobarbitone (50 mg/kg), a thoracotomy was performed and hearts rapidly excised into ice-cold perfusion fluid. The aorta was cannulated on a shortened and blunted 21 gauge needle, and perfusion initiated at a constant pressure of 80 mmHg on the apparatus depicted in Figure 2.1. Thebesian fluid accumulation into the left ventricle was vented via a polyethylene drain through the apex of the heart, and a fluid-filled balloon constructed from polyvinyl chloride film was introduced into the left ventricle through an incision in the atrial appendage. The ventricular balloon was connected via fluid-filled tubing to a pressure transducer (ADInstruments, Castle Hill, NSW, Australia) for continuous assessment of ventricular performance, and was inflated to yield a LV end-diastolic pressure of 5 mmHg during the initial 15 min of stabilization, after which it was not adjusted further.

The frequency response and damping of the balloon and transducer have been described previously [267]. Hearts were immersed in warmed perfusate in a jacketed bath maintained at 37°C, and perfusate delivered to the coronary circulation was maintained at the same temperature. Organ bath and perfusate temperatures were continuously monitored using a three-channel Physitemp TH-8 digital thermometer (Physitemp Instruments Inc., Clifton, NJ, USA). Coronary flow was measured using

an in-line Doppler flow probe (Transonic Systems Inc., Ithaca, NY, USA). Flow and LV pressure signals were recorded on a four-channel MacLab Data Acquisition System (ADInstruments). LV pressure was digitally processed to yield systolic, end diastolic and developed (LVDP) pressures, heart rate, and the peak positive and negative differentials of pressure change with time ($+dP/dt$ and $-dP/dt$, respectively).

Ventricular pacing at 420 beats/min (unless indicated otherwise) was initiated after 15 min stabilization to normalise heart rate across groups, and hearts were stabilised a further 15 min before experimentation. This heart rate corresponds to optimal LV performance in this in vitro model, based on prior work [267]. To facilitate oxygenation and limit degassing/stagnation within the apparatus at low flows, the volume between the compliance chamber and aortic cannula was minimised and perfusion fluid pumped through the compliance chamber and overflow at $\sim 10\times$ baseline coronary flow rate (Figure 2.1). A modified Krebs–Henseleit perfusion fluid was used in all experiments, except for the glucose group within the current study, as shown in Table 3.1. The fluid was bubbled with a mix of 95% O₂ and 5% CO₂ at 37°C to give a pH of 7.4, and was filtered through an in-line 0.45 μm Sterivex-HV filter (Millipore, Bedford, MA, USA) before delivery to the heart.

The volumes between the compliance chamber and heating coil (the volume of the coil being 5.5 ml), and between the heating coil and cannula, are minimised to limit ‘dead space’ and thus O₂ and heat loss at low absolute flows passing through the murine coronary vessels (1–5 ml/min). Clamping the overflow from the compliance chamber converts perfusion to constant flow, controlled via the peristaltic pump.

Table 3.1 - Recipe for formulation of modified Krebs–Henseleit solution.

<i>Salt</i>	<i>Molarity</i> (mM)	<i>MW</i>	<i>g/L</i>
NaCl	119	58.44	6.954
Glucose	11	180.16	1.982
NaHCO ₃	22	84.01	1.848
KCl	4.7	74.55	0.350
MgCl ₂	1.2	203.3	0.244
KH ₂ PO ₄	1.2	136.1	0.163
EDTA	0.5	372.24	0.186
CaCl ₂	2.5	147.02	0.368
Pyruvate*	2	110	0.220

* Pyruvate was excluded in the glucose group. MW, molecular weight.

Exclusion criteria

After the initial 15 min stabilisation, hearts were excluded from further study if any exhibited one or more of the following exclusion criteria: coronary flow greater than 5 ml/min (normally indicative of an aortic tear); LV pressure development less than 100 mmHg; intrinsic heart rate less than 320 beats/min or irregular.

Chemicals and reagents

All drugs used were purchased from Sigma-Aldrich (Castle Hill, Australia). Drug solutions were infused into hearts at $\leq 1\%$ of total coronary flow rate to achieve the final concentrations indicated.

Experimental protocol

Assessment of the normoxic functional stability

Normoxic Hearts ($n=13$): Normoxic hearts were paced following 15 min of equilibration and were aerobically perfused for a further period of 80 min. Functional parameters assessed included end diastolic pressure (EDP), systolic pressure, left ventricular developed pressure (LVDP), rate of change in LV pressure ($\pm dP/dt$), and coronary flow rate (ml/min/g).

Time course of post-ischaemic functional recovery

Hearts ($n=23$) were allowed 30 min of equilibration before being subjected to 20 min of global normothermic ischaemia and 45 min reperfusion. Recovery of functional parameters was assessed and compared at 30 and 45 min of reperfusion.

Effects of carbon substrate on functional recovery from ischaemia

Glucose only hearts ($n=6$) were perfused with the modified Krebs–Henseleit perfusion fluid described in Table 3.1, while pyruvate hearts ($n=23$) were supplemented with 2.0 mM pyruvate in the perfusion fluid. Following an initial 30 min of equilibration, all hearts were subject to 20 min global normothermic ischaemia and 45 min reperfusion.

Effects of Ado

Previous studies from the host laboratory show that Ado provides protection from ischaemia-reperfusion in isolated mouse hearts [148-159]. This series of experiments served to validate the Langendorff heart model in the investigation of potential

cardioprotective outcomes. Ado (50 μ M) was infused for 5 min before global normothermic ischaemia, and for the initial 5 min of reperfusion.

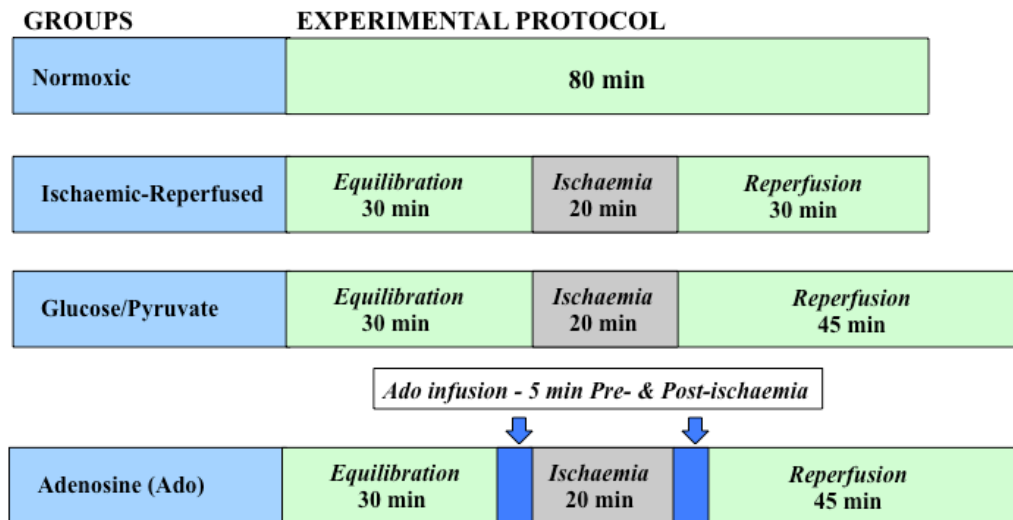


Figure 3.1 - Schematic overview of all experimental groups undertaken in the characterisation of the *ex vivo* mouse heart model.

3.4 RESULTS

Normoxic function

Normoxic cardiac function after initial equilibration and following a further 80 min of perfusion is outlined in Table 3.2. Initial (baseline) contractile function was high and in keeping with prior studies. Following 80 min of perfusion, LV pressure fell to $70 \pm 3\%$ of baseline, while coronary flow declined to $59 \pm 11\%$. LV diastolic pressure did not change significantly over this period. Changes in flow likely reflect a decline in ventricular metabolic demand at lower pressure development.

Table 3.2 - Functional parameters after stabilisation and 80 min of normoxic perfusion.

<i>Functional Parameter</i>	<i>Baseline</i>	<i>80 min Perfusion</i>
EDP (mmHg)	6±1	6±1
Systolic Pressure (mmHg)	133±2	92±4*
LVDP (mmHg)	128±2	88±4*
+dP/dt (mmHg/s)	3719±538	2943±427
-dP/dt (mmHg/s)	-2419±313	-1945±238
Coronary Flow (ml/min/g)	23±2	15±3*

Baseline functional data were measured before pacing commenced. Values are means±SEM. *, $P<0.05$ vs. Baseline.

Time course of post-ischaemic functional recovery

Functional data at 30 and 45 min of post-ischaemic reperfusion are provided in Table 3.3 and graphically in Figure 3.2. Data show that hearts recover between 50-60% of pre-ischaemic force development, with a sustained elevation in diastolic pressure of >20 mmHg. Thus, functional recovery is incomplete after this period of ischaemia, and of an intermediate level appropriate for assessment of either protective (enhancing recovery) or injurious (exaggerating recoveries) experimental stimuli. Post-ischaemic functional recoveries did not differ significantly between 30 and 45 min of reperfusion demonstrating a plateau in early post-ischaemic functional recovery by ~30 min (Figure 3.2).

Table 3.3 - Functional parameters in post-ischaemic hearts after 30 And 45 min of aerobic reperfusion.

<i>Functional Parameter</i>	<i>End of 30 min reperfusion (n=7)</i>	<i>End of 45 min reperfusion (n=23)</i>
EDP (mmHg)	24±3	23±1
Systolic Pressure (mmHg)	92±5	86±2
LVDP (mmHg)	67±6	63±2
+dP/dt mmHg/s	3557±327	2974±150
-dP/dt mmHg/s	-1894±235	-1674±52
Coronary Flow (ml/min/g)	18±1	20±2
% LVDP (pre-ischaemia)	55±5	55±2
% Coronary Flow (pre-ischaemia)	82±5	81±3

Data were measured at the end of 30 min or 45 min reperfusion. Values are means±SEM. *, $P<0.05$ vs. 30 min reperfusion.

Effects of pyruvate supplementation on ischaemic and post-ischaemic function

Functional data for glucose vs. pyruvate hearts are provided in Table 3.4. The inclusion of 2mM pyruvate altered functional responses significantly. Despite a lack of effect of pyruvate on final recovery of LVDP, a significant difference was observed in the initial 10 min of reperfusion (Figure 3.3). Similarly, no significant effect was detected for final diastolic recovery, though contracture differed significantly at 5 and 20 min of reperfusion. Interestingly, much greater (and earlier) ischaemic contracture was observed in glucose vs. pyruvate hearts (Figure 3.3).

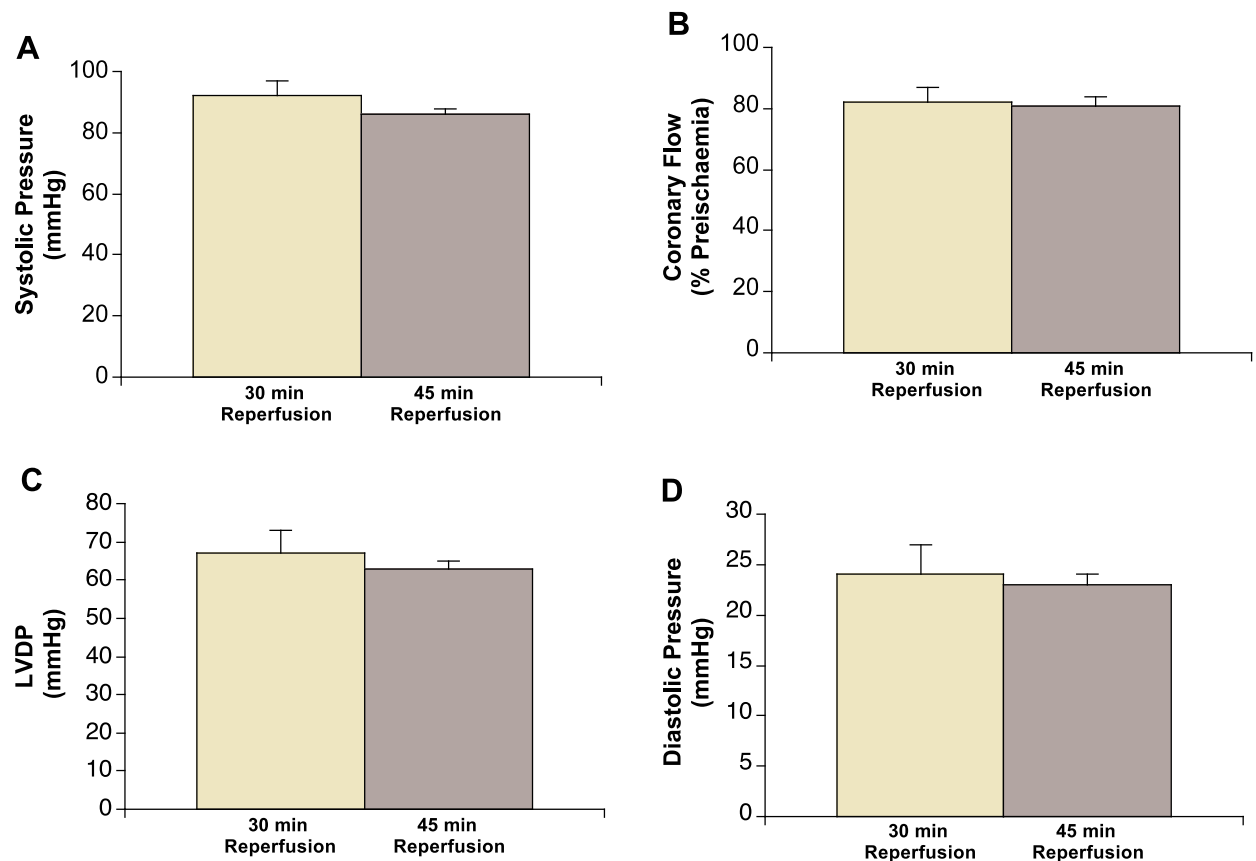


Figure 3.2. Functional outcomes from 20 min ischaemia after 30 vs. 45 min of aerobic reperfusion in pyruvate perfused hearts. Recoveries are shown for: systolic pressure (A); coronary flow rate (%Pre-ischæmia) (B); left ventricular developed pressure (C); and end-diastolic pressure (D). Values are means \pm SEM. *, $P<0.05$ vs. 30 min reperfusion.

Table 3.4 – Final post-ischæmic functional recoveries in pyruvate vs. glucose perfused mouse hearts.

<i>Functional Parameter</i>	<i>Glucose (n=6) Mean\pmSEM</i>	<i>Pyruvate (n=23) Mean\pmSEM</i>
EDP (mmHg)	24 \pm 1	23 \pm 1
Systolic Pressure (mmHg)	85 \pm 6	86 \pm 2
LVDP (mmHg)	71 \pm 4	63 \pm 2
+dP/dt mmHg/s	1686 \pm 122	2974 \pm 150
-dP/dt mmHg/s	-1400 \pm 347	-1674 \pm 52
Coronary Flow (ml/min/g)	20 \pm 1	20 \pm 2
% LVDP (pre-ischæmia)	60 \pm 4	55 \pm 2
% Coronary Flow (pre-ischæmia)	81 \pm 7	81 \pm 3

Data were measured at the end of 45 min reperfusion. Values are means \pm SEM. *, $P<0.05$ vs. glucose.

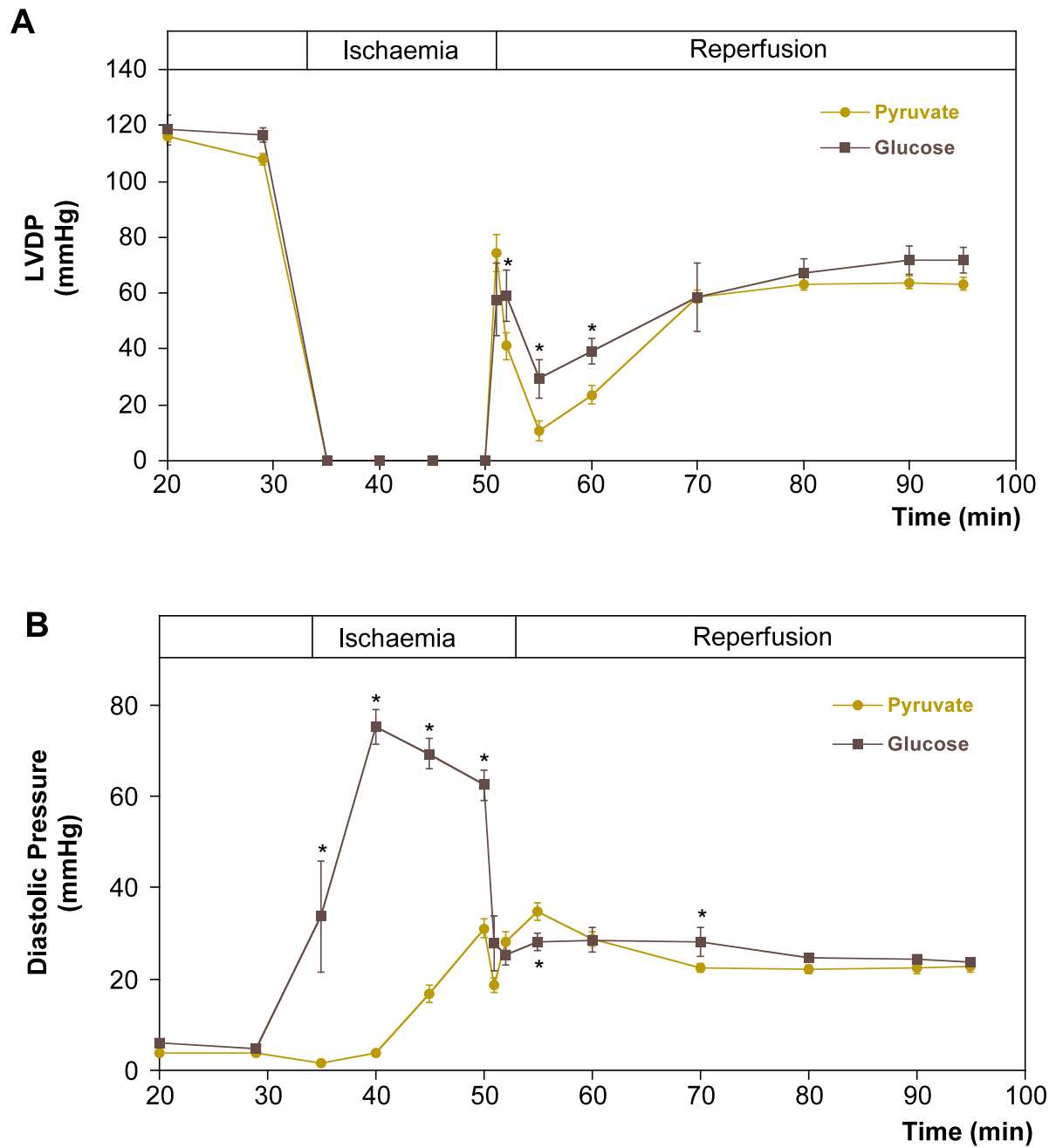


Figure 3.3. Effects of pyruvate ($n=23$) vs. glucose ($n=6$) on post-ischaemic recoveries for: (A) left ventricular developed pressure; and (B) left ventricular diastolic pressure. Values are means \pm SEM. *, $P<0.05$ vs. pyruvate.

Effects of the cardioprotectant Ado

Treatment with 50 μ M Ado significantly reduced diastolic dysfunction across all post-ischaemic time points, yet failed to alter other functional parameters (Table 3.5, Figure 3.4).

Table 3.5 – Final post-ischaemic functional recovery in control vs. Ado treated hearts.

<i>Functional Parameter</i>	<i>Control (n=23)</i>	<i>Ado (n=6)</i>
EDP (mmHg)	23 \pm 1	17 \pm 1*
Systolic Pressure (mmHg)	86 \pm 2	76 \pm 3
LVDP (mmHg)	63 \pm 2	63 \pm 1
+dP/dt mmHg/s	2974 \pm 150	3260 \pm 149
-dP/dt mmHg/s	-1674 \pm 52	-1702 \pm 66
Coronary Flow (ml/min/g)	20 \pm 2	21 \pm 1
% LVDP (pre-ischaemia)	55 \pm 2	53 \pm 2
% Coronary Flow (pre-ischaemia)	81 \pm 3	78 \pm 5

Data were measured at the end of 45 min reperfusion. Control hearts were untreated, while Ado treated hearts received 50 μ M Ado for 5 min pre and post-ischaemia. Values are means \pm SEM. *, $P<0.05$ vs. control.

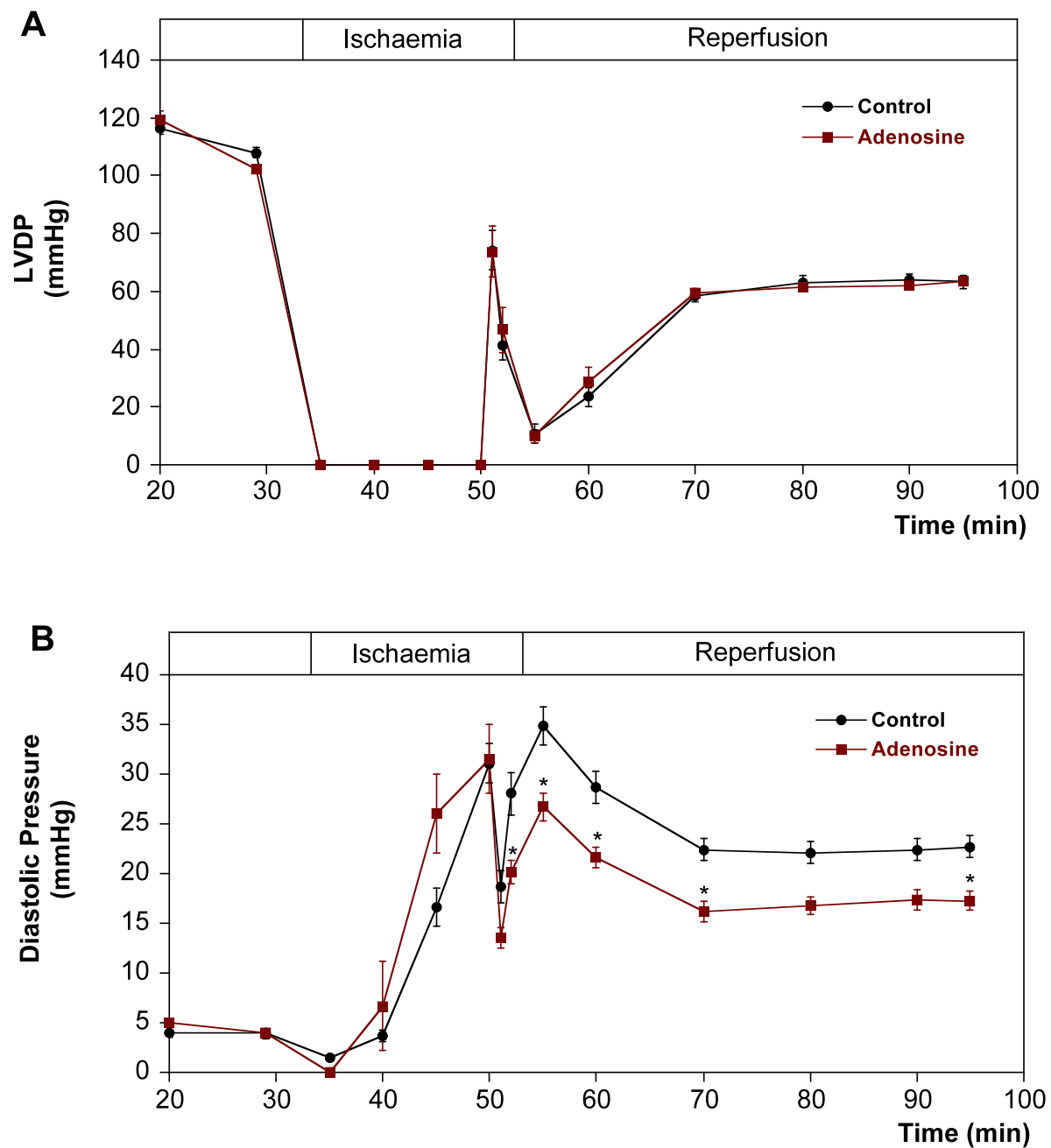


Figure 3.4 Effects of 50 μ M Ado on post-ischaemic recoveries of: (A) left ventricular developed pressure; and (B) left ventricular diastolic pressure. Data are shown for recoveries in control ($n=23$) vs. Ado ($n=6$) hearts. Values are means \pm SEM. *, $P<0.05$ vs. control.

3.5 DISCUSSION

The isolated perfused heart model is a popular tool for investigations of mammalian cardiac function. Nonetheless, relatively little data is given regarding basic properties of the model, and few have undertaken detailed characterisations, which may contribute to unacceptable variations in baseline function and ischaemic outcomes between laboratories.

Normoxic function and stability

The functional status of isolated 'crystalloid' perfused hearts is expected to deteriorate over time due to the absence of influential elements in whole blood and progressive tissue oedema that eventuates. It is therefore essential to examine functional stability over relevant experimental periods. Estimates of LVDP for isolated mouse hearts vary from as low as 50-60 mmHg, [103, 270, 288-292], to greater than 110 mmHg [154, 267, 293-295]. These values compare with *in situ* LV pressures of ~110 mmHg [296]. Thus, previous estimates of contractility are as low as 10% of *in situ* values. Here, developed pressure obtained exceeds 120 mmHg at a diastolic pressure of 5 mmHg at 37°C, in reasonable agreement with *in situ* parameters, and superior to many previous estimates.

Data in Table 3.2 shows that contractile function decreases by ~30% over an 80 min experimental period following initial stabilisation. This progressive decline is a feature of the *ex vivo* model, and should be considered when interpreting functional responses to experimental stimuli. Interestingly, time-course data reveals that LV systolic force is similar in post-ischaemic and normoxic hearts after similar perfusion periods. Thus systolic force generation does not appear to be substantially impacted

by ischaemia-reperfusion in this preparation. On the other hand, diastolic dysfunction was markedly worsened in post-ischaemic reperfused vs. normoxic heart as was (consequently) LVDP. These observations are consistent with prior work demonstrating that EDP appears a more reliable and consistent marker of cardiac injury [155, 297].

Temporal responses to ischaemia-reperfusion and effects of substrate and Ado

To confirm that 45 min reperfusion was sufficient for stabilisation of early post-ischaemic outcomes, responses at 30 and 45 min were contrasted. Data support the view that 45 min of reperfusion is sufficient for stable expression of contractile dysfunction (Figure 3.2, 3.3 and 3.4). Prior work has also established that significant cell death/infarction is manifest in this model by that time [155]. Clearly processes of injury will continue to evolve over time, however the 45 min reperfusion period should permit comparison of protective (or injurious) experimental interventions. Moreover, recovery with 20 min global ischaemia is appropriate for experimental modulation - a 50-60% recovery provides relevant scope for detecting either exacerbation or inhibition of cellular injury and functional outcomes with differing experimental interventions.

Effects of substrate (pyruvate supplementation) and Ado were also generally consistent with published responses. Pyruvate and Ado both limited contracture and diastolic dysfunction during or following ischaemia. During ischaemia itself contractile function ceases and a progressive rise in diastolic pressure occurs. The precise basis of this 'ischaemic contracture' remains to be fully resolved (though is thought to result from reduced anaerobic glycolytic ATP generation, among other

factors; [298-300]. Nonetheless, it is clear that contracture during ischaemia reflects the severity of ischaemic injury [300, 301]. Furthermore, reductions in contracture improve post-ischaemic functional recovery [301]. The present data reveal a profound reduction in contracture development in hearts supplemented with pyruvate, in agreement with prior studies [302]. How pyruvate supplementation reduces contracture is unclear. Addition of low levels of pyruvate to glucose-perfused hearts can facilitate glycolytic metabolism and ATP maintenance [303, 304]. Although pyruvate can improve oxidative metabolism via increased flux through pyruvate dehydrogenase, provide substrate for the TCA cycle [305, 306], and reduce oxidant injury in reperfused tissue [307-309], these effects do not explain reduced contracture during ischaemia. Indeed, previous investigators have observed enhanced contracture development with pyruvate (though when as a sole carbon substrate) in other species [310, 311], in agreement with the notion that glycolytic metabolism is critical in determining onset and extent of contracture [298-300].

Pre-ischaemic Ado receptor activation has also been shown to reduce contracture development [312] and mediate protective 'conditioning' effects [313-315], consistent with impaired contracture in hearts treated with 50 μ M Ado (Figure 3.4). Prior work shows that while locally generated Ado does not modify ischaemic contracture, exogenously applied Ado markedly limits contracture development [152]. The effects of Ado here are thus consistent with prior observations, and support a select impact of Ado receptors on diastolic dysfunction. Additionally, it has been shown in the current model that diastolic dysfunction and infarction are well correlated post-ischaemia [155]. Collectively the responses reported here are consistent with findings from prior

studies, supporting application of the Langendorff model in subsequent studies of ischaemia-reperfusion injuries.

CHAPTER 4

P2 PURINOCEPTOR GENE EXPRESSION PROFILES IN MOUSE MYOCARDIUM AND AORTA

4.1 ABSTRACT

Prior to subsequent investigations of P2 responses in the perfused mouse heart model, real-time PCR was employed to investigate the mRNA expression profile of the P2 purinoceptor subtypes in this organ (left vs. right ventricles) and in vascular tissue (aorta). Expression of mRNA for all nine P2 purinoceptors studied (P2X₁, P2X₄, P2X₅, P2X₇, P2Y₁, P2Y₂, P2Y₄, P2Y₆ and P2Y₁₂) was detected in aorta and ventricular tissue of the mouse. However, abundance and subtypes varied across tissues. The P2X₁, P2X₇ and P2Y₄ transcripts were most abundant in vascular tissue; P2X₇ and P2Y₂ most abundant in left ventricle; and P2X₄, P2X₅, P2Y₁, P2Y₆ and P2Y₁₂ most abundant in the right ventricle. The LinRegPCR application was used to determine mean RT-PCR reaction efficiencies, which ranged between 1.93 - 2.30. These data established the presence of all nine P2 transcripts in mouse heart, with predominant expression of P2Y₁ and P2Y₂ in myocardial vs. vascular tissues suggestive of specific cardiac roles for these subtypes. On the other hand high expression of P2X₁ supports a potential regulatory role for this subtype in vascular tissue.

4.2 INTRODUCTION

P2 purinoceptors are membrane bound receptors that mediate the diverse regulatory actions of extracellular nucleotides. P2X purinoceptors are ligand-gated ion channels whereas P2Y purinoceptors are members of the GPCR superfamily. The P2X purinoceptor has a two-transmembrane motif that is structurally related to the amiloride-sensitive epithelial Na⁺ channel [197] and is made up of between 379-472 amino acids that are inserted in the membrane, forming a pore comprised of two hydrophobic transmembrane domains and a large extracellular hydrophilic loop. P2X receptors were found to be most potently activated by stable analogues of ATP, α,β -methylene ATP (α,β -meATP), and β,γ -meATP. In contrast, P2Y purinoceptors are typically of a seven transmembrane motif and sensitive to activation by both purines (ATP, UDP) and pyrimidines (UTP, UDP). Generally, P2Y purinoceptors consist of 308 to 377 amino acid proteins.

A number of studies identify expression of P2 purinoceptors in a wide variety of tissue types in animal models and humans. Early RNA blotting studies by Tokuyama *et al.* showed that rat P2Y purinoceptor mRNA was expressed in numerous tissues including heart, brain, spleen, lung, liver, skeletal muscle and kidney [215]. Hou *et al.* identified similar P2 purinoceptor expression profiles in both rat and human myocardium [184]; involving expression of P2X₁, P2Y₁, P2Y₂, P2Y₄ and P2Y₆ in both tissue types, and the additional purinoceptor P2Y₁₁ in human myocardium. Additionally, the expression of P2X₁, P2X₃, P2X₄, P2Y₆, P2Y₂ and P2Y₄ receptor subtypes have been identified in the human foetal heart, suggesting a contributing role for purinoceptors in foetal heart development [183]. The expression of P2 purinoceptors has also been shown to be modified during development of heart

disease [184, 189, 190, 316, 317]. To date, ionotropic P2X₁₋₇ purinoceptors and metabotropic P2Y_{1,2,4,6,11} have been cloned and respective mRNAs detected in cardiomyocytes. Here we investigated the expression profile of P2 purinoceptors as a gauge of relative expression patterns, and as an initial assessment of which subtypes might play regulatory roles in murine myocardium.

4.3 MATERIALS AND METHODS

Real-Time Polymerase Chain Reaction (PCR)

RT-PCR was used to assess the gene expression profile for P2 receptor subtypes. This method amplifies small amounts of mRNA and allows the simultaneous quantification of the PCR product in an attempt to measure the level of expression of the mRNA of a specific protein. In this case, the genetic expression of the P2 receptors is quantified by performing RT-PCR on cDNA derived from the mRNA of the descending aorta and left and right ventricles of young adult mouse hearts.

PCR product is quantitated in 'real time' by measuring the increase in fluorescence emission during the course of the amplification process. SYBR green I emits fluorescence when bound to double-stranded DNA. At the beginning of the PCR amplification process, a baseline fluorescent emission is detected from the sample. After every cycle of amplification, the degree of fluorescence emission (RFU) is detected and measured. As the amount of PCR product increases due to amplification, the amount of fluorescence increases as the dye binds to the double-stranded cDNA. The change in fluorescent emission is calculated between the baseline at time zero and the amplification cycle at time 'x'. An amplification plot is derived from the data, as shown in Figure 2.2, which are characterised by a threshold,

an exponential or log phase and a plateau. The individual curves represent different input quantities. C_T is the threshold cycle, which represents the cycle at which the exponential phase begins, while ΔR_n represents the fluorescent signal.

Table 4.1 - Purinoceptors and respective Taqman products employed.

<i>Receptor</i>	<i>Taqman Product ID no. (Applied Biosystems, VIC, Australia)</i>
P2X ₁	Mm00435460_m1
P2X ₄	Mm00501787_m1
P2X ₅	Mm00473677_m1
P2X ₇	Mm00440582_m1
P2Y ₁	Mm00435471_m1
P2Y ₂	Mm00435472_m1
P2Y ₄	Mm00445136_m1
P2Y ₆	Mm01275473_m1
P2Y ₁₂	Mm00446026_m1

Tissue preparation

Investigations conformed to the Guide for the Care and Use of Laboratory Animals published by the US National Institutes of Health (NIH Publication No. 85-23, revised 1996). Hearts were acquired from male C57 mice weighing 25-35 g and anaesthetised with sodium pentobarbital IP (50mg/kg). Mouse heart tissue (descending aorta and heart complete) from 10 mice were excised and soaked in RNAlater solution. A section of ascending aorta was excised, and hearts trimmed to give left and right

ventricular myocardium which were all immediately snap-frozen in liquid nitrogen and stored at -80°C for subsequent RNA extraction.

Isolation of RNA from aorta, left and right ventricles

Frozen aorta and left and right ventricular myocardium were homogenized in TRIzol reagent (Invitrogen, Carlsbad, CA), and total RNA was isolated according to the manufacturer's protocol. Extracted total RNA was further treated with 50 U of DNase I (Promega, WI) for 15 min at 37°C, and RNeasy spin column purified (Qiagen, Hilden, Germany). Yield was determined spectrophotometrically and RNA integrity was observed via formaldehyde agarose gel electrophoresis. Total RNA was stored at -80°C prior to cDNA synthesis.

cDNA synthesis

First-strand cDNA was synthesized from 5 ug of total RNA using 200 U of Superscript III (Invitrogen, Carlsbad, CA) with 250 ng of random hexamers according to manufacturer's instructions. Random hexamers were used to enable the use of β -actin as an invariant endogenous control. After heat inactivation, RNA was alkali hydrolysed and neutralised. Synthesised cDNA was diluted 1:20 with nuclease free water and stored at -20°C before use.

Quantitative real-time PCR

Real-time quantitative PCR was performed in triplicate on an ABI PRISM 7700 Detection System using TaqMan PCR Master Mix. The final reaction volume (20 μ l) included 0.5 μ l TaqMan Universal PCR master mix, 5 μ L of diluted cDNA. The reaction cycle consisted of a 50°C step for 2 min, a second stage step to 95°C for 10 min, followed by 45 cycles consisting of 15 s at 95°C and 1 min at 60°C. Gene expression assays (Table 4.1) were purchased from Applied Biosystems (Foster City, CA). Sequences for actin primers and fluorogenic probe (ribosomal RNA Control Reagents kit) are propriety from Applied Biosystems. Optimal reaction concentrations for β -actin were as follows: 20 nM forward, 20 nM reverse primer, and 100 nM probe. All reaction plates contained a serial dilution series (1:20, 1:40, 1:80, and 1:160) of cDNA pooled from all groups, enabling inter-assay normalisation between reaction plates for the same transcript. All fluorescent signals were compared to nontemplate controls in which identical reaction constituents were added without cDNA to determine baseline noise. Gene expression changes were confirmed on at least two separate reaction plates per tissue sample. Following baseline correction the “threshold” level was set during the geometric phase of PCR amplification for quantitative measurement. This was performed separately for each P2 gene and β -actin rRNA according to Applied Biosystems guidelines. For each transcript, expression levels are expressed relative to the maximum expression level achieved in one tissue type. RT-PCR reaction efficiencies were ascertained using the application LinRegPCR, where calculations based on linear regression on the Log(Fluorescence) per cycle number derive estimated reaction efficiencies.

4.4 RESULTS

P2X purinoceptor subtype gene expression in the mouse heart

P2X₁ Purinoceptor – The P2X₁ transcripts was predominantly expressed in aorta, with only 2% of these levels evident in the left ventricle and 5% in the right ventricle.

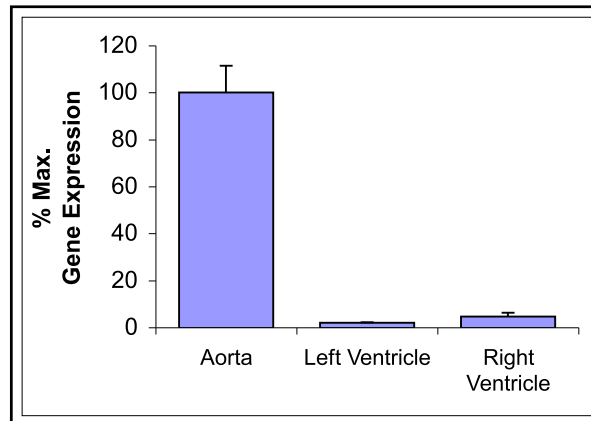


Figure 4.1. Relative vascular vs. ventricular mRNA expression of P2X₁ purinoceptor. Data expressed as a % of the maximum level achieved in the tissue (% Max Gene expression).

P2X₄ Purinoceptor - P2X₄ transcripts was expressed to a slightly higher extent in left and right ventricles vs. aorta (56%).

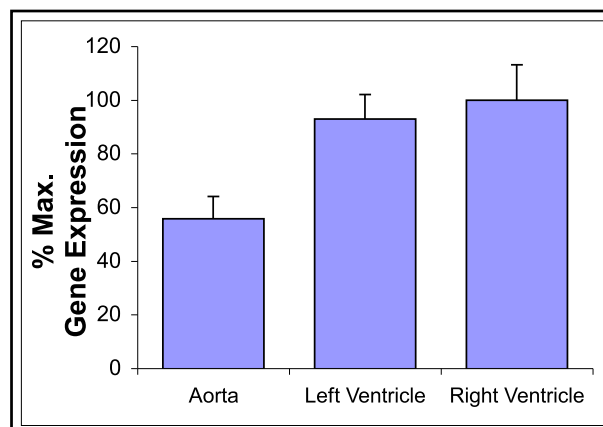


Figure 4.2. Relative vascular vs. ventricular mRNA expression of P2X₄ purinoceptor. Data expressed as a % of the maximum level achieved in the tissue (% Max Gene expression).

P2X₅ Purinoceptor – The P2X₅ was most highly expressed in the right ventricle (100%) followed by left ventricle (~70%), and was lowest in aorta (~40%).

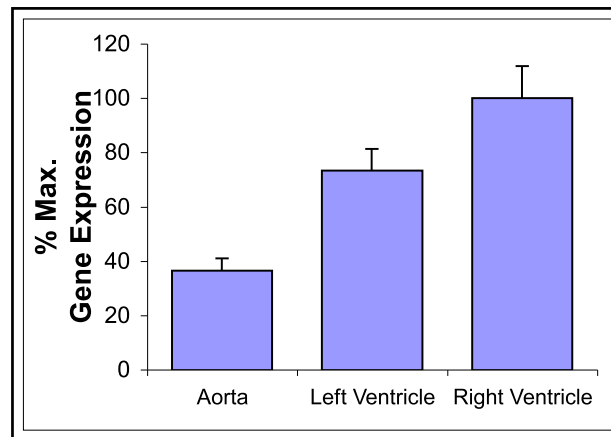


Figure 4.3. Relative vascular vs. ventricular mRNA expression of P2X₅ purinoceptor. Data expressed as a % of the maximum level achieved in the tissue (% Max Gene expression).

P2X₇ Purinoceptor - The P2X₇ transcript was commonly expressed in all three tissues.

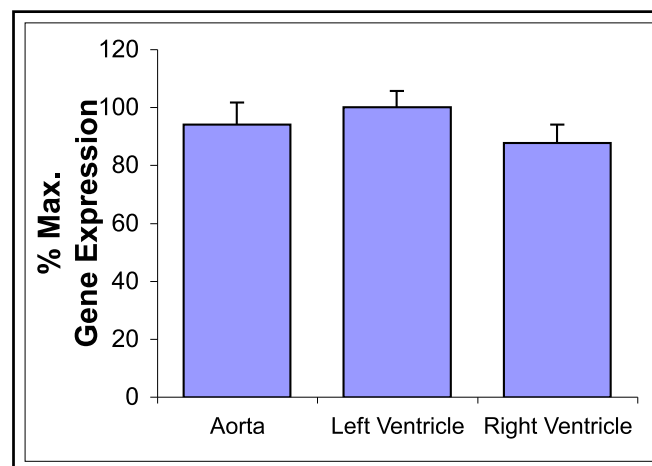


Figure 4.4. Relative vascular vs. ventricular mRNA expression of P2X₇ purinoceptor. Data expressed as a % of the maximum level achieved in the tissue (% Max Gene expression).

P2Y purinoceptor subtype gene expression in the mouse heart

P2Y₁ Purinoceptor - The P2Y₁ transcript was most highly expressed in ventricular tissue, being similar in left vs. right, and lowly expressed in aorta (~15%).

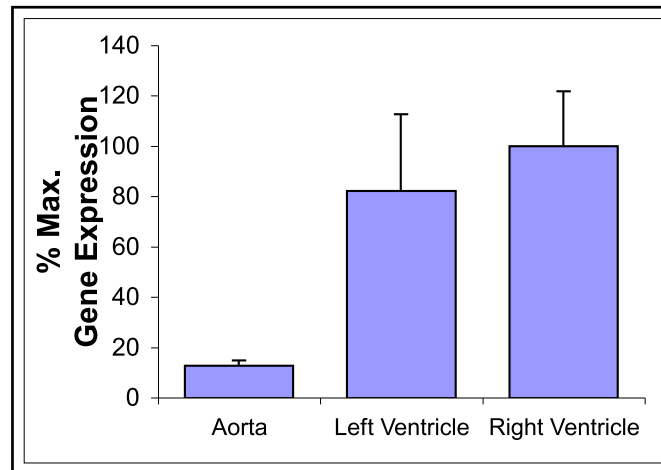


Figure 4.5. Relative vascular vs. ventricular mRNA expression of P2Y₁ purinoceptor. Data expressed as a % of the maximum level achieved in the tissue (% Max Gene expression).

P2Y₂ Purinoceptor - The mRNA expression of P2Y₂ purinoceptor was highest in the left ventricle followed by right ventricle (~70%), and lowest in aorta (~20%).

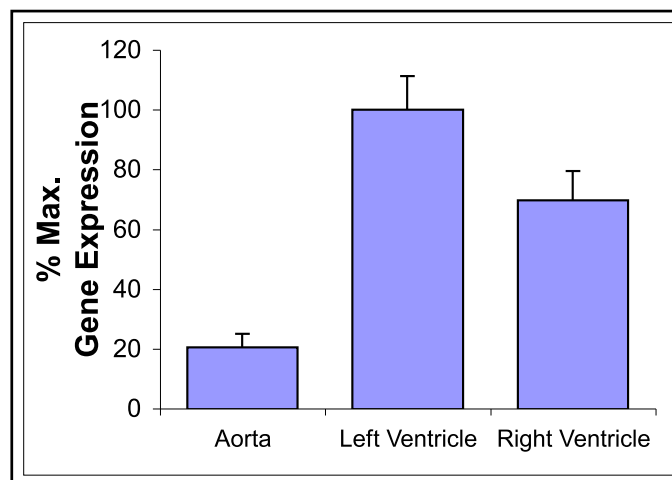


Figure 4.6. Relative vascular vs. ventricular mRNA expression of P2Y₂ purinoceptor. Data expressed as a % of the maximum level achieved in the tissue (% Max Gene expression).

P2Y₄ Purinoceptor - The P2Y₄ transcript was relatively highly expressed across all tissue types.

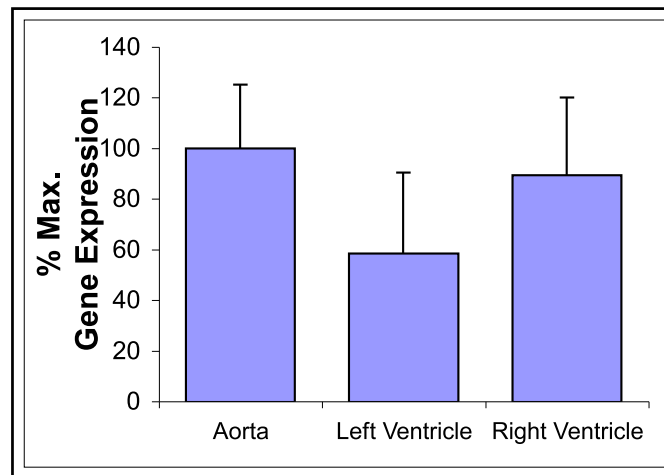


Figure 4.7. Relative vascular *vs.* ventricular mRNA expression of P2Y₄ purinoceptor. Data expressed as a % of the maximum level achieved in the tissue (% Max Gene expression).

P2Y₆ Purinoceptor - The P2Y₆ purinoceptor transcript was most highly expressed in right ventricular tissue, and equally expressed in left ventricle and aorta (50-60% of right ventricle levels).

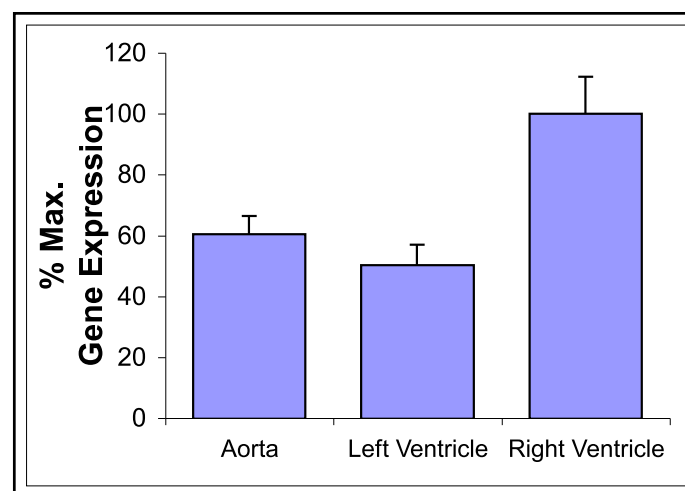


Figure 4.8. Relative vascular *vs.* ventricular mRNA expression of P2Y₆ purinoceptor. Data expressed as a % of the maximum level achieved in the tissue (% Max Gene expression).

P2Y₁₂ Purinoceptor – Like the P2Y₆, P2Y₁₂ purinoceptor transcript was most highly expressed in the right ventricle, and equally expressed in left ventricle and aorta (~50%).

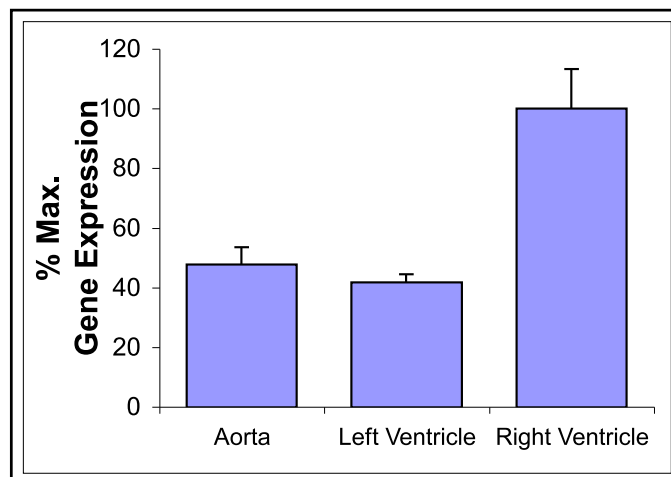


Figure 4.9. Relative vascular vs. ventricular mRNA expression of P2Y₁₂ purinoceptor. Data expressed as a % of the maximum level achieved in the tissue (% Max Gene expression).

Table 4.2 - Overview of mRNA expression for P2 purinoceptor subtypes in mouse heart and aorta.

<i>Purinoceptor Subtype</i>	<i>Aorta (n=6)</i>	<i>Left Ventricle (n=7)</i>	<i>Right Ventricle (n=7)</i>
P2X ₁	100%	2%	5%
P2X ₄	56%	93%	100%
P2X ₅	37%	73%	100%
P2X ₇	94%	100%	88%
P2Y ₁	13%	82%	100%
P2Y ₂	21%	100%	70%
P2Y ₄	100%	58%	89%
P2Y ₆	61%	50%	100%
P2Y ₁₂	48%	42%	100%

Data expressed as % Max Gene expression.

Table 4.3 - Comparison of RT-PCR efficiency, Ct(E) values and mean reaction efficiency.

<i>Purinoceptor Subtype</i>	<i>Aorta (n=6)</i>	<i>Left Ventricle (n=7)</i>	<i>Right Ventricle (n=7)</i>	<i>Mean PCR Efficiency</i>
P2X ₁	3.74±0.43	0.07±0.01	0.17±0.06	2.057
P2X ₄	0.66±0.10	1.10±0.11	1.18±0.16	2.105
P2X ₅	0.68±0.08	1.36±0.15	1.86±0.22	2.301
P2X ₇	1.03±0.08	1.10±0.06	0.96±0.07	2.117
P2Y ₁	0.16±0.02	1.04±0.38	1.26±0.28	1.935
P2Y ₂	0.25±0.06	1.24±0.14	0.86±0.12	2.148
P2Y ₄	2.85±0.72	1.67±0.91	2.55±0.88	1.933
P2Y ₆	1.11±0.11	0.92±0.12	1.83±0.22	2.132
P2Y ₁₂	0.93±0.11	0.82±0.05	1.96±0.26	2.174

Ct values presented are standardised against β -actin. Variance = 0.012

P2 purinoceptor gene expression profile in the mouse heart

Expression of mRNA for all nine P2 purinoceptors studied (P2X₁, P2X₄, P2X₅, P2X₇, P2Y₁, P2Y₂, P2Y₄, P2Y₆ and P2Y₁₂) was observed in the aorta, left and right ventricles of the mouse. However, their abundance varied in different regions of the heart as highlighted in prior figures. Thus, in general P2Y₁, P2Y₂ and P2X₄ and P2X₅ were differentially expressed in ventricle vs. aorta while P2X₁ was the only vascular subtype. Curiously, P2Y₆ and P2Y₁₂ were selectively expressed in the right ventricle. Given the similarity in RT-PCR reaction efficiencies for each purinoceptor (see Table 4.3); some general comparison of transcript expression levels between the investigated purinoceptors can be made. P2X₁ and P2Y₄ transcripts are the most

abundant in the vasculature, P2X₅ and P2Y₂ and P2Y₄ transcripts in the left ventricle, and P2Y₄, P2Y₆, P2Y₁₂ and P2X₅ are most abundant in the right ventricle.

4.5 DISCUSSION

All nine transcripts were detected in either ventricular or aorta tissue, supporting (but not confirming) protein expression of these receptors in the heart and vessels. While only a view of gene transcription, the relative mRNA levels may be of relevance to the functional importance of P2 subtypes in different tissues. Data suggests high expression (thus potential regulatory roles) for P2Y₁ and P2Y₂ in myocardial vs. vascular tissues, whereas high expression of P2X₁ may reflect an important and specific vascular role for this subtype.

P2X_{1,4,5,7} purinoceptors gene expression in heart and aorta

The P2X₁ purinoceptor mRNA was expressed at a significantly higher level in the aorta compared with the ventricles. This hints at a role for this receptor subtype in regulating vascular function. Several studies over the last two decades have implicated a role for P2X receptors in regulating the vasculature [175, 205, 318, 319]. Hopwood *et al.* first suggested in 1987 that ATP mediates vasoconstriction via P2X receptors in rat coronary vessels [175]. This receptor subtype was also found expressed on both endothelium and smooth muscle, where it may exert bi-functional roles. Vascular responses to ATP mediated via P2X₁ receptors appear dependant on cellular location, with contraction for receptors located on smooth muscle cells, and dilation for receptors expressed on endothelium (akin to effects of P2Y receptors) [319].

Vascular control via P2X₁ is supported by work showing down regulation of the P2X₁ subtype in peripheral resistance arteries as a compensatory response to enhanced peripheral sympathetic nerve activity and vascular resistance in congestive heart failure [316]. Up-regulation of P2X₁ mRNA and its protein has also been observed in congestive heart failure, suggesting a pathophysiological role for these receptors [184, 320].

P2X₄ transcript was highly expressed in murine ventricles, consistent with investigations by other groups and a role in cardiac control. Transgenic overexpression of the human P2X₄ purinoceptor in mice results in an enhanced basal level of cardiac output and contractile function compared with wild-type mice [185]. In a calsequestrin overexpression model of cardiomyopathy, P2X₄ purinoceptor exhibited a beneficial role in extending lifespan, improving LV weight-to-body weight ratio and restoring β -adrenergic responsiveness [211]. Similarly, Sonin *et al.* found P2X₄ activity improved LV pressure development and rate of contraction, significantly increasing fractional shortening and systolic thickening in non-infarcted tissue in P2X₄ overexpressing mice subjected to ischaemic heart failure [317].

Expression of P2X₅ purinoceptor mRNA was highest in right and left ventricles, although its role in ventricular myocardium remains unclear. A potential role in mammalian heart development has been forwarded: in developing rat heart, abundance of co-localised P2X₂ (this subtype not studied here) and P2X₅ receptor clusters were detected on the sarcolemma [321]. A recent study by Birdsong *et al.* suggests a role for P2X₅ purinoceptors in mediating ischaemic pain, whereby ATP

binds P2X₅ receptors to form a molecular complex with acid-sensing ion channels to detect lactic acidosis [322].

Levels of P2X₇ mRNA were similar in both aorta and ventricles. Activation of P2X₇ modulates many cellular processes, including Ca²⁺ fluxes, MAPK activation, inflammatory mediator release, and apoptosis [259, 260, 323-325]. Studies suggest the P2X₇ has a potentially pivotal role in inflammatory responses, stemming from its role in mediating ATP-triggered IL-1 β release [198, 324, 326]. Evidence for a role in apoptotic modulation has also been acquired in different tissues, including brain, immune, bone, nerve and tumour cells [325, 327-329]. Studies of ischaemia-reperfusion and conditioning responses and by Vessey *et al.* indicate that the P2X₇ purinoceptor combines with pannexin-1 to form channels that facilitate release of cardioprotectants such as Ado and sphingosine 1-phosphate [187, 213].

Co-expression of multiple P2X subtypes in ventricular and vascular tissue raises the possibility of heteromeric receptor complexes. Increasingly, research findings implicate functional heteromeric assembly between P2X purinoceptors. Studies have confirmed a heteromeric assembly of co-expressed P2X₁ and P2X₅ purinoceptors, revealing an additional ATP-gated ion channel [200, 330]. Evidence for heteropolymerisation of P2X₂ and P2X₃ purinoceptors has also been presented [199, 331]. Specifically, myocardial ischaemic nociceptive transmission in neuronal circuits is mediated by P2X₃ and P2X_{2/3} receptors, and blockade counters cardiac dysfunction [331]. Harhun *et al.* determined that two types of functional P2X receptors are expressed in renal vascular smooth muscle cells: monomeric P2X₁ and heteromeric P2X_{1/4} receptors, [332]. P2X₄ and P2X₇ purinoceptors, both playing a role in

neuropathic pain, have also been proposed to form structural and functional heteromers [333, 334]. Given evidence for structural and functional heteromeric assembly between P2X subtypes, additional to functional P2X monomers, effects of P2 purinoceptors in the heart and vessels are likely to be much more complex than initially thought.

P2Y_{1,2,4,6,12} purinoceptors gene expression in heart and aorta

Expression of P2Y₁ transcript was relatively high in ventricular compared to aortic tissue. This ADP-receptor subtype has been associated with induction of platelet aggregation [335, 336], induction of apoptosis [256], and also cardioprotection [337]. A recent study also supports involvement of the P2Y₁ in negative feedback control of the balance between myocardial O₂ consumption and coronary blood flow during exercise [338]. Expression of P2Y₂ mRNA levels was also highest in ventricle vs. aorta. Several studies provide evidence for P2Y₂ purinoceptor influences on intracellular Ca²⁺ release and in modifying Cl⁻ secretion in cystic fibrosis [339-341]. Further modulatory effects of the P2Y₂ purinoceptor on Ca²⁺ concentrations were described in cardiomyocytes. UTP activation of P2Y₂ and P2Y₄ purinoceptors produces IP₃, leading to an increase in intracellular Ca²⁺, triggering oscillatory Cl⁻ currents and membrane potential changes in rat aortic myocytes [253], together with positive inotropy [189]. Yitzhaki *et al.* demonstrated that preconditioning via UTP activation of P2Y₂ receptors reduces infarct size and improves heart function through a reduction in mitochondrial Ca²⁺ overload [255]. Together with the P2X₁, P2Y₂ mRNA expression is up-regulated in congestive heart failure [184]. Further study of UTP effects by Yitzhaki *et al.* indicates that P2Y₂ purinoceptors significantly reduce cardiomyocyte death with hypoxia [254]. More recently, the P2Y₂ was also identified

as the major purinergic receptor in human vascular endothelial cells, mediating vasorelaxation with ATP [342].

Data for P2Y₄ mRNA reveals high expression in aortic tissue. Similar to other P2Y purinoceptors (P2Y₁, P2Y₂, and P2Y₆) detected in aortic smooth muscle cells, the P2Y₄ evokes Ca²⁺ signalling via activation of PLC [235, 236]. P2Y₆ transcript was most abundant in the right ventricle, and several studies have described its effects on cardiomyocytes. According to Wihlborg *et al.*, UDP acting on this receptor subtype produces positive inotropy via an IP₃-dependent path, and may be involved in development of cardiac disease [189]. Nishida *et al.* found that extracellular nucleotide-stimulated P2Y₆ activation of G $\alpha_{(12/13)}$ in cardiomyocytes triggers fibrosis during pressure overload [190]. A role in cardioprotection has also been noted: P2Y₁₁ (not studied here) and P2Y₆ purinoceptors have been shown to be involved in pyridoxal-5'-phosphate induced cardiac preconditioning [192].

Similar to P2Y₆ mRNA expression, P2Y₁₂ transcript was highest in the right ventricle. This receptor subtype has an important role in platelet aggregation [343, 344], while cardiac roles are less clear. Reciprocal cross-talk between P2Y₁ and P2Y₁₂ (where P2Y₁₂ positively regulates P2Y₁ actions, while P2Y₁ negatively regulates the P2Y₁₂) may maintain a balance between platelet activation and inhibition during haemostasis [244]. The P2Y₁₂ (a ADP receptor) is linked to G_i and plays a special role in amplification of platelet activation initiated by varied paths [345]. Furthermore, 2MeSADP activation of P2Y₁₂ purinoceptors antagonises TNF α -induced apoptosis, suggesting a possible cytoprotective role for this subtype [257]. The role of this purinoceptor subtype within the heart is yet to be defined.

It is important to note that exclusion of P2X₂, P2X₃, P2X₆, P2Y₃ and P2Y₁₁ in this gene expression study limits a more complete view of P2 purinoceptor co-expression and within mouse heart and vessels. Unfortunately, at the time of this work Taqman gene expression products were unavailable for these subtypes.

4.6 CONCLUSION

All nine P2 purinoceptors studied - P2X₁, P2X₄, P2X₅, P2X₇, P2Y₁, P2Y₂, P2Y₄, P2Y₆ and P2Y₁₂ were identified in the mouse heart, with relative abundances varying between aorta, and right and left ventricles. Of the P2 purinoceptors, P2X₁ and P2Y₄ transcripts were predominant in the aorta, with remaining purinoceptor transcripts expressed more highly in ventricular tissue. Relatively high expression of multiple subtypes in cardiac tissue supports potentially complex cardiovascular control by these receptors. Having established expression of multiple cardiac P2 transcripts, the aim of subsequent studies was to assess potential functional relevance of these receptors.

CHAPTER 5

P2 PURINOCEPTOR ANTAGONIST EFFECTS IN ISCHAEMIC-REPERFUSED MOUSE HEART - ROLES FOR INTRINSIC P2 ACTIVITY

5.1 ABSTRACT

Having established cardiac mRNA expression of a range of P2Y and P2X subtypes in the prior study, the current work addresses the potential roles of intrinsic P2 purinoceptor activity in determining cardiac stress tolerance (specifically, modifying myocardial responses to global ischaemia-reperfusion). Perfused C57/B16 mouse hearts were subjected to 20 min global ischaemia and 45 min reperfusion. Effects of P2 antagonists on post-ischaemic recoveries and oncosis (LDH efflux) were assessed. Antagonists were infused 5 mins prior to ischaemia and for the initial 5 mins of reperfusion, bracketing the primary period of stress. Control (CTRL) hearts recovered 65 ± 4 mmHg ventricular pressure development ($\sim 50\%$ of pre-ischaemia) and exhibited sustained diastolic contracture (24 ± 2 mmHg). P2Y antagonism with 1 or 100 μM reactive blue 2 (RB2) depressed post-ischaemic recovery (diastolic contracture increased to 37-45 mmHg, ventricular pressure development reduced to 15-30% of pre-ischaemia). Similarly, the P2Y antagonist suramin (200 μM) reduced functional recovery (40 ± 3 mmHg EDP, $\sim 28\%$ recovery of ventricular pressure development). Data also indicate that P2Y₁ antagonism with 3 μM 2'-deoxy-N⁶-methyladenosine-3', 5'-biphosphate (MRS2179) modestly depresses post-ischaemic recoveries. A role for P2X receptors was also supported by diminished post-ischaemic recovery with the P2X antagonists pyridoxal-5'-phosphate-6-azophenyl-4'-carboxylate (MRS2159) (3 μM) or 200 nM pyridoxal-5'-phosphate-6-(2'-naphthylazo-6-nitro-4',8'-disulphonate) (PPNDS), with diastolic contracture increased to 35-41 mmHg, and ventricular pressure development reduced to 25-35% of pre-ischaemia. Overall, detrimental effects of P2Y and P2X purinoceptor antagonists support some intrinsic protective function for both P2Y and also P2X receptors during cardiac ischaemia-reperfusion.

5.2 INTRODUCTION

Extracellular purines and pyrimidines modulate cellular function by interacting with P2 purinoceptors located in a variety of cell types, including the cardiomyocyte. P2 purinoceptors are classified into two main families of ligand-gated ion channels and G protein-coupled receptors termed P2X and P2Y purinoceptors. To date, seven subtypes of P2X (P2X₁₋₇) have been identified whilst eight mammalian P2Y subtypes have been established (P2Y₁, P2Y₂, P2Y₄, P2Y₆, P2Y₁₁, P2Y₁₂, P2Y₁₃ and P2Y₁₄).

In the heart, P2 purinoceptors have been implicated in aortic and coronary vasoconstriction and vasodilatation [161, 176, 223, 235, 346-349], cardiac inotropy [173, 186, 189, 209, 350-353], cardioprotection including pre- and post-conditioning [181, 187, 192, 213, 254, 255, 354, 355], and in the development of cardiac dysfunction [184, 190, 250, 331, 356, 357]. Furthermore, several P2 purinoceptors have a role in different aspects of platelet activity [335, 336, 358-361] that contributes to shifts in cardiac function *in vivo*. In the previous chapter, significant P2X_{1,4,5,7} and P2Y_{1,2,4,6,12} receptor transcript expression was detected in mouse heart and vasculature. However, potential functional roles of these receptors in terms of myocardial responses to ischaemic insult require more direct exploration. To determine whether accumulation of endogenous nucleotides (or other P2 agonists) might modify functional outcome from ischaemia-reperfusion, contractile and coronary responses of perfused hearts to ischaemia-reperfusion were assessed in the absence and presence of differing P2 antagonists.

5.3 MATERIALS AND METHODS

Perfused heart preparation and experimental protocol

Hearts were prepared as described in detail in **Chapter 2**. Investigations conformed to the Guide for the Care and Use of Laboratory Animals published by the US National Institute of Health (NIH Publication No 85-23, revised 1996). Experiments were undertaken in hearts removed from male C57 mice weighing 25-35g anaesthetised with a bolus injection sodium pentobarbital of (50 mg/kg) intraperitoneally.

Hearts were allowed 30 min of equilibration following aortic cannulation. After the initial 20 min of equilibration, hearts were paced at a fixed rate of 428 beats/min. All hearts were subjected to 20 min of global normothermic ischaemia followed by 45 min of aerobic reperfusion. Test drugs were infused via the cannulation port for 5 min prior to ischaemia and for the initial 5 min of reperfusion (Figure 5.1). Coronary effluent was collected on ice for assessment of tissue necrosis from LDH efflux.

Exclusion criteria

After the initial 15 min stabilisation, hearts were excluded from further study if any exhibited one or more of the following exclusion criteria: coronary flow greater than 5 ml/min (normally indicative of an aortic tear); LV pressure development less than 100 mmHg; intrinsic heart rate less than 320 beats/min or irregular.

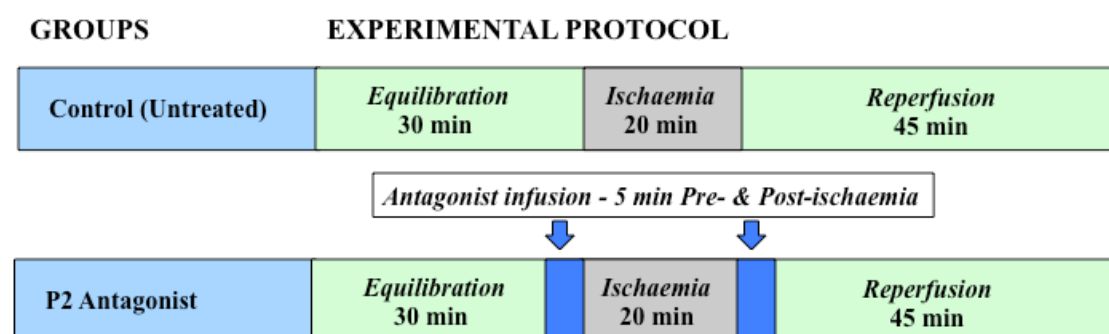


Figure 5.1. Experimental time course in investigations of P2 antagonism in ischaemia-reperfusion.

Table 5.1 – Summary of experimental groups, antagonists used selectivity and concentrations used in targeting P2 purinoceptors in ischaemic-reperfused hearts.

Group	Drug Concentration	pIC_{50} values	Receptor Targeted	Order of Selectivity
CTRL (n=10)	Untreated	N/A	N/A	N/A
RB2-100 (n=7)	100 μ M	4.3 (m)	P2Y	P2Y ₁ >P2Y ₆ >P2Y ₁₂ *>P2Y ₂ =P2Y ₆ >P2Y ₁₁ >P2Y ₄ *P2Y ₁₂ decrease by 100% at 30 μ M
RB2-1 (n=8)	1 μ M	4.3 (m)	P2Y	
Suramin (n=8)	200 μ M	pA_2 = 4.9~4.3 (h)	P2Y	P2Y ₁₁ >P2Y ₁ =P2Y ₁₂ >P2Y ₂ >P2Y ₆ Not active at P2Y ₄ (300 μ M no effect)
MRS2179 (n=4)	3 μ M	6.5 (h)	P2Y ₁	P2Y ₁ No effect on other subtypes at 10, 30 or 100 μ M
MRS2159 (n=8)	3 μ M	8.0 (r)	P2X ₁	P2X ₁ >P2X ₂ >P2X ₄
PPNDS (n=9)	200 nM	7.8 (r)	P2X ₁	P2X ₁ >P2X ₂ >P2X ₄ > P2X ₃ >P2X ₇

Potency indices for antagonists (pIC_{50} or pA_2) and receptor selectivity in rat (r), mouse (m) or human (h) P2Y and P2X receptor subtypes presented as $-\log_{10}IC_{50}$ (pIC_{50}) values [197, 362, 363].

Chemicals and reagents

All drugs used were purchased from Sigma-Aldrich (Castle Hill, Australia). Drug solutions were infused into hearts at $\leq 1\%$ of total coronary flow rate to achieve the final concentrations indicated.

Statistical analyses

The study was divided into effects of P2Y antagonists and effects of P2X antagonists. Post-ischaemic functional recoveries were compared via one-way ANOVA, and where inter-group significance were detected a Newman-Keuls post-hoc test was applied for specific comparisons. Significance was accepted for $P < 0.05$. Data are presented as means \pm SEM.

5.4 RESULTS

Pre-ischaemic function

Baseline data is shown in Table 5.2. Only 100 μ M RB2 affected contractile force (increasing force). Coronary flow was also increased by RB2 (both 1 and 100 μ M) and also by suramin. MRS2179 and MRS2159 and PPNDS did not modify function at baseline.

Effects of P2Y purinoceptor antagonism on post-ischaemic recoveries

Suramin, RB2 and MRS2179 were used to test effects of P2Y purinoceptor blockade on myocardial functional tolerance to ischaemia-reperfusion. Recoveries are shown in Figures 5.2-4. At the end of 45 min reperfusion, CTRL hearts recovered $\sim 55\%$ of pressure development, 80% flow and exhibited a sustained 25 mmHg rise in diastolic pressure. Both concentrations of RB2 (100 μ M, 1 μ M) significantly depressed LV

contractile recovery at the end of reperfusion, and worsened diastolic contracture (Figure 5.2 and 5.3). Interestingly, RB2 at the higher concentration of 100 μ M also impaired recovery of coronary flow. Suramin at 200 μ M significantly worsened post-ischaemic outcome, increasing diastolic dysfunction and limiting recovery of ventricular pressure development. Selective P2Y₁ antagonism by 3 μ M MRS2179 also significantly increased diastolic dysfunction but exerted no effect on LVDP or flow recovery (Figure 5.2, 5.3 and 5.4).

Table 5.2 Pre-ischaemic contractile function and coronary flow in all experimental groups.

<i>Experimental Group</i>	<i>LVDP (mmHg)</i>	<i>Coronary Flow (ml/min/g)</i>
CTRL (n=10)	114 \pm 4	20 \pm 1
<i>P2Y Antagonists</i>		
100 μ M RB2 (n=7)	146 \pm 6*	28 \pm 6*
1 μ M RB2 (n=8)	124 \pm 7	32 \pm 2*
200 μ M suramin (n=9)	120 \pm 3	27 \pm 2*
<i>P2Y₁ Antagonist</i>		
3 μ M MRS2179 (n=4)	126 \pm 10	24 \pm 2
<i>P2X₁ Antagonists</i>		
3 μ M MRS2159 (n=8)	127 \pm 4	19 \pm 2
200 nM PPNDs (n=9)	118 \pm 2	22 \pm 1

Functional parameters were measured immediately prior to induction of global ischaemia. Values are means \pm SEM. *, P <0.05 vs. CTRL.

Effects of P2X₁ purinoceptor antagonism on post-ischaemic recoveries

The P2X₁ selective antagonists MRS2159 and PPNDS were used to assess effects of P2X₁ activity on functional tolerance to ischaemia-reperfusion. Both antagonists significantly depressed LV recovery (PPNDS, to a greater extent than MRS2159) and increased diastolic dysfunction (Figure 5.2 and 5.3). Final coronary flow rate was not affected by either MRS2159 or PPNDS (Figure 5.4).

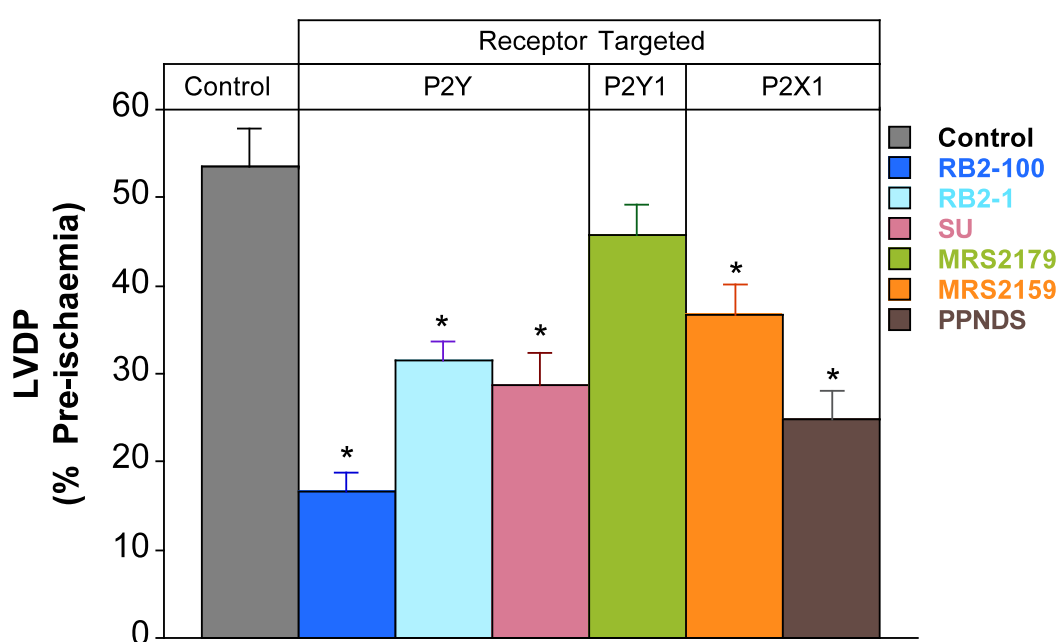


Figure 5.2. Effects of P2 purinoceptor antagonists on left ventricular developed pressure at the end of 45 min reperfusion. Data are shown for treatment with RB2 (100 μ M, 1 μ M), suramin (SU; 200 μ M), MRS2179 (3 μ M), MRS2159 (3 μ M), and PPNDS (200 nM). Values shown are means \pm SEM. *, $P < 0.05$ vs. untreated control hearts.

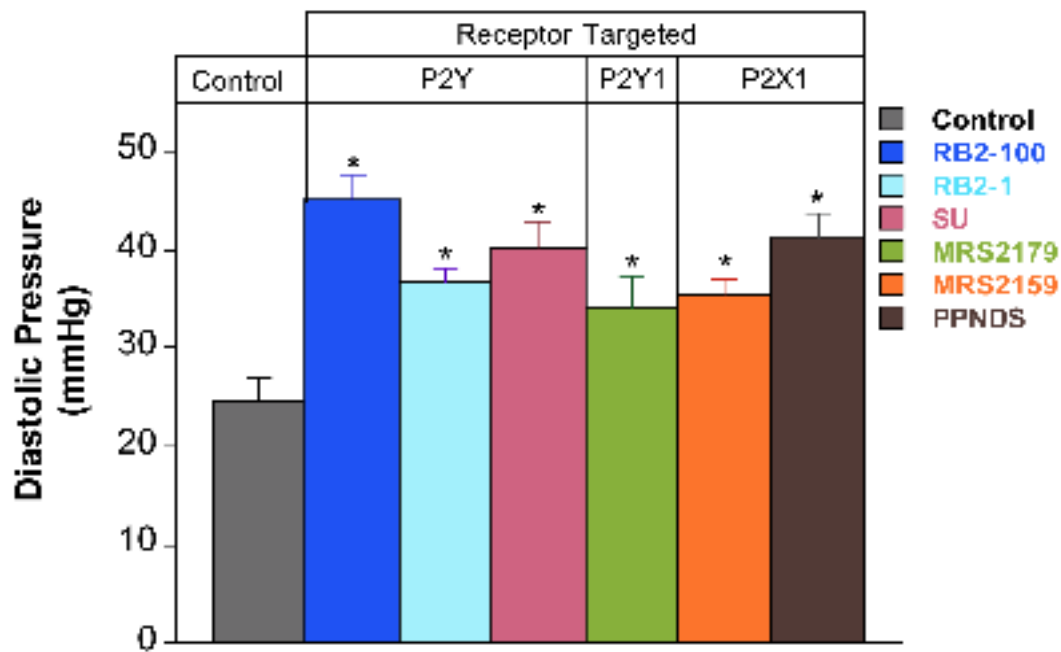


Figure 5.3. Effects of P2 purinoceptor antagonists on left ventricular diastolic pressure at the end of 45 min reperfusion. Data are shown for treatment with RB2 (100 μ M, 1 μ M), suramin (SU; 200 μ M), MRS2179 (3 μ M), MRS2159 (3 μ M), and PPND5 (200 nM). Values shown are means \pm SEM. *, $P < 0.05$ vs. untreated control hearts.

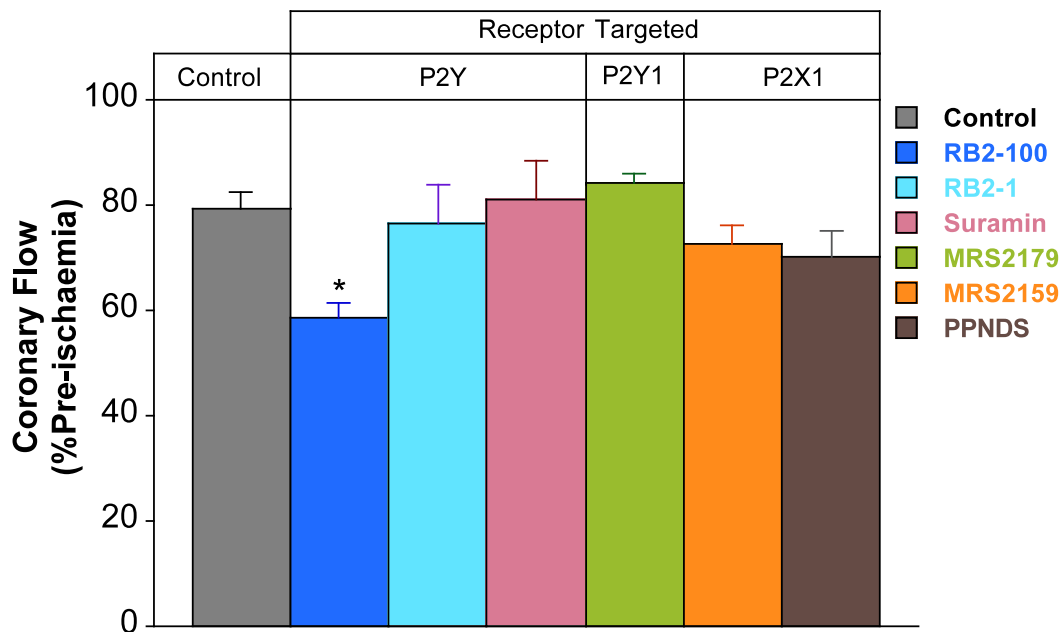


Figure 5.4. Effects of P2 purinoceptor antagonists on coronary flow (% Pre-ischæmia) at the end of 45 min reperfusion. Data are shown for treatment with RB2 (100 μ M, 1 μ M), suramin (200 μ M), MRS2179 (3 μ M), MRS2159 (3 μ M), and PPND5 (200 nM). Values shown are means \pm SEM. *, $P < 0.05$ vs. untreated control hearts.

Time course of effects of P2Y antagonism during ischaemia-reperfusion

The effects of P2Y antagonist treatments were examined in more detail over the full time-course of ischaemia-reperfusion. This analysis shows a general biphasic pattern of contractile recovery, with initial recovery of LVDP in the first minutes of reperfusion, followed by a decline and subsequent more gradual recovery. This pattern likely evidences emergence of initial reperfusion injury in the first minutes of reperfusion. The P2 antagonists decreased recovery of LVDP throughout much of the reperfusion period. Diastolic pressure also evidenced a biphasic recovery (falling initially then rising before gradually dissipating over time). Again, antagonists worsened EDP recovery throughout reperfusion.

Time course of effects of P2X₁ antagonism during ischaemia-reperfusion

Recovery of LVDP was decreased by both P2X antagonists throughout reperfusion, with PPNDS exerting a greater effect than MRS2159. Post-ischaemic diastolic contracture was significantly worsened by both P2X₁ antagonists at all time points during reperfusion (Figure 5.3). Interestingly, although both antagonists targeted the same purinoceptor, diastolic pressures in MRS2159 treated hearts differed significantly from PPNDS treated hearts, with PPNDS triggering greater ventricular dysfunction in response to ischaemia-reperfusion.

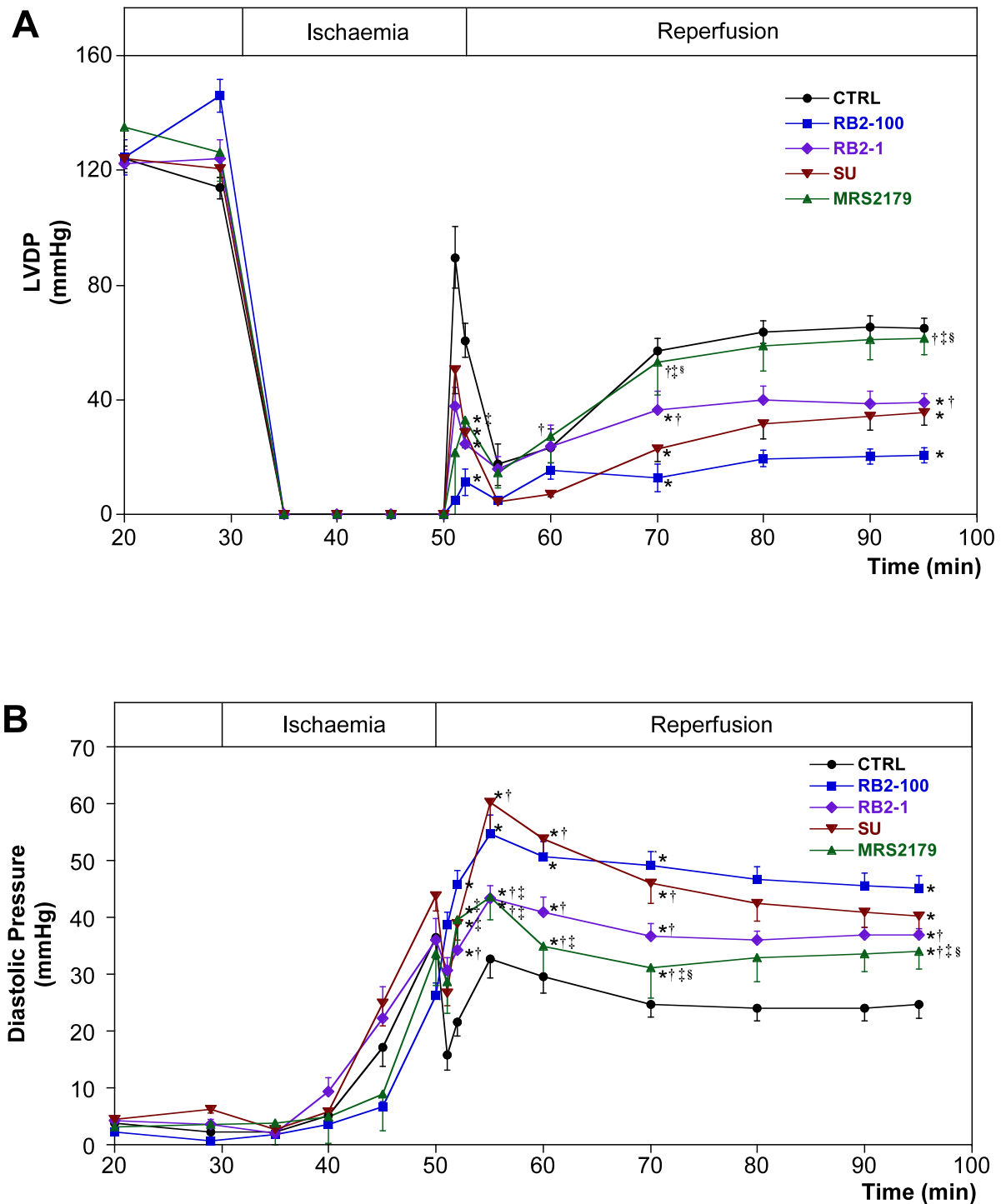


Figure 5.5. Effects of P2Y purinoceptor antagonists on post-ischaemic recoveries for (A) left ventricular developed pressure and (B) left ventricular diastolic pressure. Data are shown for recoveries in CTRL ($n=10$), 100 μ M RB2-100 ($n=7$), 1 μ M RB2-1 ($n=8$), 200 μ M suramin ($n=9$) and 3 μ M MRS2179 ($n=4$) treated hearts. Values are means \pm SEM. *, $P<0.05$ vs. CTRL. †, $P<0.05$ vs. RB2-100. ‡, $P<0.05$ vs. SU. §, $P<0.05$ vs. RB2-1.

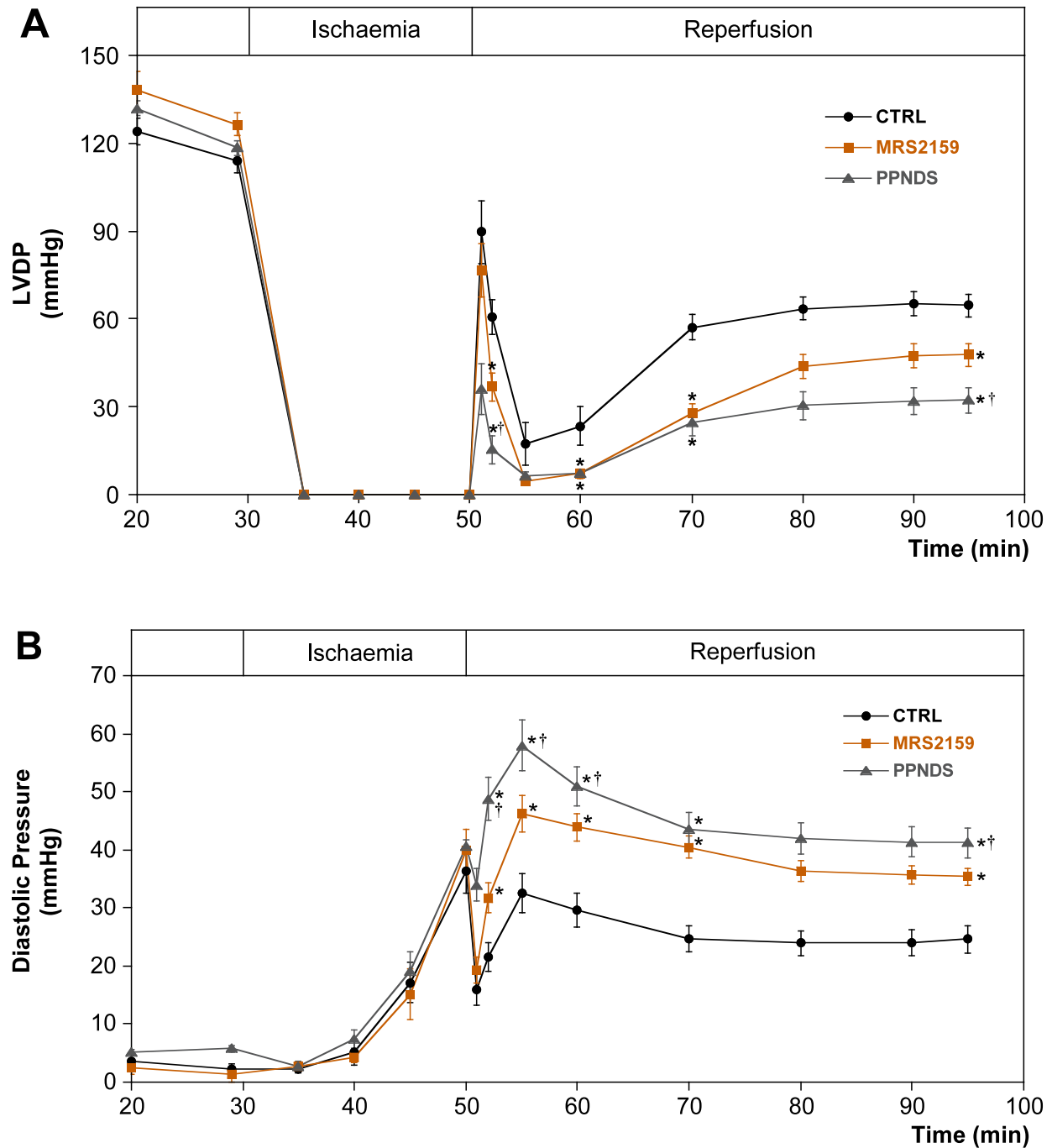


Figure 5.6. Effects of P2X purinoceptor antagonism on post-ischaemic recoveries for (A) left ventricular developed pressure and (B) left ventricular diastolic pressure. Data are shown for recoveries in CTRL ($n=10$), 3 μ M MRS2159 ($n=8$) and 200 nM PPNDS ($n=9$) hearts. Values are means \pm SEM. *, $P<0.05$ vs. CTRL. †, $P<0.05$ vs. MRS2159.

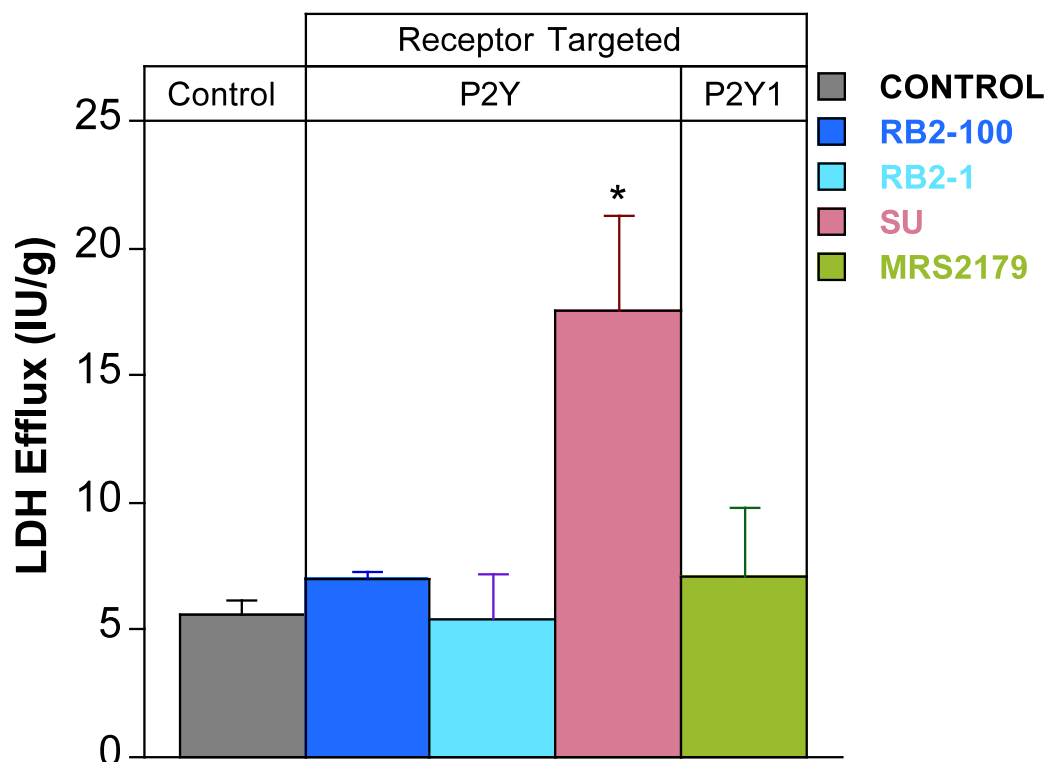


Figure 5.7. Post-ischaemic efflux of lactate dehydrogenase (LDH) following 20 min ischaemia for control hearts and hearts treated with RB2 (100 μ M, 1 μ M), suramin (200 μ M) and MRS2179 (3 μ M). Values shown are means \pm SEM.

Effects of P2 antagonists on post-ischaemic oncosis (LDH efflux)

Coronary effluent was collected for the assessment of tissue oncosis/necrosis by measuring LDH efflux. The non-selective P2Y antagonist, suramin (200 μ M) significantly increased LDH loss (Figure 5.7), indicating a greater level of cell death compared to CTRL, RB2 (100 μ M, 1 μ M) and 3 μ M MRS2179 treated hearts. Unfortunately LDH activity in hearts treated with P2X₁ antagonists, 3 μ M MRS2159 and 200 nM PPNDs was not assessed due to accidental degradation of coronary effluent sample prior to LDH assessment.

5.5 DISCUSSION

P2 purinoceptors are structurally classed into two major families of P2X, ligand-gated ion channels and P2Y, G protein-coupled purinoceptors [174, 197, 364, 365]. In the previous chapter, transcripts for both P2X and P2Y purinoceptors were detected in mouse hearts and vasculature. Relatively few investigators have undertaken to define the functions of P2 purinoceptors in terms of myocardial stress resistance and protection.

Cardiac effects

In the present study, exogenous blockade of P2 purinoceptors worsened post-ischaemic myocardial recovery, supporting cardiac protection via intrinsic P2 purinoceptor activation. Specifically, significant limitation of post-ischaemic recoveries through P2Y blockade with RB2 and suramin, and P2X₁ antagonism with MRS2159 and PPNDS, supports intrinsic protective activation of both P2Y and possibly P2X₁ purinoceptors. Depressed ventricular recovery was also apparent with specific blockade of P2X₁ receptors with MRS2159 and PPNDS (although transcript for P2X₁ was found to be very low in myocardium). Given evidence for heteromeric assembly of P2X purinoceptors between P2X₁ and P2X₄ subunits [332] and P2X₁ and P2X₅ subunits [200, 330], the present data cannot exclude possible activation of heteromeric assemblies involving P2X purinoceptors. Recent studies of conditioning responses and ischaemic injury by Vessey *et al.* also indicate that the P2X₇ purinoceptor combines with pannexin-1 to form channels that facilitate release of other cardioprotectants [187, 213]. There is also evidence that MRS2159 and PPNDS may also block P2X₇ purinoceptors despite apparent specificity for P2X₁ subtype [366, 367].

These data for inhibitory effects of P2 antagonists are consistent with prior studies of similar agents in other different cardiac models [181, 192, 254, 263, 346, 355]. For example, in ischaemic-preconditioning studies, Ninomiya *et al.* found that suramin and RB2 inhibited protective effects in terms of diastolic dysfunction [181], and ATP- and UTP-enhanced cardioprotective responses [355]. Additionally, UTP-mediated reductions in infarct size and improvement in myocardial function are also abolished by suramin and RB2 in ischaemic-reperfused myocardium [263].

Vascular effects

Interestingly, P2Y antagonists (RB2 and suramin) enhanced coronary flow rate prior to the 20 min global ischaemia. However, among antagonists tested only blockade of P2Y purinoceptors by 100 μ M RB2 significantly impaired coronary flow at the end of reperfusion. Prior evidence has been provided by several investigators for a role for P2Y₂ purinoceptors in endothelium-dependent vasorelaxation [175-177, 205, 241, 342, 368, 369]. Results for normoxic flow suggest that P2Y activity may actually limit flow, given the stimulatory effects of RB2 and suramin. This may reflect mixed effects of purinoceptors based on cellular location, with relaxation arising from endothelial receptors *vs.* constriction via smooth muscle receptors [370, 371]. Similarly, Harrington *et al.* propose that the P2X₁ subtype exerts vasodilatory effects dependent on its vascular location [205, 318, 319]. Selective blockade by both P2X₁ antagonists had no effect on coronary flow rate pre- or post-ischaemia in the current study.

Different P2 purinoceptors have been directly implicated in development of cardiac dysfunction under other disease states. The P2Y subtype is cited as playing a role in

calcification of aortic valves [357]; up-regulation of mRNA transcripts for P2X₁, P2Y₂ and P2Y₆ has been documented in congestive heart failure [184, 250]; the P2Y₆ triggers pressure overload-induced cardiac fibrosis [190]; blockade of P2X₃ and P2X_{2/3} may improve cardiac dysfunction associated with P2X nociceptive pain transmission by a reduction in the sympathoexcitatory reflex that exaggerates myocardial tissue injury [331]; and P2X₇ activation produces several responses including Ca²⁺ fluxes, MAPK activation, inflammatory mediator release, and apoptosis [325, 328]. In addition, and though not relevant in the current model, platelet activation via P2Y₁ [359], P2Y₁₂ [335, 336, 358-361] can also contribute to myocardial dysfunction.

Limitations

Delineating how each P2 subtype contributes to functional responses is hindered by incomplete selectivity of currently available antagonists. Although RB2 exhibits some selectivity for P2Y purinoceptors; suramin and RB2 are widely used as non-specific antagonists [197, 365]. Additionally, suramin affects downstream signal transduction and G-proteins [372]. Data interpretation is further complicated by a potential blockade of ectonucleotidase activity by suramin and other P2 antagonists. Several studies have demonstrated that P2 antagonists may inhibit ectonucleotidase activity in different species and tissues [373, 374]. The inhibitory effects on ectonucleotidase activity could limit responses mediated by hydrolysis products of extracellular nucleotides, and contribute to the negative influences of these agents on post-ischaemic recovery. As evident in the LDH loss/necrosis data, P2Y blockade by suramin increased LDH efflux beyond that with all other antagonists tested.

5.6 CONCLUSION

The present data indicate that intrinsic P2Y purinoceptor activity mediates protection against post-ischaemic injury, and that P2X purinoceptors may also have a protective role. Post-ischaemic recovery was reduced by blocking endogenous activation of P2Y receptors (RB2, suramin, MRS2179) and by blockade of endogenous activation of P2X purinoceptors (MRS2159 and PPNDS). The role of P2 endogenous nucleotides in the ischaemic myocardium warrants further study. In the following Chapter, the aim was to explore the effects of P2 receptor activation in the pre- vs. post-ischaemic periods.

CHAPTER 6

PRE- VS. POST-ISCHAEMIC CARDIOPROTECTION VIA THE P2 AGONIST UTP

6.1 ABSTRACT

Having acquired evidence of ventricular expression of P2Y₁ and P2Y₂, and of potential protective functions of intrinsic P2Y_{1/2} activity, the current study specifically addresses concentration and timing dependent properties of P2Y agonist mediated cardioprotection. Effects of the P2Y agonist UTP were investigated in isolated perfused mouse hearts subjected to 20 min global ischaemia followed by 45 min of reperfusion. Six experimental groups were assessed, with hearts subjected to either 250 nM or 1 μ M UTP treatment: i) 5 min pre-ischaemia; ii) 5 min post-ischaemia (early reperfusion); or iii) 5 min pre- and 5 min post-ischaemia. Control (CTRL) hearts recovered 67 ± 3 mmHg left ventricular developed pressure (LVDP) (~50% of pre-ischaemia) and exhibited sustained diastolic contracture (31 ± 2 mmHg) at the end of 45 min reperfusion. Pre-ischaemic UTP treatment (250 nM) did not modify LVDP recovery, while end-diastolic contracture was significantly reduced (17 ± 1 mmHg; $P<0.05$), suggestive of a distinct effect on diastolic vs. systolic function. In contrast, pre-ischaemic UTP at 1 μ M enhanced LVDP recovery and reduced diastolic dysfunction (90 ± 6 mmHg and 21 ± 4 mmHg, respectively; $P<0.05$). Pre-ischaemic UTP treatment also resulted in a significantly higher (~95% of pre-ischaemia) recovery of coronary flow compared to CTRL hearts (~75% of pre-ischaemia; $P<0.05$). Functional recovery was not improved by post-ischaemic UTP treatment at either concentration. Interestingly, combined pre- and post-ischaemic UTP at 250 nM significantly reduced diastolic contracture (17 ± 3 mmHg) and resulted in higher recovery of LVDP (89 ± 6 mmHg), whereas a higher 1 μ M level did not. Thus, UTP has complex concentration and time dependent effects on functional tolerance to ischaemia-reperfusion.

6.2 INTRODUCTION

Whether P2Y GPCRs, currently entailing 8 mammalian subtypes (P2Y_{1,2,4,6,11,12,13,14}), may modify the hearts ability to withstand injury and cell damage with stress has not been extensively studied. However, P2 receptors and the natural ligand UTP do modify other vascular and cardiac functions. P2Y purinoceptors localised to vascular smooth muscle cells have been shown to promote vascular contraction, while P2Y purinoceptors on endothelium mediate relaxation via factors such as NO, prostaglandins and endothelium-derived hyperpolarising factor [195, 375, 376]. Harden *et al.* proposed at least four P2Y subtypes to be involved in vascular effects of extracellular nucleotides – the P2Y₁, P2Y₂, P2Y₄ and P2Y₆ subtypes. UTP and UDP are inactive at the P2Y₁ subtype [377] while the P2Y₄ purinoceptor is highly sensitive to UTP [233]. The P2Y₂ purinoceptor is activated equipotently by UTP and ATP [378, 379].

In the myocardium, these nucleotides exert dual inotropic effects: first a rapid decrease in contractility, and secondly a subsequent increase in contractile tension. UTP has been shown to induce positive inotropic effects while ATP induces negative inotropism via activation of P1 Ado receptors [380, 381]. It is proposed that UTP exerts positive inotropy via activation of the P2Y₂ subtype while UDP acts via P2Y₆ receptors [189].

There is evidence local P2 agonists such as UTP are enhanced during stress, providing scope for P2 modulation under such conditions. The release of the endogenous P2 ligand UTP during cardiac ischaemia was first documented by Erlinge *et al.*: UTP levels increased during early ischaemia and early reperfusion in pigs enhancing blood

flow, ventricular arrhythmias and t-PA release [252]. UTP levels also increase in humans during myocardial infarction [189]. Data from prior chapters in this thesis indicate that P2 antagonism worsens post-ischaemic outcome, supporting some protective roles for intrinsically activated P2 receptors. From the perspective of cytoprotection, Yitzhaki *et al.* report that UTP significantly reduces cardiomyocyte death induced by hypoxia [254]. Subsequent *in vivo* studies reveal that UTP reduces mitochondrial Ca^{2+} levels following hypoxia, and that UTP “preconditioning” can reduce infarct size and improve myocardial function post-ischaemia [254, 255]. Thus, pre-ischaemic activation of P2 receptors may be an effective “pre-conditioning” stimulus.

In previous chapters evidence was presented for potential cardioprotective roles of P2Y purinoceptors activation by locally generated ligands. Specific involvement of the P2Y₂ subtype was evidenced (though not conclusively). The aim of the current study was to investigate the time and concentration dependent effects of P2Y_{2/4} purinoceptor agonism via exogenous UTP in ischaemic-reperfused mouse hearts.

6.3 MATERIALS AND METHODS

Perfused heart preparation and experimental protocol

Hearts were prepared as described in detail in **Chapter 2**. Investigations conformed to the Guide for the Care and Use of Laboratory Animals published by the US National Institute of Health (NIH Publication No 85-23, revised 1996). Experiments were undertaken in hearts removed from male C57 mice weighing 25-35g anaesthetised with a bolus injection sodium pentobarbital of (50 mg/kg) intraperitoneally.

UTP treatments

Hearts were allowed 30 min of equilibration following aortic cannulation. After the initial 20 min of equilibration, hearts were paced at a rate of 420 ± 5 beats/min. All hearts were subjected to 20 min of global normothermic ischaemia followed by 45 min of aerobic reperfusion (and thus during ischaemia). UTP (250 nM or $1 \mu\text{M}$) was infused as outlined in Figure 6.1: i) 5 min pre-ischaemia; ii) 5 min post-ischaemia; or iii) 5 min pre- and 5 min post-ischaemia.

Chemicals and reagents

All drugs used were purchased from Sigma-Aldrich (Castle Hill, Australia). Drug solutions were infused into hearts at $\leq 1\%$ of total coronary flow rate to achieve the final concentrations indicated.

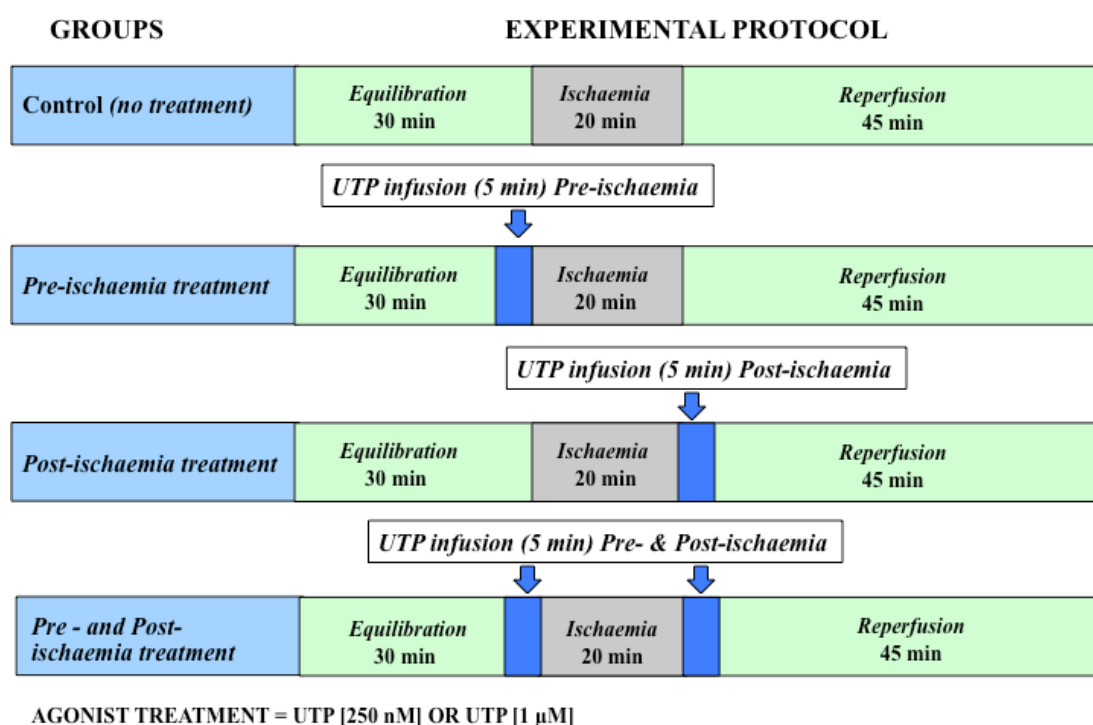


Figure 6.1. Overview of experimental groups in the investigations of P2 agonism with UTP pre-ischaemia, post-ischaemia, and pre-and post-ischaemia.

Statistical analyses

Post-ischaemic functional recoveries were compared via one-way ANOVA. Where inter-group significance was detected, a Newman-Keuls post-hoc test was applied for specific comparisons. Significance was accepted for $P < 0.05$. Data are presented as means \pm SEM.

6.4 RESULTS

Pre-ischaemic functional parameters

CTRL hearts exhibited pre-ischaemic LVDP of 133 ± 4 mmHg and a coronary flow rate of 26 ± 2 ml/min/g. All other experimental groups exhibited comparable LVDP and coronary flow rates (Table 6.1).

Table 6.1 Pre-ischaemic contractile function and coronary flow.

<i>Experimental Group</i>	<i>LVDP (mmHg)</i>	<i>Coronary Flow (ml/min/g)</i>
CTRL ($n=19$)	133 ± 4	26 ± 2
<i>250 nM UTP</i>		
Pre-ischaemia ($n=10$)	117 ± 4	25 ± 2
Post-ischaemia ($n=8$)	132 ± 6	23 ± 2
Pre & Post-ischaemia ($n=12$)	139 ± 11	22 ± 2
<i>1 μM UTP</i>		
Pre-ischaemia ($n=8$)	140 ± 7	21 ± 1
Post-ischaemia ($n=8$)	129 ± 5	22 ± 2
Pre & Post-ischaemia ($n=12$)	126 ± 4	26 ± 2

Functional parameters were measured at the end of normoxic stabilisation, immediately prior to induction of global ischaemia. Values are means \pm SEM. *, $P < 0.05$ vs. CTRL.

Effects of UTP treatment on post-ischaemic function

UTP at 250 nM and 1 μ M was used to assess effects of P2Y_{2/4} activation on functional tolerance to ischaemia-reperfusion. At the end of 45 min reperfusion, untreated hearts exhibited an LVDP of 67 ± 3 mmHg ($46 \pm 2\%$ of pre-ischaemia), diastolic contracture of 31 ± 2 mmHg, and a coronary flow rate equivalent to $75 \pm 2\%$ of pre-ischaemic levels. These outcomes were modified by UTP in a concentration and time-dependent manner (Table 6.2, Figures 6.2, 6.3, 6.4).

Pre-ischaemic UTP

Pre-ischaemic treatment with 250 nM UTP failed to modify recovery of LVDP after 45 min reperfusion, while diastolic pressure was significantly reduced (Table 6.2 and Figure 6.2, 6.3). In contrast, pre-ischaemic UTP at a higher 1 μ M level improved both LVDP as well as diastolic contracture. Pre-ischaemic UTP also significantly improved coronary flow rate compared to control hearts (Table 6.2 and Figure 6.4).

Post-ischaemic UTP

Functional recovery was not altered by post-ischaemic treatment with UTP at either concentration. LVDP recoveries in treated hearts were comparable to CTRL (untreated) hearts (Table 6.2 and Figure 6.2). Hearts treated with 250 nM UTP exhibited modestly reduced diastolic contracture, though this effect was not significant compared to CTRL (Table 6.2 and Figure 6.3). Post-ischaemic treatment with 1 μ M UTP did not alter diastolic function. Coronary flow was modestly increased by treatment with the higher concentration of UTP (Table 6.2 and Figure 6.4).

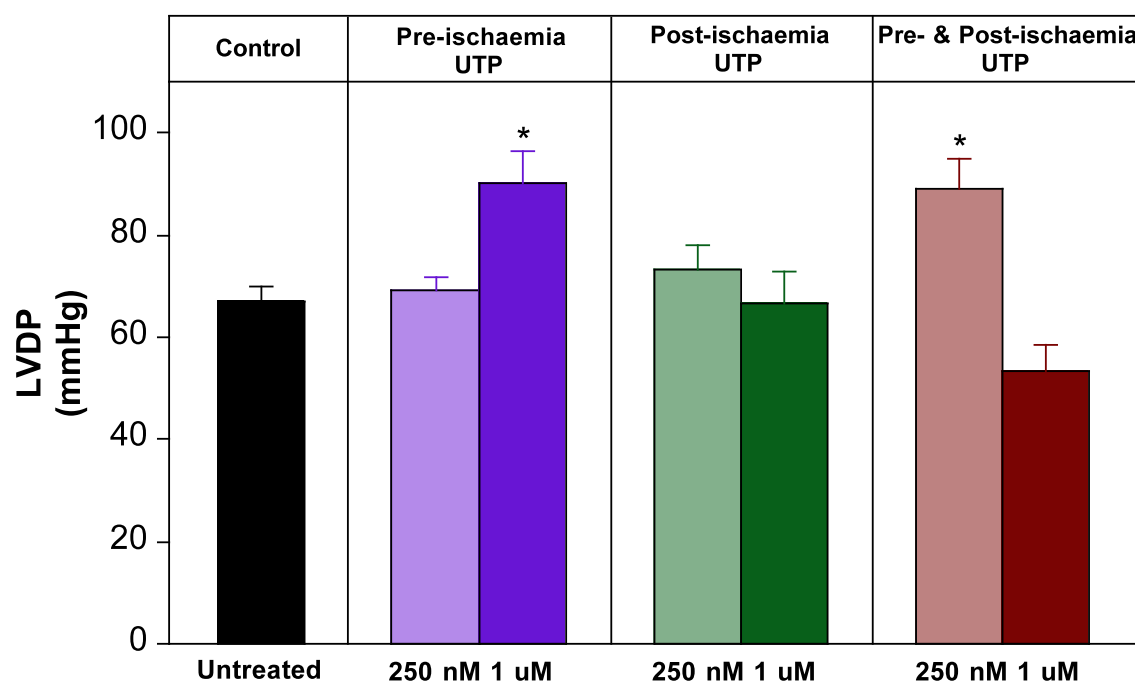


Figure 6.2. Effects of UTP treatment (250 nM or 1 µM) on final post-ischæmic recoveries of left ventricular (LV) developed pressure. Values are means±SEM. *, $P<0.05$ vs. control.

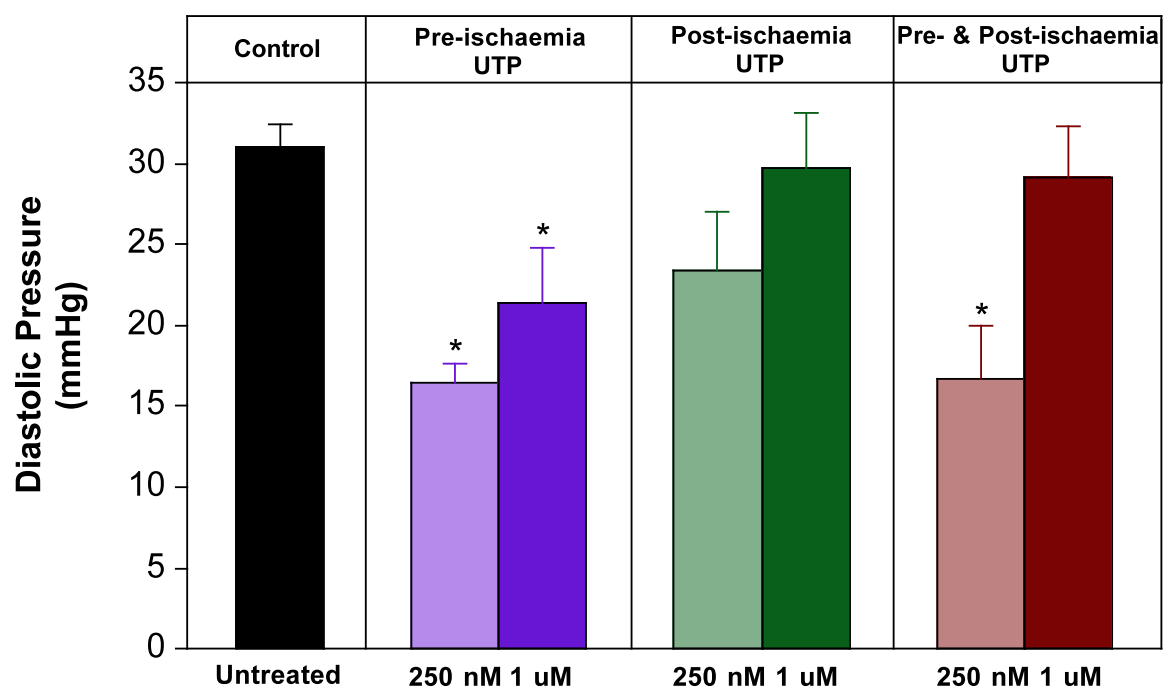


Figure 6.3. Effects of UTP treatment (250 nM or 1 µM) on final post-ischæmic recoveries of left ventricular diastolic pressure. Values are means±SEM. *, $P<0.05$ vs. control.

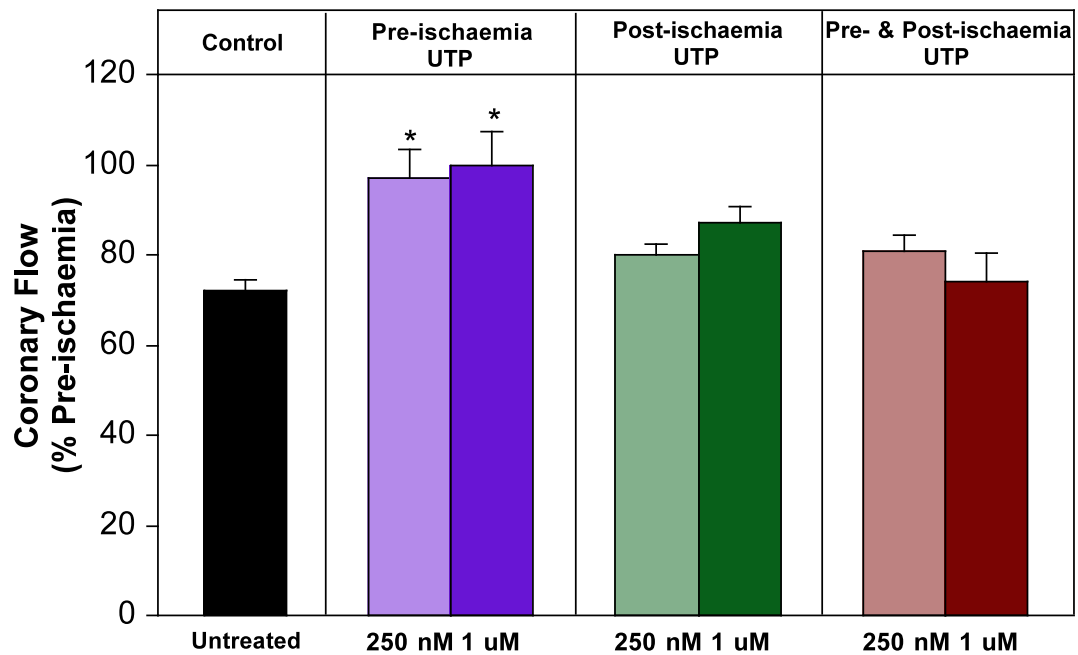


Figure 6.4. Effects of UTP treatment (250 nM or 1 μ M) on final post-ischaemic recoveries of coronary flow (% pre-ischaemia). Values are means \pm SEM. *, $P<0.05$ vs. control.

Pre- and post-ischaemic UTP

Interestingly, pre- and post-ischaemic treatment of 250 nM UTP not only significantly reduced diastolic contracture, but also resulted in higher recovery of LVDP (Table 6.2, Figure 6.2, 6.3). However, paradoxically, pre- and post-ischaemic treatment with the higher 1 μ M concentration had no effect on functional recoveries (Table 6.2, Figure 6.2, 6.3, 6.4).

Table 6.2 - Final post-ischaemic functional recoveries in mouse hearts untreated (Control) or treated with UTP (250 nM or 1 μ M) at different times.

<i>Group</i>	<i>EDP (mmHg)</i>	<i>LVDP (mmHg)</i>	<i>LVDP (%Pre-ischaemia)</i>	<i>Coronary Flow</i>
CTRL (<i>n</i> =10)	31 \pm 2	67 \pm 3	46 \pm 2	75 \pm 2
<i>250nM UTP Treatment</i>				
UTP Pre (<i>n</i> =10)	17 \pm 1*	69 \pm 3	54 \pm 3	97 \pm 7*
UTP Post (<i>n</i> =8)	23 \pm 4	73 \pm 5	51 \pm 4	80 \pm 3
UTP Pre & Post (<i>n</i> =12)	17 \pm 3*	89 \pm 6*	60 \pm 2	81 \pm 4
<i>1 μM UTP Treatment</i>				
UTP Pre (<i>n</i> =8)	21 \pm 3*	90 \pm 6*	58 \pm 3	100 \pm 7*
UTP Post (<i>n</i> =8)	30 \pm 3	67 \pm 6	47 \pm 4	87 \pm 4
UTP Pre & Post (<i>n</i> =12)	30 \pm 3	53 \pm 5	38 \pm 3	74 \pm 6

All parameters were measured at the end of 45-min reperfusion following 20 min global normothermic ischaemia. EDP, end diastolic pressure; LVDP, left ventricular developed pressure. Values are means \pm SEM. *, P <0.05 vs. CTRL.

Time dependent recoveries in CTRL and UTP treated hearts

The effects of UTP treatments were examined in detail over the time course of 45 min reperfusion (see Figures 6.5 and 6.6).

Pre-ischaemic UTP

Hearts treated with 250 nM UTP exhibited lower LV function in the early minutes of reperfusion but recovered comparable function to CTRL hearts after 45 min reperfusion (Figure 6.5A). Treatment with 1 μ M UTP resulted in higher LV function

from early through to end reperfusion (Figure 6.6A). A sustained reduction in diastolic pressure was also observed throughout reperfusion with both concentrations of UTP (Figure 6.5B and Figure 6.6B).

Pre- and post-ischaemic UTP

In hearts treated with 250 nM UTP, a higher LV function and lower diastolic contracture were evident from the early minutes of reperfusion through to the end of the experiment (Figure 6.5A and Figure 6.6B). Hearts treated with 1 μ M UTP exhibited lower LV function in the early minutes of reperfusion yet appeared to exhibit worsened LVDP recovery at the end of 45 min reperfusion (Figure 6.6A). At this concentration, lower diastolic contracture was detected initially in reperfusion while contracture was similar to Control hearts at the end of 45 min reperfusion.

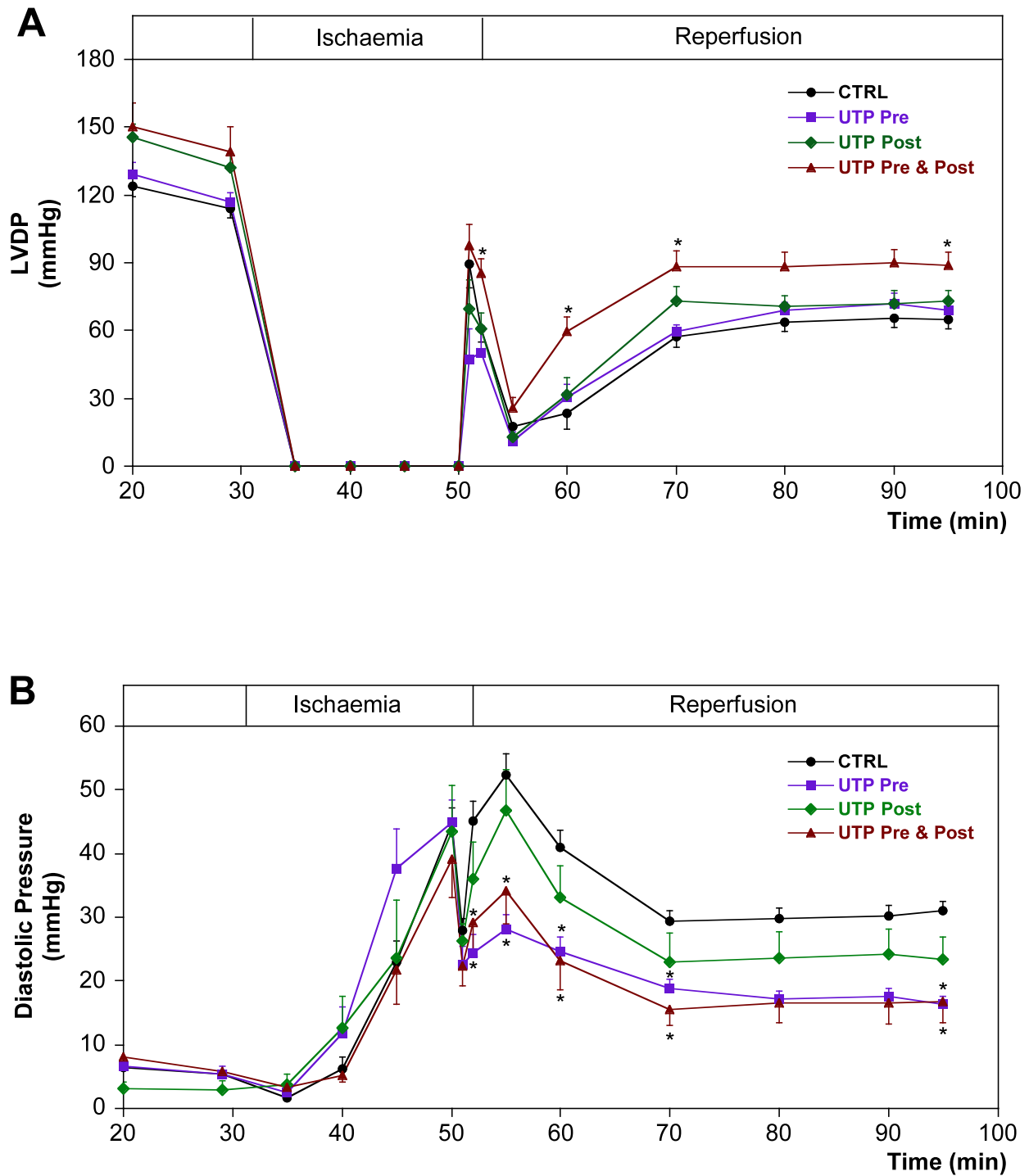


Figure 6.5. Effects of 250 nM UTP treatment (5 min pre-ischaemia, 5 min post-ischaemia, 5 min pre- and post-ischaemia) on post-ischaemic recoveries for: (A) left ventricular developed pressure; and (B) left ventricular diastolic pressure. Data are shown for recoveries for Control ($n=19$) versus UTP Pre ($n=10$), UTP Post ($n=8$) and UTP Pre & Post ($n=12$) treated hearts. Values are means \pm SEM. *, $P<0.05$ vs. CTRL.

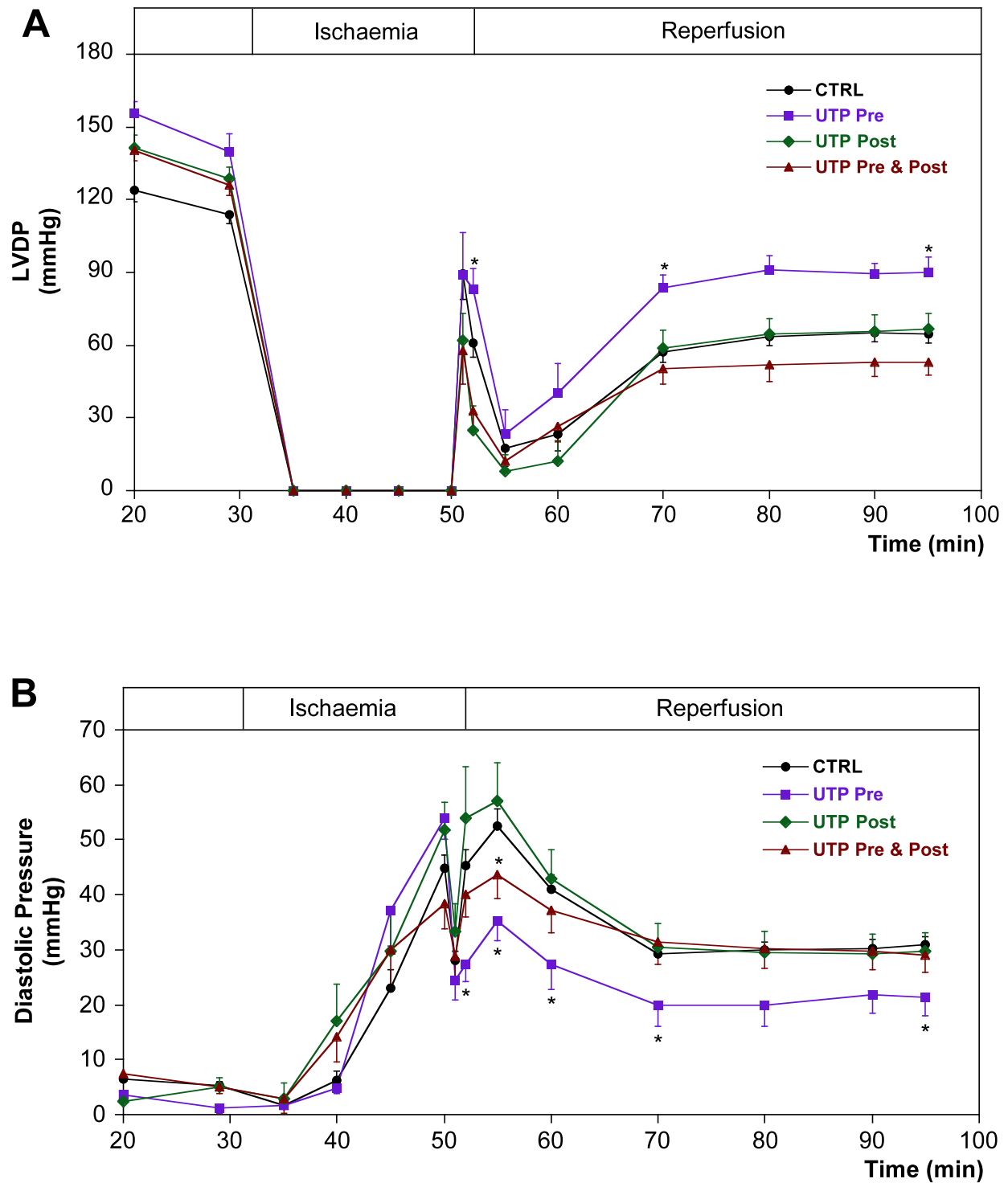


Figure 6.6. Effects of 1 μ M UTP treatment (5 min pre-ischaemia, 5 min post-ischaemia, 5 min pre- and post-ischaemia) on post-ischaemic recoveries for: (A) left ventricular developed pressure; and (B) left ventricular diastolic pressure. Data are shown for recoveries in Control ($n=19$) versus UTP Pre ($n=8$), UTP Post ($n=8$) and UTP Pre & Post ($n=12$) treated hearts. Values are means \pm SEM. *, $P<0.05$ vs. CTRL.

6.5 DISCUSSION

The protective effects of the nucleotide UTP have been studied in varied cell types, including cardiomyocytes [263, 382-384]. This nucleotide may interact with multiple P2 receptor subtypes in the heart and vessels. Investigators have shown that the P2Y₂ purinoceptor is activated equipotently by ATP and UTP [378], while the P2Y₄ purinoceptor is potently activated by UTP [233], and the P2Y₆ purinoceptor is selectively activated by UDP [385, 386]. Known cardiovascular effects of extracellular UDP and UTP include vasoconstriction via P2Y purinoceptors on vascular smooth muscles cells and vasodilatation via P2Y receptors on endothelial cells [387]. UTP and UDP also stimulate cell growth and migration of vascular smooth muscle cells, and intimal hyperplasia via P2Y₁, P2Y₂, P2Y₄ and P2Y₆ subtypes [240, 388-390]. UDP sensitive P2Y₆ was recently implicated in cardiac preconditioning in the isolated rat heart model [192].

Cardioprotective effects of UTP have been described by other investigators: pre-treatment with UTP protects cultured rat cardiomyocytes during hypoxia [254]; and *in vivo* UTP treatment after myocardial infarction decreases infarct size and improves myocardial function in rats [254, 255, 263]. Furthermore, UTP is proposed to play a role in ischaemic preconditioning, given evidence of its release during cardiac ischaemia [252]. Here 250 nM or 1 μ M UTP was applied pre-, post- and both pre- and post-ischaemia to assess when activation of receptors confers protection. At these levels UTP is likely to predominantly target P2Y₂ and P2Y₄ receptors. Protective effects were detected, though these were both time- and concentration-dependent. While it is known that UTP elicits inotropic effects in cardiomyocytes [189, 209, 248, 380, 381], likely of the P2Y₂ and P2Y₆ subtype in mice (Wihlborg et al., 2006),

effects of UTP on post-ischaemic contractile recovery here are unlikely to reflect direct inotropism, since UTP is only applied immediately prior to ischaemia or in the initial minutes of reperfusion, and is rapidly catabolised and washed from the heart.

Time-dependent protection with UTP

Time-dependent effects of UTP were observed: pre-ischaemic treatment with UTP afforded protection while functional recovery was not altered by post-ischaemic treatment (Figures 6.2 and 6.3). Efficacy of UTP pretreatment suggests a potential 'preconditioning-like' effect of P2 receptor activation prior to ischaemia. Multiple GPCRs appear able to activate RISK signalling involved in conditioning response, and several studies implicate P2 purinoceptors in [181, 192, 254, 255, 355, 384]. Ninomiya *et al.* found that ATP and Ado appear to play complementary roles in ischaemic-preconditioning via P2Y purinoceptors and Ado (P1) receptors, respectively. Prior data supports P2Y₂ subtype involvement in such UTP-dependent preconditioning effects [254, 255]. The current results are consistent with UTP mediated protection via pre-ischaemia P2Y₂ activity, though P2Y₄ subtype may also be involved.

In contrast to pre-ischaemic treatment, post-ischaemic application of UTP failed to modify functional outcomes from ischaemia-reperfusion (Figures 6.2 and 6.3). This argues against a 'postconditioning' effect of P2Y purinoceptors. There is prior support for postconditioning actions of P2 receptors, with the P2X₇ subtype found to combine with pannexin-1 to form channels that mediate release of multiple cardioprotectants in response to pre- and post-ischaemic ATP [187, 213]. However Vessey *et al.* also reported that the P2 antagonist suramin was ineffective in modifying ATP-mediated

postconditioning, suggesting no involvement of P2Y subtypes in this response [187]. This is consistent with the current data that indicate no protective efficacy of post-ischaemic P2Y agonism with UTP (Figures 6.2-6).

Concentration-dependent Protection with UTP

An apparent (somewhat paradoxical) concentration-dependent action of UTP was observed: pre-ischaemic treatment with both concentrations of UTP afforded protection, as did combined pre- and post-ischaemic treatment with the low UTP concentration (Figures 6.2-6). In contrast, combined pre- and post-ischaemic treatment with the higher 1 μ M UTP failed to modify outcomes (Figures 6.2-6). As noted above, pre-ischaemic application of either concentration of UTP confers protection, in agreement with P2-mediated preconditioning effects [254, 255]. Thus, failure of protection with combined pre- and post-ischaemic UTP (1 μ M) implies a negative action of intra-ischaemic UTP that compensates for benefit from pre-ischaemic P2 agonism.

A potential explanation for this effect is that high levels of applied UTP in combination with endogenously generated UTP (or other P2 agonists) during ischaemia may mediate alternate (detrimental) actions via P2Y_{2/4} receptors, or target other P2 sub-types as a result of both high agonist levels and potential degradation of UTP to alternate P2 ligands. UTP release has been documented during cardiac ischaemia [252], and Wihlborg *et al.* (2006) confirmed plasma UTP (10^{-7} mol/L range) increased 57% in patients with acute myocardial infarction. Concentration-dependent and differential P2Y responses have been described previously. For example, Horiuchi *et al.* found that low levels of UTP (10^{-12} M) dilated arterioles

whilst high levels (10^{-4} and 10^{-6} M) induced constriction [391]. High levels of P2Y_{2/4} activity have also been associated with cellular dysfunction, for example with increased P2Y₂ and P2Y₄ expression in cancers [225, 392-395], with UTP increasing cellular proliferation [225, 394, 396] or inducing apoptosis [397] in a tissue- and dose-dependent manner. UTP at high concentrations (10-100 μ M) has also been shown to induce P2Y₂ fibrotic responses in cardiac fibroblasts [193]. Hou *et al.* also reported increases in myocardial P2Y₂ receptor mRNA levels (4.7 fold) and P2X₁ (2.7 fold) in congestive heart failure [184].

Applied UTP can also activate P2Y₄ receptors [233], and Communi *et al.* propose that the P2Y₄ exists in two distinct activation states that differ in terms of temporal responses, specificity for uridine nucleotides, and G-protein coupling [398]. Prolonged P2Y₄ activation by UTP also induces cell death in neuronal cells [399] and other cell types [393, 400, 401]. Additionally, high levels of UTP can lead to P2Y₆ activation via degradation products, with evidence that NTPDases dephosphorylate UTP to generate significant P2Y₆ activation via UDP [402-404]. Ectonucleotidases on myocardial cell surfaces rapidly hydrolyse nucleotides (ATP \rightarrow ADP \rightarrow AMP \rightarrow adenosine; UTP \rightarrow UDP \rightarrow UMP \rightarrow uridine) [402-404]. Furthermore, rapid degradation of UTP may result in the transfer of phosphate to generate ATP [189, 405]. Thus, paradoxical effects of high vs. low levels of UTP (Figures 6.2-6) could arise from excessive P2Y_{2/4} agonism (combination of exogenous and endogenous ligands) and/or degradation of UTP to UDP to target other P2Y subtypes.

These data draw attention to the general fact that effects of applied nucleotides must be considered in the context of potential degradation by ectonucleotidases, and the

impact of such activity on subsequent activation of other P2Y purinoceptors (e.g. P2Y₆, and the consequence of parallel metabolism of extracellular ATP). For example, recent findings by Kauffenstein *et al.* indicate that triphosphate diphosphohydrolase-1 (NTPDase1 or CD39), the major ectonucleotidase in cardiac endothelial cells [406], controls endothelial P2Y receptor-dependent relaxation, regulating agonist levels and P2 receptor responses [407, 408]. Additionally, NTPDase1 expression was shown to increase with hypoxia, diminishing vasodilatory effects of nucleotides and increasing vascular tone [409].

Limitations

A limitation in this study, and in other sections of this thesis, is that post-ischaemic outcome is assessed via shifts in cardiac contractile function. Clearly recovery of force development, and of diastolic function, is a primary and critical end-point following ischaemia or infarction (as the primary purpose of the heart is to pump ventricular volume to peripheral and pulmonary circuits). Ischaemia-reperfusion injury entails a mix of reversible mechanical/electrophysiological dysfunction together with irreversible cell death/infarction [155, 267]. While contractile function is a major determinant of outcome and thus an important clinical or experimental end point, a limitation is that we do not delineate relative effects of protective stimuli on differing components of acute injury. Nonetheless, it has been previously established that contractile recoveries and diastolic dysfunction correlate strongly with cell death [155]. It is likely that changes in cell death and dysfunction are both involved in benefit with UTP, although their relative contributions cannot be directly ascertained here.

6.6 CONCLUSION

The present data indicate that P2Y_{2/4} receptor activation by UTP mediates myocardial protection during ischaemia-reperfusion. UTP, when infused pre-ischaemia, may enhance myocardial tolerance to ischaemia in a preconditioning-like fashion, given evidence that multiple GPCRs are able to engage common protective RISK signals. Post-ischaemic UTP treatment fails to modify functional response to ischaemia-reperfusion, indicating that targeted P2Y_{2/4} subtypes do not exert postconditioning like effects after the ischaemic event. The UTP-mediated cardioprotection was also found to be concentration-dependent, with low (250 nM) UTP affording protection whereas high 1 µM levels were ineffective. The basis of this paradoxical concentration-dependence is not clear, but potentially arises as a result of mixed and non-selective actions of high UTP (combined endogenous and exogenous) and/or hydrolysis of high levels to other P2 agonists.

CHAPTER 7

**P2 PURINOCEPTOR-
MEDIATED
CARDIOPROTECTION IN
ISCHAEMIC-REPERFUSED
MOUSE HEART**

7.1 ABSTRACT

P2 purinoceptor modulation of injury during ischaemia-reperfusion was further studied with P2 agonists or antagonists, and the interstitial accumulation of endogenous P2 agonists (UTP, ATP, ADP) also assessed in Langendorff perfused hearts during 20 min ischaemia and 45 min reperfusion. In control hearts ventricular pressure development recovered to 68 ± 4 mmHg ($63 \pm 3\%$ of baseline), diastolic pressure remained elevated (23 ± 2 mmHg), and 26 ± 4 U/g LDH was released during reperfusion, evidencing necrosis. Treatment with 250 nM UTP improved pressure development (85 ± 5 mmHg, or $77 \pm 2\%$), and reduced diastolic contracture (by $\sim 70\%$, to 7 ± 1 mmHg) and LDH loss (by $\sim 60\%$, to 11 ± 2 U/g). In contrast, P2Y₁ agonism with 50 nM 2-methyl-thio-ATP (2-MeSATP) was ineffective. In the presence of the P2Y antagonist suramin (10 or 200 μ M), UTP no longer improved post-ischaemic outcomes. Ischaemia also substantially elevated interstitial [UTP], [ATP] and [ADP], potentially activating P2 receptors. This was supported in part by effects of antagonists: 200 μ M suramin worsened LDH efflux (53 ± 9 IU/g) and contractile dysfunction (41 ± 2 mmHg diastolic pressure; 28 ± 3 mmHg developed pressure), as did P2Y antagonism with either 10 or 100 μ M reactive blue 2 (RB2). However, a 10 μ M concentration of suramin failed to alter outcome. P2X antagonism with 10 μ M pyridoxal phosphate-6-azo(benzene-2,4-disulfonic acid (PPADS) and P2X₁ selective MRS2159 (30 μ M) was ineffective. Data collectively support cardioprotection with low concentrations of UTP, and are consistent with P2Y₂ involvement. Endogenous nucleotides may also play a protective role, as evidenced by their significant accumulation within the interstitial compartment to active levels, together with effects of P2 antagonists.

7.2 INTRODUCTION

As has already been outlined in detail in prior Chapters, extracellular nucleotides may play important regulatory roles within the cardiovascular system [174, 364], with recent evidence implicating P2 purinergic receptors in protection of ischaemic or reperfused myocardium [174, 181, 355]. While purine nucleotides have been the most widely studied P2 agonists, it is clear pyrimidines such as UTP also possess important regulatory functions. Two recent studies provide evidence UTP may mediate protective actions in ischaemic hearts [255] and hypoxic myocytes [254] from rats. However, not all investigations detect such effects of UTP under similar conditions [355], and a number of issues arise from prior studies, foremost among these being use of very high UTP concentrations to trigger protection [254, 355]. These prior studies employ levels >2-orders of magnitude above those required to activate the P2Y₂ receptors implicated in the responses [197, 363, 365]. The physiological (even pathological) relevance of responses to such high agonist levels is questionable, and it is difficult to ascribe effects to specific receptor sub-types, since such concentrations will even activate P2 receptors classified as UTP insensitive (e.g. P2Y₁ receptors). Additionally, in the only study of intact perfused hearts [355] myocyte death was not assessed, and the primary measure of ischaemic outcome (contractile recovery) was complicated by uncontrolled and thus variable heart rate. This renders interpretation of rate-dependent contractile function problematic, potentially explaining lack of effect of UTP in this work [355]. Another unresolved issue relates to potential roles of endogenous P2 agonists. Whether ischaemia enhances interstitial pyrimidine nucleotide levels sufficiently to activate P2 receptors is not known. Interestingly, recent work does reveal elevated vascular UTP in humans suffering myocardial ischaemia [189], providing indirect support for cardiac UTP release.

Four inter-related questions emerge regarding UTP and cardiac protection, to be addressed in part here: i) do low and physiologically relevant concentrations of UTP enhance ischaemic tolerance; ii) is observed protection with UTP dependent upon P2 receptor activation; iii) does ischaemia trigger significant accumulation of UTP and other P2 agonists in cardiac interstitium; and iv) are these interstitial agonist concentrations sufficient to activate P2 receptors and so modify ischaemic tolerance? We tested the ability of 250 nM UTP to modify functional outcomes and cell death following ischaemia-reperfusion, assessed the impact of P2 antagonism on UTP responses, characterized the impact of ischaemia on cardiac interstitial [UTP], and tested for protection in response to intrinsic P2 agonism (through P2 antagonism with suramin, RB2, PPADS, and MRS2159).

7.3 MATERIALS AND METHODS

Animals

Experiments were performed in accordance with the *Guide for the Care and Use of Laboratory Animals* (NIH Publication No. 85-23, revised 1996), and work approved by the Institutional Animal Care and Use committee. Young male C57/Bl6 mice of 16-20 weeks of age were used in the studies. All animals were allowed at least 4 days of in-house acclimatization before experimental procedures.

Chemicals and reagents

All drugs used were purchased from Sigma-Aldrich (Castle Hill, Australia). Drug solutions were infused into hearts at $\leq 1\%$ of total coronary flow rate to achieve the final concentrations indicated.

Perfused heart preparation and experimental protocol

The Langendorff mouse heart model, described and characterized previously [151, 155, 267], was employed. Hearts were isolated from 16-20 week old male C57/Bl6 mice (23.4 ± 0.5 g body weight, $n=119$) anaesthetised with 50 mg/kg sodium pentobarbital administered intraperitoneally, and perfused as outlined in **Chapter 2**.

Hearts stabilized for 20 min at intrinsic heart rate were switched to ventricular pacing at 420 beats/min (2 ms pulse duration, amplitude 20% above the pacing threshold) for a further 10 min. Baseline function was then assessed and 20 min global ischaemia initiated followed by 45 min reperfusion. Pacing was terminated during ischaemia and reinstated at 2 min reperfusion [155, 267]. Hearts were either untreated ($n=19$), or subjected to P2 purinoceptor antagonism (200 μ M suramin, 100 μ M RB2, 50 μ M PPADS, or 30 μ M MRS2159) applied 15 min prior to ischaemia and for the initial 10 min of reperfusion ($n=8$ for each drug), P2 purinoceptor agonism with 250 nM UTP (applied 10 min prior to ischaemia and for the initial 10 min of reperfusion; $n=12$), or co-treatment with UTP + SU ($n=8$) according to the same protocols. Upon detection of significant effects of both 200 μ M suramin and 100 μ M RB2 on intrinsic ischaemic tolerance (see **7.4 RESULTS**), effects of lower 10 μ M concentrations of these antagonists were tested alone ($n=7$ for SU, $n=7$ for RB2), together with 10 μ M SU + 250 nM UTP ($n=9$). In addition, P2Y₁ agonism with 50 nM 2-MeSATP ($n=11$) was studied. As the primary goal was identifying whether P2 agonism or antagonism modifies responses to ischaemic insult, drug infusion protocols were used to effectively bracket the ischaemic episode and early reperfusion.

For assessment of necrotic cell death, efflux of the intracellular enzyme LDH was assessed [151, 155, 267]. Myocardial LDH efflux has been shown to correlate linearly with infarct size in this model [155]. Coronary effluent was collected on ice and stored at -80°C (≤ 7 days) until analysis for LDH via a CytoTox assay kit (Promega Corporation, Annandale, Australia), a colorimetric assay coupling LDH content to conversion of a tetrazolium salt to a coloured formazan product. Total LDH washed from hearts during reperfusion was calculated as the product of LDH content (per ml) and total coronary effluent over the measurement period [155, 267].

Cardiac microdialysis assessment of interstitial nucleotides

To test for elevations in endogenous P2 agonists in the interstitial compartment, a second group of untreated hearts ($n=14$) was instrumented with cardiac microdialysis probes according to the method outlined by us previously [154]. Probes were constantly perfused at 1 $\mu\text{l}/\text{min}$ and eluents collected on ice over 10 min periods. After a 60 min stabilization period half of these hearts were subjected to 20 min global ischaemia and 45 min reperfusion while the remainder were perfused normally (non-ischaemic control). Consecutive 10 min samples of dialysate were collected and frozen at -80°C until analysed via HPLC, using an adaptation of prior techniques [410, 411]. Briefly, dialysate samples were injected onto a Suplecasil C18S column (maintained at 27°C) and eluted at 1 ml/min using a buffer gradient (60% solution A/40% solution B at 0 min to 40% solution A/60% solution B at 25 min, followed by isocratic elution to 60 min). Solution A consisted of a 10 mM KH_2PO_4 buffer containing 0.25% MeOH and 10 mM tetrabutylammonium hydroxide (pH 6.9), and solution B consisted of a 50 mM KH_2PO_4 buffer containing 30% MeOH and 5.3 mM tetrabutylammonium hydroxide (pH 7.0). Eluent absorbance was continuously

monitored on a Waters photodiode array detector (Waters, NSW, Australia), and nucleotide concentrations calculated based on comparison to absorbances for known standards run each day of analysis.

Statistical analysis

Data are presented as mean \pm SEM. Baseline data and functional outcomes from ischaemia in different experimental groups were compared via one-way ANOVA. When significant effects were identified a Newman-Keuls post hoc test was employed for individual comparisons. A value of $P < 0.05$ was considered significant in all tests.

7.4 RESULTS

Normoxic function

Baseline functional data are provided in Table 7.1. Pressure development, and inotropy and rate of relaxation were high, and coronary flow sub-maximal based on prior data for flow responses in murine hearts [267]. Treatment with UTP failed to modify ventricular contractile function in normoxic hearts. Similarly, most antagonist treatments did not alter contractility, although 100 (but not 10) μ M RB2 did generate a significant increase in force development and inotropic state (Table 7.1). Interestingly, suramin (at 200 μ M) and RB2 (at both 10 and 100 μ M) generated significant elevations in baseline coronary flow, while there was a tendency (albeit insignificant) for modestly decreased coronary flow with UTP (Table 7.1).

Table 7.1 – Pre-ischaemic contractile function and coronary flow in all experimental groups.

<i>Treatment</i>	<i>LVDP</i> (mmHg)	<i>+dP/dt</i> (mmHg/s)	<i>-dP/dt</i> (mmHg/s)	<i>Flow</i> (ml/min/g)
Untreated (n=19)	115±4	4388±218	-2962±116	20.0±1.0
250 nM UTP (n=12)	109±5	3866±275	-2730±153	17.3±0.9
10 µM suramin (n=7)	127±5	5056±392	-3083±184	25.5±2.3
200 µM suramin (n=8)	115±6	4664±417	-3023±355	28.9±1.3*
UTP + 10 µM suramin (n=9)	116±4	5035±370	-3078±192	25.9±1.8†
UTP + 200 µM suramin (n=8)	104±4	4316±243	-2635±160	26.4±0.5*†
10 µM RB2 (n=7)	128±7	5249±351	-3409±172	30.0±2.4*
100 µM RB2 (n=8)	136±4*	6249±351*	-4160±164*	28.6±1.5*
50 µM PPADS (n=8)	108±3	4834±183	-3139±136	19.7±0.5
30 µM MRS2159 (n=8)	126±4	4769±232	-3205±127	19.3±1.7

Data were measured immediately prior to ischaemia. LVDP, left ventricular developed pressure; +dP/dt and -dP/dt, positive and negative differentials of left ventricular force development, respectively. Values are means±SEM. *, $P<0.05$ vs. untreated hearts; †, $P<0.05$ vs. UTP alone.

Effects of ischaemia and UTP on cardiovascular function and cell death

Ischaemia resulted in sustained depression of contractile function over the 45 min reperfusion period (Figure 7.1). Diastolic pressure remained elevated at ~20 mmHg (Figure 7.1A), and ventricular pressure development recovered to ~65% of pre-ischaemic levels (Figure 7.1B). Coronary flow recovered to slightly less than pre-ischaemic levels (Figure 7.1C). Ischaemia-reperfusion was also associated with significant efflux of LDH (Figure 7.2), reflecting necrotic death [155]. Treatment of hearts with 250 nM UTP significantly reduced post-ischaemic diastolic dysfunction, and moderately enhanced ventricular pressure development (Figure 7.1). These effects were not associated with significant differences in final recovery of flow rate (expressed as ml/min/g; Figure 7.1C).

Treatment with UTP also significantly reduced LDH loss (Figure 7.2). We additionally tested for effects of the P2Y₁ agonist 2-MeSATP (50 nM), but the agent was found to exert no effects on any markers of ischaemic injury at this concentration (data not shown). To test for P2 involvement in UTP-mediated cardioprotection, we co-treated hearts with the antagonist suramin, which was found to exert concentration-dependent effects on ischaemic outcome. When applied at 200 μ M, suramin worsened functional recovery from ischaemia (Figure 7.1) and LDH washout (Figure 7.2). However, a lower 10 μ M concentration was without effect on functional recovery from ischaemia (Figure 7.1). Importantly, UTP was unable to modify responses to ischaemia in the presence of 10 or 200 μ M suramin, failing to reduce contractile dysfunction (Figures 7.1A and B) below levels observed in the presence of suramin alone. Similarly, UTP no longer reduced LDH washout in the presence of 200 μ M suramin (Figure 7.2)

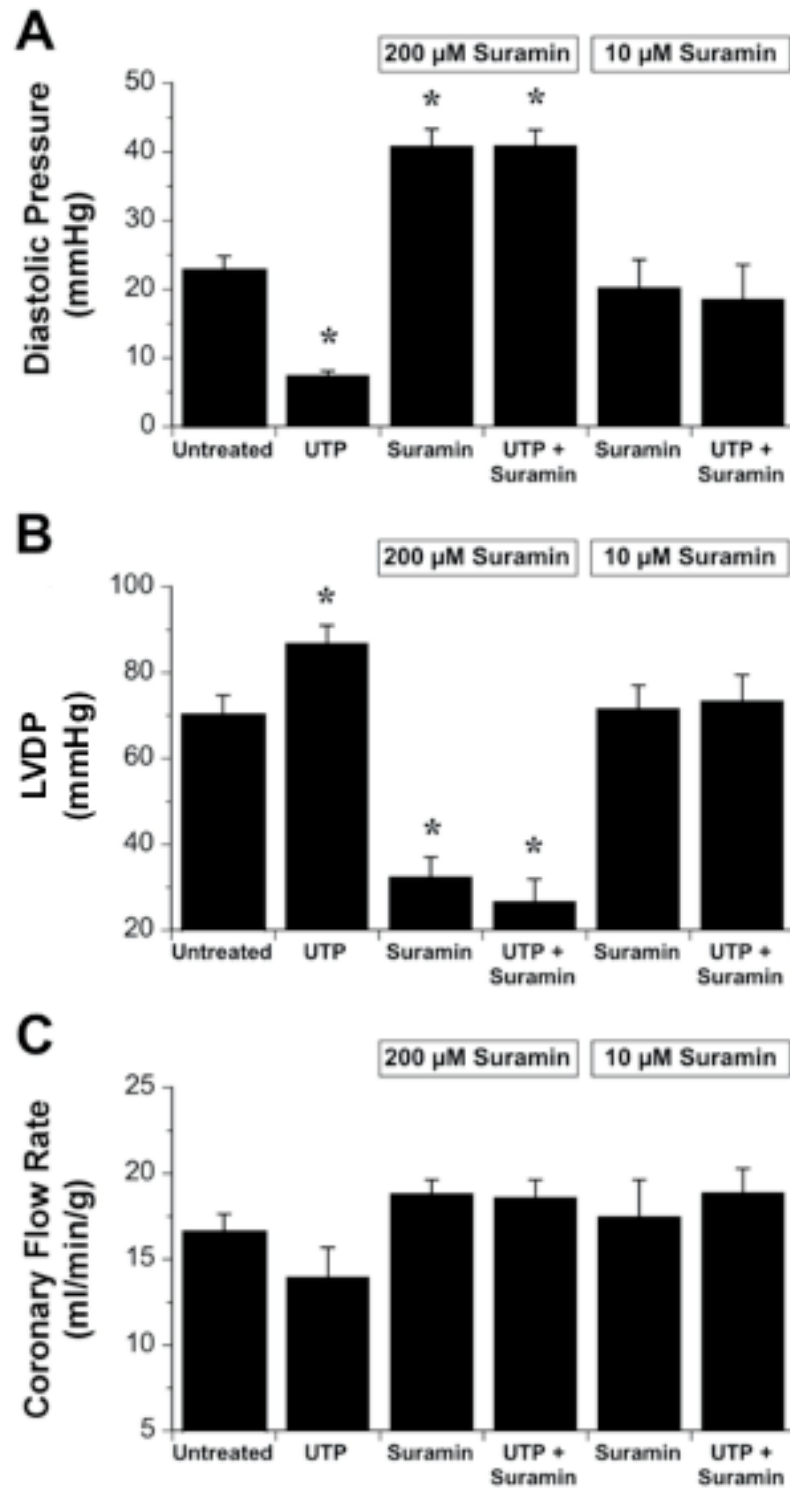


Figure 7.1. Effects of UTP on post-ischaemic recoveries of left ventricular contractile function and coronary flow. Measures were made at the end of 45 min reperfusion (following 20 min global ischaemia) in untreated hearts ($n=19$), and in hearts treated with 250 nM UTP ($n=12$), 200 μ M suramin ($n=8$), 250 nM UTP + 200 μ M suramin ($n=8$), 10 μ M suramin ($n=7$), or 250 nM UTP + 10 μ M suramin ($n=9$). Shown are recoveries for left ventricular (LV) diastolic pressure (A), left ventricular (LV) developed pressure (B), and coronary flow rate (C). Values are means \pm SEM. * $P<0.05$ vs. corresponding values from control (Untreated) hearts.

Effects of ischaemia on myocardial interstitial UTP, ATP and ADP concentrations

Based on apparent reduction in ischaemic tolerance with 200 μ M suramin alone, we assessed release of P2 agonists into the interstitial compartment (Figure 7.3). Under normoxic conditions we were able to detect ATP in most cases, yet could not consistently detect ADP or UTP in cardiac microdialysate samples (Figure 7.3). However, during 20 min of global ischaemia the accumulation of all three nucleotides was significantly enhanced, with ATP levels exceeding those for ADP, and in turn UTP. Nucleotide concentrations peaked within the initial 10 min of ischaemia and then declined during the ensuing 10 min (although remaining substantially elevated above normoxic levels). Subsequent reperfusion led to a gradual decline in dialysate UTP, ATP and ADP levels, such that only ATP remained detectable during the final 20 min of reperfusion. No changes in nucleotide levels were detected in normoxically perfused hearts (Figure 7.3).

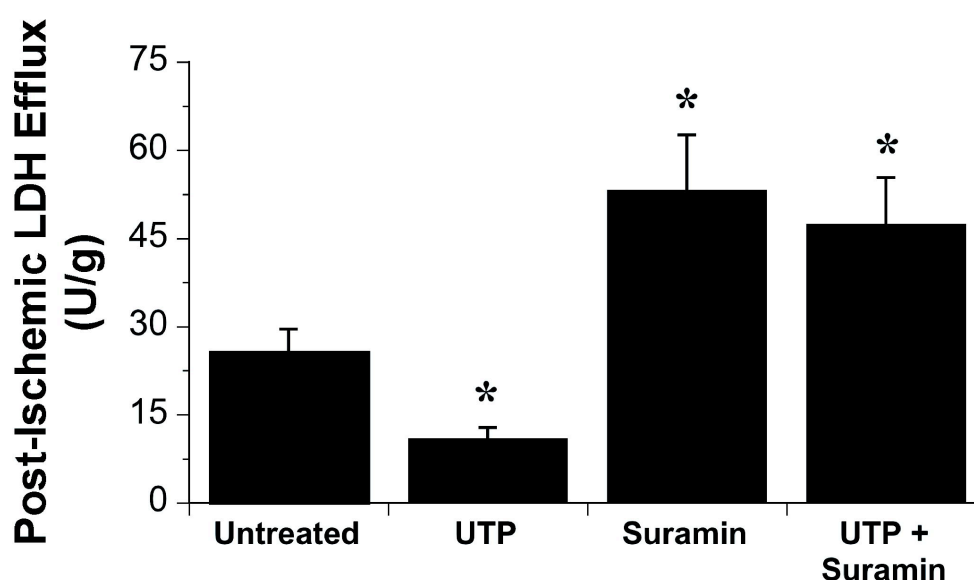


Figure 7.2. Myocardial LDH efflux (indicating extent of oncosis) throughout post-ischaemic reperfusion. Efflux was measured in untreated hearts ($n=19$), and in hearts treated with 250 nM UTP ($n=12$), 200 μ M suramin ($n=8$), or UTP + suramin ($n=8$). Values are means \pm SEM. *, $P<0.05$ vs. corresponding values from control (Untreated) hearts.

Effects of P2 purinoceptor antagonism on functional tolerance to ischaemia

To determine whether accumulation of endogenous nucleotides in the interstitium might indeed modify functional outcome from ischaemia we re-assessed contractile responses to ischaemia-reperfusion in the presence of differing P2 antagonists (Figure 7.4). As already noted, treatment with 200 μ M suramin worsened post-ischaemic outcome, increasing diastolic dysfunction and limiting recovery of ventricular pressure development (Figures 7.1 and 7.4) and enhancing cell death (Figure 7.2). Greater contractile dysfunction was accompanied by impaired recovery of coronary flow (to ~65%) (Figure 7.4C). The alternate P2 antagonist RB2 (at 100 μ M) also worsened contractile dysfunction. Interestingly, while a lower 10 μ M concentration of RB2 also worsened ischaemic outcomes, this concentration of suramin was without effect on post-ischaemic functional recovery (Figure 7.4), though it remained effective in blocking the protective effects of UTP (Figure 7.1). Neither 10 μ M PPADS or 30 μ M MRS2159 exerted any effect on post-ischaemic recoveries (Figure 7.4)

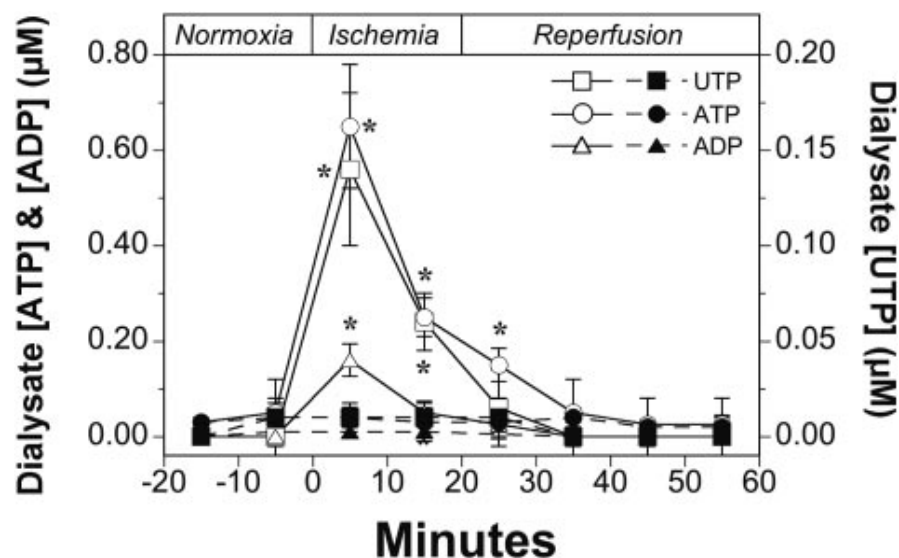


Figure 7.3. Microdialysate levels of ATP, ADP and UTP during ischaemia-reperfusion in control (untreated; $n=7$) hearts. Microdialysate levels are also shown for normally perfused, non-ischaemic hearts (closed symbols; $n=7$). Values are means \pm SEM. *, $P<0.05$ vs. pre-ischaemic levels.

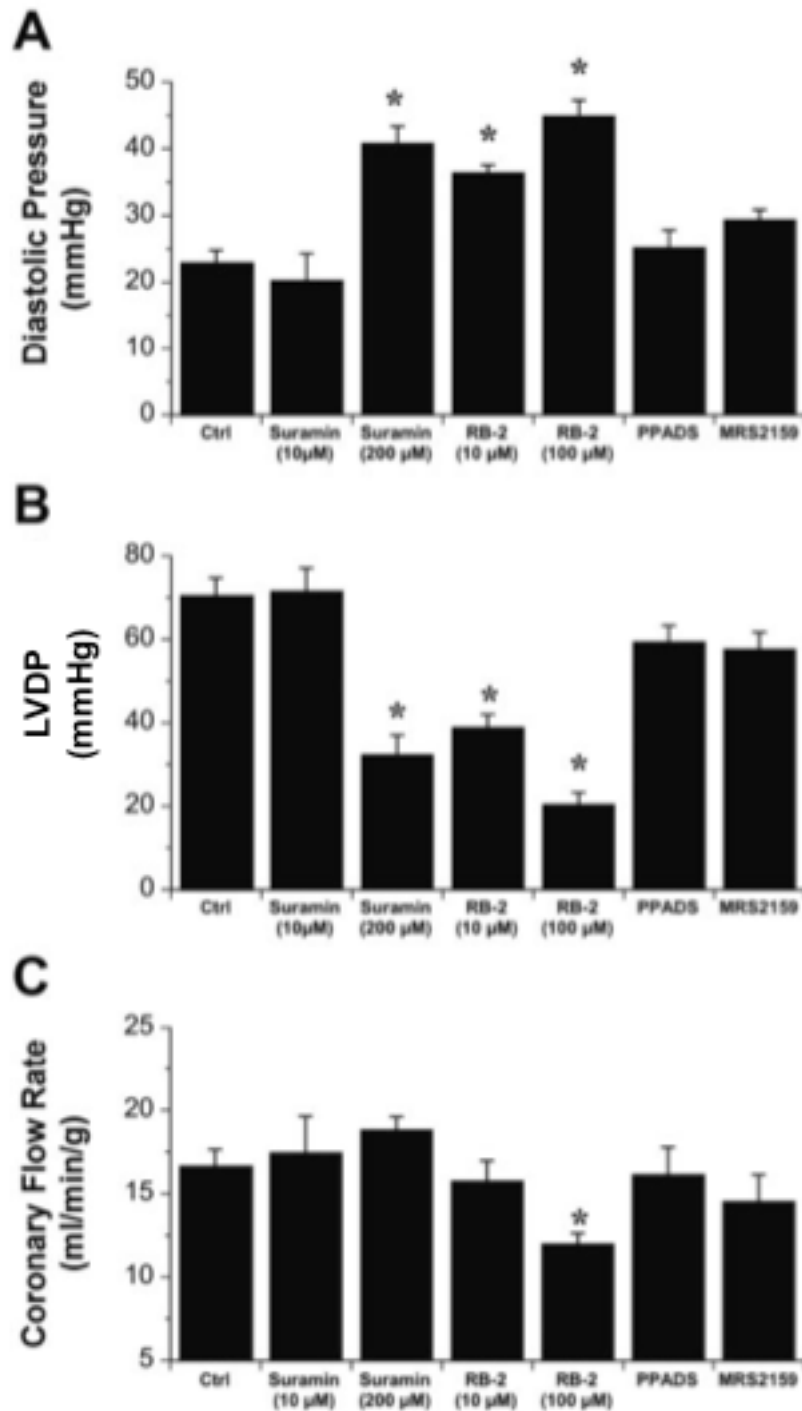


Figure 7.4. Effects of P2 antagonists on post-ischaemic recoveries of contractile function and coronary flow. Measures were made after 45 min reperfusion in untreated hearts ($n=19$), and in hearts treated with 10 μ M ($n=7$) or 200 μ M ($n=8$) suramin, 10 μ M ($n=7$) or 100 μ M ($n=8$) RB2, 50 μ M PPADS ($n=8$), or 30 μ M MRS2159 ($n=8$). Shown are recoveries for left ventricular (LV) diastolic pressure (A), left ventricular (LV) developed pressure (B), and coronary flow rate (C). Values are means \pm SEM. *, $P<0.05$ vs. corresponding values from control (Untreated) hearts.

7.5 DISCUSSION

Recent studies provide good support for UTP-dependent cardioprotection in the rat [254, 255]. However, these findings are not universal (e.g. Ninomiya *et al.*, 2002a), and a number of interesting questions arise from these prior investigations. Here we confirm P2-mediated cardioprotection in response to sub-micromolar concentrations of UTP, document significant accumulation of UTP (together with ATP and ADP) in the interstitium of ischaemic hearts, and show that high levels of the P2 antagonists suramin and RB2 (and not PPADS or MRS2159) worsen ischaemic outcome. Interestingly, while a lower 10 μ M concentration of RB2 also limited post-ischaemic outcome, suramin at this concentration was ineffective. Collectively, these findings evidence cardioprotection via exogenous UTP (involving limitation of ventricular contractile dysfunction and necrosis), and implicate the P2Y₂ receptor as the most likely mediator of this protection. Mixed effects of P2 antagonists alone also support protection via endogenous P2 agonists, though these responses may potentially involve P2-independent effects and deserve further attention (see below).

P2 purinoceptors and cardioprotection

Based on structural similarities the P2Y receptor family is grouped into P2Y₁, P2Y₂, P2Y₄, P2Y₆, and P2Y₁₁ receptors, and a dissimilar group containing P2Y₁₂ and P2Y₁₃ receptors [174, 197, 364, 365]. These G-coupled receptors, or their mRNA's, have been localized to cardiomyocytes [412], cardiac fibroblasts [191], and vascular smooth muscle and endothelium [413], and are known to regulate the activity of multiple intracellular kinases [365] to modify cellular function. Relatively little work has been undertaken to delineate functions of P2Y purinoceptors in myocardial stress resistance and protection. Unfortunately, delineating contributions of individual P2

sub-types to functional responses in intact tissue is hampered by mixed selectivities of agonists and (particularly) antagonists [197, 365]. While judicious choice of drug concentration can limit the range of receptor candidates, recent studies of cardiac protection have employed very high (3-100 μ M) UTP concentrations [254, 355], sufficient to maximally activate P2Y₂, P2Y₄, and P2Y₆ receptors, and potentially activate P2Y₁ and P2Y₁₁ receptors at which UTP is generally considered a poor agonist [197, 365]. Here we employ a low UTP concentration (250 nM) that, based on known potencies [197], should be selective for P2Y₂ receptors but may also activate P2Y₄ receptors to a limited extent. Since UTP possesses EC₅₀ values at P2Y₁, P2Y₆ and P2Y₁₁ receptors as much as 3-orders of magnitude higher than the concentration applied here, these receptors should not be significantly activated. Furthermore, we observed no effects of P2Y₁ agonism with 2-MeSATP (see **7.4 RESULTS**). Finally, the 10 and 200 μ M concentrations of the non-selective P2Y antagonist suramin shown to inhibit UTP-mediated protection (Figure 7.1) should exert greatest effects at P2Y₂, P2Y₁ (eliminated as a candidate due to lack of effect of 2-MeSATP) and P2Y₁₁ receptors (eliminated as a candidate owing to their insensitivity to 250 nM UTP). Collectively, the effects of 250 nM UTP and suramin, and lack of effect of 2-MeSATP, implicate P2Y₂ receptor involvement in UTP-dependent cardioprotection.

In contrast to our data, a prior study in rats found that myocardial P2Y activation alone does not generate protection, although endogenous P2 agonists apparently contributed to benefit with ischaemic preconditioning [181, 355]. Limitation of ischaemic injury observed here (Figures 7.1 and 7.2) is consistent with UTP-mediated protection of hypoxic cardiomyocytes [254]. Furthermore, in the course of the current study Yitzhaki *et al.* (2006) published details of infarct-sparing effects of transient

UTP pre-treatment in an *in vivo* rat model. These investigators found UTP reduced hypoxia-dependent mitochondrial Ca^{2+} load in isolated myocytes, potentially underlying observed protection. Reasons for the lack of effect of UTP in the earlier study of Ninomiya *et al.* (2002a) vs. protection observed here and by Yitzhaki *et al.* (2006) are not known, although high UTP levels employed in prior studies raises the possibility of confounding effects of multiple P2Y sub-type activation. Moreover, Ninomiya *et al.* (2006) did not assess markers of cell death, and heart rate was uncontrolled, complicating interpretation of rate-dependent contractility.

Ischaemic accumulation of interstitial nucleotides

Cardiac microdialysis provides a useful tool for monitoring accumulation of signalling compounds in the myocardial interstitium [154, 181, 411]. While some degree of tissue injury is unavoidable in microdialysis studies, and is perhaps exaggerated in small technically challenging models such as the mouse [154], our data nonetheless reveal substantial ischaemia-specific elevations in UTP, ATP and ADP in cardiac microdialysate (Figure 7.3). Although prior studies have documented similar elevations in ATP and ADP in rat myocardium [181], together with elevations in the related P1 agonist Ado in rat and mouse hearts [154, 181, 411], this is the first report of ischaemic elevations in myocardial interstitial UTP. Recent observations of vascular accumulation of UTP in patients suffering myocardial ischaemia are consistent with cardiac UTP release [189].

The source and identity of nucleotides released during ischaemia remains unclear: nucleotides may be released from endothelium by G-coupled receptor activation [414], from sympathetic and parasympathetic nerve endings [415] and from cardiac

myocytes during hypoxic or ischaemic stress [416, 417]. The changes in interstitial nucleotides observed here could play a regulatory role during or following ischaemia: interstitial UTP, ATP, or ADP may all activate G-coupled P2Y receptors (with ATP and ADP additionally modulating ion channel-coupled P2X purinoceptors) in coronary vessels [413, 418], cardiac fibroblasts [191], and myocytes [412]. Though it is problematic to estimate precise solute concentrations from microdialysate levels, our data suggest that low μM levels of UTP and ATP may be achieved with severe ischaemic stress, sufficient to activate P2Y₂ receptors at which these nucleotides possess EC₅₀ values $\leq 0.25 \mu\text{M}$ [197].

Modulation of ischaemic tolerance by P2 antagonism

Having established that low levels of exogenous UTP trigger P2-dependent cardioprotection (Figures 7.1 and 7.2), and that ischaemia generates substantial elevations in this and other P2 agonists (Figure 7.3), we sought to identify effects of endogenous nucleotides via co-treatment with differing P2 antagonists (Figure 7.4). suramin, RB2 and PPADS are relatively broad-spectrum antagonists, RB2 exhibiting some selectivity for P2Y vs. P2X while PPADS is partially selective for P2X vs. P2Y receptors [197, 363]. The drug MRS2159 is selective at P2X₁ receptors. It is worth noting that suramin and PPADS can exert effects on signal transduction and G-proteins [372, 419]. However, the polar nature of the agents prevents them from crossing the cell membrane, minimizing these effects in intact tissue.

Detrimental effects of 200 μM suramin and 10-100 μM RB2 on post-ischaemic recovery (Figures 7.1 and 7.4), together with lack of effect of PPADS and MRS2159, tend to support intrinsic activation of P2Y purinoceptors. Since suramin selectively

blocks P2Y₂ vs. P2Y₄ receptors (at which it exhibits very poor potency) [363, 365], inhibitory effects of this agent on both UTP-mediated protection and intrinsic ischaemic tolerance support involvement of P2Y₂ receptors. Lack of effect of PPADS on ischaemic outcome is also consistent with P2Y₂ involvement, as PPADS is most potent at P2Y₁ and possibly P2Y₆ receptors, but ineffective at rodent P2Y₄ and human P2Y₂ receptors [363, 365]. In contrast, RB2 will more broadly antagonize P2Y receptor sub-types, and is also shown to impact on post-ischaemic recovery at low and high concentrations (Figure 7.4). However, a complication in this interpretation relates to potential blockade of ectonucleotidase activity by suramin and other P2 antagonists.

Several studies confirm that different P2 antagonists may non-competitively inhibit ectonucleotidase activity in different species and tissues [373, 374]. Studying Mg²⁺-sensitive ectonucleotidase from rats, Yegutkin and Burnstock (2000) arrived at an IC₅₀ of 20-30 µM for suramin (with values of 50 µM for RB2, and ~1 mM for PPADS). Chen *et al.* (1996) acquired IC₅₀ values of 40 to >100 µM for suramin in rat and mouse cells (and 15-20 µM for both RB2 and PPADS). These inhibitory effects will limit responses mediated by hydrolysis products of extracellular nucleotides, which may be responsible (at least in part) for the detrimental actions of these agents during ischaemia-reperfusion. In assessing this possibility, we examined responses to lower 10 µM concentrations of suramin and RB2 (Figure 7.1 and 7.4), which we reasoned should retain some P2 inhibitory efficacy but be less effective in inhibiting ectonucleotidases. Curiously, though the lower RB2 concentration still effectively impaired post-ischaemic outcome, 10 µM suramin was without effect on the response to ischaemia (Figure 7.4). This likely stems from differing inhibitory potencies of the

two agents at different P2 receptors (see above), but may additionally reflect effects of SU on other processes dictating post-ischaemic outcome (including inhibition of ectonucleotidase activity) at high concentrations. In this regard, findings of Colgan *et al.* (2006) revealed that gene ablation of CD73 worsens outcome from ischaemia *in vivo* [420], and we have recently confirmed that P1 receptor activation by endogenous Ado (which is generated via CD73 activity) does limit injury during ischaemia-reperfusion [151]. We must temper our conclusion then, that effects of the P2 antagonist SU may involve a combination of receptor antagonism and/or inhibition of beneficial actions of ectonucleotidase activity. Future work might address the impact of these agents on interstitial accumulation of nucleotides and their hydrolysis products.

Injurious effects of suramin and RB2 in ischaemic myocardium have not been documented previously. The studies of Ninomiya and colleagues (2000a,b) in rat hearts do not report on effects of P2 antagonism alone, and in any case employ an index of post-ischaemic outcome that is difficult to interpret (rate-dependent contractile function in un-paced hearts). However, other evidence does support endogenous P2 receptor activation or roles for nucleotides in ischaemic myocardium: cardiac t-PA release during ischaemia is modulated by endogenous nucleotides acting at P2Y receptors [337]; intrinsic P2 receptor activation contributes to preconditioning with transient ischaemia [181]; and as already noted, CD73 knockout may worsen ischaemic tolerance [420], supporting a contribution of extracellular nucleotide hydrolysis to cardiac protection. Thus, there is evidence for roles of endogenous nucleotides in ischaemic myocardium.

P2 purinoceptor-dependent coronary constriction

Unexpected coronary dilation in response to suramin and RB2 is of interest - both antagonists significantly enhanced coronary flow in normoxic hearts (Table 7.1). Additionally, and perhaps related, the P2 agonist UTP elicited a small (albeit insignificant) decline in baseline flow. There is some prior support for P2Y-mediated smooth muscle constriction, in addition to dilation [421, 422], although substantial species differences exist in these responses. This may explain the modest dilatory effect of extremely high (50 μ M) UTP reported by Ninomiya *et al.* (2002a) in rat hearts *vs.* modest (insignificant) constriction observed with UTP in the mouse (Table 7.1). Other studies report on novel UTP-sensitive coronary P2Y receptors exhibiting some properties relevant to the current observations [423], and support UTP-mediated coronary constriction [161]. Rayment *et al.* (2007) most recently presented evidence for P2Y₂-dependent UTP mediated coronary artery contraction, which is sensitive to suramin [347]. Thus, despite P2-mediated endothelium-dependent dilation of intact vessels [245, 424], evidence also reveals a P2Y-mediated coronary constriction [161, 425]. The nature of these different vascular responses deserves further attention, as does the identity of P2 receptors involved. For example, while evidence is presented for P2Y₂ involvement in coronary constriction [347], P2Y₆-dependent contraction detected in other vessel types [241] could conceivably play some role.

7.6 CONCLUSION

This study builds on prior evidence of UTP-mediated tissue protection [254, 255]. Our observations reveal that low concentrations of UTP improve post-ischaemic outcomes in a P2-dependent manner. While the receptor sub-type(s) involved remains

to be unequivocally identified, the P2Y₂ sub-type is most strongly implicated based on the effects of UTP and suramin. Ischaemia itself also triggers elevations in interstitial UTP and other P2 agonists (ATP, ADP) to active levels, and P2 antagonism with suramin and RB2 does limit intrinsic ischaemic tolerance. Concentration dependent actions of suramin warrant further study, and may reflect differing potencies at relevant P2 receptors and/or other inhibitory actions (such as blockade of ectonucleotidase activity).

CHAPTER 8

EFFECTS OF SELECTIVE P2Y₆ AND P2Y_{2/4} AGONISTS IN ISCHAEMIC-REPERFUSED MYOCARDIUM

8.1 ABSTRACT

Prior work detailed UTP-mediated cardioprotection in ischaemic myocardium, with evidence implicating the P2Y₂ as the likely receptor involved. However, identification of subtype involvement is hampered by partial selectivity of antagonists and potential conversion of UTP to other P2 agonists. Thus, the current study assesses more selective P2Y agonists (stable pyrimidines *UDPβS* and *UTPγS*) to identify effects of selective activation of P2Y₆ and P2Y_{2/4} purinoceptors, respectively. These agents were not readily available at the time of earlier studies. Interestingly, significant changes in normoxic function were apparent with *UTPγS* and *UDPβS*. A reduction in rate of relaxation ($-dP/dt$ declined from -3239 ± 222 to -2944 ± 118 ; $P < 0.05$) and coronary flow (from 23 ± 1 to 20 ± 1 ml/min/g; $P < 0.05$) occurred with 50 nM *UTPγS*. Treatment with 50 nM *UDPβS* not only reduced baseline rate of relaxation ($-dP/dt$ fell to -2507 ± 150 ; $P < 0.05$) and coronary flow (to 19 ± 2 ml/min/g, $P < 0.05$), but also unexpectedly depressed LVDP (from 122 ± 4 to 97 ± 4 mmHg; $P < 0.05$). Hearts subject to 20 min ischaemia and 45 min reperfusion exhibited depression of LVDP to $57 \pm 3\%$ of pre-ischaemic levels (74 ± 6 mmHg), with substantial diastolic contracture (23 ± 2 mmHg). The latter diastolic contracture was significantly and concentration-dependently reduced by both 50 and 150 nM of the P2Y_{2/4} agonist *UTPγS* (to 15 ± 2 mmHg with 50 nM, and 10 ± 1 mmHg with 150 nM; $P < 0.05$). *UTPγS* did not modify absolute recovery of LVDP. However, 50 nM *UTPγS*, appeared to improve % recovery of LVDP ($74 \pm 4\%$ of pre-ischaemia; $P < 0.05$) whilst hearts treated 150 nM *UTPγS* exhibited comparable relative recovery to untreated hearts ($61 \pm 5\%$). Post-ischaemic recovery of contractile function was also improved with *UDPβS*, with enhanced relative recovery of LVDP ($73 \pm 4\%$ of pre-ischaemia) and $-dP/dt$ ($94 \pm 6\%$ of pre-ischaemia). *UDPβS* did not modify recovery of diastolic pressure, but did enhance

recovery of coronary flow. Paradoxically, *UTP* γ *S* failed to alter LDH efflux, while *UDP* β *S* actually enhanced LDH loss suggesting exaggeration of tissue damage. These results collectively support a cardioprotective role for select P2Y_{2/4} purinoceptor activation, which appears restricted to functional improvements. Results also provide the first evidence of P2Y₆ mediated functional protection in ischaemic-reperfused mouse hearts, though evidence suggests cell damage may be paradoxically exaggerated.

8.2 INTRODUCTION

Multiple cell types release P2 agonists into the extracellular compartment with hypoxic or ischaemic stress. The receptors may mediate both protective and detrimental effects under such conditions, as evidenced in prior studies in this thesis. Discriminating between the effects of P2Y purinoceptors is difficult because of a lack of highly selective agonists and antagonists. In addition, ligand instability further complicates analyses in intact tissues, with nucleotide tri-phosphates and di-phosphates metabolised by ectonucleotidases on the cell surface [426]. The P2Y₂, P2Y₄ and P2Y₆ purinoceptors are all activated by uracil nucleotides, with the P2Y₂ activated equipotently by ATP and UTP [195, 427]. Whilst ATP is a competitive antagonist at the human P2Y₄ receptor, UTP is a selective agonist [405]. However, species differences between the rat and mouse reveal that P2Y₄ receptors can be activated by both UTP and ATP [428]. The P2Y₆ receptor is selectively activated by UDP and UTP is a weak agonist or inactive at this receptor subtype [385, 386].

The stable pyrimidines *UDPβS* and *UTPγS* have been used to pharmacologically define roles of P2Y purinoceptor subtypes. These nucleotides contain a modification of the triphosphate group in the form of a thio-substitution at the terminal phosphate, providing stability against ectonucleotidase activity. *UTPγS* is a potent and enzymatically stable agonist at human P2Y₂ and P2Y₄ purinoceptors, while *UDPβS* has been shown to selectively activate the P2Y₆ subtype [240, 429]. Since UTP is susceptible to hydrolysis through UDP to UMP and uridine via nucleotidase and phosphatase activities in intact tissues, these stable pyrimidine analogues enable better discrimination of P2Y purinoceptor specific responses. In **Chapter 4** it was shown that murine expression of P2Y₂ transcript was highest in the left ventricle. Although

the expression of P2Y₄ transcript was highest in aorta, transcript was also expressed in the left ventricle (~50% of P2Y₂ transcript expression). Therefore, observable protective effects of UTP may be attributed to activation of P2Y₂ subtype, though it may also lead to generation of other local P2 ligands as a result of hydrolysis by ectoenzymes. The aim of the present study was to further discriminate between P2Y_{2/4} and P2Y₆ effects in normoxic and ischaemic-reperfused tissue, employing the stable pyrimidines *UTP* γ *S* (acting selectively on P2Y_{2/4}) and *UDP* β *S* (acting selectively on P2Y₆).

8.3 MATERIALS AND METHODS

Perfused heart preparation and experimental protocol

Investigations conformed to the Guide for the Care and Use of Laboratory Animals published by the US National Institute of Health (NIH Publication No 85-23, revised 1996). Male C57/B16 mice weighing 25-35g were anaesthetised with a bolus injection sodium pentobarbital (50 mg/kg) administered intraperitoneally. Mouse hearts were excised *en bloc* with the lungs and arrested by immersion in ice-cold perfusion fluid. Hearts were cannulated via the aorta and retrogradely perfused as outlined in detail in **Chapter 2**.

Hearts stabilised for 20 min at intrinsic heart rate were switched to ventricular pacing at 420 beats/min (2 ms pulse duration, amplitude 20% above the pacing threshold) for a further 10 min. Baseline function was then assessed and 20 min global ischaemia initiated followed by 45 min of aerobic reperfusion. Pacing was terminated during ischaemia and reinstated at 2 min reperfusion [155, 267]. Hearts were untreated ($n=10$) or subjected to treatment with: i) 50 nM *UTP* γ *S* ($n=10$); ii) 150 nM *UTP* γ *S*

($n=10$); or iii) 50 nM $UDP\beta S$ ($n=8$). Agents were applied for 10 min pre-ischaemia and the initial 10 min of reperfusion. For assessment of necrotic cell death, efflux of the intracellular enzyme LDH was assessed [151, 155, 267], as outlined in **Chapter 2**.

Chemicals and reagents

The stable pyrimidines $UDP\beta S$ and $UTP\gamma S$ were kindly donated by Prof David Erlinge. Drug solutions were infused into hearts at $\leq 1\%$ of coronary flow rate to achieve the final concentrations indicated.

Statistical analyses

Post-ischaemic functional recoveries were compared via one-way ANOVA. Where inter-group significance was detected, a Newman-Keuls post-hoc test was applied for specific comparisons. In all tests, significance was accepted for $P < 0.05$. Data are presented as means \pm SEM.

8.4 RESULTS

Effects of $UDP\beta S$ and $UTP\gamma S$ on normoxic function

Normoxic function in control (untreated) hearts is shown in Table 8.1. Treatment with 50 nM $UTP\gamma S$ reduced rate of relaxation (indicated by $-dP/dt$) without modifying inotropic state ($+dP/dt$) or LV pressure development (Table 8.1). However, 50 nM $UDP\beta S$ reduced developed pressure and rate of relaxation (Table 8.1). Treatment with 50 nM of either $UTP\gamma S$ or $UDP\beta S$ also reduced coronary flow. Pressure development, rate of relaxation and coronary flow differed significantly between hearts treated with $UTP\gamma S$ vs. $UDP\beta S$ (50 nM) (Table 8.1).

Effects of the selective P2Y_{2/4} agonist UTP γ S on post-ischaemic outcomes

Post-ischaemic recovery of LV diastolic pressure was significantly improved by UTP γ S (Figure 8.4) in a concentration-dependent manner. UTP γ S at either concentration had no effect on absolute LV developed pressure at the end of reperfusion (Figure 8.1A).

Table 8.1 – Effects of UTP γ S and UDP β S on normoxic cardiovascular function.

<i>Treatment</i>	<i>LVDP (mmHg)</i>	<i>+dP/dt (mmHg/s)</i>	<i>-dP/dt (mmHg/s)</i>	<i>Flow (ml/min/g)</i>
Untreated (n=10)	129 \pm 8	5173 \pm 504	-3465 \pm 196	25 \pm 1
UTP γ S (50 nM) (n=10)	121 \pm 5	4813 \pm 279	-2944 \pm 118*	20 \pm 1*
UTP γ S (150 nM) (n=10)	124 \pm 8	4759 \pm 642	-3476 \pm 262	26 \pm 2 [†]
UDP β S (50 nM) (n=8)	97 \pm 4* [‡]	3849 \pm 235	-2507 \pm 150* [‡]	19 \pm 2* [‡]

Data were measured immediately prior to ischaemia. LVDP, left ventricular developed pressure; +dP/dt and -dP/dt, positive and negative differentials with respect to time or left ventricular force development and relaxation, respectively. Values are means \pm SEM. *, $P < 0.05$ vs. untreated hearts; [†], $P < 0.05$ vs. UTP γ S (50 nM), [‡], $P < 0.05$ vs. UTP γ S (150 nM).

Interestingly, hearts treated with the lower concentration of 50 nM UTP γ S exhibited a greater relative recovery of LVDP than hearts treated with 150 nM UTP γ S (Figure 8.1) while hearts treated with the higher concentration exhibited comparable recovery to untreated hearts. However, this may stem in part from effects on pre-ischaemic function. Recovery of coronary flow was not significantly altered by either concentration of UTP γ S (Figure 8.5A and 8.5B).

Effects of the Selective P2Y₆ Agonist UDPβS on Post-Ischaemic Outcomes

Recovery of LV contractile function was improved by UDPβS, with significant differences detected for LVDP and +dP/dt (Figures 8.1B and 8.2B). In addition, UDPβS enhanced coronary flow recovery to levels exceeding pre-ischaemia (Figure 8.5B). However, UDPβS did not modify recovery of diastolic pressure (Figure 8.4).

Effects of P2Y_{2/4} and P2Y₆ agonism on time-dependent recovery of LV function

The temporal patterns of effects of P2Y_{2/4} and P2Y₆ agonist treatments were examined over 45 min of reperfusion (Figures 8.6A and B). Hearts treated with UTPγS (50 nM or 150 nM) exhibited improved LV function in the initial minutes of reperfusion but not later in the final stages of reperfusion (compared to untreated hearts) (Figure 8.6A). Although hearts treated with UDPβS exhibited reduced LV pressure development in the initial 10 minutes of reperfusion, recovery of function was comparable to untreated hearts at the end of reperfusion (Figure 8.6A).

Diastolic contracture was significantly reduced by application of UTPγS (50 nM or 150 nM), with reduction of post-ischaemic contracture statistically significant at 20 and 45 min of reperfusion compared to untreated hearts (and to hearts treated with UDPβS). Selective activation of P2Y₆ purinoceptors with 50 nM UDPβS did not modify diastolic contracture at any point of reperfusion (Figure 8.6B).

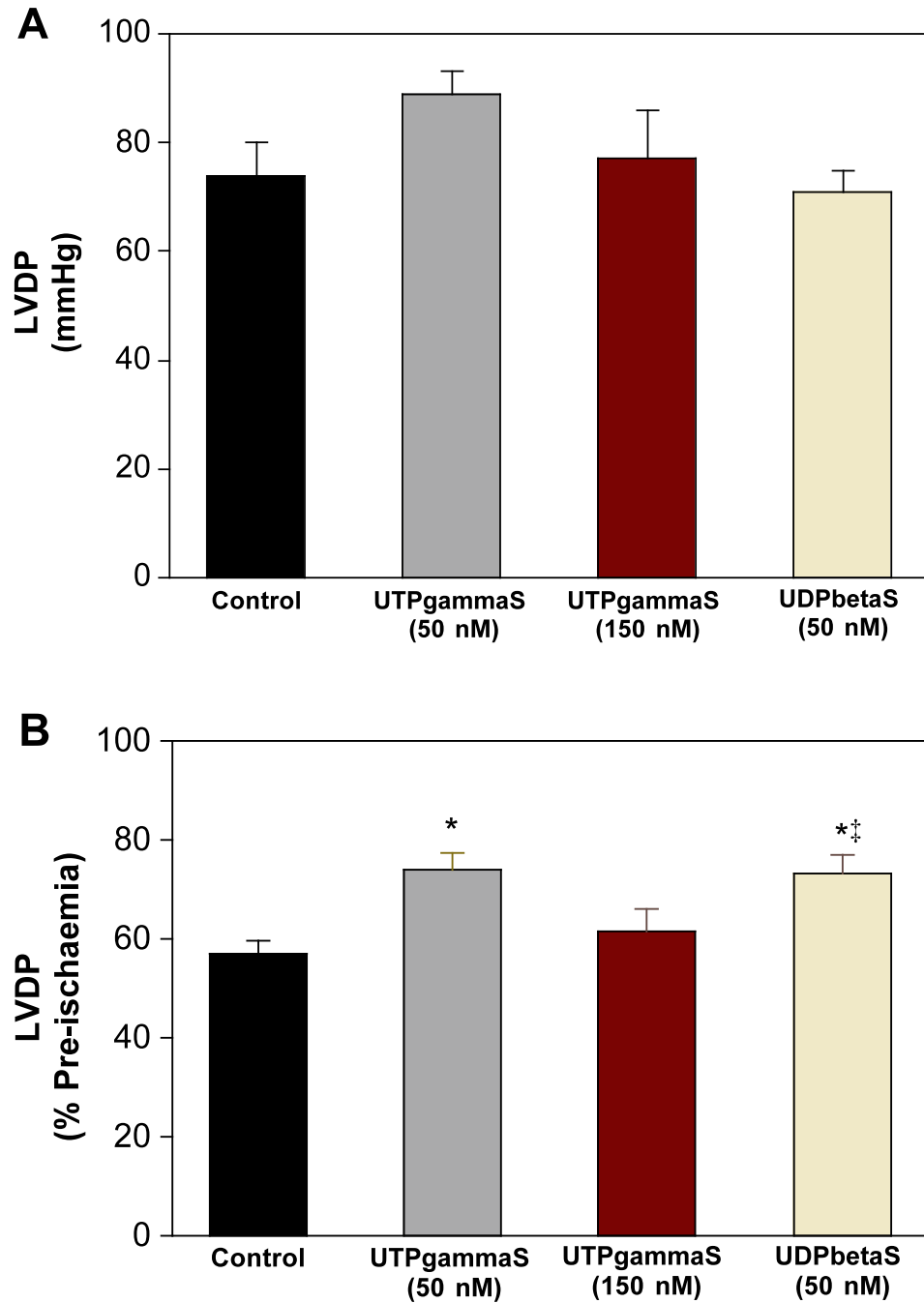


Figure 8.1. Effects of $UTP\gamma S$ (50 nM or 150 nM) or $UDP\beta S$ (50 nM) on post-ischaemic recoveries of: A) LVDP (absolute units); and B) LVDP (% of pre-ischaemic levels). Values are means \pm SEM. *, $P<0.05$ vs. control; †, $P<0.05$ vs. $UTP\gamma S$ (50 nM); ‡, $P<0.05$ vs. $UTP\gamma S$ (150 nM).

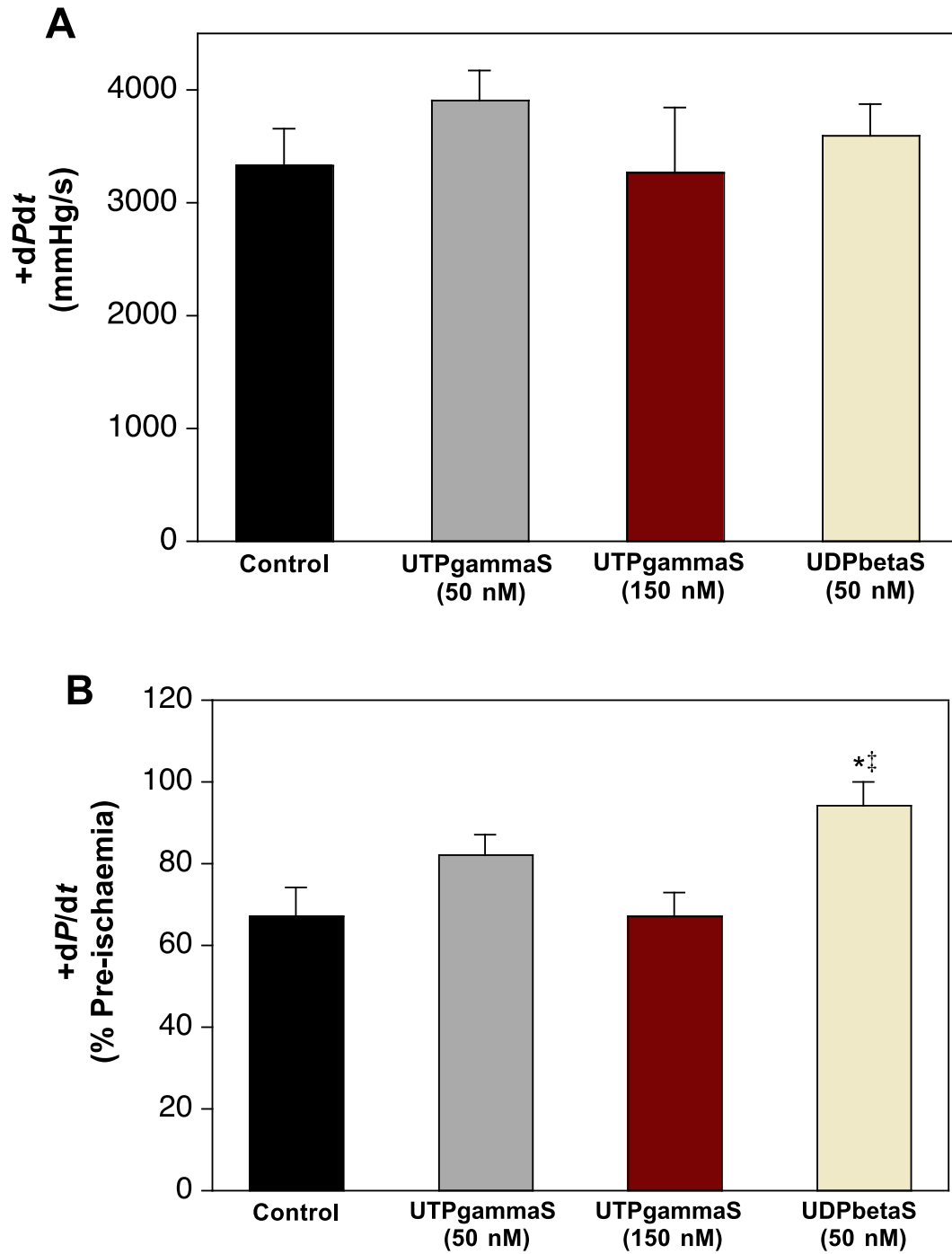


Figure 8.2. Effects of *UTP*γ*S* (50 nM or 150 nM) or *UDP*β*S* (50 nM) on post-ischaemic recoveries of: A) +d*P*/d*t* (absolute units); and B) +d*P*/d*t* (% of pre-ischaemia). Values are means±SEM. *, *P*<0.05 vs. control; †, *P*<0.05 vs. *UTP*γ*S* (50 nM); ‡, *P*<0.05 vs. *UTP*γ*S* (150 nM).

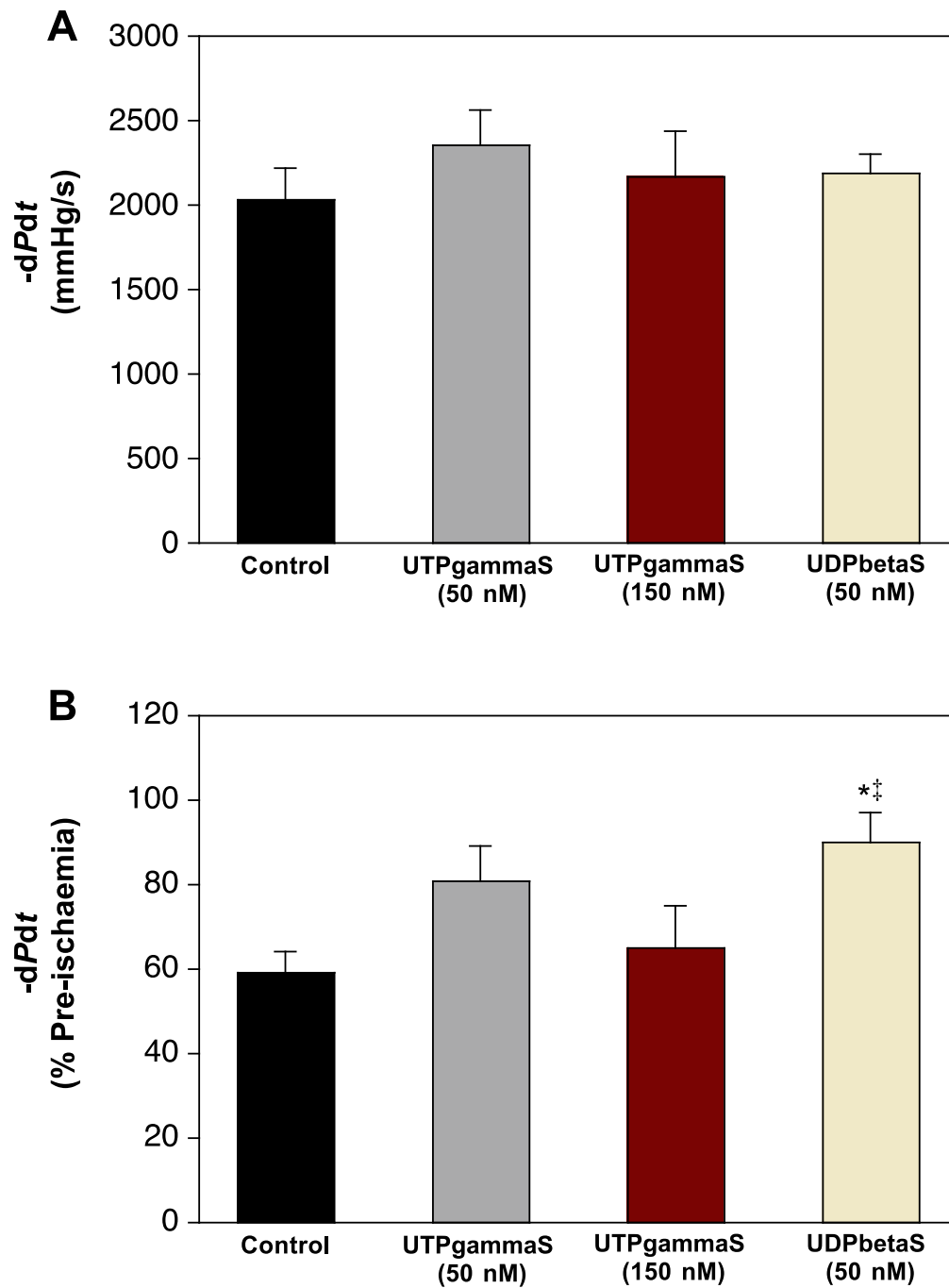


Figure 8.3. Effects of *UTP* γ *S* (50 nM or 150 nM) or *UDP* β *S* (50 nM) on post-ischaemic recoveries of: A) $-dP/dt$ (absolute units); and B) $-dP/dt$ (% of pre-ischaemia). Values are means \pm SEM. *, $P<0.05$ vs. control; †, $P<0.05$ vs. *UTP* γ *S* (50 nM); ‡, $P<0.05$ vs. *UTP* γ *S* (150 nM).

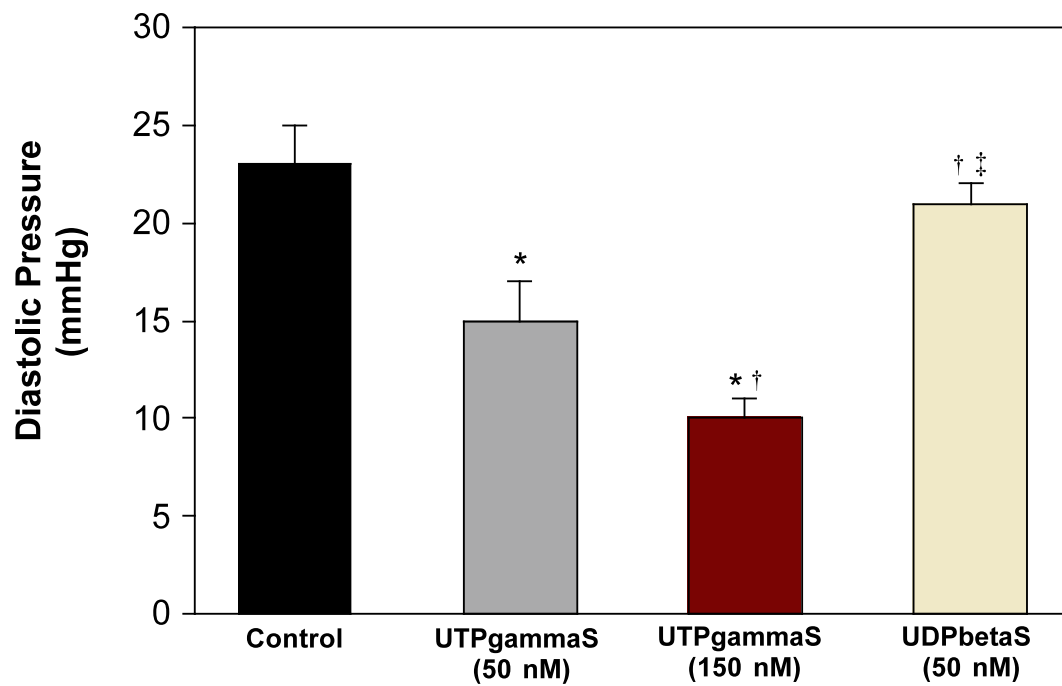


Figure 8.4. Effects of *UTP γ S* (50 nM or 150 nM) or *UDP β S* (50 nM) treatment on post-ischaemic recovery of end-diastolic pressure. Values are means \pm SEM. *, $P<0.05$ vs. control; †, $P<0.05$ vs. *UTP γ S* (50 nM); ‡, $P<0.05$ vs. *UTP γ S* (150 nM).

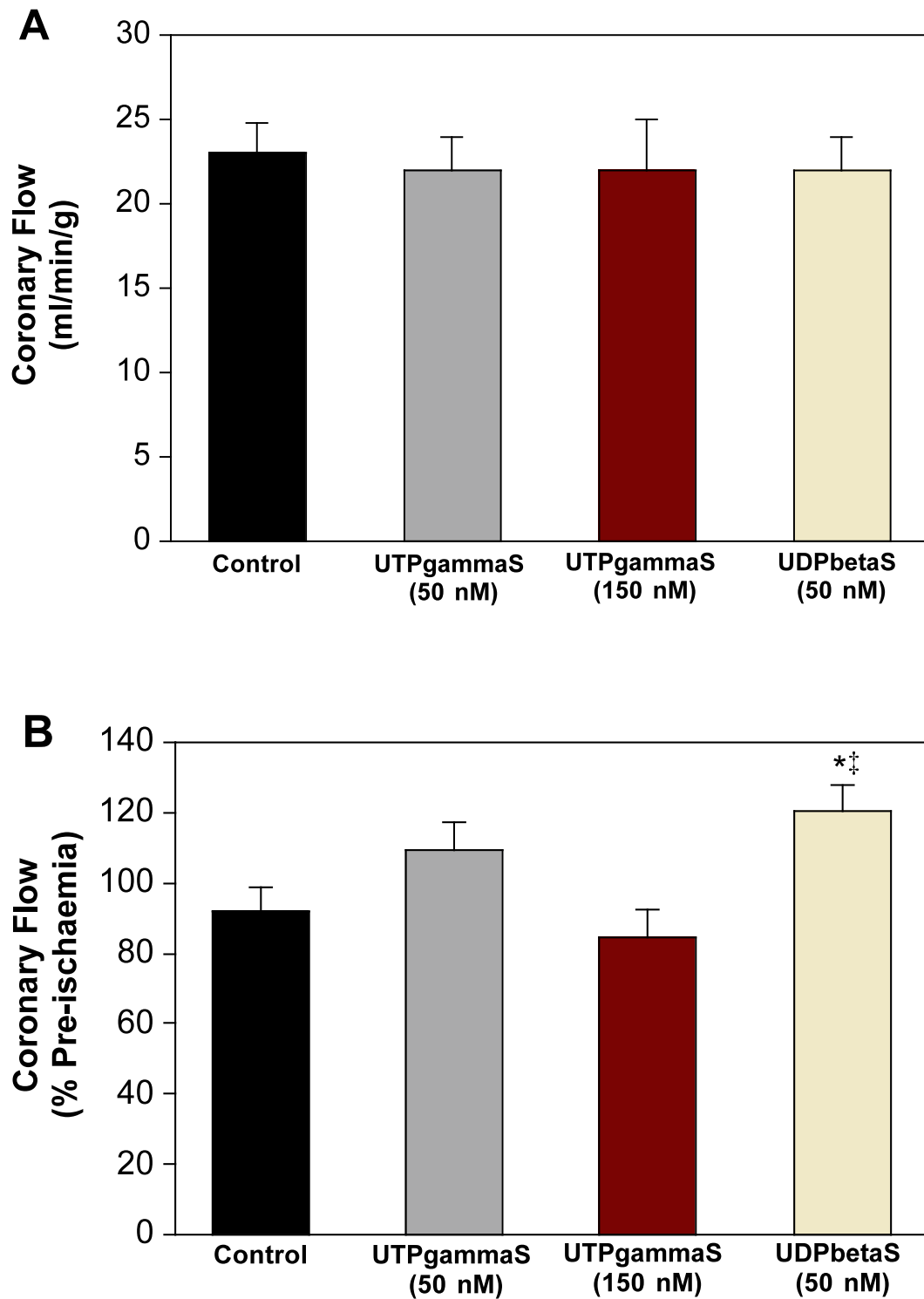


Figure 8.5. Effects of *UTP* γ *S* (50 nM or 150 nM) or *UDP* β *S* (50 nM) treatment on post-ischæmic recovery of: A) coronary flow (absolute units); and (B) coronary flow (% of pre-ischæmia). Values are means \pm SEM. *, $P < 0.05$ vs. control; †, $P < 0.05$ vs. *UTP* γ *S* (50 nM); ‡, $P < 0.05$ vs. *UTP* γ *S* (150 nM).

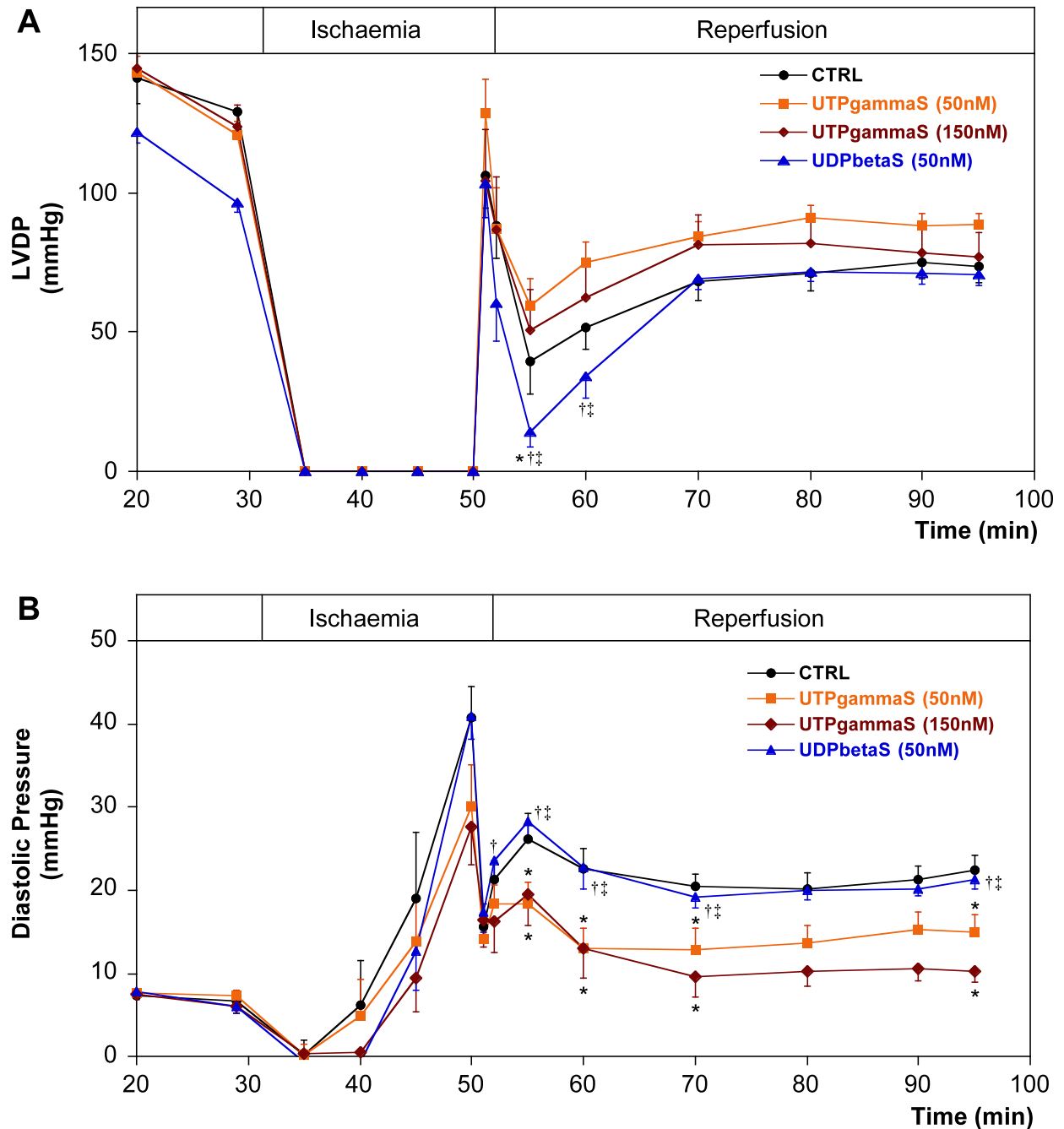


Figure 8.6. Effects of $UTP\gamma S$ (50 nM or 150 nM) or $UDP\beta S$ (50 nM) on post-ischaemic recoveries for: A) LVDP; and B) left ventricular diastolic pressure. Data are shown for recoveries in untreated control hearts ($n=10$) vs. 50 nM $UTP\gamma S$ ($n=10$), 150 nM $UTP\gamma S$ ($n=10$), and 50 nM $UDP\beta S$ ($n=8$) treated hearts. Values are means \pm SEM. *, $P<0.05$ vs. Control; †, $P<0.05$ vs. 50 nM $UTP\gamma S$; ‡, $P<0.05$ vs. 150 nM $UTP\gamma S$.

Effects of P2Y_{2/4} and P2Y₆ agonism on post-ischaemic LDH efflux

Post-ischaemic LDH efflux from Control and *UTP* γ *S* treated hearts was comparable, whereas hearts treated with 50 nM *UDP* β *S* exhibited significantly exaggerated tissue injury over 45 min reperfusion (Figure 8.7).

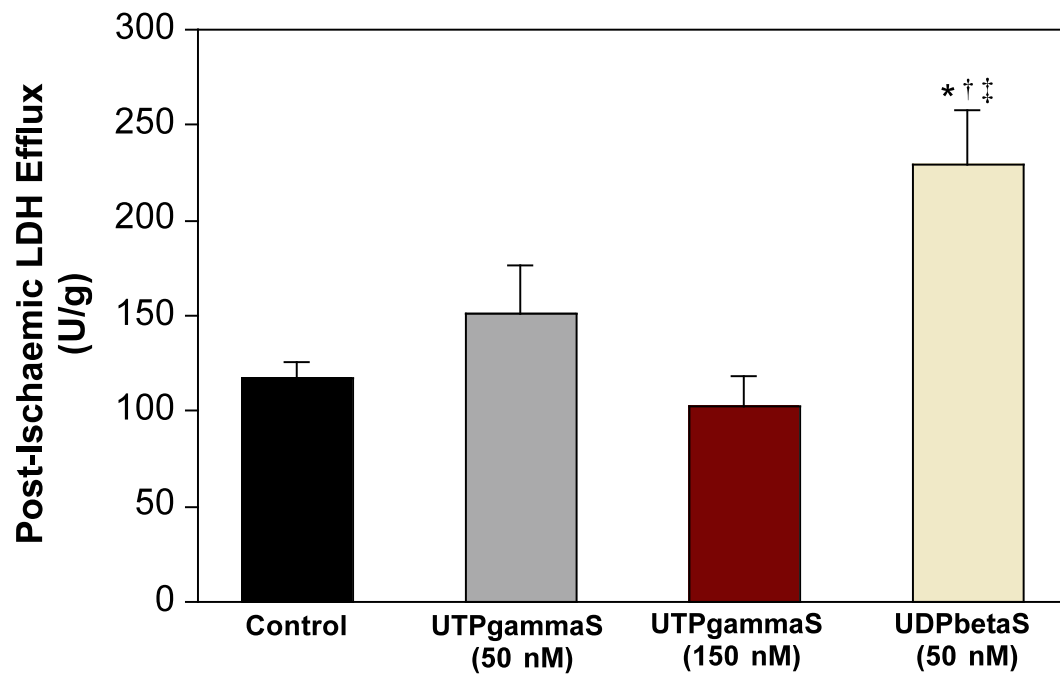


Figure 8.7. Effects of *UTP* γ *S* (50 nM or 150 nM) and *UDP* β *S* (50 nM) on post-ischaemic LDH efflux (indicating extent of oncosis). Values are means \pm SEM. *, $P<0.05$ vs. control; †, $P<0.05$ vs. 50 nM *UTP* γ *S*; ‡, $P<0.05$ vs. 150 nM *UTP* γ *S*.

8.5 DISCUSSION

Protective effects of UTP-dependent activation of P2Y_{2/4} purinoceptors have been studied by several groups [254, 255, 263, 383, 384]. However, inter-conversion of UTP and other nucleotides may occur at the cell surface: ectonucleoside diphosphokinase can interconvert 5'-di- and -triphosphates such as UTP and ADP to UDP and ATP, respectively. Therefore, application of UTP (or ATP) in intact tissues may result in mutual activation or inactivation of ATP, ADP, UTP or UDP sensitive receptors, significantly complicating interpretation of responses triggered by these ligands [402]. To analyse the specific cardiac effects of pyrimidine selective receptors, the stable UTP analogues *UTP* γ *S* and *UDP* β *S*, resistant to ectonucleotidases degradation were used to specifically activate P2Y_{2/4} and P2Y₆ receptors, respectively.

Cardiovascular Effects of UTP γ S and UDP β S in Normoxic Hearts

Purinoceptor activation by *UTP* γ *S* and *UDP* β *S* triggered unexpected changes in normoxic myocardial function not detected in prior studies of UTP. Treatment with UTP (250 nM or 1 μ M) did not modify baseline functional parameters (see **Chapter 6**). However, the pyrimidine analogues *UTP* γ *S* and *UDP* β *S* significantly reduced LV relaxation rate ($-dP/dt$) and reduced coronary flow (Table 8.1). This highlights the importance of employing stable and selective compounds in intact tissue, and based on earlier observations in this thesis is suggestive of differential effects of UTP and its degradation products. The reduction in relaxation rate with *UTP* γ *S* may be partially explained by dual inotropic effects of ATP and UTP, reported previously by Froldi *et al.* [381]. ATP and UTP were reported to trigger an initial rapid decrease in contractility followed by an increase in contractile function [381]. Reduced rate of

relaxation with *UDPβS* suggests P2Y₆ receptors may inhibit this functional parameter. Prior studies report P2Y₆ mediated positive inotropic effects in mouse cardiomyocytes [189], attenuation of apoptosis in ischaemic-reperfused skeletal muscle [430], and triggering cardiac fibrosis in pressure overload [190]. The reduction in coronary flow observed here is somewhat consistent support with prior studies: in coronary vasculature, UDP and UTP induce vasoconstriction via vascular smooth muscle receptors [195, 387, 426, 431]. Previously, UTP and *UTPγS* have been shown to mediate constriction in human coronary arteries [431], and UDP and *UDPβS* mediate contraction of human cerebral arteries [241, 432]. Interestingly, the higher 150 nM concentration of *UTPγS* did not modify cardiac function (Table 8.1).

Activation of P2Y_{2/4} and P2Y₆ purinoceptors during ischaemia-reperfusion

The stable pyrimidine, *UTPγS* (EC₅₀ = 240 nM at P2Y₂) has been shown to be equipotent to UTP and ATP [429] in activating P2Y_{2/4} receptors. The P2Y₆ receptor is selectively activated by UDP, while UTP is a weak agonist or inactive at this subtype [385, 386]. To investigate specific effects of P2Y_{2/4} and P2Y₆ receptors, *UTPγS* (50 nM or 150 nM) or *UDPβS* (50 nM) were applied pre- and post-ischaemia. *UTPγS* at both concentrations protected hearts significantly against ischaemia-reperfusion in a concentration-dependent manner - the higher concentration exerting a greater reduction in end-diastolic contracture compared to 50 nM. Contractile function indicated by LVDP (% pre-ischaemia) was significantly improved with 50 nM *UTPγS*, however the higher 150 nM concentration was ineffective. At this higher concentration *UTPγS* reduced diastolic contracture alone, but not other functional parameters. LV effects of 50 nM *UTPγS* are similar to unstable effects in previous studies (see **Chapters 6 and 7**). Concentration-dependence of *UTPγS* effects are

consistent with previous UTP studies in which low concentrations of exogenous UTP conferred cardioprotection while a higher concentration did not. Since dose-dependency in UTP protective effects has also been reported by other investigators [249, 383, 391, 405], it is conceivable that stable *UTP γ S* also affords cardioprotection up to a concentration threshold beyond which, in combination with endogenous UTP, may lead to negative cardiac effects. Under baseline conditions UTP is detected in low nanomolar concentrations in the extracellular medium in several tissue types, primary astrocytes, primary airway epithelial cells, isolated human platelets and several cell lines [219], while data in **Chapter 7** confirms substantial interstitial accumulation of UTP in ischaemic-reperfused mouse heart. In a pig model Erlinge *et al.* demonstrated almost 3-fold elevations in UTP release during cardiac ischaemia [252]. Subsequently, UTP release during cardiac ischaemia in humans was determined to generate 10^{-7} mol/L in the plasma [189].

To date, known effects of P2Y₆ activation include the growth and contraction of vascular muscles [240], enhancement of osteoclast survival through NF- κ B activation [433], regulation of electrolyte transport in the airways [239], production of pro-inflammatory cytokines and chemokines [434, 435], positive inotropic effects [189], contraction of arteries [241], concentration dependent anti-apoptotic effects [430], and cardiac fibrosis in pressure overload (a known cause of heart failure and impairment of cardiac function) [190]. Stable *UDP β S* significantly enhanced recovery of LV function and coronary flow, but did not modify diastolic contracture. Improved contractile recovery with both pyrimidine analogues is consistent with prior findings: UTP, UDP and respective stable analogues, have been shown to exert positive inotropic effects via P2Y purinoceptors [189]. To our knowledge, this is the first

report of protection against ischaemia-reperfusion injury with P2Y₆ activation in murine myocardium. Some evidence exists to support such an effect: the P2Y₆ subtype has recently been implicated in pyridoxal-5'-phosphate, PLP-induced cardiac pre-conditioning in the isolated rat heart model [192]. Additionally, Krylova *et al.* [436] showed that extracellular UDP precursors (uridine and uridine-5'-monophosphate) decreased infarct zone by 1.9 and 3.5 times respectively in rat myocardium, and partially limited rhythm disorders with ischaemia. The investigators proposed that UDP provides protection via mitoK_{ATP} activation, however this study failed to address potential issues with unstable UDP and its modulation via cell surface ectonucleotidase activity [436]. In contrast, improved ventricular functional recovery and coronary flow in *UDPβS* targeting of P2Y₆ has not been reported previously.

In coronary vasculature, UDP and UTP induce direct vasoconstriction of vascular smooth muscle cells as well as endothelium mediated vasodilatation [195, 387, 426, 431]; such effects may explain the significant increase in coronary flow (~120 % pre-ischaemia) in hearts treated with *UDPβS*. However, others also show that UDP and *UDPβS* mediate contraction of rat mesenteric artery [437] and human cerebral arteries [241, 432], though it was also determined in this study that P2Y₆ receptors were absent in human coronary arteries. Species differences may provide an explanation for the vasodilatory effect seen here, as it has been shown that P2Y₆ mRNA is expressed in murine myocardium (see **Chapter 4**). Malmstro *et al.* also proposed that UTP mediated vasoconstriction is mediated by P2Y₆ receptors with a lesser contribution from the P2Y₂. In the current study, evidence is provided that activation by both

stable $UTP\gamma S$ and $UDP\beta S$ elicits vasoconstriction, reducing coronary flow in normoxic tissue.

Paradoxical Increase in LDH Efflux

The extent of LDH loss (Figure 8.7), a marker of oncosis, was paradoxically enhanced by treatment with $UDP\beta S$. The basis of this response is not clear. Cardiomyocyte $G\alpha_{(12/13)}$ activation by $P2Y_6$ receptors could contribute [190], since cardiomyocytes $G\alpha_{(12/13)}$ activity has also been implicated in apoptosis [438-440]. However, other studies indicate $P2Y_6$ activation is anti-apoptotic in other cell types [430, 441, 442], and $P2Y_6$ agonism protects against skeletal muscle ischaemia-reperfusion injury (Mamedova *et al.*). On the other hand, a recent study by Apolloni *et al.*, indicates UDP causes mitochondrial damage via release of cytochrome *c*, and stimulation of caspase-3, 7 and 8 activities [442]. The basis of $UDP\beta S$ exaggeration of tissue oncosis here is unclear and warrants further investigation .

8.6 CONCLUSION

Potent activation of $P2Y_{2/4}$ purinoceptors by stable pyrimidines $UTP\gamma S$ enhanced myocardial functional tolerance to ischaemia reperfusion in a concentration-dependent manner. A low concentration of extracellular $UTP\gamma S$ may act together with endogenous UTP to enhance myocardial tolerance, whereas cardioprotection may be lost when high concentration of potent $UTP\gamma S$ are applied. For the first time it is demonstrated here that activation of $P2Y_6$ purinoceptors also provides cardioprotection against contractile dysfunction in ischaemic-reperfused mouse hearts, though a paradoxical effect on cell death may arise.

CHAPTER 9

PHARMACOLOGICAL INTERROGATION OF P2 PURINOCEPTOR COUPLED SIGNALING IN ISCHAEMIC- REPERFUSED MOUSE HEART

9.1 ABSTRACT

The current study represents a basic pharmacological interrogation of downstream signalling pathways associated with P2Y-mediated protection. P2Y activation has been linked to multiple signalling paths, but primarily stimulation of PIP₂ – PLC signals, leading to increased IP₃ and DAG, with IP₃ mobilising intracellular Ca²⁺. This, in turn, activates other signalling intermediates including PKC, PLA₂, Ca²⁺-dependent K⁺ channels, NOS, voltage-operated Ca²⁺ channels and MAPKs. To identify potential mechanisms involved in P2Y_{2/4} purinoceptor-mediated cardioprotection, ischaemic-reperfused mouse hearts (20 min ischaemia/45 min reperfusion) were either untreated (*n*=30) or subjected to treatment with: i) 250 nM of the P2Y agonist UTP (*n*=15); ii) UTP + 200 μM suramin (a P2 antagonist; *n*=8); iii) 100 μM 5-HD (mitochondrial K_{ATP} channel inhibitor; *n*=11); iv) UTP + 5-HD (*n*=9); v) 30 nM wortmannin (a PI3K inhibitor; *n*=9); vi) UTP + wortmannin (*n*=9); vii) 3 μM GW5074 (a Raf-1 inhibitor; *n*=13); or viii) UTP + GW5074 (*n*=13). The P2Y agonist UTP was applied 10 min prior to and for the initial 10 min following ischaemia, with inhibitors applied 5 min prior to UTP. Baseline contractile function was comparable in all groups. In terms of post-ischaemic recoveries, untreated hearts exhibited diastolic dysfunction (EDP = 23±2 mmHg), partial recovery of LVDP (76±4 mmHg, or 62±3% of pre-ischaemic levels), and partial recovery of coronary flow (86±2% of pre-ischaemia). Treatment with UTP was protective, reducing EDP (10±1 mmHg; *P*<0.05) and enhancing recovery of LVDP (89±2 mmHg; *P*<0.05). Suramin abolished this protection, confirming P2 purinoceptor involvement. UTP-mediated functional protection was also significantly attenuated by wortmannin, GW5074 and 5-HD. Treatment with UTP also reduced post-ischaemic LDH efflux (a marker of oncosis), while wortmannin and 5-HD alone exaggerated cell death. UTP

was unable to improve LDH efflux in the presence of these inhibitors, supporting PI3K and K_{ATP} channel involvement in cytoprotection. The Raf-1 inhibitor GW5074 also limited the effects of UTP on LDH efflux (and also reduced LDH efflux when applied alone). These results collectively indicate that UTP-mediated cardioprotection involves Raf-1 (immediately downstream of Ras in MAPK signalling), PI3K activation, and opening of mitochondrial K_{ATP} channels. Data further suggests that intrinsic activities of PI3K and K_{ATP} channels may normally limit cell death with ischaemia-reperfusion.

9.2 INTRODUCTION

The G-coupled P2Y purinoceptors mediate diverse actions through distinct G-protein coupling and engagement of different signalling pathways. P2Y purinoceptors are subdivided into five G_q-coupled subtypes (P2Y₁, P2Y₂, P2Y₄, P2Y₆, P2Y₁₁) and three G_i-coupled subtypes (P2Y₁₂, P2Y₁₃ and P2Y₁₄). Expression of G_q-coupled subtypes has been reported in mammalian cardiac myocytes [174]. As outlined in prior Chapters, both exogenous and endogenous P2Y activity appears to modify myocardial ischaemic tolerance. The mechanistic basis of these cardioprotective effects are unclear.

As outlined by Hausenloy and Yellon [126], cardioprotective RISK signalling cascades appear to be responsive to a range of GPCRs, and are involved in conditioning responses in which P2 receptors are also implicated [443]. Thus, P2Y protection may well involve such signalling. The P2Y purinoceptors are conventionally attributed with stimulation of PIP₂ and PLC, leading to increased IP₃ and DAG, with subsequent activation of Ca²⁺ and protein kinase signalling [162, 197]. This cascade also leads to activation of other signalling paths and intermediates, including PKC, PLA₂, and MAPK paths. Some P2Y purinoceptors are also linked to inhibition of adenylate cyclase activity [222], namely P2Y₁₂, P2Y₁₃ and P2Y₁₄ [218], and regulation of ion channel function [444]. Sauzeau *et al.* propose that P2Y₁, P2Y₂, P2Y₄ and P2Y₆ purinoceptors couple to Rho/Rho-kinase activation [223]. Montiel *et al.* suggest that P2Y purinoceptors activate MAPK/ERK through PI3K-dependent mechanisms, with PDK1 and PKC- ζ identified as key components [221]. P2Y purinoceptors may also form homo-and hetero-multimeric assemblies under certain conditions, increasing the potential complexity of P2Y signalling. All of the above

paths have been implicated in cellular protection responses to other stimuli in different models.

In cardiomyocytes, extracellular UTP and ATP stimulate DAG, PKC, p38 MAPK and K_{ATP} channels [162, 197], indicating that exogenous or endogenously released UTP may trigger intracellular signalling associated with protective preconditioning [129, 142, 147, 162, 445]. Alvarez *et al.* demonstrated $P2Y_2$ stimulation of PLC β -dependent activation of heteromeric transient receptor potential channels 3/7 (TRPC3/7) [232]. Shainberg *et al.* propose that UTP triggers cardioprotective responses via transient increases in $[Ca^{2+}]_i$, phosphorylation of Erk1/2 and Akt, and a reduction in mitochondrial Ca^{2+} loading [263].

In order to assess potential cytoprotection signalling coupled to $P2Y_{2/4}$ activation, known inhibitors of key signalling intermediates were employed to test for ability to negate or limit cardioprotection mediated by UTP. Specifically, wortmannin was employed to inhibit PI3K signals, 5-HD to inhibit K_{ATP} channels, and GW5074 to inhibit Raf-1 dependent kinase signalling (immediately downstream of Ras in MAPK signalling paths).

9.3 MATERIALS AND METHODS

Experimental preparation and protocol

Experiments were performed in accordance with the *Guide for the Care and Use of Laboratory Animals* (NIH Publication No. 85-23, revised 1996), and work approved by the Institutional Animal Care and Use committee. Young male C57/Bl6 mice of 16-20 weeks of age were used in all studies, and were anaesthetised with a bolus injection sodium pentobarbital (50 mg/kg) administered intraperitoneally. Mouse hearts were excised *en bloc* with the lungs and arrested by immersion in ice-cold perfusion fluid. Hearts were cannulated via the aorta and retrogradely perfused as outlined in detail in **Chapter 2**.

Hearts stabilized for 20 min at intrinsic heart rate were switched to ventricular pacing at 420 beats/min (2 ms pulse duration, amplitude 20% above the pacing threshold) for a further 10 min. Baseline function was then assessed and 20 min global ischaemia initiated followed by 45 min reperfusion. Pacing was terminated during ischaemia and reinstated at 2 min reperfusion [155, 267]. Hearts were either untreated ($n=30$) or subjected to treatment with: i) 250 nM of the P2Y agonist UTP ($n=15$); ii) UTP + 200 μ M suramin (a P2 antagonist; $n=8$); iii) 100 μ M 5-HD (mitochondrial K_{ATP} channel inhibitor; $n=11$); iv) UTP + 5-HD ($n=9$); v) 30 nM wortmannin (a PI3K inhibitor; $n=9$); vi) UTP + wortmannin ($n=9$); vii) 3 μ M GW5074 (a Raf-1 inhibitor; $n=13$); or viii) UTP + GW5074 ($n=13$). The P2Y agonist UTP was applied 10 min prior to and for the initial 10 min following ischaemia, with inhibitors applied 5 min prior to UTP and also for 10 min post-ischaemia. For assessment of necrotic cell death, efflux of the intracellular enzyme LDH throughout reperfusion was measured [151, 155, 267].

Chemicals and reagents

All drugs were purchased from Sigma-Aldrich (Castle Hill, Australia). Drug solutions were infused into hearts at $\leq 1\%$ of total coronary flow rate to achieve the final concentrations indicated. Final concentrations of drugs applied were: UTP (250 nM), suramin (200 μ M), 5-HD (100 μ M), wortmannin (30 nM) and GW5074 (3 μ M).

Statistical analyses

Post-ischaemic recoveries and LDH efflux were compared via one-way ANOVA. Where inter-group significance was detected, a Newman-Keuls post-hoc test was applied for specific comparisons. In all tests, significance was accepted for $P < 0.05$. Data are presented as means \pm SEM.

9.4 RESULTS

Pre-ischaemic Function

Baseline (normoxic) functional data is presented in Table 9.1. All groups exhibited comparable contractile function under normoxic conditions. However, coronary flow rates were significantly different in several treatment groups: co-infusion of suramin and 5-HD with UTP apparently increased coronary flow above that for UTP treatment alone.

Table 9.1 – Pre-ischaemic contractile function and coronary flow.

<i>Treatment</i>	<i>LVDP</i> (mmHg)	<i>+dP/dt</i> (mmHg/s)	<i>-dP/dt</i> (mmHg/s)	<i>Flow</i> (ml/min/g)
Untreated (n=30)	121±3	4470±176	-3046±86	22±1
UTP (250 nM) (n=15)	118±7	4243±348	-2947±197	17±1
Suramin+UTP (n=8)	104±4	4316±243	-2635±160	27±1 [†]
GW5074 (3 µM) (n=13)	129±9	4898±516	-3411±338	23±2
GW5074+UTP (n=13)	127±11	4346±660	-2968±363	21±2
Wortmannin (30 nM) (n=9)	122±6	4449±277	-2969±203	25±2 [†]
Wortmannin+UTP (n=9)	127±12	4763±674	-3330±222	18±1
5-HD (100 µM) (n=11)	113±5	3828±419	-2755±217	21±1
5-HD+UTP (n=9)	112±5	3851±316	-3107±221	25±3 [†]

Data were measured immediately prior to ischaemia. LVDP, left ventricular developed pressure; +dP/dt and -dP/dt, positive and negative differentials of left ventricular force development, respectively. Values are means±SEM. *, $P<0.05$ vs. untreated hearts; †, $P<0.05$ vs. UTP alone.

Functional response to ischaemia-reperfusion

Untreated hearts exhibited diastolic dysfunction and impaired recovery of LVDP (Table 9.1) following 20 min global ischaemia and 45 min reperfusion. Treatment with UTP was protective, reducing diastolic contracture and improving LV contractile function (Figures 9.1 and 9.2).

The Raf-1 inhibitor GW5074 significantly reduced end diastolic dysfunction and enhanced coronary flow recovery compared to untreated hearts. GW5074 also inhibited UTP cardioprotective effects, worsening diastolic dysfunction and depressing LVDP recovery (Figures 9.1 and 9.2). Wortmannin treated hearts exhibited comparable post-ischaemic recovery to untreated hearts (Figures 9.1 and 9.2). Wortmannin abolished UTP-mediated protective effects (Figures 9.1 and 9.2). Hearts treated with 5-HD also exhibited comparable recovery of EDP, LVDP and coronary flow compared with untreated hearts. However, 5-HD abolished UTP-mediated cardioprotective effects, worsening diastolic contracture and impaired LVDP recovery (Figures 9.1 and 9.2).

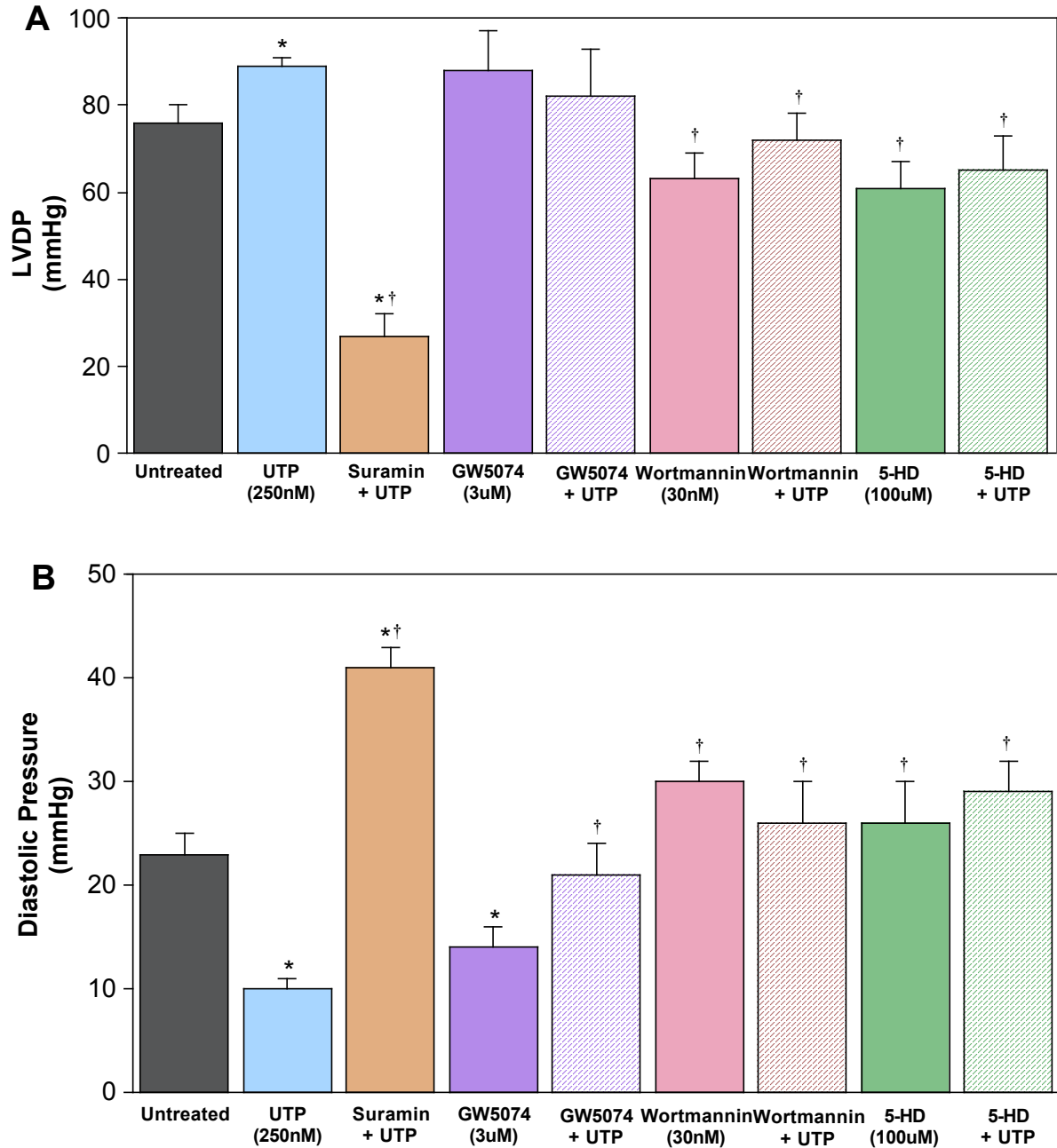


Figure 9.1. Effects of UTP and signalling inhibitors on post-ischaemic recoveries for: (A) left ventricular developed pressure (mmHg); and (B) left ventricular end diastolic pressure (mmHg). Data are shown for untreated hearts ($n=30$) and UTP ($n=15$), suramin+UTP ($n=8$), 5-HD ($n=11$), 5-HD+UTP ($n=9$), wortmannin ($n=9$), wortmannin+UTP ($n=9$), GW5074 ($n=13$), and GW5074+UTP ($n=13$) treated hearts. Values are means \pm SEM. *, $P<0.05$ vs. Control; †, $P<0.05$ vs. UTP.

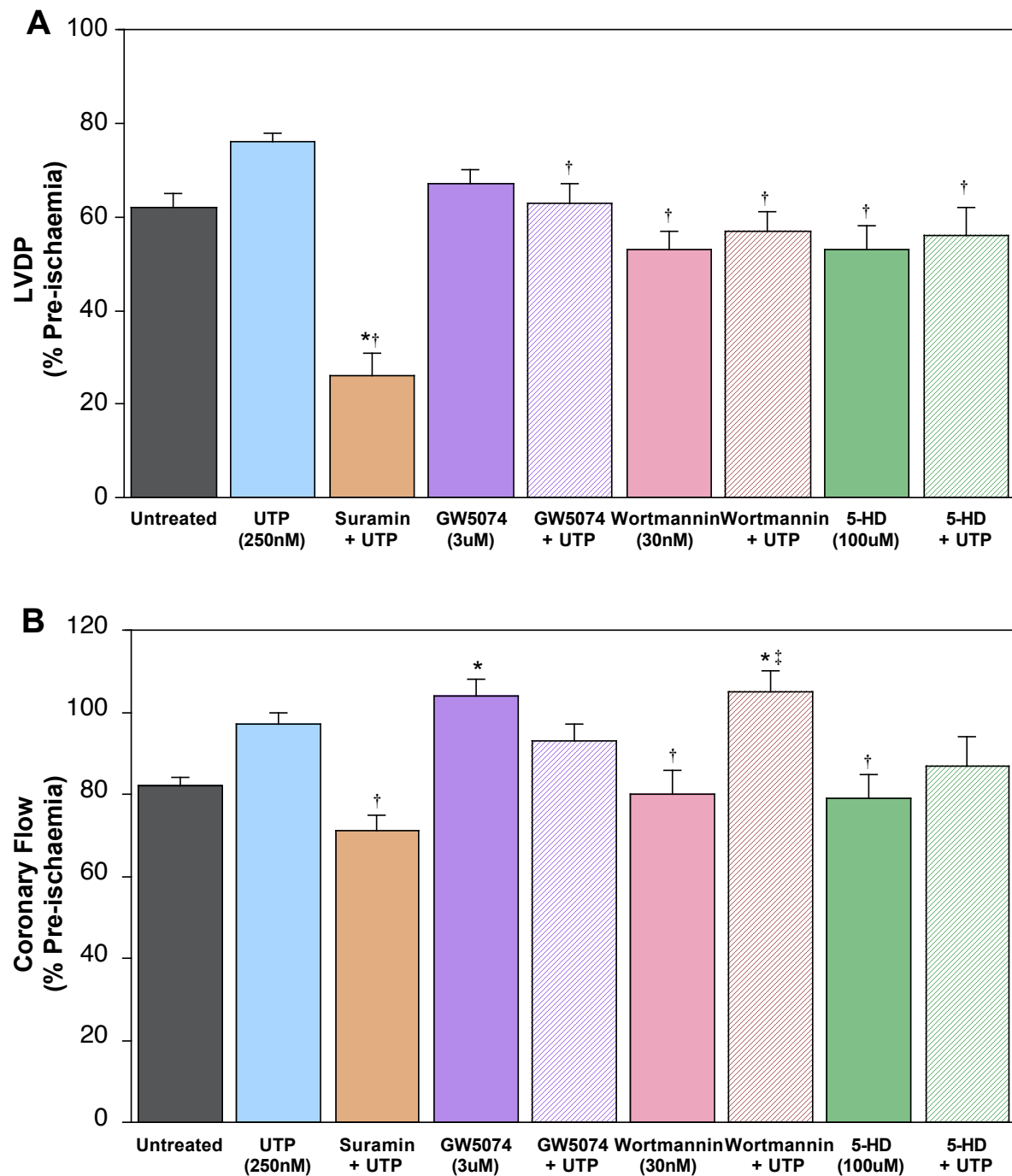


Figure 9.2. Effects of UTP and signalling inhibitors on post-ischaemic recoveries for: (A) left ventricular developed pressure (% pre-ischæmia); and (B) coronary flow (% pre-ischæmia). Data are shown for untreated hearts ($n=30$), and UTP ($n=15$), suramin+UTP ($n=8$), 5-HD ($n=11$), 5HD+UTP ($n=9$), wortmannin ($n=9$), wortmannin+UTP ($n=9$), GW5074 ($n=13$), and GW5074+UTP ($n=13$) treated hearts. Values are means \pm SEM. *, $P<0.05$ vs. Control; †, $P<0.05$ vs. UTP; ‡, $P<0.05$ vs. wortmannin.

Effects of UTP and signalling inhibitors on cell death

For assessment of necrotic cell death, we measured efflux of the intracellular enzyme LDH. LDH efflux for untreated hearts was ~120 U/g (Figure 9.3). Treatment with UTP significantly lowered myocardial release of LDH. In the presence of GW5074 UTP was ineffective in lowering LDH release (Figure 9.3). Interestingly, LDH efflux were significantly enhanced by both wortmannin and 5-HD, and again UTP was unable to modify LDH efflux in these inhibitor treatment groups (Figure 9.3).

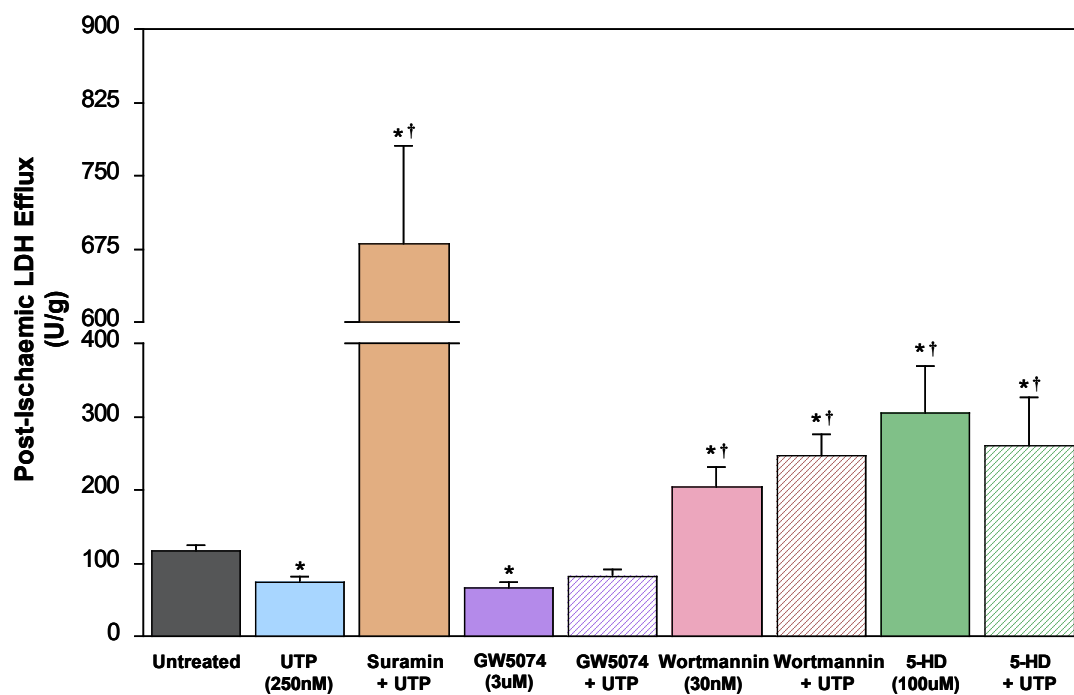


Figure 9.3. Effects of UTP and signalling inhibitors on post-ischaemic efflux of lactate dehydrogenase (LDH) over 45 min reperfusion. Values are means \pm SEM. *, $P < 0.05$ vs. Control; †, $P < 0.05$ vs. UTP.

9.5 DISCUSSION

To investigate the signalling mechanisms involved in cardioprotection mediated by UTP activation of P2Y_{2/4} purinoceptors, several inhibitory agents were employed: non-selective P2Y antagonism with suramin, PI3K inhibition with wortmannin, Raf-1 kinase inhibition with GW5074, and mitochondrial selective K_{ATP} antagonism with 5-HD. The data reveal that cardioprotection via UTP is impaired by each of these inhibitors, implicating Raf-1 and PI3K dependent signalling, and K_{ATP} channel activity, in P2Y-mediated cardioprotection. Data for inhibitors alone also hints at an intrinsic cytoprotective function for PI3K and K_{ATP} channels.

P2 involvement in UTP protection

To confirm P2Y involvement suramin was employed as an antagonist. While widely employed, it is important to note that suramin is also an ecto-ATPase inhibitor [373], and may uncouple G proteins from P2 receptors [446]. Pharmacological studies indicate that suramin is a potent antagonist for P2Y₂ receptors (IC₅₀, 9±3 µM) in rodents [447], and confirm that P2Y₄ receptors are suramin-insensitive (IC₅₀, 1027±32 µM) [363, 398, 447-449]. Suramin abrogated cardioprotective effects of UTP and generally worsened outcomes from ischaemia, resulting in higher diastolic contracture, impaired LV function and coronary flow recovery post-ischaemia (Figures 9.1 and 9.2). Since suramin is inactive at P2Y₄ receptors, these effects implicate the P2Y₂ in UTP mediated (and intrinsic) cardioprotection.

Raf-1 dependent signalling

GPCRs including P2Y receptors have been linked to control of extracellular signal-regulated kinases (Erk1/2) of the MAPK family [450, 451]. GPCR activation of

GTPase Ras localized in the plasma membrane, leads to recruitment of a Raf kinase from the cytosol to the membrane. Through poorly understood interactions of adapter proteins and protein phosphorylation, members of the Ras family (Raf-1, B-Raf and A-Raf) can activate MEK which, in turn phosphorylates and activates MAPKs such as Erk1/2 [452, 453]. This Raf/MEK/Erk signalling path is implicated in cardioprotection [126], and regulates diverse cellular processes including proliferation [454], differentiation, and death via apoptosis [455].

There is prior support for P2Y_{2/4} coupling to this path: Tu *et al.* found that P2Y₂-mediated mitogenic effects of UTP involve activation of Ras/Raf/MEK/MAPK in C(6) glioma cells [454]; the P2Y₂ activates Erk1/2 to promote mitogenic responses and cell migration in monocytes [450]; and down-regulation of P2Y₂ receptors leads to attenuated phosphorylation of Src and Erk1/2 in epithelial tissue [456]. Cardiac-specific Raf-1 effects include: cardiac hypertrophy and regulation of myocyte survival and growth in pressure overload [457, 458]; modulation of cardiac remodelling and apoptosis [455]; and action as a novel cardiac troponin T kinase linking growth factor-dependent signalling to cardiac contractility [459]. Support also exists for Raf-1 and Raf/MEK/ERK signalling in ischaemic preconditioning [460, 461]. Here GW5074 was used as a Raf-1 blocker to test for involvement of this signalling in UTP-mediated protection. Interestingly, GW5074 treatment alone modestly reduced LV diastolic contracture and enhanced coronary flow in normoxic hearts, and abolished UTP effects on post-ischaemic functional recovery (Figures 9.1 and 9.2). These effects are consistent with findings regarding the role of Raf-1 in regulating contractile function, and in cardiac protection. The data thus supports Raf-1 dependent signal involvement in UTP-mediated protection.

PI3K dependent signalling

PI3K activation promotes cell survival and inhibits apoptosis via Akt/PKB activity in many cell types including cardiomyocytes, cardiac fibroblasts, vascular smooth muscle cells, and endothelial cells [462]. The PI3K signalling cascade is one of several survival protein kinase cascades implicated in cardioprotection [126]. In ischaemic preconditioning, it is proposed that signalling through a PI3K–Akt–eNos–cGMP–PKG path [147] leads to opening of mitochondrial K_{ATP} channels [125], and survival kinase activation via reactive oxygen species [463]. Activation of the PI3K–Akt pathway at the time of myocardial reperfusion protects the myocardium in ischaemic postconditioning [126, 464]. Additional studies also implicate PI3K dependent signalling in sustained morphine-activated preconditioning via δ -opioid receptors [297, 465], and in luteolin-mediated cardioprotection [466], among other protective responses. Recent studies also reveal a role for PI3Ks in regulation of myocardial and vascular contractility [467-470].

There is prior support for P2 coupling to PI3K. For example, wortmannin inhibits P2Y-mediated phosphorylation of MAPK/Erk1/2 in endothelial cells [221]. P2Y₁ and P2Y₂ were also proposed to mediate wortmannin-surmountable ATP stimulation of mouse embryonic stem cell proliferation via PKC, PI3K/Akt, and MAPK signalling [471]. ATP- and UTP-mediated P2Y₂ anti-apoptotic effects in neuronal and renal cells have been found to rely on PI3K signalling [472, 473]. In the current study, wortmannin inhibited UTP-dependent functional protection (Figures 9.1 and 9.2), exaggerated cell death/ LDH efflux alone, and negated the ability of UTP to reduce LDH efflux (Figure 9.3). These data support PI3K involvement in UTP cardioprotection, and furthermore provide support for an important role for intrinsic

PI3K activity. This is consistent with the findings of Shainberg *et al.*, who found that UTP protects hypoxic cardiomyocytes via signalling involving phosphorylation of Erk1/2 and Akt (the latter downstream of PI3K) [263].

K_{ATP} channel involvement

The K_{ATP} channels have been widely implicated in multiple cardioprotective responses [138]. Mitochondrial K_{ATP} channel opening mimics ischaemic preconditioning in intact cardiac tissue [474], and PKC-dependent control of K_{ATP} channel function is important in induction and maintenance of preconditioning responses [120, 142, 475]. Sarcolemmal K_{ATP} channels have also been implicated in triggering or mediating cardioprotective effects of PKC [171, 476, 477]. The sarcolemmal K_{ATP} and mitochondrial K_{ATP} channels may have a complementary role in mediating protection in preconditioning [478]. Oketani *et al.* found that extracellular ATP modulates K_{ATP} channel activity through P2Y purinoceptors coupled to PLC and PIP₂ signalling in mammalian cardiomyocytes [251]. Thus, protection via UTP may well involve K_{ATP} channel modulation. Nonetheless, Yitzhaki *et al.* (2005, 2007) have proposed that UTP bypasses mitochondrial K_{ATP} channels in exerting its protective effects.

The agent 5-HD is a putative selective inhibitor of mitochondrial K_{ATP} channels. In the current study 5-HD inhibited UTP-dependent effects on post-ischaemic function recovery (Figures 9.1 and 9.2). In contrast to Yitzhaki *et al.* (2005, 2007), it is also shown here that 5-HD effectively inhibits UTP reductions in cell death. Interestingly, 5-HD exaggerated efflux of LDH alone, suggesting some role for intrinsic K_{ATP} channel activity in dictating ischaemic tolerance. This latter is consistent with the

findings of some prior studies [294], though contrast others who find no effect of this inhibitor on intrinsic ischaemic tolerance [479]. These findings add to an extensive literature supporting convergence of protective signals on mitochondrial proteins and complexes [74, 106, 133, 138, 474, 480-483].

9.6 CONCLUSION

Based on effects of signalling inhibitors applied alone and in conjunction with the protectant UTP, the current study supports involvement of Raf-1, PI3K and mitochondrial K_{ATP} channels in UTP-mediated protection. Such signalling involvement is consistent with a variety of studies implicating similar components in conditioning responses, and with the role of RISK signalling in cardiac protection. Interestingly, effects of wortmannin and 5-HD also support some role for endogenous PI3K and K_{ATP} channel activity in determining intrinsic myocardial resistance to ischaemic insult.

CHAPTER 10

GENERAL CONCLUSIONS

This doctoral research has assessed the role of a widely expressed receptor family in modifying outcomes from myocardial ischaemia-reperfusion. It is important both fundamentally and in terms of clinical development that we evolve our understanding of mechanisms dictating progression of cellular injury with ischaemia-reperfusion. This may ultimately improve our ability to limit injury in the setting of acute myocardial infarction, or in surgical ischaemia. The Australian health authorities have invested a significant amount of funding and effort in preventing cardiovascular disease and reducing associated death in Australia. Ischaemic heart diseases have been the leading cause of death in Australia since 2000, and despite a steady decline in the number of deaths due to ischaemic heart disease (from almost 24% in 1995; [4], it remained the underlying cause of 16% of all death in 2009 [5]. On a global scale, the incidence and prevalence of cardiovascular disease is expected to increase and become the leading public health problem in coming decades, due in part to ageing of populations and the 'Westernising' of developing countries. Economic affluence brings about sedentary lifestyles and ready access to calorie dense foods, with a resultant rise in chronic diseases such as obesity and Type II diabetes, compounding the incidence and management of cardiovascular disease. The current study addresses the role of a widely distributed receptor family in modifying outcomes from the major consequence of ischaemic heart disease (acute ischaemia-reperfusion) in a small animal model, focussing on an isolated heart preparation to identify specific cardiac responses.

The findings from the current series of studies indicate that P2Y purinoceptors are able to limit contractile dysfunction and cell death during and following myocardial ischaemia, and may be both activated by endogenously generated ligands as well as

remaining responsive to exogenous agonists. This receptor system may thus ultimately prove of value in understanding the pathogenesis of injury during ischaemia-reperfusion, and as a potential therapeutic target for amelioration of such damage.

Initial interrogation of mRNA expression profiles in ventricular and vascular tissue identified significant transcript for all nine P2 purinoceptors studied - P2X₁, P2X₄, P2X₅, P2X₇, P2Y₁, P2Y₂, P2Y₄, P2Y₆ and P2Y₁₂ receptors. Of these, transcript for P2X₁ was highest in vascular tissue, whereas P2Y₁ and P2Y₂ receptors predominated in myocardial vs. vascular tissue. These data support potentially multifaceted P2-dependent control of vascular and cardiac function. Subsequent investigations revealed significant worsening of myocardial ischaemic outcomes with varying P2 receptor antagonists, implicating both P2Y and P2X purinoceptors as local determinants of intrinsic myocardial resistance to ischaemic insult.

Analysis of time and concentration dependent responses to the P2Y_{2/4} agonist UTP in ischaemic-reperfused mouse hearts indicates external activation of these receptors prior to ischaemia exerts a preconditioning-like effect, whereas post-ischaemic activation is ineffective. Paradoxically, high levels of applied UTP throughout ischaemia-reperfusion fail to modify outcome, potentially due to mixed effects of UTP by-products and/or activation of other potentially detrimental P2-mediated actions. Data reveals that endogenous P2 agonists do accumulate substantially within the interstitial compartment during ischaemia, consistent with pharmacological evidence of P2-modulation of ischaemic tolerance. Effects of applied UTP must thus be considered within this context of locally generated P2 agonism. Overall, data for

agonists and antagonists tends to support protection via local and exogenous activation of P2Y₂ (and potentially P2Y₆) receptors. The downstream signalling harnessed by these receptors appears to involve Raf-1 dependent signals, PI3K activation, and opening of mitochondrial K_{ATP} channels.

Given the multiple P2 receptors localised to cardiac and vascular tissue, and their varying, sometimes opposing actions, it may be a challenge to selectively harness and modify P2-mediated cardioprotection. Nonetheless, as more selective pharmacological agents are developed, and our understanding of the roles and interactions between these receptors evolves, it may ultimately become feasible to manipulate this ancient receptor system to modify myocardial outcomes from ischaemic insult.

REFERENCES

1. Bolli, R., *Oxygen-derived free radicals and postischemic myocardial dysfunction ("stunned myocardium")*. J Am Coll Cardiol, 1988. **12**(1): p. 239-49.
2. Granger, D.N., *Role of xanthine oxidase and granulocytes in ischemia-reperfusion injury*. Am J Physiol, 1988. **255**(6 Pt 2): p. H1269-75.
3. Maxwell, S.R. and G.Y. Lip, *Reperfusion injury: a review of the pathophysiology, clinical manifestations and therapeutic options*. Int J Cardiol, 1997. **58**(2): p. 95-117.
4. Statistics, A.B.o., *Causes of Death, Australia*. ABS, Canberra, 2005. **viewed 14 March 2007**(cat. no 3303.0).
5. Statistics, A.B.o., *Causes of Death, Australia*. ABS, Canberra, 2009. **viewed on 20 October 2011**(cat. no 3303.0).
6. Statistics, A.B.o., *Cardiovascular Disease in Australia: A Snapshot, 2004-05*. ABS, Canberra, 2004-05(cat. no. 4821.0.55.001).
7. Stanley, W.C. and M.P. Chandler, *Energy metabolism in the normal and failing heart: potential for therapeutic interventions*. Heart Fail Rev, 2002. **7**(2): p. 115-30.
8. Ventura-Clapier, R., A. Garnier, and V. Veksler, *Energy metabolism in heart failure*. J Physiol, 2004. **555**(Pt 1): p. 1-13.
9. Lopaschuk, G.D., *Advantages and limitations of experimental techniques used to measure cardiac energy metabolism*. J Nucl Cardiol, 1997. **4**(4): p. 316-28.
10. Russell RR, I., Yin R, Caplan MJ, Hu X, Ren J, Shulman GI, Sinusas AJ, Young LH., *Additive effects of hyperinsulinemia and ischemia on myocardial GLUT1 and GLUT4 translocation in vivo*. Circulation, 1998. **98**: p. 2180-2186.
11. Ferrari, R., et al., *Different outcomes of the reperfused myocardium: insights into the comments of stunning and hibernation*. Int J Cardiol, 1998. **65 Suppl 1**: p. S7-16.
12. Piper, H.M., D. Garcia_Dorado, and M. Ovize, *A fresh look at reperfusion injury*. Cardiovascular Research, 1998. **38**(2): p. 291-300.
13. Piper, H.M., K. Meuter, and C. Schafer, *Cellular mechanisms of ischemia-reperfusion injury*. The Annals of Thoracic Surgery, 2003. **75**(2): p. S644-8.
14. Akiyama, K., et al., *Production of oxidative products of nitric oxide in infarcted human heart*. J Am Coll Cardiol, 1998. **32**(2): p. 373-9.
15. Kawahara, K., et al., *Ischemia/reperfusion-induced death of cardiac myocytes: possible involvement of nitric oxide in the coordination of ATP supply and demand during ischemia*. J Mol Cell Cardiol, 2006. **40**(1): p. 35-46.
16. Ambrosio, G., et al., *Effects of ischemia and reperfusion on cardiac tolerance to oxidative stress*. Am J Physiol, 1992. **262**(1 Pt 2): p. H23-30.
17. Hanich, R.F., et al., *Electrophysiologic recovery in postischemic, stunned myocardium despite persistent systolic dysfunction*. Am Heart J, 1993. **125**(1): p. 23-32.
18. Bolli, R. and E. Marban, *Molecular and cellular mechanisms of myocardial stunning*. Physiol Rev, 1999. **79**(2): p. 609-34.
19. Buja, L.M., *Modulation of the myocardial response to ischemia*. Lab Invest, 1998. **78**(11): p. 1345-73.
20. Duncker, D.J., et al., *"Myocardial stunning" remaining questions*. Cardiovasc Res, 1998. **38**(3): p. 549-58.

21. Krause, S.M., W.E. Jacobus, and L.C. Becker, *Alterations in cardiac sarcoplasmic reticulum calcium transport in the postischemic "stunned" myocardium*. Circ Res, 1989. **65**(2): p. 526-30.
22. Limbruno, U., et al., *Sarcoplasmic reticulum function in the "stunned" myocardium*. J Mol Cell Cardiol, 1989. **21**(10): p. 1063-72.
23. Carrozza, J.P., Jr., et al., *Decreased myofilament responsiveness in myocardial stunning follows transient calcium overload during ischemia and reperfusion*. Circ Res, 1992. **71**(6): p. 1334-40.
24. Gao, W.D., et al., *Relationship between intracellular calcium and contractile force in stunned myocardium. Direct evidence for decreased myofilament Ca²⁺ responsiveness and altered diastolic function in intact ventricular muscle*. Circ Res, 1995. **76**(6): p. 1036-48.
25. Hampton, T.G., et al., *Intracellular calcium dynamics in mouse model of myocardial stunning*. Am J Physiol, 1998. **274**(5 Pt 2): p. H1821-7.
26. Ferrari, R., et al., *Oxygen-mediated myocardial damage during ischaemia and reperfusion: role of the cellular defences against oxygen toxicity*. J Mol Cell Cardiol, 1985. **17**(10): p. 937-45.
27. Steare, S.E. and D.M. Yellon, *The potential for endogenous myocardial antioxidants to protect the myocardium against ischaemia-reperfusion injury: refreshing the parts exogenous antioxidants cannot reach?* J Mol Cell Cardiol, 1995. **27**(1): p. 65-74.
28. Pierce, G.N. and M.P. Czubryt, *The contribution of ionic imbalance to ischemia/reperfusion-induced injury*. J Mol Cell Cardiol, 1995. **27**(1): p. 53-63.
29. Piper, H.M., Y. Abdallah, and C. Schafer, *The first minutes of reperfusion: a window of opportunity for cardioprotection*. Cardiovasc Res, 2004. **61**(3): p. 365-71.
30. Saris, N.E. and E. Carafoli, *A historical review of cellular calcium handling, with emphasis on mitochondria*. Biochemistry (Mosc), 2005. **70**(2): p. 187-94.
31. Ruiz-Meana, M., et al., *Propagation of cardiomyocyte hypercontracture by passage of Na(+) through gap junctions*. Circ Res, 1999. **85**(3): p. 280-7.
32. Majno, G. and I. Joris, *Apoptosis, oncosis, and necrosis. An overview of cell death*. Am J Pathol, 1995. **146**(1): p. 3-15.
33. Van Cruchten, S. and W. Van Den Broeck, *Morphological and biochemical aspects of apoptosis, oncosis and necrosis*. Anat Histol Embryol, 2002. **31**(4): p. 214-23.
34. Weiland, U., et al., *Inhibition of endogenous nitric oxide synthase potentiates ischemia-reperfusion-induced myocardial apoptosis via a caspase-3 dependent pathway*. Cardiovasc Res, 2000. **45**(3): p. 671-8.
35. Haunstetter, A. and S. Izumo, *Future perspectives and potential implications of cardiac myocyte apoptosis*. Cardiovasc Res, 2000. **45**(3): p. 795-801.
36. Zhao, Z.Q., et al., *Reperfusion induces myocardial apoptotic cell death*. Cardiovasc Res, 2000. **45**(3): p. 651-60.
37. Kajstura, J., et al., *Apoptotic and necrotic myocyte cell deaths are independent contributing variables of infarct size in rats*. Lab Invest, 1996. **74**(1): p. 86-107.
38. Gottlieb, R.A., et al., *Reperfusion injury induces apoptosis in rabbit cardiomyocytes*. J Clin Invest, 1994. **94**(4): p. 1621-8.
39. Fliss, H. and D. Gatteringer, *Apoptosis in ischemic and reperfused rat myocardium*. Circ Res, 1996. **79**(5): p. 949-56.

40. Eefting, F., et al., *Role of apoptosis in reperfusion injury*. Cardiovasc Res, 2004. **61**(3): p. 414-26.
41. Hetts, S.W., *To die or not to die: an overview of apoptosis and its role in disease*. Jama, 1998. **279**(4): p. 300-7.
42. Liu, X., et al., *Induction of apoptotic program in cell-free extracts: requirement for dATP and cytochrome c*. Cell, 1996. **86**(1): p. 147-57.
43. Buja, L.M. and M.L. Entman, *Modes of myocardial cell injury and cell death in ischemic heart disease*. Circulation, 1998. **98**(14): p. 1355-7.
44. Borutaite, V. and G.C. Brown, *Mitochondria in apoptosis of ischemic heart*. FEBS Lett, 2003. **541**(1-3): p. 1-5.
45. Zhao, Z.Q. and J. Vinten-Johansen, *Myocardial apoptosis and ischemic preconditioning*. Cardiovasc Res, 2002. **55**(3): p. 438-55.
46. Bishopric, N.H., et al., *Molecular mechanisms of apoptosis in the cardiac myocyte*. Curr Opin Pharmacol, 2001. **1**(2): p. 141-50.
47. Mocanu, M.M., G.F. Baxter, and D.M. Yellon, *Caspase inhibition and limitation of myocardial infarct size: protection against lethal reperfusion injury*. Br J Pharmacol, 2000. **130**(2): p. 197-200.
48. Gustafsson, A.B. and R.A. Gottlieb, *Bcl-2 family members and apoptosis, taken to heart*. Am J Physiol Cell Physiol, 2007. **292**(1): p. C45-51.
49. Saraste, A. and K. Pulkki, *Morphologic and biochemical hallmarks of apoptosis*. Cardiovasc Res, 2000. **45**(3): p. 528-37.
50. Yaoita, H., et al., *Apoptosis in relevant clinical situations: contribution of apoptosis in myocardial infarction*. Cardiovasc Res, 2000. **45**(3): p. 630-41.
51. Yasuda, M., et al., *Adenovirus E1B-19K/BCL-2 interacting protein BNIP3 contains a BH3 domain and a mitochondrial targeting sequence*. J Biol Chem, 1998. **273**(20): p. 12415-21.
52. Chen, G., et al., *The E1B 19K/Bcl-2-binding protein Nip3 is a dimeric mitochondrial protein that activates apoptosis*. J Exp Med, 1997. **186**(12): p. 1975-83.
53. Hamacher-Brady, A., et al., *Response to myocardial ischemia/reperfusion injury involves Bnip3 and autophagy*. Cell Death Differ, 2007. **14**(1): p. 146-57.
54. Vande Velde, C., et al., *BNIP3 and genetic control of necrosis-like cell death through the mitochondrial permeability transition pore*. Mol Cell Biol, 2000. **20**(15): p. 5454-68.
55. Regula, K.M., K. Ens, and L.A. Kirshenbaum, *Inducible expression of BNIP3 provokes mitochondrial defects and hypoxia-mediated cell death of ventricular myocytes*. Circ Res, 2002. **91**(3): p. 226-31.
56. Kubli, D.A., J.E. Ycaza, and A.B. Gustafsson, *Bnip3 mediates mitochondrial dysfunction and cell death through Bax and Bak*. Biochem J, 2007. **405**(3): p. 407-15.
57. Kubasiak, L.A., et al., *Hypoxia and acidosis activate cardiac myocyte death through the Bcl-2 family protein BNIP3*. Proc Natl Acad Sci U S A, 2002. **99**(20): p. 12825-30.
58. Diwan, A., et al., *Inhibition of ischemic cardiomyocyte apoptosis through targeted ablation of Bnip3 restrains postinfarction remodeling in mice*. J Clin Invest, 2007. **117**(10): p. 2825-33.
59. Kubli, D.A., et al., *Bnip3 functions as a mitochondrial sensor of oxidative stress during myocardial ischemia and reperfusion*. Am J Physiol Heart Circ Physiol, 2008. **295**(5): p. H2025-31.

60. Azad, M.B., et al., *Hypoxia induces autophagic cell death in apoptosis-competent cells through a mechanism involving BNIP3*. *Autophagy*, 2008. **4**(2): p. 195-204.
61. Zhang, J. and P.A. Ney, *Role of BNIP3 and NIX in cell death, autophagy, and mitophagy*. *Cell Death Differ*, 2009. **16**(7): p. 939-46.
62. Thomas, R.L., D.A. Kubli, and A.B. Gustafsson, *Bnip3-mediated defects in oxidative phosphorylation promote mitophagy*. *Autophagy*, 2011. **7**(7).
63. Zhang, J., et al., *EndoG Links Bnip3-Induced Mitochondrial Damage and Caspase-Independent DNA Fragmentation in Ischemic Cardiomyocytes*. *PLoS One*, 2011. **6**(3): p. e17998.
64. Parrish, J.Z., et al., *CRN-1, a Caenorhabditis elegans FEN-1 homologue, cooperates with CPS-6/EndoG to promote apoptotic DNA degradation*. *Embo J*, 2003. **22**(13): p. 3451-60.
65. Li, L.Y., X. Luo, and X. Wang, *Endonuclease G is an apoptotic DNase when released from mitochondria*. *Nature*, 2001. **412**(6842): p. 95-9.
66. Bahi, N., et al., *Switch from caspase-dependent to caspase-independent death during heart development: essential role of endonuclease G in ischemia-induced DNA processing of differentiated cardiomyocytes*. *J Biol Chem*, 2006. **281**(32): p. 22943-52.
67. Chinnadurai, G., S. Vijayalingam, and S.B. Gibson, *BNIP3 subfamily BH3-only proteins: mitochondrial stress sensors in normal and pathological functions*. *Oncogene*, 2008. **27 Suppl 1**: p. S114-27.
68. Javadov, S., et al., *Targeting the mitochondrial permeability transition: cardiac ischemia-reperfusion versus carcinogenesis*. *Cell Physiol Biochem*, 2011. **27**(3-4): p. 179-90.
69. Chipuk, J.E., L. Bouchier-Hayes, and D.R. Green, *Mitochondrial outer membrane permeabilization during apoptosis: the innocent bystander scenario*. *Cell Death Differ*, 2006. **13**(8): p. 1396-402.
70. Lucken-Ardjomande, S., S. Montessuit, and J.C. Martinou, *Contributions to Bax insertion and oligomerization of lipids of the mitochondrial outer membrane*. *Cell Death Differ*, 2008. **15**(5): p. 929-37.
71. Halestrap, A.P. and P. Pasdois, *The role of the mitochondrial permeability transition pore in heart disease*. *Biochim Biophys Acta*, 2009. **1787**(11): p. 1402-15.
72. Argaud, L., et al., *Specific inhibition of the mitochondrial permeability transition prevents lethal reperfusion injury*. *J Mol Cell Cardiol*, 2005. **38**(2): p. 367-74.
73. Hausenloy, D.J. and D.M. Yellon, *The mitochondrial permeability transition pore: its fundamental role in mediating cell death during ischaemia and reperfusion*. *J Mol Cell Cardiol*, 2003. **35**(4): p. 339-41.
74. Javadov, S.A., et al., *Ischaemic preconditioning inhibits opening of mitochondrial permeability transition pores in the reperfused rat heart*. *J Physiol*, 2003. **549**(Pt 2): p. 513-24.
75. Piot, C., et al., *Effect of cyclosporine on reperfusion injury in acute myocardial infarction*. *N Engl J Med*, 2008. **359**(5): p. 473-81.
76. Shanmuganathan, S., et al., *Mitochondrial permeability transition pore as a target for cardioprotection in the human heart*. *Am J Physiol Heart Circ Physiol*, 2005. **289**(1): p. H237-42.
77. Krauskopf, A., et al., *Properties of the permeability transition in VDAC1(-/-) mitochondria*. *Biochim Biophys Acta*, 2006. **1757**(5-6): p. 590-5.

78. Baines, C.P., et al., *Voltage-dependent anion channels are dispensable for mitochondrial-dependent cell death*. Nat Cell Biol, 2007. **9**(5): p. 550-5.
79. Nakagawa, T., et al., *Cyclophilin D-dependent mitochondrial permeability transition regulates some necrotic but not apoptotic cell death*. Nature, 2005. **434**(7033): p. 652-8.
80. Basso, E., et al., *Properties of the permeability transition pore in mitochondria devoid of Cyclophilin D*. J Biol Chem, 2005. **280**(19): p. 18558-61.
81. Baines, C.P., et al., *Loss of cyclophilin D reveals a critical role for mitochondrial permeability transition in cell death*. Nature, 2005. **434**(7033): p. 658-62.
82. Leung, A.W., P. Varanyuwatana, and A.P. Halestrap, *The mitochondrial phosphate carrier interacts with cyclophilin D and may play a key role in the permeability transition*. J Biol Chem, 2008. **283**(39): p. 26312-23.
83. Bernardi, P., et al., *Modulation of the mitochondrial permeability transition pore. Effect of protons and divalent cations*. J Biol Chem, 1992. **267**(5): p. 2934-9.
84. Griffiths, E.J. and A.P. Halestrap, *Mitochondrial non-specific pores remain closed during cardiac ischaemia, but open upon reperfusion*. Biochem J, 1995. **307** (Pt 1): p. 93-8.
85. Kerr, P.M., M.S. Suleiman, and A.P. Halestrap, *Reversal of permeability transition during recovery of hearts from ischemia and its enhancement by pyruvate*. Am J Physiol, 1999. **276**(2 Pt 2): p. H496-502.
86. Javadov, S., et al., *NHE-1 inhibition-induced cardioprotection against ischaemia/reperfusion is associated with attenuation of the mitochondrial permeability transition*. Cardiovasc Res, 2008. **77**(2): p. 416-24.
87. Prendes, M.G., et al., *Protection of ischaemic-reperfused rat heart by dimethylamiloride is associated with inhibition of mitochondrial permeability transition*. Clin Exp Pharmacol Physiol, 2008. **35**(2): p. 201-6.
88. Murray, C.E., et al., *Preconditioning with ischaemia: a delay of lethal cell injury in ischaemic myocardium*. Circulation, 1986. **74**: p. 1124-1136.
89. Opie, L.H., *The multifarious spectrum of ischemic left ventricular dysfunction: relevance of new ischemic syndromes*. J Mol Cell Cardiol, 1996. **28**(12): p. 2403-14.
90. Heusch, G. and R. Schulz, *Endogenous protective mechanisms in myocardial ischemia: hibernation and ischemic preconditioning*. Am J Cardiol, 1997. **80**(3A): p. 26A-33A.
91. Cave, A.C., *Preconditioning induced protection against post-ischaemic contractile dysfunction: characteristics and mechanisms*. J Mol Cell Cardiol, 1995. **27**(4): p. 969-79.
92. Parratt, J. and A. Vegh, *Pronounced antiarrhythmic effects of ischemic preconditioning*. Cardioscience, 1994. **5**(1): p. 9-18.
93. Fatehi-Hassanabad, Z. and J.R. Parratt, *Genistein, an inhibitor of tyrosine kinase, prevents the antiarrhythmic effects of preconditioning*. Eur J Pharmacol, 1997. **338**(1): p. 67-70.
94. Gottlieb, R.A., et al., *Preconditioning rabbit cardiomyocytes: role of pH, vacuolar proton ATPase, and apoptosis*. J Clin Invest, 1996. **97**(10): p. 2391-8.
95. Piot, C.A., et al., *Ischemic preconditioning decreases apoptosis in rat hearts in vivo*. Circulation, 1997. **96**(5): p. 1598-604.

96. Rehring, T.F., et al., *Cardiac preconditioning protects against irreversible injury rather than attenuating stunning*. J Surg Res, 1995. **59**(1): p. 111-4.
97. Ovize, M., et al., *Preconditioning does not attenuate myocardial stunning*. Circulation, 1992. **85**(6): p. 2247-54.
98. Jenkins, D.P., W.B. Pugsley, and D.M. Yellon, *Ischaemic preconditioning in a model of global ischaemia: infarct size limitation, but no reduction of stunning*. J Mol Cell Cardiol, 1995. **27**(8): p. 1623-32.
99. Downey, J.M., Cohen M.V., *Preconditioning: what it is and how it works*. Dialogues Cardiovas Med, 1997(2): p. 179-196.
100. Pasupathy, S. and S. Homer-Vanniasinkam, *Ischaemic preconditioning protects against ischaemia/reperfusion injury: emerging concepts*. Eur J Vasc Endovasc Surg, 2005. **29**(2): p. 106-15.
101. Liang, B.T. and K.A. Jacobson, *Adenosine and ischemic preconditioning*. Curr Pharm Des, 1999. **5**(12): p. 1029-41.
102. Yellon, D.M., et al., *Ischaemic preconditioning: present position and future directions*. Cardiovasc Res, 1998. **37**(1): p. 21-33.
103. Zhao, T., et al., *Inducible nitric oxide synthase mediates delayed myocardial protection induced by activation of adenosine A(1) receptors: evidence from gene-knockout mice*. Circulation, 2000. **102**(8): p. 902-7.
104. Carini, R., et al., *Ischemic preconditioning reduces Na(+) accumulation and cell killing in isolated rat hepatocytes exposed to hypoxia*. Hepatology, 2000. **31**(1): p. 166-72.
105. Takano, H., X.L. Tang, and R. Bolli, *Differential role of K(ATP) channels in late preconditioning against myocardial stunning and infarction in rabbits*. Am J Physiol Heart Circ Physiol, 2000. **279**(5): p. H2350-9.
106. Hausenloy, D.J., et al., *Preconditioning protects by inhibiting the mitochondrial permeability transition*. Am J Physiol Heart Circ Physiol, 2004. **287**(2): p. H841-9.
107. Hausenloy, D.J. and D.M. Yellon, *Adenosine-induced second window of protection is mediated by inhibition of mitochondrial permeability transition pore opening at the time of reperfusion*. Cardiovasc Drugs Ther, 2004. **18**(1): p. 79-80.
108. Dhalla, N.S., et al., *Status of myocardial antioxidants in ischemia-reperfusion injury*. Cardiovasc Res, 2000. **47**(3): p. 446-56.
109. Haramaki, N., et al., *Networking antioxidants in the isolated rat heart are selectively depleted by ischemia-reperfusion*. Free Radic Biol Med, 1998. **25**(3): p. 329-39.
110. Takemura, G., et al., *Demonstration of hydroxyl radical and its role in hydrogen peroxide-induced myocardial injury: hydroxyl radical dependent and independent mechanisms*. Free Radic Biol Med, 1993. **15**(1): p. 13-25.
111. Zweier, J.L., *Measurement of superoxide-derived free radicals in the reperfused heart. Evidence for a free radical mechanism of reperfusion injury*. J Biol Chem, 1988. **263**(3): p. 1353-7.
112. Zweier, J.L. and M.A. Talukder, *The role of oxidants and free radicals in reperfusion injury*. Cardiovasc Res, 2006. **70**(2): p. 181-90.
113. Xu, K.Y., J.L. Zweier, and L.C. Becker, *Hydroxyl radical inhibits sarcoplasmic reticulum Ca(2+)-ATPase function by direct attack on the ATP binding site*. Circ Res, 1997. **80**(1): p. 76-81.

114. Hearse, D.J. and A. Tosaki, *Reperfusion-induced arrhythmias and free radicals: studies in the rat heart with DMPO*. J Cardiovasc Pharmacol, 1987. **9**(6): p. 641-50.
115. Kim, M.S. and T. Akera, *O₂ free radicals: cause of ischemia-reperfusion injury to cardiac Na⁺-K⁺-ATPase*. Am J Physiol, 1987. **252**(2 Pt 2): p. H252-7.
116. Le Grand, B., et al., *Alleviation of contractile dysfunction in ischemic hearts by slowly inactivating Na⁺ current blockers*. Am J Physiol, 1995. **269**(2 Pt 2): p. H533-40.
117. Przyklenk, K. and R.A. Kloner, *Superoxide dismutase plus catalase improve contractile function in the canine model of the "stunned myocardium"*. Circ Res, 1986. **58**(1): p. 148-56.
118. Halliwell, B. and J.M. Gutteridge, *The antioxidants of human extracellular fluids*. Arch Biochem Biophys, 1990. **280**(1): p. 1-8.
119. Petrosillo, G., et al., *Melatonin protects against heart ischemia-reperfusion injury by inhibiting mitochondrial permeability transition pore opening*. Am J Physiol Heart Circ Physiol, 2009. **297**(4): p. H1487-93.
120. Sato, T., B. O'Rourke, and E. Marban, *Modulation of mitochondrial ATP-dependent K⁺ channels by protein kinase C*. Circ Res, 1998. **83**(1): p. 110-4.
121. Fryer, R.M., A.K. Hsu, and G.J. Gross, *Mitochondrial K(ATP) channel opening is important during index ischemia and following myocardial reperfusion in ischemic preconditioned rat hearts*. J Mol Cell Cardiol, 2001. **33**(4): p. 831-4.
122. Haruna, T., et al., *Coordinate interaction between ATP-sensitive K⁺ channel and Na⁺, K⁺-ATPase modulates ischemic preconditioning*. Circulation, 1998. **98**(25): p. 2905-10.
123. Hu, K., et al., *Protein kinase C activates ATP-sensitive K⁺ current in human and rabbit ventricular myocytes*. Circ Res, 1996. **78**(3): p. 492-8.
124. Yang, X.M., et al., *Multiple, brief coronary occlusions during early reperfusion protect rabbit hearts by targeting cell signaling pathways*. J Am Coll Cardiol, 2004. **44**(5): p. 1103-10.
125. Costa, A.D., et al., *Protein kinase G transmits the cardioprotective signal from cytosol to mitochondria*. Circ Res, 2005. **97**(4): p. 329-36.
126. Hausenloy, D.J. and D.M. Yellon, *Survival kinases in ischemic preconditioning and postconditioning*. Cardiovasc Res, 2006. **70**(2): p. 240-53.
127. Costa, A.D., et al., *cGMP signalling in pre- and post-conditioning: the role of mitochondria*. Cardiovasc Res, 2008. **77**(2): p. 344-52.
128. Grover, G.J. and K.D. Garlid, *ATP-Sensitive potassium channels: a review of their cardioprotective pharmacology*. J Mol Cell Cardiol, 2000. **32**(4): p. 677-95.
129. Peart, J.N. and G.J. Gross, *Sarcolemmal and mitochondrial K(ATP) channels and myocardial ischemic preconditioning*. J Cell Mol Med, 2002. **6**(4): p. 453-64.
130. Yao, Z., I. Cavero, and G.J. Gross, *Activation of cardiac KATP channels: an endogenous protective mechanism during repetitive ischemia*. Am J Physiol, 1993. **264**(2 Pt 2): p. H495-504.
131. Grover, G.J., et al., *The KATP blocker sodium 5-hydroxydecanoate does not abolish preconditioning in isolated rat hearts*. Eur J Pharmacol, 1995. **277**(2-3): p. 271-4.

132. Yao, Z. and G.J. Gross, *Effects of the KATP channel opener bimakalim on coronary blood flow, monophasic action potential duration, and infarct size in dogs*. Circulation, 1994. **89**(4): p. 1769-75.
133. Liu, Y., et al., *Mitochondrial ATP-dependent potassium channels: novel effectors of cardioprotection?* Circulation, 1998. **97**(24): p. 2463-9.
134. Fukuda, H., et al., *The effect of K(atp)channel activation on myocardial cationic and energetic status during ischemia and reperfusion: role in cardioprotection*. J Mol Cell Cardiol, 2001. **33**(3): p. 545-60.
135. Babenko, A. and G. Vassort, *Enhancement of the ATP-sensitive K⁺ current by extracellular ATP in rat ventricular myocytes. Involvement of adenylyl cyclase-induced subsarcolemmal ATP depletion*. Circ Res, 1997. **80**(4): p. 589-600.
136. McPherson, C.D., G.N. Pierce, and W.C. Cole, *Ischemic cardioprotection by ATP-sensitive K⁺ channels involves high-energy phosphate preservation*. Am J Physiol, 1993. **265**(5 Pt 2): p. H1809-18.
137. Grover, G.J., et al., *Cardioprotective effects of the potassium channel opener cromakalim: stereoselectivity and effects on myocardial adenine nucleotides*. J Pharmacol Exp Ther, 1991. **257**(1): p. 156-62.
138. Garlid, K.D., et al., *Cardioprotective signaling to mitochondria*. J Mol Cell Cardiol, 2009. **46**(6): p. 858-66.
139. Clarke, S.J., et al., *Inhibition of mitochondrial permeability transition pore opening by ischemic preconditioning is probably mediated by reduction of oxidative stress rather than mitochondrial protein phosphorylation*. Circ Res, 2008. **102**(9): p. 1082-90.
140. Liu, G.S., et al., *Protection against infarction afforded by preconditioning is mediated by A1 adenosine receptors in rabbit heart*. Circulation, 1991. **84**(1): p. 350-6.
141. Qin, Q., J.M. Downey, and M.V. Cohen, *Acetylcholine but not adenosine triggers preconditioning through PI3-kinase and a tyrosine kinase*. Am J Physiol Heart Circ Physiol, 2003. **284**(2): p. H727-34.
142. Cohen, M.V., et al., *Acetylcholine, bradykinin, opioids, and phenylephrine, but not adenosine, trigger preconditioning by generating free radicals and opening mitochondrial K(ATP) channels*. Circ Res, 2001. **89**(3): p. 273-8.
143. Solenkova, N.V., et al., *Endogenous adenosine protects preconditioned heart during early minutes of reperfusion by activating Akt*. Am J Physiol Heart Circ Physiol, 2006. **290**(1): p. H441-9.
144. Philipp, S., et al., *Postconditioning protects rabbit hearts through a protein kinase C-adenosine A2b receptor cascade*. Cardiovasc Res, 2006. **70**(2): p. 308-14.
145. Liu, G.S., et al., *Evidence that the adenosine A3 receptor may mediate the protection afforded by preconditioning in the isolated rabbit heart*. Cardiovasc Res, 1994. **28**(7): p. 1057-61.
146. Downey, J.M. and M.V. Cohen, *Signal transduction in ischemic preconditioning*. Adv Exp Med Biol, 1997. **430**: p. 39-55.
147. Downey, J.M., A.M. Davis, and M.V. Cohen, *Signaling pathways in ischemic preconditioning*. Heart Fail Rev, 2007. **12**(3-4): p. 181-8.
148. Willems, L., K.J. Ashton, and J.P. Headrick, *Adenosine-mediated cardioprotection in the aging myocardium*. Cardiovasc Res, 2005. **66**(2): p. 245-55.

149. Zatta, A.J., G.P. Matherne, and J.P. Headrick, *Adenosine receptor-mediated coronary vascular protection in post-ischemic mouse heart*. Life Sci, 2006. **78**(21): p. 2426-37.
150. Reichelt, M.E., et al., *Endogenous adenosine selectively modulates oxidant stress via the A1 receptor in ischemic hearts*. Antioxid Redox Signal, 2009. **11**(11): p. 2641-50.
151. Reichelt, M.E., et al., *Genetic deletion of the A1 adenosine receptor limits myocardial ischemic tolerance*. Circ Res, 2005. **96**(3): p. 363-7.
152. Reichelt, M.E., et al., *Modulation of ischaemic contracture in mouse hearts: a 'supraphysiological' response to adenosine*. Exp Physiol, 2007. **92**(1): p. 175-85.
153. Peart, J., et al., *Adenosine-mediated cardioprotection in ischemic-reperfused mouse heart*. J Cardiovasc Pharmacol, 2002. **39**(1): p. 117-29.
154. Peart, J. and J.P. Headrick, *Intrinsic A(1) adenosine receptor activation during ischemia or reperfusion improves recovery in mouse hearts*. Am J Physiol Heart Circ Physiol, 2000. **279**(5): p. H2166-75.
155. Peart, J. and J.P. Headrick, *Adenosine-mediated early preconditioning in mouse: protective signaling and concentration dependent effects*. Cardiovasc Res, 2003. **58**(3): p. 589-601.
156. Peart, J., et al., *Cardioprotection with adenosine metabolism inhibitors in ischemic-reperfused mouse heart*. Cardiovasc Res, 2001. **52**(1): p. 120-9.
157. Peart, J., L. Willems, and J.P. Headrick, *Receptor and non-receptor-dependent mechanisms of cardioprotection with adenosine*. Am J Physiol Heart Circ Physiol, 2003. **284**(2): p. H519-27.
158. Headrick, J.P. and R.D. Lasley, *Adenosine receptors and reperfusion injury of the heart*. Handb Exp Pharmacol, 2009(193): p. 189-214.
159. Hack, B., et al., *Oxidant stress and damage in post-ischemic mouse hearts: effects of adenosine*. Mol Cell Biochem, 2006. **287**(1-2): p. 165-75.
160. Drury, A.N. and A. Szent-Gyorgyi, *The physiological activity of adenine compounds with especial reference to their action upon the mammalian heart*. J Physiol, 1929. **68**(3): p. 213-37.
161. Matsumoto, T., T. Nakane, and S. Chiba, *Pharmacological analysis of responses to ATP in the isolated and perfused canine coronary artery*. European Journal of Pharmacology, 1997. **334**(2-3): p. 173-80.
162. Harden, T.K., J.L. Boyer, and R.A. Nicholas, *P2-purinergic receptors: subtype-associated signaling responses and structure*. Annu Rev Pharmacol Toxicol, 1995. **35**: p. 541-79.
163. Tanaka, N., et al., *ATP participates in the regulation of microvessel permeability*. J Pharm Pharmacol, 2006. **58**(4): p. 481-7.
164. Yoshida, H., et al., *ATP stimulates interleukin-6 production via P2Y receptors in human HaCaT keratinocytes*. Eur J Pharmacol, 2006. **540**(1-3): p. 1-9.
165. Deli, T., et al., *Contribution from P2X and P2Y purinoreceptors to ATP-evoked changes in intracellular calcium concentration on cultured myotubes*. Pflugers Arch, 2007. **453**(4): p. 519-29.
166. Locovei, S., J. Wang, and G. Dahl, *Activation of pannexin 1 channels by ATP through P2Y receptors and by cytoplasmic calcium*. FEBS Lett, 2006. **580**(1): p. 239-44.
167. Lee, Y.J. and H.J. Han, *Role of ATP in DNA synthesis of renal proximal tubule cells: involvement of calcium, MAPKs, and CDKs*. Am J Physiol Renal Physiol, 2006. **291**(1): p. F98-106.

168. Lakshmi, S. and P.G. Joshi, *Activation of Src/kinase/phospholipase C/mitogen-activated protein kinase and induction of neurite expression by ATP, independent of nerve growth factor*. Neuroscience, 2006. **141**(1): p. 179-89.
169. Williams, M. and M.F. Jarvis, *Purinergic and pyrimidinergic receptors as potential drug targets*. Biochemical Pharmacology, 2000. **59**(10): p. 1173-85.
170. Burnstock, G. and M. Williams, *P2 purinergic receptors: modulation of cell function and therapeutic potential*. The Journal of Pharmacology and Experimental Therapeutics, 2000. **295**(3): p. 862-9.
171. Noma, A., *ATP-regulated K⁺ channels in cardiac muscle*. Nature, 1983. **305**(5930): p. 147-8.
172. Mei, Q. and B.T. Liang, *P2 purinergic receptor activation enhances cardiac contractility in isolated rat and mouse hearts*. American Journal of Physiology. Heart and Circulatory Physiology, 2001. **281**(1): p. H334-41.
173. Balogh, J., et al., *Phospholipase C and cAMP-dependent positive inotropic effects of ATP in mouse cardiomyocytes via P2Y11-like receptors*. J Mol Cell Cardiol, 2005. **39**(2): p. 223-30.
174. Vassort, G., *Adenosine 5'-triphosphate: a P2-purinergic agonist in the myocardium*. Physiological Reviews, 2001. **81**(2): p. 767-806.
175. Hopwood, A.M. and G. Burnstock, *ATP mediates coronary vasoconstriction via P2x-purinoceptors and coronary vasodilatation via P2y-purinoceptors in the isolated perfused rat heart*. European Journal of Pharmacology, 1987. **136**(1): p. 49-54.
176. Burnstock, G., *Vascular control by purines with emphasis on the coronary system*. Eur Heart J, 1989. **10 Suppl F**: p. 15-21.
177. Hansmann, G., et al., *Nucleotide-evoked relaxation of human coronary artery*. European Journal of Pharmacology, 1998. **359**(1): p. 59-67.
178. Yamamoto, T., et al., *P2 purinoceptors contribute to ATP-induced inhibition of L-type Ca²⁺ current in rabbit atrial myocytes*. Cardiovascular Research, 1999. **41**(1): p. 166-74.
179. Fischer, Y., C. Becker, and C. Loken, *Purinergic inhibition of glucose transport in cardiomyocytes*. J Biol Chem, 1999. **274**(2): p. 755-61.
180. Zenteno_Savin, T., et al., *Effects of arginine vasopressin in the heart are mediated by specific intravascular endothelial receptors*. European Journal of Pharmacology, 2000. **410**(1): p. 15-23.
181. Ninomiya, H., et al., *Complementary role of extracellular ATP and adenosine in ischemic preconditioning in the rat heart*. American Journal of Physiology. Heart and Circulatory Physiology, 2002a. **282**(5): p. H1810-20.
182. Fu, L.W. and J.C. Longhurst, *A new function for ATP: activating cardiac sympathetic afferents during myocardial ischemia*. Am J Physiol Heart Circ Physiol, 2010. **299**(6): p. H1762-71.
183. Bogdanov, Y., A. Rubino, and G. Burnstock, *Characterisation of subtypes of the P2X and P2Y families of ATP receptors in the foetal human heart*. Life Sciences, 1998. **62**(8): p. 697-703.
184. Hou, M., et al., *Increase in cardiac P2X1-and P2Y2-receptor mRNA levels in congestive heart failure*. Life Sciences, 1999. **65**(11): p. 1195-206.
185. Hu, B., et al., *A novel contractile phenotype with cardiac transgenic expression of the human P2X4 receptor*. Faseb J, 2001. **15**(14): p. 2739-41.

186. Gurung, I.S., et al., *Activation of purinergic receptors by ATP induces ventricular tachycardia by membrane depolarization and modifications of Ca²⁺ homeostasis*. J Mol Cell Cardiol, 2009. **47**(5): p. 622-33.
187. Vessey, D.A., L. Li, and M. Kelley, *P2X7 Receptor Agonists Pre- and Post-Condition the Heart Against Ischemia Reperfusion Injury by Opening Pannexin-1/P2X7 Channels*. Am J Physiol Heart Circ Physiol, 2011.
188. Korchazhkina, O., G. Wright, and C. Exley, *Intravascular ATP and coronary vasodilation in the isolated working rat heart*. Br J Pharmacol, 1999. **127**(3): p. 701-8.
189. Wihlborg, A.K., et al., *Positive inotropic effects by uridine triphosphate (UTP) and uridine diphosphate (UDP) via P2Y2 and P2Y6 receptors on cardiomyocytes and release of UTP in man during myocardial infarction*. Circ Res, 2006. **98**(7): p. 970-6.
190. Nishida, M., et al., *P2Y6 receptor-Galpha12/13 signalling in cardiomyocytes triggers pressure overload-induced cardiac fibrosis*. Embo J, 2008. **27**(23): p. 3104-15.
191. Zheng, J.S., et al., *Stimulation of P2Y receptors activates c-fos gene expression and inhibits DNA synthesis in cultured cardiac fibroblasts*. Cardiovasc Res, 1998. **37**(3): p. 718-28.
192. Millart, H., et al., *Involvement of P2Y receptors in pyridoxal-5'-phosphate-induced cardiac preconditioning*. Fundam Clin Pharmacol, 2009. **23**(3): p. 279-92.
193. Braun, O.O., et al., *Uridine triphosphate (UTP) induces profibrotic responses in cardiac fibroblasts by activation of P2Y2 receptors*. J Mol Cell Cardiol, 2010. **49**(3): p. 362-9.
194. Fredholm, B.B., et al., *Nomenclature and classification of purinoceptors*. Pharmacological Reviews, 1994. **46**(2): p. 143-56.
195. Ralevic, V. and G. Burnstock, *Receptors for purines and pyrimidines*. Pharmacological Reviews, 1998. **50**(3): p. 413-92.
196. Abbracchio, M.P. and G. Burnstock, *Purinoceptors: are there families of P2X and P2Y purinoceptors?* Pharmacology & Therapeutics, 1994. **64**(3): p. 445-75.
197. Jacobson, K.A., M.F. Jarvis, and M. Williams, *Purine and pyrimidine (P2) receptors as drug targets*. Journal of Medicinal Chemistry, 2002. **45**(19): p. 4057-93.
198. North, R.A., *Molecular physiology of P2X receptors*. Physiol Rev, 2002. **82**(4): p. 1013-67.
199. Radford KM, e.a., *Baculovirus expression provides direct evidence for heteromeric assembly of P2X2 and P2X3 receptors*. Journal of Neuroscience, 1997. **17**: p. 6529-6533.
200. Torres, G.E., et al., *Co-expression of P2X1 and P2X5 receptor subunits reveals a novel ATP-gated ion channel*. Mol Pharmacol, 1998. **54**(6): p. 989-93.
201. Brown, S.G., et al., *Heteromultimeric P2X(1/2) receptors show a novel sensitivity to extracellular pH*. J Pharmacol Exp Ther, 2002. **300**(2): p. 673-80.
202. Zemkova, H., et al., *Roles of purinergic P2X receptors as pacemaking channels and modulators of calcium-mobilizing pathway in pituitary gonadotrophs*. Mol Endocrinol, 2006. **20**(6): p. 1423-36.
203. Solle, M., et al., *Altered cytokine production in mice lacking P2X(7) receptors*. The Journal of Biological Chemistry, 2001. **276**(1): p. 125-32.

204. Schwiebert, L.M., et al., *Extracellular ATP signaling and P2X nucleotide receptors in monolayers of primary human vascular endothelial cells*. American Journal of Physiology. Cell Physiology, 2002. **282**(2): p. C289-301.
205. Harrington, L.S. and J.A. Mitchell, *Novel role for P2X receptor activation in endothelium-dependent vasodilation*. Br J Pharmacol, 2004. **143**(5): p. 611-7.
206. Burnstock, G., *Local control of blood pressure by purines*. Blood Vessels, 1987. **24**(3): p. 156-60.
207. Bean, B.P., *Pharmacology and electrophysiology of ATP-activated ion channels*. Trends in Pharmacological Sciences, 1992. **13**(3): p. 87-90.
208. Dubyak, G.R. and C. el_Moatassim, *Signal transduction via P2-purinergic receptors for extracellular ATP and other nucleotides*. The American Journal of Physiology, 1993. **265**(3 Pt 1): p. C577-606.
209. Froldi, G., et al., *P2X-purinoceptors in the heart: actions of ATP and UTP*. Life Sci, 1997. **60**(17): p. 1419-30.
210. Scislo, T.J., E. Ergene, and D.S. O'Leary, *Impaired arterial baroreflex regulation of heart rate after blockade of P2-purinoceptors in the nucleus tractus solitarius*. Brain Research Bulletin, 1998. **47**(1): p. 63-7.
211. Yang, A., et al., *A beneficial role of cardiac P2X4 receptors in heart failure: rescue of the calsequestrin overexpression model of cardiomyopathy*. Am J Physiol Heart Circ Physiol, 2004. **287**(3): p. H1096-103.
212. Anikina, T.A., et al., *Role of purinoceptors in cardiac function in rats during ontogeny*. Bull Exp Biol Med, 2005. **140**(5): p. 483-5.
213. Vessey, D.A., L. Li, and M. Kelley, *Pannexin-1/P2X 7 purinergic receptor channels mediate the release of cardioprotectants induced by ischemic pre- and postconditioning*. J Cardiovasc Pharmacol Ther, 2010. **15**(2): p. 190-5.
214. Barnard, E.A., et al., *Signalling pathways and ion channel regulations of P2Y receptors*. Drug Development Research, 2003. **59**(1): p. 36-48.
215. Tokuyama, Y., et al., *Cloning of rat and mouse P2Y purinoceptors*. Biochemical and Biophysical Research Communications, 1995. **211**(1): p. 211-8.
216. Nakata, H., K. Yoshioka, and O. Saitoh, *Hetero-oligomerization between adenosine A1 and P2Y1 receptors in living cells: Formation of ATP-sensitive adenosine receptors*. Drug Development Research Volume, Issue, 2003. Pages:, 2003. **58**(4): p. 340-349.
217. Boeynaems, J.-M., et al., *P2Y receptors: New subtypes, new functions*. Drug Development Research, 2003. **59**(1): p. 30-35.
218. Jacobson, K.A., et al., *Action of nucleosides and nucleotides at 7 transmembrane-spanning receptors*. Nucleosides Nucleotides Nucleic Acids, 2006. **25**(12): p. 1425-36.
219. Lazarowski, E.R., R.C. Boucher, and T.K. Harden, *Mechanisms of release of nucleotides and integration of their action as P2X- and P2Y-receptor activating molecules*. Mol Pharmacol, 2003. **64**(4): p. 785-95.
220. Erb, L., et al., *P2 receptors: intracellular signaling*. Pflugers Arch, 2006. **452**(5): p. 552-62.
221. Montiel, M., E.P. de la Blanca, and E. Jimenez, *P2Y receptors activate MAPK/ERK through a pathway involving PI3K/PDK1/PKC-zeta in human vein endothelial cells*. Cell Physiol Biochem, 2006. **18**(1-3): p. 123-34.
222. Communi, D., et al., *Cloning of a human purinergic P2Y receptor coupled to phospholipase C and adenylyl cyclase*. The Journal of Biological Chemistry, 1997. **272**(51): p. 31969-73.

223. Sauzeau, V., et al., *P2Y(1), P2Y(2), P2Y(4), and P2Y(6) receptors are coupled to Rho and Rho kinase activation in vascular myocytes*. American Journal of Physiology. Heart and Circulatory Physiology, 2000. **278**(6): p. H1751-61.
224. Hechler, B., et al., *MRS2500 [2-iodo-N6-methyl-(N)-methanocarba-2'-deoxyadenosine-3',5'-bisphosphate], a potent, selective, and stable antagonist of the platelet P2Y1 receptor with strong antithrombotic activity in mice*. J Pharmacol Exp Ther, 2006. **316**(2): p. 556-63.
225. White, N., et al., *P2Y purinergic receptors regulate the growth of human melanomas*. Cancer Lett, 2005. **224**(1): p. 81-91.
226. Suh, B.C., et al., *Selective inhibition of beta(2)-adrenergic receptor-mediated cAMP generation by activation of the P2Y(2) receptor in mouse pineal gland tumor cells*. J Neurochem, 2001. **77**(6): p. 1475-85.
227. Mosbacher, J., et al., *P2Y receptor subtypes differentially couple to inwardly-rectifying potassium channels*. FEBS Lett, 1998. **436**(1): p. 104-10.
228. Brambilla, R., et al., *A novel gliotic P2 receptor mediating cyclooxygenase-2 induction in rat and human astrocytes*. J Auton Nerv Syst, 2000. **81**(1-3): p. 3-9.
229. Soltoff, S.P., et al., *Activation of P2Y2 receptors by UTP and ATP stimulates mitogen-activated kinase activity through a pathway that involves related adhesion focal tyrosine kinase and protein kinase C*. The Journal of Biological Chemistry, 1998a. **273**(5): p. 2653-60.
230. Soltoff, S.P., *Related adhesion focal tyrosine kinase and the epidermal growth factor receptor mediate the stimulation of mitogen-activated protein kinase by the G-protein-coupled P2Y2 receptor. Phorbol ester or [Ca2+]i elevation can substitute for receptor activation*. The Journal of Biological Chemistry, 1998. **273**(36): p. 23110-7.
231. Homolya, L., et al., *Nucleotide-regulated calcium signaling in lung fibroblasts and epithelial cells from normal and P2Y(2) receptor (-/-) mice*. The Journal of Biological Chemistry, 1999. **274**(37): p. 26454-60.
232. Alvarez, J., et al., *ATP/UTP activate cation-permeable channels with TRPC3/7 properties in rat cardiomyocytes*. Am J Physiol Heart Circ Physiol, 2008. **295**(1): p. H21-8.
233. Communi, D., et al., *Cloning and functional expression of a human uridine nucleotide receptor*. The Journal of Biological Chemistry, 1995. **270**(52): p. 30849-52.
234. Bogdanov, Y.D., et al., *Molecular cloning and characterization of rat P2Y4 nucleotide receptor*. Br J Pharmacol, 1998. **124**(3): p. 428-30.
235. Govindan, S., E.J. Taylor, and C.W. Taylor, *Ca(2+) signalling by P2Y receptors in cultured rat aortic smooth muscle cells*. Br J Pharmacol, 2010. **160**(8): p. 1953-62.
236. Harper, S., et al., *Evidence that P2Y4 nucleotide receptors are involved in the regulation of rat aortic smooth muscle cells by UTP and ATP*. British Journal of Pharmacology, 1998. **124**(4): p. 703-10.
237. Warny, M., et al., *P2Y(6) nucleotide receptor mediates monocyte interleukin-8 production in response to UDP or lipopolysaccharide*. J Biol Chem, 2001. **276**(28): p. 26051-6.
238. Filippov, A.K., et al., *Dual coupling of heterologously-expressed rat P2Y6 nucleotide receptors to N-type Ca2+ and M-type K+ currents in rat sympathetic neurones*. Br J Pharmacol, 1999. **126**(4): p. 1009-17.

239. Schreiber, R. and K. Kunzelmann, *Purinergic P2Y6 receptors induce Ca²⁺ and CFTR dependent Cl⁻ secretion in mouse trachea*. Cell Physiol Biochem, 2005. **16**(1-3): p. 99-108.
240. Hou, M., et al., *UDP acts as a growth factor for vascular smooth muscle cells by activation of P2Y(6) receptors*. Am J Physiol Heart Circ Physiol, 2002. **282**(2): p. H784-92.
241. Malmstro, M., et al., *Potent P2Y6 receptor mediated contractions in human cerebral arteries*. BMC Pharmacol, 2003. **3**: p. 4.
242. Nakata, H., et al., *Functions of heteromeric association between adenosine and P2Y receptors*. J Mol Neurosci, 2005. **26**(2-3): p. 233-8.
243. Suzuki, T., et al., *Regulation of pharmacology by hetero-oligomerization between A1 adenosine receptor and P2Y2 receptor*. Biochem Biophys Res Commun, 2006. **351**(2): p. 559-65.
244. Hardy, A.R., et al., *Reciprocal cross-talk between P2Y1 and P2Y12 receptors at the level of calcium signaling in human platelets*. Blood, 2004. **104**(6): p. 1745-52.
245. Vials, A.J. and G. Burnstock, *Differential effects of ATP- and 2-methylthioATP-induced relaxation in guinea pig coronary vasculature*. J Cardiovasc Pharmacol, 1994. **23**(5): p. 757-64.
246. Chinellato, A., et al., *Pharmacological characterization of ATP receptors mediating vasodilation on isolated rabbit aorta*. General Pharmacology, 1992. **23**(5): p. 861-5.
247. Simonsen, U., A. Garcia-Sacristan, and D. Prieto, *Involvement of ATP in the non-adrenergic non-cholinergic inhibitory neurotransmission of lamb isolated coronary small arteries*. Br J Pharmacol, 1997. **120**(3): p. 411-20.
248. Podrasky, E., D. Xu, and B.T. Liang, *A novel phospholipase C- and cAMP-independent positive inotropic mechanism via a P2 purinoceptor*. The American Journal of Physiology, 1997. **273**(5 Pt 2): p. H2380-7.
249. Guns, P.J., et al., *Pharmacological characterization of nucleotide P2Y receptors on endothelial cells of the mouse aorta*. Br J Pharmacol, 2005. **146**(2): p. 288-95.
250. Banfi, C., et al., *P2 receptors in human heart: upregulation of P2X6 in patients undergoing heart transplantation, interaction with TNFalpha and potential role in myocardial cell death*. J Mol Cell Cardiol, 2005. **39**(6): p. 929-39.
251. Oketani, N., et al., *Regulation of K(ATP) channels by P(2Y) purinoceptors coupled to PIP(2) metabolism in guinea pig ventricular cells*. American Journal of Physiology. Heart and Circulatory Physiology, 2002. **282**(2): p. H757-65.
252. Erlinge, D., et al., *Uridine triphosphate (UTP) is released during cardiac ischemia*. Int J Cardiol, 2005. **100**(3): p. 427-33.
253. Muraki, K., Y. Imaizumi, and M. Watanabe, *Effects of UTP on membrane current and potential in rat aortic myocytes*. European Journal of Pharmacology, 1998. **360**(2-3): p. 239-47.
254. Yitzhaki, S., et al., *Involvement of uracil nucleotides in protection of cardiomyocytes from hypoxic stress*. Biochem Pharmacol, 2005. **69**(8): p. 1215-23.
255. Yitzhaki, S., et al., *Uridine-5'-triphosphate (UTP) reduces infarct size and improves rat heart function after myocardial infarct*. Biochem Pharmacol, 2006. **72**(8): p. 949-55.

256. Sellers, L.A., et al., *Adenosine nucleotides acting at the human P2Y₁ receptor stimulate mitogen-activated protein kinases and induce apoptosis*. The Journal of Biological Chemistry, 2001. **276**(19): p. 16379-90.
257. Mamedova, L.K., Z.G. Gao, and K.A. Jacobson, *Regulation of death and survival in astrocytes by ADP activating P2Y₁ and P2Y₁₂ receptors*. Biochem Pharmacol, 2006. **72**(8): p. 1031-41.
258. Nihei, O.K., et al., *Pharmacologic properties of P(2Z)/P2X(7) receptor characterized in murine dendritic cells: role on the induction of apoptosis*. Blood, 2000. **96**(3): p. 996-1005.
259. Schulze-Lohoff, E., et al., *Extracellular ATP causes apoptosis and necrosis of cultured mesangial cells via P2Z/P2X₇ receptors*. Am J Physiol, 1998. **275**(6 Pt 2): p. F962-71.
260. Coutinho-Silva, R., et al., *P2Z/P2X₇ receptor-dependent apoptosis of dendritic cells*. Am J Physiol, 1999. **276**(5 Pt 1): p. C1139-47.
261. Ferrari, D., et al., *P2Z purinoreceptor ligation induces activation of caspases with distinct roles in apoptotic and necrotic alterations of cell death*. FEBS Lett, 1999. **447**(1): p. 71-5.
262. Mazzola, A., et al., *Opposite effects of uracil and adenine nucleotides on the survival of murine cardiomyocytes*. J Cell Mol Med, 2008. **12**(2): p. 522-36.
263. Shainberg, A., et al., *Involvement of UTP in protection of cardiomyocytes from hypoxic stress*. Can J Physiol Pharmacol, 2009. **87**(4): p. 287-99.
264. Cosentino, S., et al., *Cardiomyocyte death induced by ischemic/hypoxic stress is differentially affected by distinct purinergic P2 receptors*. J Cell Mol Med, 2011.
265. Sumeray, M.S. and D.M. Yellon, *Characterisation and validation of a murine model of global ischaemia-reperfusion injury*. Mol Cell Biochem, 1998. **186**(1-2): p. 61-8.
266. Sutherland, F.J. and D.J. Hearse, *The isolated blood and perfusion fluid perfused heart*. Pharmacological Research : the Official Journal of the Italian Pharmacological Society, 2000. **41**(6): p. 613-27.
267. Headrick, J.P., et al., *Functional properties and responses to ischaemia-reperfusion in Langendorff perfused mouse heart*. Exp Physiol, 2001a. **86**(6): p. 703-16.
268. Sutherland, F.J., et al., *Mouse isolated perfused heart: characteristics and cautions*. Clin Exp Pharmacol Physiol, 2003. **30**(11): p. 867-78.
269. Skrzypiec-Spring, M., et al., *Isolated heart perfusion according to Langendorff-Still viable in the new millennium*. J Pharmacol Toxicol Methods, 2007. **55**(2): p. 113-26.
270. Chen, Z., et al., *Overexpression of MnSOD protects against myocardial ischemia/reperfusion injury in transgenic mice*. J Mol Cell Cardiol, 1998. **30**(11): p. 2281-9.
271. Asimakis, G.K., S. Lick, and C. Patterson, *Postischemic recovery of contractile function is impaired in SOD2(+/-) but not SOD1(+/-) mouse hearts*. Circulation, 2002. **105**(8): p. 981-6.
272. Jin, Z.Q., et al., *Cardioprotection mediated by sphingosine-1-phosphate and ganglioside GM-1 in wild-type and PKC epsilon knockout mouse hearts*. Am J Physiol Heart Circ Physiol, 2002. **282**(6): p. H1970-7.
273. Said, M., et al., *Role of dual-site phospholamban phosphorylation in the stunned heart: insights from phospholamban site-specific mutants*. Am J Physiol Heart Circ Physiol, 2003. **285**(3): p. H1198-205.

274. Tanno, M., et al., *Diverse mechanisms of myocardial p38 mitogen-activated protein kinase activation: evidence for MKK-independent activation by a TAB1-associated mechanism contributing to injury during myocardial ischemia.* Circ Res, 2003. **93**(3): p. 254-61.
275. Moseley, A.E., et al., *Attenuation of cardiac contractility in Na,K-ATPase α 1 isoform-deficient hearts under reduced calcium conditions.* J Mol Cell Cardiol, 2004. **37**(5): p. 913-9.
276. Palmer, B.M., et al., *Effect of cardiac myosin binding protein-C on mechanoenergetics in mouse myocardium.* Circ Res, 2004. **94**(12): p. 1615-22.
277. Huang, R., et al., *Deletion of the mouse alpha-calcitonin gene-related peptide gene increases the vulnerability of the heart to ischemia-reperfusion injury.* Am J Physiol Heart Circ Physiol, 2008. **294**(3): p. H1291-7.
278. Hannan, R.L., et al., *Deletion of endothelial nitric oxide synthase exacerbates myocardial stunning in an isolated mouse heart model.* J Surg Res, 2000. **93**(1): p. 127-32.
279. Willems, L., et al., *Age-related changes in ischemic tolerance in male and female mouse hearts.* J Mol Cell Cardiol, 2005. **38**(2): p. 245-56.
280. Yet, S.F., et al., *Cardiac-specific expression of heme oxygenase-1 protects against ischemia and reperfusion injury in transgenic mice.* Circ Res, 2001. **89**(2): p. 168-73.
281. Imahashi, K., et al., *Male/female differences in intracellular Na⁺ regulation during ischemia/reperfusion in mouse heart.* J Mol Cell Cardiol, 2004. **37**(3): p. 747-53.
282. Seubert, J., et al., *Enhanced postischemic functional recovery in CYP2J2 transgenic hearts involves mitochondrial ATP-sensitive K⁺ channels and p42/p44 MAPK pathway.* Circ Res, 2004. **95**(5): p. 506-14.
283. Jin, Z.Q., et al., *A sphingosine kinase 1 mutation sensitizes the myocardium to ischemia/reperfusion injury.* Cardiovasc Res, 2007. **76**(1): p. 41-50.
284. Schulte, G., et al., *Adenosine A receptors are necessary for protection of the murine heart by remote, delayed adaptation to ischaemia.* Acta Physiol Scand, 2004. **182**(2): p. 133-43.
285. Leary, P.J., et al., *A cardioprotective role for platelet-activating factor through NOS-dependent S-nitrosylation.* Am J Physiol Heart Circ Physiol, 2008. **294**(6): p. H2775-84.
286. Toth, A., et al., *Targeted deletion of Puma attenuates cardiomyocyte death and improves cardiac function during ischemia-reperfusion.* Am J Physiol Heart Circ Physiol, 2006. **291**(1): p. H52-60.
287. Gonon, A.T., et al., *Cardioprotection mediated by rosiglitazone, a peroxisome proliferator-activated receptor gamma ligand, in relation to nitric oxide.* Basic Res Cardiol, 2007. **102**(1): p. 80-9.
288. Kameyama, T., et al., *Mechanoenergetic studies in isolated mouse hearts.* Am J Physiol, 1998. **274**(1 Pt 2): p. H366-74.
289. Sato, R., J. Yamazaki, and T. Nagao, *Temporal differences in actions of calcium channel blockers on K⁺ accumulation, cardiac function, and high-energy phosphate levels in ischemic guinea pig hearts.* J Pharmacol Exp Ther, 1999. **289**(2): p. 831-9.
290. Gyurko, R., et al., *Modulation of mouse cardiac function in vivo by eNOS and ANP.* Am J Physiol Heart Circ Physiol, 2000. **278**(3): p. H971-81.

291. Pazos-Moura, C., et al., *Cardiac dysfunction caused by myocardium-specific expression of a mutant thyroid hormone receptor*. Circ Res, 2000. **86**(6): p. 700-6.
292. MacGowan, G.A., et al., *Ischemic dysfunction in transgenic mice expressing troponin I lacking protein kinase C phosphorylation sites*. Am J Physiol Heart Circ Physiol, 2001. **280**(2): p. H835-43.
293. Brooks, W.W. and C.S. Apstein, *Effect of treppe on isovolumic function in the isolated blood-perfused mouse heart*. J Mol Cell Cardiol, 1996. **28**(8): p. 1817-22.
294. Headrick, J.P., et al., *Cardioprotection by K(ATP) channels in wild-type hearts and hearts overexpressing A(1)-adenosine receptors*. Am J Physiol Heart Circ Physiol, 2000a. **279**(4): p. H1690-7.
295. Headrick, J.P., et al., *Chronotropic and vasodilatory responses to adenosine and isoproterenol in mouse heart: effects of adenosine A1 receptor overexpression*. Clin Exp Pharmacol Physiol, 2000. **27**(3): p. 185-90.
296. Georgakopoulos, D., et al., *In vivo murine left ventricular pressure-volume relations by miniaturized conductance micromanometry*. Am J Physiol, 1998. **274**(4 Pt 2): p. H1416-22.
297. Peart, J.N., et al., *Sustained ligand-activated preconditioning via delta-opioid receptors*. J Pharmacol Exp Ther, 2011. **336**(1): p. 274-81.
298. Cross, H.R., et al., *Is a high glycogen content beneficial or detrimental to the ischemic rat heart? A controversy resolved*. Circ Res, 1996. **78**(3): p. 482-91.
299. King, L.M., F. Boucher, and L.H. Opie, *Coronary flow and glucose delivery as determinants of contracture in the ischemic myocardium*. J Mol Cell Cardiol, 1995. **27**(1): p. 701-20.
300. Kingsley, P.B., et al., *Ischemic contracture begins when anaerobic glycolysis stops: a ³¹P-NMR study of isolated rat hearts*. Am J Physiol, 1991. **261**(2 Pt 2): p. H469-78.
301. Tani, M., et al., *Protection of ischemic myocardium by inhibition of contracture in isolated rat heart*. Am J Physiol, 1996. **271**(6 Pt 2): p. H2515-9.
302. Flood, A., B.D. Hack, and J.P. Headrick, *Pyruvate-dependent preconditioning and cardioprotection in murine myocardium*. Clin Exp Pharmacol Physiol, 2003. **30**(3): p. 145-52.
303. Bunger, R., R.T. Mallet, and D.A. Hartman, *Pyruvate-enhanced phosphorylation potential and inotropism in normoxic and postischemic isolated working heart. Near-complete prevention of reperfusion contractile failure*. Eur J Biochem, 1989. **180**(1): p. 221-33.
304. Bunger, R., et al., *Pyruvate attenuation of hypoxia damage in isolated working guinea-pig heart*. J Mol Cell Cardiol, 1986. **18**(4): p. 423-38.
305. Randle, P.J., E.A. Newsholme, and P.B. Garland, *Regulation of glucose uptake by muscle. 8. Effects of fatty acids, ketone bodies and pyruvate, and of alloxan-diabetes and starvation, on the uptake and metabolic fate of glucose in rat heart and diaphragm muscles*. Biochem J, 1964. **93**(3): p. 652-65.
306. Williamson, J.R., *Glycolytic control mechanisms. II. Kinetics of intermediate changes during the aerobic-anoxic transition in perfused rat heart*. J Biol Chem, 1966. **241**(21): p. 5026-36.
307. Bindoli, A., E. Barzon, and M.P. Rigobello, *Inhibitory effect of pyruvate on release of glutathione and swelling of rat heart mitochondria*. Cardiovasc Res, 1995. **30**(5): p. 821-4.

308. Crestanello, J.A., et al., *Pyruvate improves myocardial tolerance to reperfusion injury by acting as an antioxidant: a chemiluminescence study*. Surgery, 1998. **124**(1): p. 92-9.
309. DeBoer, L.W., et al., *Pyruvate enhances recovery of rat hearts after ischemia and reperfusion by preventing free radical generation*. Am J Physiol, 1993. **265**(5 Pt 2): p. H1571-6.
310. Lewandowski, E.D., D.L. Johnston, and R. Roberts, *Effects of inosine on glycolysis and contracture during myocardial ischemia*. Circ Res, 1991. **68**(2): p. 578-87.
311. Cavallini, L., M. Valente, and M.P. Rigobello, *The protective action of pyruvate on recovery of ischemic rat heart: comparison with other oxidizable substrates*. J Mol Cell Cardiol, 1990. **22**(2): p. 143-54.
312. Lasley, R.D., et al., *Adenosine A1 receptor mediated protection of the globally ischemic isolated rat heart*. J Mol Cell Cardiol, 1990. **22**(1): p. 39-47.
313. Cohen, M.V., C.P. Baines, and J.M. Downey, *Ischemic preconditioning: from adenosine receptor to KATP channel*. Annu Rev Physiol, 2000. **62**: p. 79-109.
314. de Jong, J.W., et al., *The role of adenosine in preconditioning*. Pharmacol Ther, 2000. **87**(2-3): p. 141-9.
315. Headrick, J.P., *Ischemic preconditioning: bioenergetic and metabolic changes and the role of endogenous adenosine*. J Mol Cell Cardiol, 1996. **28**(6): p. 1227-40.
316. Malmsjo, M., et al., *Congestive heart failure induces downregulation of P2X1-receptors in resistance arteries*. Cardiovascular Research, 1999. **43**(1): p. 219-27.
317. Sonin, D., et al., *Role of P2X purinergic receptors in the rescue of ischemic heart failure*. Am J Physiol Heart Circ Physiol, 2008. **295**(3): p. H1191-H1197.
318. Harrington, L.S. and J.A. Mitchell, *P2X1 receptors and the endothelium*. Mem Inst Oswaldo Cruz, 2005. **100 Suppl 1**: p. 111-2.
319. Harrington, L.S., et al., *Purinergic 2X1 receptors mediate endothelial dependent vasodilation to ATP*. Mol Pharmacol, 2007. **72**(5): p. 1132-6.
320. Jiang, L., et al., *P2X1 receptors are closely associated with connexin 43 in human ventricular myocardium*. Int J Cardiol, 2005. **98**(2): p. 291-7.
321. Hansen, M.A., M.R. Bennett, and J.A. Barden, *Distribution of purinergic P2X receptors in the rat heart*. J Auton Nerv Syst, 1999. **78**(1): p. 1-9.
322. Birdsong, W.T., et al., *Sensing muscle ischemia: coincident detection of acid and ATP via interplay of two ion channels*. Neuron, 2010. **68**(4): p. 739-49.
323. Leon, D., C. Hervas, and M.T. Miras-Portugal, *P2Y1 and P2X7 receptors induce calcium/calmodulin-dependent protein kinase II phosphorylation in cerebellar granule neurons*. Eur J Neurosci, 2006. **23**(11): p. 2999-3013.
324. Arulkumaran, N., R.J. Unwin, and F.W. Tam, *A potential therapeutic role for P2X7 receptor (P2X7R) antagonists in the treatment of inflammatory diseases*. Expert Opin Investig Drugs, 2011.
325. Lenertz, L.Y., et al., *Transcriptional control mechanisms associated with the nucleotide receptor P2X7, a critical regulator of immunologic, osteogenic, and neurologic functions*. Immunol Res, 2011. **50**(1): p. 22-38.
326. Bours, M.J., et al., *P2 receptors and extracellular ATP: a novel homeostatic pathway in inflammation*. Front Biosci (Schol Ed), 2011. **3**: p. 1443-56.
327. Wesselius, A., et al., *Role of purinergic receptor polymorphisms in human bone*. Front Biosci, 2011. **17**: p. 2572-85.

328. Roger, S. and P. Pelegrin, *P2X7 receptor antagonism in the treatment of cancers*. Expert Opin Investig Drugs, 2011.
329. Franke, H., et al., *P2X7 receptor expression after ischemia in the cerebral cortex of rats*. J Neuropathol Exp Neurol, 2004. **63**(7): p. 686-99.
330. Lalo, U., et al., *P2X1 and P2X5 subunits form the functional P2X receptor in mouse cortical astrocytes*. J Neurosci, 2008. **28**(21): p. 5473-80.
331. Liang, S., et al., *P2X receptors and modulation of pain transmission: focus on effects of drugs and compounds used in traditional Chinese medicine*. Neurochem Int, 2010. **57**(7): p. 705-12.
332. Harhun, M.I., O.V. Povstyan, and D.V. Gordienko, *Purinoreceptor-mediated current in myocytes from renal resistance arteries*. Br J Pharmacol, 2010. **160**(4): p. 987-97.
333. Guo, C., et al., *Evidence for functional P2X4/P2X7 heteromeric receptors*. Mol Pharmacol, 2007. **72**(6): p. 1447-56.
334. Nicke, A., *Homotrimeric complexes are the dominant assembly state of native P2X7 subunits*. Biochem Biophys Res Commun, 2008. **377**(3): p. 803-8.
335. Fabre, J.E., et al., *Decreased platelet aggregation, increased bleeding time and resistance to thromboembolism in P2Y1-deficient mice*. Nature Medicine, 1999. **5**(10): p. 1199-202.
336. Leon, C., et al., *Defective platelet aggregation and increased resistance to thrombosis in purinergic P2Y(1) receptor-null mice*. The Journal of Clinical Investigation, 1999. **104**(12): p. 1731-7.
337. Olivecrona, G.K., et al., *The ADP receptor P2Y(1) mediates t-PA release in pigs during cardiac ischemia*. J Thromb Thrombolysis, 2007. **24**(2): p. 115-22.
338. Gorman, M.W., et al., *Adenine nucleotide control of coronary blood flow during exercise*. Am J Physiol Heart Circ Physiol, 2010. **299**(6): p. H1981-9.
339. Buscher, R., et al., *P2Y2 receptor polymorphisms and haplotypes in cystic fibrosis and their impact on Ca²⁺ influx*. Pharmacogenet Genomics, 2006. **16**(3): p. 199-205.
340. Watt, W.C., E.R. Lazarowski, and R.C. Boucher, *Cystic fibrosis transmembrane regulator-independent release of ATP. Its implications for the regulation of P2Y2 receptors in airway epithelia*. J Biol Chem, 1998. **273**(22): p. 14053-8.
341. Faria, D., R. Schreiber, and K. Kunzelmann, *CFTR is activated through stimulation of purinergic P2Y2 receptors*. Pflugers Arch, 2009. **457**(6): p. 1373-80.
342. Raqeeb, A., et al., *Purinergic P2Y2 receptors mediate rapid Ca(2+) mobilization, membrane hyperpolarization and nitric oxide production in human vascular endothelial cells*. Cell Calcium, 2011. **49**(4): p. 240-8.
343. van der Meijden, P.E., et al., *Platelet P2Y12 receptors enhance signalling towards procoagulant activity and thrombin generation. A study with healthy subjects and patients at thrombotic risk*. Thromb Haemost, 2005. **93**(6): p. 1128-36.
344. van Giezen, J.J. and R.G. Humphries, *Preclinical and clinical studies with selective reversible direct P2Y12 antagonists*. Semin Thromb Hemost, 2005. **31**(2): p. 195-204.
345. Storey, R.F., *Biology and pharmacology of the platelet P2Y12 receptor*. Curr Pharm Des, 2006. **12**(10): p. 1255-9.

346. Garcia-Villalon, A.L., et al., *Coronary response to diadenosine pentaphosphate after ischaemia-reperfusion in the isolated rat heart*. Cardiovasc Res, 2009. **81**(2): p. 336-43.
347. Rayment, S.J., et al., *Evidence for the Expression of Multiple Uracil Nucleotide-Stimulated P2 Receptors Coupled to Smooth Muscle Contraction in Porcine Isolated Arteries*. Br J Pharmacol, 2007.
348. Judkins, C.P., et al., *NADPH-induced contractions of mouse aorta do not involve NADPH oxidase: a role for P2X receptors*. J Pharmacol Exp Ther, 2006. **317**(2): p. 644-50.
349. Borna, C., et al., *Contractions in human coronary bypass vessels stimulated by extracellular nucleotides*. The Annals of Thoracic Surgery, 2003. **76**(1): p. 50-7.
350. Legssyer, A., et al., *ATP and other adenine compounds increase mechanical activity and inositol trisphosphate production in rat heart*. J Physiol (Lond), 1988. **401**(1): p. 185-199.
351. Zverev, A.A., T.A. Anikina, and F.G. Sitdicov, *Role of P2X receptors in positive inotropic effect of rat myocardium during ontogeny*. Bull Exp Biol Med, 2008. **145**(2): p. 174-6.
352. Anikina, T.A., et al., *Role of P2X and P2Y receptors in rat myocardial contractility during ontogeny*. Bull Exp Biol Med, 2007. **143**(6): p. 695-8.
353. Musa, H., et al., *P2 purinergic receptor mRNA in rat and human sinoatrial node and other heart regions*. Naunyn Schmiedebergs Arch Pharmacol, 2009. **379**(6): p. 541-9.
354. Ahmet, I., et al., *Diadenosine tetraphosphate (AP4A) mimics cardioprotective effect of ischemic preconditioning in the rat heart: contribution of KATP channel and PKC*. Basic Res Cardiol, 2000. **95**(3): p. 235-42.
355. Ninomiya, H., et al., *Enhanced IPC by activation of pertussis toxin-sensitive and -insensitive G protein-coupled purinoceptors*. American Journal of Physiology. Heart and Circulatory Physiology, 2002b. **282**(5): p. H1933-43.
356. Barrabes, J.A., et al., *Antagonism of P2Y12 or GPIIb/IIIa receptors reduces platelet-mediated myocardial injury after ischaemia and reperfusion in isolated rat hearts*. Thromb Haemost, 2010. **104**(1): p. 128-35.
357. Osman, L., et al., *A novel role of extracellular nucleotides in valve calcification: a potential target for atorvastatin*. Circulation, 2006. **114**(1 Suppl): p. I566-72.
358. Evans, D.J., et al., *Platelet P2Y(12) receptor influences the vessel wall response to arterial injury and thrombosis*. Circulation, 2009. **119**(1): p. 116-22.
359. Jin, J., J.L. Daniel, and S.P. Kunapuli, *Molecular basis for ADP-induced platelet activation. II. The P2Y1 receptor mediates ADP-induced intracellular calcium mobilization and shape change in platelets*. The Journal of Biological Chemistry, 1998. **273**(4): p. 2030-4.
360. Nylander, S., et al., *Synergistic action between inhibition of P2Y12/P2Y1 and P2Y12/thrombin in ADP- and thrombin-induced human platelet activation*. Br J Pharmacol, 2004. **142**(8): p. 1325-31.
361. Fung, C.Y., et al., *P2X(1) receptor inhibition and soluble CD39 administration as novel approaches to widen the cardiovascular therapeutic window*. Trends Cardiovasc Med, 2009. **19**(1): p. 1-5.
362. King, B.F. and A. Townsend-Nicholson, *Nucleotide and Nucleoside Receptors*. Tocris Reviews, 2003. **23**: p. 1-11.

363. von Kugelgen, I., *Pharmacological profiles of cloned mammalian P2Y-receptor subtypes*. Pharmacol Ther, 2006. **110**(3): p. 415-32.
364. Kunapuli, S.P. and J.L. Daniel, *P2 receptor subtypes in the cardiovascular system*. The Biochemical Journal, 1998. **336** (Pt 3): p. 513-23.
365. von Kugelgen, I. and A. Wetter, *Molecular pharmacology of P2Y-receptors*. Naunyn Schmiedebergs Arch Pharmacol, 2000. **362**(4-5): p. 310-23.
366. Lambrecht, G., *Agonists and antagonists acting at P2X receptors: selectivity profiles and functional implications*. Naunyn Schmiedebergs Arch Pharmacol, 2000. **362**(4-5): p. 340-50.
367. Kim, M., et al., *Proteomic and functional evidence for a P2X7 receptor signalling complex*. Embo J, 2001. **20**(22): p. 6347-58.
368. Hopwood, A.M., et al., *Adenosine 5'-triphosphate, adenosine and endothelium-derived relaxing factor in hypoxic vasodilatation of the heart*. European Journal of Pharmacology, 1989. **165**(2-3): p. 323-6.
369. Guns, P.J., et al., *Endothelium-dependent relaxation evoked by ATP and UTP in the aorta of P2Y2-deficient mice*. Br J Pharmacol, 2006. **147**(5): p. 569-74.
370. Burnstock, G. and C. Kennedy, *A dual function for adenosine 5'-triphosphate in the regulation of vascular tone. Excitatory cotransmitter with noradrenaline from perivascular nerves and locally released inhibitory intravascular agent*. Circ Res, 1986. **58**(3): p. 319-30.
371. Rongen, G.A., et al., *Cardiovascular pharmacology of purines*. Clin Sci (Lond), 1997. **92**(1): p. 13-24.
372. Shehnaz, D., et al., *Pyridoxal-phosphate-6-azophenyl-2',4'-disulfonate (PPADS), a putative P2Y(1) receptor antagonist, blocks signaling at a site distal to the receptor in Madin-Darby canine kidney-D(1) cells*. J Pharmacol Exp Ther, 2000. **292**(1): p. 346-50.
373. Chen, B.C., C.M. Lee, and W.W. Lin, *Inhibition of ecto-ATPase by PPADS, suramin and reactive blue in endothelial cells, C6 glioma cells and RAW 264.7 macrophages*. Br J Pharmacol, 1996. **119**(8): p. 1628-34.
374. Yegutkin, G.G. and G. Burnstock, *Inhibitory effects of some purinergic agents on ecto-ATPase activity and pattern of stepwise ATP hydrolysis in rat liver plasma membranes*. Biochim Biophys Acta, 2000. **1466**(1-2): p. 234-44.
375. Malmsjo, M., L. Edvinsson, and D. Erlinge, *P2U-receptor mediated endothelium-dependent but nitric oxide-independent vascular relaxation*. British Journal of Pharmacology, 1998. **123**(4): p. 719-29.
376. Malmsjo, M., et al., *Endothelial P2Y receptors induce hyperpolarisation of vascular smooth muscle by release of endothelium-derived hyperpolarising factor*. European Journal of Pharmacology, 1999. **364**(2-3): p. 169-73.
377. Leon, C., et al., *The P2Y1 receptor is an ADP receptor antagonized by ATP and expressed in platelets and megakaryoblastic cells*. FEBS Lett, 1997. **403**(1): p. 26-30.
378. Lustig, K.D., et al., *Expression cloning of an ATP receptor from mouse neuroblastoma cells*. Proc Natl Acad Sci U S A, 1993. **90**(11): p. 5113-7.
379. Parr, C.E., et al., *Cloning and expression of a human P2U nucleotide receptor, a target for cystic fibrosis pharmacotherapy*. Proc Natl Acad Sci U S A, 1994. **91**(26): p. 13067.
380. Froldi, G., E. Ragazzi, and L. Caparrotta, *Do ATP and UTP involve cGMP in positive inotropism on rat atria?* Comp Biochem Physiol C Toxicol Pharmacol, 2001. **128**(2): p. 265-74.

381. Frolidi, G., et al., *Dual effect of ATP and UTP on rat atria: which types of receptors are involved?* Naunyn Schmiedebergs Arch Pharmacol, 1994. **349**(4): p. 381-6.
382. Ben-Ari, Z., et al., *Uridine-5'-triphosphate protects against hepatic-ischemic/reperfusion injury in mice.* Transplantation, 2009. **87**(8): p. 1155-62.
383. Tian, M.L., et al., *Uridine 5'-triphosphate (UTP) protects against cerebral ischemia reperfusion injury in rats.* Neurosci Lett, 2009. **465**(1): p. 55-60.
384. Yitzhaki, S., et al., *Uridine-5'-triphosphate (UTP) maintains cardiac mitochondrial function following chemical and hypoxic stress.* J Mol Cell Cardiol, 2007. **43**(5): p. 653-62.
385. Nicholas, R.A., et al., *Uridine nucleotide selectivity of three phospholipase C-activating P2 receptors: identification of a UDP-selective, a UTP-selective, and an ATP- and UTP-specific receptor.* Mol Pharmacol, 1996. **50**(2): p. 224-9.
386. Chang, K., et al., *Molecular cloning and functional analysis of a novel P2 nucleotide receptor.* The Journal of Biological Chemistry, 1995. **270**(44): p. 26152-8.
387. Wihlborg, A.K., et al., *Extracellular nucleotides induce vasodilatation in human arteries via prostaglandins, nitric oxide and endothelium-derived hyperpolarising factor.* Br J Pharmacol, 2003. **138**(8): p. 1451-8.
388. Erlinge, D., et al., *Mitogenic effects of ATP on vascular smooth muscle cells vs. other growth factors and sympathetic cotransmitters.* Am J Physiol, 1993. **265**(4 Pt 2): p. H1089-97.
389. Seye, C.I., et al., *Functional P2Y2 nucleotide receptors mediate uridine 5'-triphosphate-induced intimal hyperplasia in collared rabbit carotid arteries.* Circulation, 2002. **106**(21): p. 2720-6.
390. Pillois, X., et al., *Nucleotide receptors involved in UTP-induced rat arterial smooth muscle cell migration.* Circ Res, 2002. **90**(6): p. 678-81.
391. Horiuchi, T., et al., *Analysis of purine- and pyrimidine-induced vascular responses in the isolated rat cerebral arteriole.* Am J Physiol Heart Circ Physiol, 2001. **280**(2): p. H767-76.
392. Greig, A.V., et al., *Expression of purinergic receptors in non-melanoma skin cancers and their functional roles in A431 cells.* J Invest Dermatol, 2003. **121**(2): p. 315-27.
393. Coutinho-Silva, R., et al., *P2X and P2Y purinergic receptors on human intestinal epithelial carcinoma cells: effects of extracellular nucleotides on apoptosis and cell proliferation.* Am J Physiol Gastrointest Liver Physiol, 2005. **288**(5): p. G1024-35.
394. White, N. and G. Burnstock, *P2 receptors and cancer.* Trends Pharmacol Sci, 2006. **27**(4): p. 211-7.
395. Nylund, G., et al., *P2Y2- and P2Y4 purinergic receptors are over-expressed in human colon cancer.* Auton Autacoid Pharmacol, 2007. **27**(2): p. 79-84.
396. Schafer, R., et al., *ATP- and UTP-activated P2Y receptors differently regulate proliferation of human lung epithelial tumor cells.* Am J Physiol Lung Cell Mol Physiol, 2003. **285**(2): p. L376-85.
397. Hopfner, M., et al., *Growth inhibition and apoptosis induced by P2Y2 receptors in human colorectal carcinoma cells: involvement of intracellular calcium and cyclic adenosine monophosphate.* Int J Colorectal Dis, 2001. **16**(3): p. 154-66.

398. Communi, D., et al., *Pharmacological characterization of the human P2Y₄ receptor*. Eur J Pharmacol, 1996. **317**(2-3): p. 383-9.
399. Cavaliere, F., et al., *The metabotropic P2Y₄ receptor participates in the commitment to differentiation and cell death of human neuroblastoma SH-SY5Y cells*. Neurobiol Dis, 2005. **18**(1): p. 100-9.
400. Harada, H., et al., *Induction of proliferation and apoptotic cell death via P2Y and P2X receptors, respectively, in rat glomerular mesangial cells*. Kidney Int, 2000. **57**(3): p. 949-58.
401. Kaczmarek, E., et al., *Modulation of endothelial cell migration by extracellular nucleotides: involvement of focal adhesion kinase and phosphatidylinositol 3-kinase-mediated pathways*. Thromb Haemost, 2005. **93**(4): p. 735-42.
402. Harden, T.K., E.R. Lazarowski, and R.C. Boucher, *Release, metabolism and interconversion of adenine and uridine nucleotides: implications for G protein-coupled P2 receptor agonist selectivity*. Trends Pharmacol Sci, 1997. **18**(2): p. 43-6.
403. Lazarowski, E.R., R.C. Boucher, and T.K. Harden, *Constitutive release of ATP and evidence for major contribution of ecto-nucleotide pyrophosphatase and nucleoside diphosphokinase to extracellular nucleotide concentrations*. J Biol Chem, 2000. **275**(40): p. 31061-8.
404. Kukulski, F., et al., *Comparative hydrolysis of P2 receptor agonists by NTPDases 1, 2, 3 and 8*. Purinergic Signal, 2005. **1**(2): p. 193-204.
405. Kennedy, C., et al., *ATP, an agonist at the rat P2Y₄ receptor, is an antagonist at the human P2Y₄ receptor*. Mol Pharmacol, 2000. **57**(5): p. 926-31.
406. Enjyoji, K., et al., *Targeted disruption of cd39/ATP diphosphohydrolase results in disordered hemostasis and thromboregulation*. Nat Med, 1999. **5**(9): p. 1010-7.
407. Kauffenstein, G., et al., *NTPDase1 (CD39) controls nucleotide-dependent vasoconstriction in mouse*. Cardiovasc Res, 2009. **85**(1): p. 204-13.
408. Kauffenstein, G., et al., *The ecto-nucleotidase NTPDase1 differentially regulates P2Y₁ and P2Y₂ receptor-dependent vasorelaxation*. Br J Pharmacol, 2010. **159**(3): p. 576-85.
409. Eltzschig, H.K., et al., *Coordinated adenine nucleotide phosphohydrolysis and nucleoside signaling in posthypoxic endothelium: role of ectonucleotidases and adenosine A2B receptors*. J Exp Med, 2003. **198**(5): p. 783-96.
410. Headrick, J. and R.J. Willis, *Endogenous adenosine improves work rate to oxygen consumption ratio in catecholamine stimulated isovolumic rat heart*. Pflugers Arch, 1989. **413**(4): p. 354-8.
411. Harrison, G.J., R.J. Willis, and J.P. Headrick, *Extracellular adenosine levels and cellular energy metabolism in ischemically preconditioned rat heart*. Cardiovasc Res, 1998. **40**(1): p. 74-87.
412. Webb, T.E., M.O. Boluyt, and E.A. Barnard, *Molecular biology of P2Y purinoceptors: expression in rat heart*. Journal of Autonomic Pharmacology, 1996. **16**(6): p. 303-7.
413. Wang, L., et al., *P2 receptor expression profiles in human vascular smooth muscle and endothelial cells*. J Cardiovasc Pharmacol, 2002. **40**(6): p. 841-53.
414. Yang, S., et al., *Purinergic axis in cardiac blood vessels. Agonist-mediated release of ATP from cardiac endothelial cells*. Circ Res, 1994. **74**(3): p. 401-7.

415. Burnstock, G., *Purinergic receptors in the heart*. Circ Res, 1980. **46**(6 Pt 2): p. I175-82.
416. Forrester, T. and C.A. Williams, *Release of adenosine triphosphate from isolated adult heart cells in response to hypoxia*. J Physiol, 1977. **268**(2): p. 371-90.
417. Clemens, M.G. and T. Forrester, *Appearance of ATP in the coronary sinus effluent from isolated working rat heart in response to hypoxia [proceedings]*. J Physiol, 1979. **295**: p. 50P-51P.
418. Strobaek, D., et al., *P2-purinoceptor-mediated formation of inositol phosphates and intracellular Ca²⁺ transients in human coronary artery smooth muscle cells*. Br J Pharmacol, 1996. **118**(7): p. 1645-52.
419. Freissmuth, M., et al., *Suramin analogues as subtype-selective G protein inhibitors*. Mol Pharmacol, 1996. **49**(4): p. 602-11.
420. Colgan, S.P., et al., *Physiological roles for ecto-5'-nucleotidase (CD73)*. Purinergic Signal, 2006. **2**(2): p. 351-60.
421. Corr, L. and G. Burnstock, *Vasodilator response of coronary smooth muscle to the sympathetic co-transmitters noradrenaline and adenosine 5'-triphosphate*. Br J Pharmacol, 1991. **104**(2): p. 337-42.
422. Murthy, K.S. and G.M. Makhoulf, *Coexpression of ligand-gated P2X and G protein-coupled P2Y receptors in smooth muscle. Preferential activation of P2Y receptors coupled to phospholipase C (PLC)-beta1 via Galphaq/11 and to PLC-beta3 via Gbetagamma3*. The Journal of Biological Chemistry, 1998. **273**(8): p. 4695-704.
423. Hill, B.J. and M. Sturek, *Pharmacological characterization of a UTP-sensitive P2Y nucleotide receptor in organ cultured coronary arteries*. 2002. **39**(1-2): p. 83-8.
424. Marrelli, S.P., *Mechanisms of endothelial P2Y(1)- and P2Y(2)-mediated vasodilatation involve differential [Ca²⁺]_i responses*. American Journal of Physiology. Heart and Circulatory Physiology, 2001. **281**(4): p. H1759-66.
425. Sugimura, A., et al., *Effect of diadenosine tetraphosphate (AP4A) on coronary arterial microvessels in the beating canine heart*. Jpn Circ J, 2000. **64**(11): p. 868-75.
426. Gordon, J.L., *Extracellular ATP: effects, sources and fate*. Biochem J, 1986. **233**(2): p. 309-19.
427. Lazarowski, E.R. and R.C. Boucher, *UTP as an extracellular signaling molecule*. News Physiol Sci, 2001. **16**: p. 1-5.
428. Jacobson, K.A., et al., *Structure activity and molecular modeling analyses of ribose- and base-modified uridine 5'-triphosphate analogues at the human P2Y2 and P2Y4 receptors*. Biochem Pharmacol, 2006. **71**(4): p. 540-9.
429. Lazarowski, E.R., et al., *Enzymatic synthesis of UTP gamma S, a potent hydrolysis resistant agonist of P2U-purinoceptors*. Br J Pharmacol, 1996. **117**(1): p. 203-9.
430. Mamedova, L.K., et al., *Attenuation of apoptosis in vitro and ischemia/reperfusion injury in vivo in mouse skeletal muscle by P2Y6 receptor activation*. Pharmacol Res, 2008. **58**(3-4): p. 232-9.
431. Malmsjo, M., et al., *Characterization of contractile P2 receptors in human coronary arteries by use of the stable pyrimidines uridine 5'-O-thiodiphosphate and uridine 5'-O-3-thiotriphosphate*. The Journal of Pharmacology and Experimental Therapeutics, 2000. **293**(3): p. 755-60.

432. Malmsjo, M., et al., *The stable pyrimidines UDPbetaS and UTPgammaS discriminate between contractile cerebrovascular P2 receptors*. European Journal of Pharmacology, 2003a. **458**(3): p. 305-11.
433. Korcok, J., et al., *P2Y6 nucleotide receptors activate NF-kappaB and increase survival of osteoclasts*. J Biol Chem, 2005. **280**(17): p. 16909-15.
434. Cox, M.A., et al., *The pyrimidinergic P2Y6 receptor mediates a novel release of proinflammatory cytokines and chemokines in monocytic cells stimulated with UDP*. Biochem Biophys Res Commun, 2005. **330**(2): p. 467-73.
435. Khine, A.A., et al., *Human neutrophil peptides induce interleukin-8 production through the P2Y6 signaling pathway*. Blood, 2006. **107**(7): p. 2936-42.
436. Krylova, I.B., et al., *The cardioprotective effect of uridine and uridine-5'-monophosphate: the role of the mitochondrial ATP-dependent potassium channel*. Exp Gerontol, 2006. **41**(7): p. 697-703.
437. Malmsjo, M., et al., *The stable pyrimidines UDPbetaS and UTPgammaS discriminate between the P2 receptors that mediate vascular contraction and relaxation of the rat mesenteric artery*. Br J Pharmacol, 2000. **131**(1): p. 51-6.
438. Kurose, H., *Galpha12 and Galpha13 as key regulatory mediator in signal transduction*. Life Sci, 2003. **74**(2-3): p. 155-61.
439. Dermott, J.M., et al., *Differential regulation of Jun N-terminal kinase and p38MAP kinase by Galpha12*. Oncogene, 2004. **23**(1): p. 226-32.
440. Hayakawa, Y., et al., *Inhibition of cardiac myocyte apoptosis improves cardiac function and abolishes mortality in the peripartum cardiomyopathy of Galpha(q) transgenic mice*. Circulation, 2003. **108**(24): p. 3036-41.
441. Kim, S.G., et al., *P2Y6 nucleotide receptor activates PKC to protect 1321NI astrocytoma cells against tumor necrosis factor-induced apoptosis*. Cell Mol Neurobiol, 2003. **23**(3): p. 401-18.
442. Apolloni, S., et al., *UDP exerts cytostatic and cytotoxic actions in human neuroblastoma SH-SY5Y cells over-expressing P2Y6 receptor*. Neurochem Int, 2010. **56**(5): p. 670-8.
443. Hausenloy, D.J. and D.M. Yellon, *Reperfusion injury salvage kinase signalling: taking a RISK for cardioprotection*. Heart Fail Rev, 2007. **12**(3-4): p. 217-34.
444. Abbracchio, M.P., et al., *Characterization of the UDP-glucose receptor (re-named here the P2Y14 receptor) adds diversity to the P2Y receptor family*. Trends Pharmacol Sci, 2003. **24**(2): p. 52-5.
445. Carroll, R. and D.M. Yellon, *Delayed cardioprotection in a human cardiomyocyte-derived cell line: the role of adenosine, p38MAP kinase and mitochondrial KATP*. Basic Res Cardiol, 2000. **95**(3): p. 243-9.
446. Beindl, W., et al., *Inhibition of receptor/G protein coupling by suramin analogues*. Molecular Pharmacology, 1996. **50**(2): p. 415-23.
447. Wildman, S.S., R.J. Unwin, and B.F. King, *Extended pharmacological profiles of rat P2Y2 and rat P2Y4 receptors and their sensitivity to extracellular H⁺ and Zn²⁺ ions*. Br J Pharmacol, 2003. **140**(7): p. 1177-86.
448. Charlton, S.J., et al., *PPADS and suramin as antagonists at cloned P2Y- and P2U-purinoceptors*. British Journal of Pharmacology, 1996. **118**(3): p. 704-10.
449. Suarez-Huerta, N., et al., *Molecular cloning and characterization of the mouse P2Y4 nucleotide receptor*. Eur J Pharmacol, 2001. **416**(3): p. 197-202.

450. Chorna, N.E., et al., *P2Y(2) receptors induced cell surface redistribution of alpha(v) integrin is required for activation of ERK 1/2 in U937 cells*. J Cell Physiol, 2006. **211**(2): p. 410-422.
451. da Cruz, C.M., et al., *Activation of ERK1/2 by extracellular nucleotides in macrophages is mediated by multiple P2 receptors independently of P2X7-associated pore or channel formation*. Br J Pharmacol, 2006. **147**(3): p. 324-34.
452. Kolch, W., M. Calder, and D. Gilbert, *When kinases meet mathematics: the systems biology of MAPK signalling*. FEBS Lett, 2005. **579**(8): p. 1891-5.
453. Seko, Y., et al., *Hypoxia and hypoxia/reoxygenation activate Raf-1, mitogen-activated protein kinase kinase, mitogen-activated protein kinases, and S6 kinase in cultured rat cardiac myocytes*. Circ Res, 1996. **78**(1): p. 82-90.
454. Tu, M.T., et al., *P2Y(2) receptor-mediated proliferation of C(6) glioma cells via activation of Ras/Raf/MEK/MAPK pathway*. Br J Pharmacol, 2000. **129**(7): p. 1481-9.
455. Yamaguchi, O., et al., *Cardiac-specific disruption of the c-raf-1 gene induces cardiac dysfunction and apoptosis*. J Clin Invest, 2004. **114**(7): p. 937-43.
456. Boucher, I., et al., *The P2Y2 receptor mediates the epithelial injury response and cell migration*. Am J Physiol Cell Physiol, 2010. **299**(2): p. C411-21.
457. Harris, I.S., et al., *Raf-1 kinase is required for cardiac hypertrophy and cardiomyocyte survival in response to pressure overload*. Circulation, 2004. **110**(6): p. 718-23.
458. Muslin, A.J., *Role of raf proteins in cardiac hypertrophy and cardiomyocyte survival*. Trends Cardiovasc Med, 2005. **15**(6): p. 225-9.
459. Pfeleiderer, P., et al., *Raf-1: a novel cardiac troponin T kinase*. J Muscle Res Cell Motil, 2009. **30**(1-2): p. 67-72.
460. Xuan, Y.T., et al., *Role of the protein kinase C-epsilon-Raf-1-MEK-1/2-p44/42 MAPK signaling cascade in the activation of signal transducers and activators of transcription 1 and 3 and induction of cyclooxygenase-2 after ischemic preconditioning*. Circulation, 2005. **112**(13): p. 1971-8.
461. Cao, Q., et al., *Negative feedback regulation of Raf/MEK/ERK cascade after sublethal cerebral ischemia in the rat hippocampus*. Neurochem Res, 2011. **36**(1): p. 153-62.
462. Oudit, G.Y., et al., *The role of phosphoinositide-3 kinase and PTEN in cardiovascular physiology and disease*. J Mol Cell Cardiol, 2004. **37**(2): p. 449-71.
463. Samavati, L., et al., *Mitochondrial K(ATP) channel openers activate the ERK kinase by an oxidant-dependent mechanism*. Am J Physiol Cell Physiol, 2002. **283**(1): p. C273-81.
464. Tsang, A., et al., *Postconditioning: a form of "modified reperfusion" protects the myocardium by activating the phosphatidylinositol 3-kinase-Akt pathway*. Circ Res, 2004. **95**(3): p. 230-2.
465. Peart, J.N., et al., *Activation of kappa-opioid receptors at reperfusion affords cardioprotection in both rat and mouse hearts*. Basic Res Cardiol, 2008. **103**(5): p. 454-63.
466. Fang, F., et al., *Luteolin Inhibits Apoptosis and Improves Cardiomyocyte Contractile Function through the PI3K/Akt Pathway in Simulated Ischemia/Reperfusion*. Pharmacology, 2011. **88**(3-4): p. 149-158.
467. Lu, Z., et al., *Loss of cardiac phosphoinositide 3-kinase p110 alpha results in contractile dysfunction*. Circulation, 2009. **120**(4): p. 318-25.

468. Wu, C.Y., et al., *PI3Ks Maintain the Structural Integrity of T-Tubules in Cardiac Myocytes*. PLoS One, 2011. **6**(9): p. e24404.
469. Pinho, J.F., et al., *Phosphatidylinositol 3-kinase-delta up-regulates L-type Ca²⁺ currents and increases vascular contractility in a mouse model of type 1 diabetes*. Br J Pharmacol, 2010. **161**(7): p. 1458-71.
470. Oudit, G.Y. and J.M. Penninger, *Cardiac regulation by phosphoinositide 3-kinases and PTEN*. Cardiovasc Res, 2009. **82**(2): p. 250-60.
471. Heo, J.S. and H.J. Han, *ATP stimulates mouse embryonic stem cell proliferation via protein kinase C, phosphatidylinositol 3-kinase/Akt, and mitogen-activated protein kinase signaling pathways*. Stem Cells, 2006. **24**(12): p. 2637-48.
472. Huwiler, A., et al., *Extracellular ATP and UTP activate the protein kinase B/Akt cascade via the P2Y(2) purinoceptor in renal mesangial cells*. Br J Pharmacol, 2002. **136**(4): p. 520-9.
473. Arthur, D.B., et al., *Inhibition of apoptosis by P2Y2 receptor activation: novel pathways for neuronal survival*. J Neurosci, 2006. **26**(14): p. 3798-804.
474. Gross, G.J. and J.A. Auchampach, *Blockade of ATP-sensitive potassium channels prevents myocardial preconditioning in dogs*. Circ Res, 1992. **70**(2): p. 223-33.
475. Oldenburg, O., M.V. Cohen, and J.M. Downey, *Mitochondrial K(ATP) channels in preconditioning*. J Mol Cell Cardiol, 2003. **35**(6): p. 569-75.
476. Cole, W.C., C.D. McPherson, and D. Sontag, *ATP-regulated K⁺ channels protect the myocardium against ischemia/reperfusion damage*. Circ Res, 1991. **69**(3): p. 571-81.
477. Suzuki, M., et al., *Role of sarcolemmal K(ATP) channels in cardioprotection against ischemia/reperfusion injury in mice*. J Clin Invest, 2002. **109**(4): p. 509-16.
478. Gross, G.J. and J.N. Peart, *KATP channels and myocardial preconditioning: an update*. Am J Physiol Heart Circ Physiol, 2003. **285**(3): p. H921-30.
479. McCullough, J.R., et al., *Specific block of the anti-ischemic actions of cromakalim by sodium 5-hydroxydecanoate*. Circ Res, 1991. **69**(4): p. 949-58.
480. Garlid, K.D., et al., *Mitochondrial potassium transport: the role of the mitochondrial ATP-sensitive K(+) channel in cardiac function and cardioprotection*. Biochim Biophys Acta, 2003. **1606**(1-3): p. 1-21.
481. Garlid, K.D., et al., *Cardioprotective effect of diazoxide and its interaction with mitochondrial ATP-sensitive K⁺ channels. Possible mechanism of cardioprotection*. Circ Res, 1997. **81**(6): p. 1072-82.
482. Sato, T. and E. Marban, *The role of mitochondrial K(ATP) channels in cardioprotection*. Basic Res Cardiol, 2000. **95**(4): p. 285-9.
483. Murphy, E., *Primary and secondary signaling pathways in early preconditioning that converge on the mitochondria to produce cardioprotection*. Circ Res, 2004. **94**(1): p. 7-16.